BRL-CR-646

DTIC FILE COPY

(2)

CONTRACTOR REPORT BRL-CR-646

BRL

AD-A229 661

EVALUATION OF ELECTROMAGNETIC AND ELECTROTHERMAL LAUNCHERS FOR THE BRL ADVANCED TEST FACILITY

R.M. DEL VECCHIO
G. GIBSON
H. RIEMERSMA
D.W. SCHERBARTH
WESTINGHOUSE SCIENCE & TECHNOLOGY CENTER
PITTSBURGH, PENNSYLVANIA

NOVEMBER 1990

U.S. ARMY LABORATORY COMMAND

BALLISTIC RESEARCH LABORATORY
ABERDEEN PROVING GROUND, MARYLAND

NOTICES

UNCLASSIFIED

REPORT DOCUMENTATION PAGE

Form Approved
OMB No. 0704-0188

1. AGENCY USE ONLY *(Leave blank)*

2. REPORT DATE
November 1990

3. REPORT TYPE AND DATES COVERED
Final, 17 Aug 88 - 16 Aug 89

4. TITLE AND SUBTITLE
Evaluation of Electromagnetic and Electrothermal Launchers for the BRL Advanced Test Facility

5. FUNDING NUMBERS
C: DAAA15-88-C-0012

6. AUTHOR(S)
R. M. Del Vecchio, G. Gibson, H. Riemersma, D. W. Scherbarth

7. PERFORMING ORGANIZATION NAME(S) AND ADDRESS(ES)
Westinghouse Science & Technology Center
1310 Beulah Road
Pittsburgh, Pennsylvania 15235

8. PERFORMING ORGANIZATION REPORT NUMBER
89-9E6-EMBRL-R2

9. SPONSORING / MONITORING AGENCY NAME(S) AND ADDRESS(ES)
US Army Ballistic Research Laboratory
ATTN: SLCBR-DD-T
Aberdeen Proving Ground, MD 21005-5066

10. SPONSORING / MONITORING AGENCY REPORT NUMBER
BRL-CR-646

11. SUPPLEMENTARY NOTES
BRL Technical Monitor: Henry Burden (301) 278-4363

12a. DISTRIBUTION / AVAILABILITY STATEMENT
Approved for public release; distribution unlimited.

12b. DISTRIBUTION CODE

13. ABSTRACT *(Maximum 200 words)*
Optimum designs have been developed for three types of electric launchers that can be used for conducting terminal ballistic research. The U.S. Army Ballistic Research Laboratory (BRL), which is located at Aberdeen, MD, specified the operational requirements, viz., to accelerate penetrators having a mass in the 60-200 g range and a length-to-diameter ratio in the 10-40 range to velocities in the 2.5-3.5 km/s range. Capacitor-driven electromagnetic launchers (EMLs), homopolar-generator-driven EMLs, and capacitor-driven electrothermal launchers have been evaluated and compared on the basis of technical risks and capital costs. A capacitor-driven EML is recommended as the best option for meeting BRL's requirements. Based on the design of the preferred launcher option, a one-year commissioning/test (C/T) program has been defined. The C/T Program addresses the technical issues that can be identified that impact on facility performance, reliability and cost of operation. The resolution of these issues by the conclusion of the C/T Program, will allow routine operation of the facility for terminal ballistic research to commence. At that time, the BRL team should thoroughly understand the operation and maintenance of the advanced gun facility.

14. SUBJECT TERMS
Launcher; Electrothermal; Electromagnetic Guns; Terminal Ballistics; Penetrator; Commissioning

15. NUMBER OF PAGES
251

16. PRICE CODE

17. SECURITY CLASSIFICATION OF REPORT	18. SECURITY CLASSIFICATION OF THIS PAGE	19. SECURITY CLASSIFICATION OF ABSTRACT	20. LIMITATION OF ABSTRACT
UNCLASSIFIED	UNCLASSIFIED	UNCLASSIFIED	SAR

INTENTIONALLY LEFT BLANK.

Contents

INTENTIONALLY LEFT BLANK.

List of Figures

List of Tables

INTENTIONALLY LEFT BLANK.

ACKNOWLEDGEMENTS

H. Burden of the Engineering/Physics Department of the Army's Ballistic Research Laboratory was the technical monitor for this work. He provided guidance, helped establish the ground rules under which this study was conducted, closely followed the progress of the study, and critiqued the reports. He also arranged a tour of the BRL facilities which provided insight into the needs and requirements for the type of research conducted at BRL.

In addition to the authors, significant contributions were made to the program by the following engineers and scientists at the Westinghouse STC:

R. G. Colclaser......... ETL Circuit Analysis
D. W. Deis.............. Design Reviews
T. K. Deis.............. ETL Mechanical Design/Bore Reaming Tool
J. A. Hendrickson....... Preaccelerator
T. D. Hordubay.......... Mechanical Design Reviews
D. A. Fikse............. Program Management
D. C. Johnson........... Electrical Design Reviews
D. Marschik............. Electrical Systems/Design Reviews
D. Pavlik............... HPG Analysis
H. Riemersma............ EML Costs/Design Reviews
J. A. Spitznagle........ Bore Materials
B. W. Swanson........... ETL Analysis

H. A. Calvin of the Westinghouse Marine Division in Sunnyvale, CA contributed to the design of the HPG-driven EML. Prior to his leaving Westinghouse, D. A. Sink made major contributions to the design of the capacitor-driven EML.

INTENTIONALLY LEFT BLANK.

1. INTRODUCTION

This report documents the results of the "Program to Improve Launcher Performance for High Velocity Terminal Ballistic Research" that was conducted by the Westinghouse Science and Technology Center under contract to the U.S. Army Ballistic Research Laboratory (BRL). Essentially two tasks were conducted during the course of this program. Task 1 can be described in terms of the following three subtasks:

a) Development of optimized conceptual designs for capacitor- and homopolar generator (HPG)-driven electromagnetic launchers (EMLs) and an electrothermal launcher (ETL) that will satisfy the BRL lethality test stand requirements. The design must be in sufficient depth to allow subtasks b and c to be conducted.

b) Evaluation and comparison of the launchers on the basis of technical risks and capital costs.

c) Selection of the best design concept to satisfy the Army Ballistic Research Laboratory's needs.

The requirements for the test stand, which form the basis of the Task 1 study, are presented in Section 1.1. A simple scoping analysis that provides preliminary dimensions for the launcher barrel is given in Section 1.2. Some qualitative features of the three launcher options are also presented in Section 1.2; these features are quantified in the detailed designs presented in Sections 2, 3 and 4.

Task 2 which addresses a commissioning plan plus a test plan that will prepare the launcher selected during Task 1 (and the operating crew) for the type of routine operation required for a terminal ballistic research tool is described in Section 1.3.

1.1 REQUIRED PERFORMANCE FOR THE BRL

The requirements that BRL has established for their Advanced Lethality Test Stand are shown in Table 1. It must be noted that in order to accelerate a rod-shaped penetrator, a projectile package of much larger mass must be accelerated. Figure 1 is an example of a 500-g projectile consisting of a 200-g penetrator, a 175-g sabot/rider, and a 125-g aluminum armature. No engineering of projectile packages was conducted during task 1 of this study. Figure 1 simply illustrates our assumptions in obtaining a total mass for the projectile. For the ETL the corresponding mass of the projectile package would be 375 g since an armature would not be required. For this example, an EML having a barrel of length 5 m and a bore diameter of 5.6 cm has been assumed. Under standard atmospheric conditions, 15 g of air which is located initially in the bore would also be accelerated. For efficient operation, it is important to minimize the mass of the sabot and armature.

Before beginning the detailed analyses of the three advanced launcher options under consideration, (see Sections 2, 3 and 4) a scoping analysis based on a simple model was performed to determine some of the launcher parameters. These parameters served as a starting-point design for the more detailed analysis and engineering design.

1.2 SIMPLE SCOPING ANALYSIS

A simple expression can be obtained for the projectile motion down the bore of any launcher if the following assumptions are made:

- frictional effects can be ignored
- atmospheric effects are not important
- there is no preacceleration of the projectile
- the mass of the projectile package does not change during acceleration

Table 1   BRL LETHALITY TEST STAND REQUIREMENTS

- Single shot launcher.

- High density (e.g., tungsten alloy at 17 g/cm^3) penetrators in the mass range:

$$60 \text{ g} \lesssim m \lesssim 200 \text{ g}$$

- Penetrator length-to-diameter ratios in the range:

$$10 \lesssim \frac{L}{D} \lesssim 40 ,$$

  - For 65-g penetrator:

    D = 6.2 mm, L = 12.4 cm for L/D = 20

    D = 5.4 mm, L = 16.3 cm for L/D = 30

  - For 200-g penetrator:

    D = 9.0 mm, L = 18.0 cm for L/D = 20

    D = 7.9 mm, L = 23.7 cm for L/D = 30

- Projectile velocities at the muzzle in the range:

$$2.5 \text{ km/s} \lesssim v_m \lesssim 3.5 \text{ km/s}$$

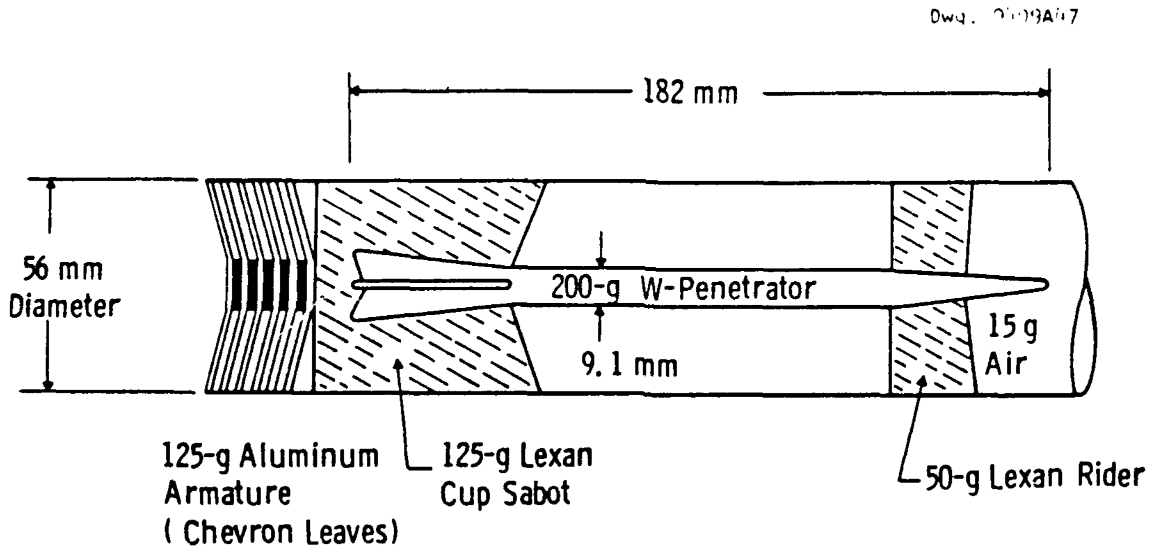

Figure 1. A projectile package for a 200 g penetrator.

The force equation $f = m\ a$

can be written as $P\ A = m\ v\ \frac{dv}{dX}$.

The solution to this equation is: $v_m = \left(\frac{2\ A\ L\ \bar{P}}{m}\right)^{1/2}$

where P = pressure driving the projectile

$$\bar{P} = \frac{1}{L} \int_0^L P\ dX$$

L = length of barrel

A = cross sectional area of bore

m = total mass of projectile package, and

v_m = velocity of projectile at the muzzle.

Therefore if we can estimate the average driving pressure and specify the bore dimensions, the achievable velocity can be obtained as a function of the mass of the projectile package. The average driving pressure depends on the peak pressure attainable and the profile of the pressure at the base of the projectile as it accelerates down the bore. For example, for an EML there is an engineering constraint on the peak driving pressure viz $\hat{P} \simeq 345$ MPa (50 ksi). Furthermore, it is known for capacitor-driven EMLs that the average driving pressure $\bar{P} \simeq 1/2\ \hat{P}$. Figure 2 shows the velocity, which has been obtained from the equation given above, that can be achieved as a function of the projectile mass. The different curves correspond to different core diameters. These curves are valid for any type launcher, provided that $\bar{P} = 173$ MPa and the barrel length equals 5 m. It can be seen that the velocity varies inversely as the square root of the mass. This means the kinetic energy of a projectile at any point down the bore is independent of its mass! In order to accelerate a 500-g projectile package into the velocity range 2.5 km/s-3.5 km/s, it can be seen that for a 5-m long barrel a bore diameter ≥ 5 cm is required. Of course, as the diameter of the bore increases, the total mass of the projectile package will tend to increase also.

A number of sets of curves such as shown in Figure 2 which correspond to different barrel lengths were generated. Based on meeting the BRL requirements and having a compact device (for ease of maintenance, efficiency, and low cost) a barrel length of 5 m was chosen as the starting point for the analyses that follows in subsequent sections.

In order to optimize the performance of a launcher, we would like to achieve the highest peak driving pressure possible and to have a pressure profile, i.e., pressure as a function of projectile position down the bore, that minimizes the piezometric ratio, $\hat{P}/\bar{P}$. However, in minimizing the piezometric ratio, there is an engineering constraint that the driving pressure must decrease just prior to the projectile exiting the muzzle in order to not damage the projectile package and perturb the motion of the penetrator.

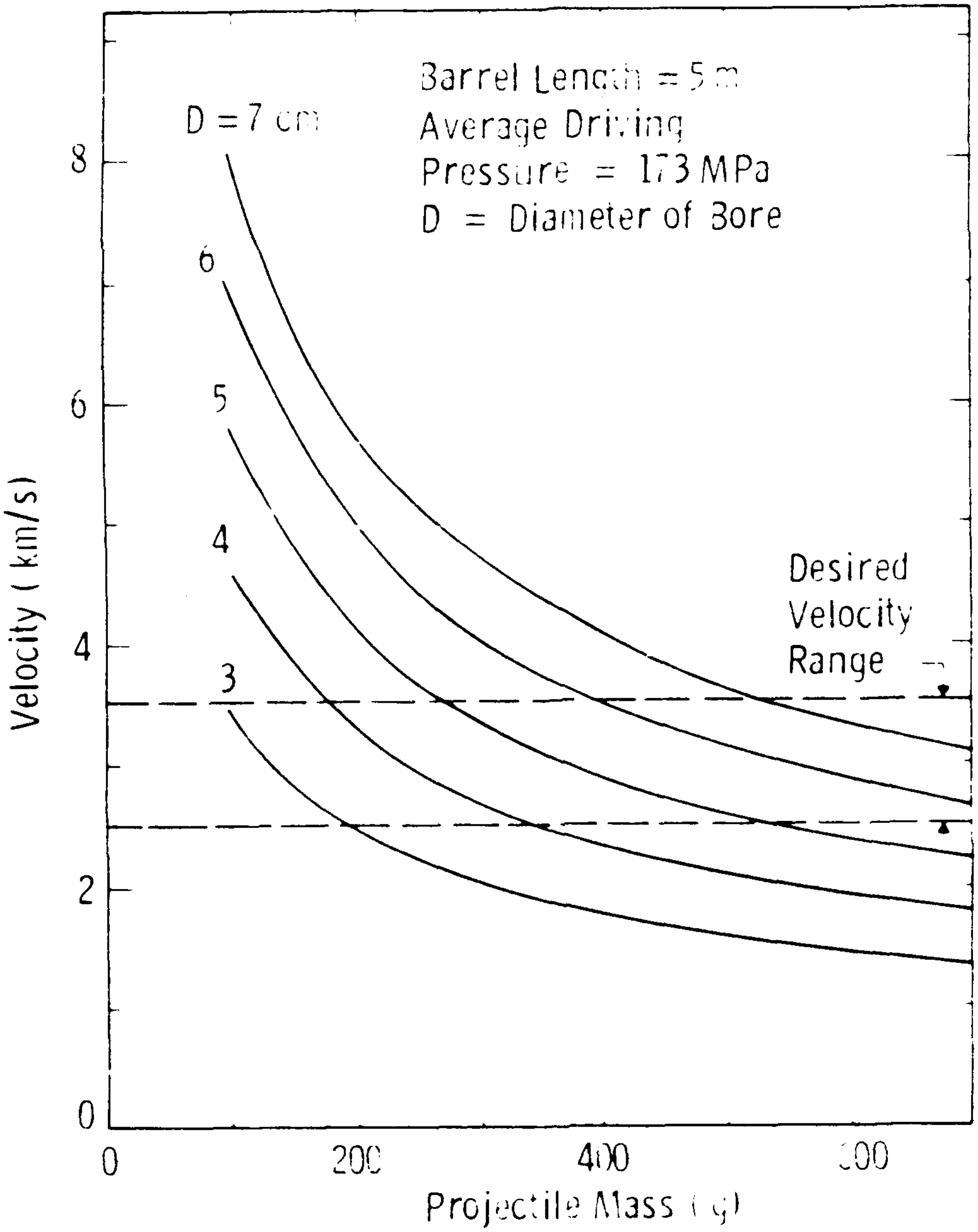

Figure 2. Velocity of projectile at the muzzle as a function of projectile mass. The bore diameter is the parameter.

Electromagnetic guns have an advantage over electrothermal guns in achieving a favorable pressure profile since the electrical power is directly coupled to the projectile and the driving (Lorentz) force can be maintained. In electrothermal guns the electrical power is indirectly coupled to the projectile through a pressurized propellant. As the projectile velocity increases in an electrothermal gun, the driving force decreases rapidly as the projectile tends to pull away from the propellant gas. However, the barrel design of an EML is more complicated than that for an ETL because of the necessity to couple the electrical power directly to the projectile armature. As a result, larger peak pressures are tolerable in ETLs.

Capacitor-driven EMLs have an advantage in that the capacitors can be divided into a number of banks and the input-power can be programmed to optimize the current and pressure profiles.

In principle, any one of the launchers can satisfy the Army's Ballistic Research Lab (BRL) requirements. In Sections 2, 3, and 4, results of detailed analyses, discussions of technical issues and risks, and cost estimates for each of the launcher options are presented. Based on comparative analyses, a recommendation is made in Section 5 of the option which best meets the needs of BRL. It was recommended to BRL that the capacitor-driven EML be selected as the preferred option. This recommendation was made at a presentation by Westinghouse to BRL personnel at the BRL, Aberdeen, MD on Feb. 24, 1989. At a meeting immediately following the presentation it was agreed that the capacitor-driven EML would form the basis for Task 2, and the scope of work for Task 2 was defined.

1.3 TASK 2 DESCRIPTION

Essentially three subtasks have been performed for Task 2:

2.1 System design requirements have been defined that will allow necessary tests for verifying that the components/system are in a condition for reliable operation to be conducted, see Section 6.

2.2 A commissioning plan/test program (Sections 7 and 8) has been defined on the basis that the equipment is fully assembled in the test cell, the system meets the design requirements defined in Subtask 2.1, and all of the components have satisfied the acceptance tests. The commissioning plan/test program addresses all of the technical issues that can be identified that impact on the facility performance, reliability, and cost of operation.

2.3 A schedule and cost estimate have been prepared for conducting the commissioning/test program, see Section 9.

Two goals were established for Subtask 2.2, viz., to define:

- A commissioning plan that will verify the operational capability of the integrated launcher system.

- A test program that will allow the full capability of the facility to be exploited and to result in a reliable, cost effective, high velocity gun.

The elements of the commissioning plan (Section 7) are a) the commissioning of the power supply, b) the commissioning of the preaccelerator, followed by c) the commissioning of the integrated EML system. The commissioning plus maintenance plans are defined so as to avoid ignitron failure, high voltage breakdown, and instrumentation and control failures. All of these technical issues can impact on schedule, cost, and desired performance.

The test program that has been defined (Section 8) and which follows the commissioning of the facility addresses four key issues that are presented below:

Issue 1: Lack of a data base; lack of predictive capability. Solution: Conduct tests with the integrated EML system to a) develop performance tables, i.e., muzzle velocity versus operational parameters such as projectile-package mass, time delays before switching capacitor banks, capacitor voltage, etc., b) develop statistics on failure modes, and c) associate diagnostic measurements, such as rail voltage, with performance.

Issue 2: Need for a standard armature. Solution: Conduct tests with solid, plasma and hybrid armatures. Select one or more standard armatures for all masses of projectile packages that provides reliable performance in the operating parameter range of interest and results in minimum bore damage.

Issue 3: Need for a standard projectile package for the terminal ballistic research application. Solution: Conduct tests to develop a standard projectile package with a four-piece, fly-away sabot that minimizes total mass, provides optimum performance with no tip-off on exit from muzzle, and is adjustable to changing bore diameter.

Issue 4: Deterioration of performance due to bore damage. Solution: Develop criteria for determining when boring of the barrel is required, quick method of bore inspection, and boring techniques for reconditioning the bore of the barrel. This work can be conducted in parallel with the other tests that require operation of the EML.

In addressing issues 2, 3, and 4 engineering design work was conducted in order to develop conceptual designs for the projectile package and the reaming tool.

The commissioning/test program that has been defined will require one year to conduct. At the conclusion of the commissioning/test program, routine operation of the facility should follow where the emphasis will be on terminal ballistic research. By the time this research phase commences, the BRL team will thoroughly understand the operation and maintenance of the gun system.

2.0 DESIGN OF THE CAPACITOR-DRIVEN EML

2.1 SYSTEMS ANALYSIS

2.1.1 Description of PARATRANS Computer Code

The PARATRANS computer code has been used to conduct the analyses of the capacitor-driven EML. PARATRANS is a multi-stage railgun simulation code written in FORTRAN 77 at the Westinghouse STC. It models distributed energy sources as well as independently energized augmenting rails. The current version of PARATRANS includes the following features:

- Provision to model up to 13 stages of current
- Armature modeled as a combination of fixed resistance and fixed voltage drop in series
- Added mass due to ablation (assumed to be proportional to the ohmic heating power dissipated in the armature)
- Computes performance loss due to growth of plasma mass and armature viscous drag forces
- Complete energy balance, including dissipative losses
- Provision for initial velocity (preaccelerated projectile)
- Triggering delay to allow plasma to fully enter a given stage before firing that stage
- Crowbar option for capacitors
- All computations in double precision
- Output available in text and/or graphic format

PARATRANS is based on a lumped parameter model of the railgun circuit shown in Figure 3.

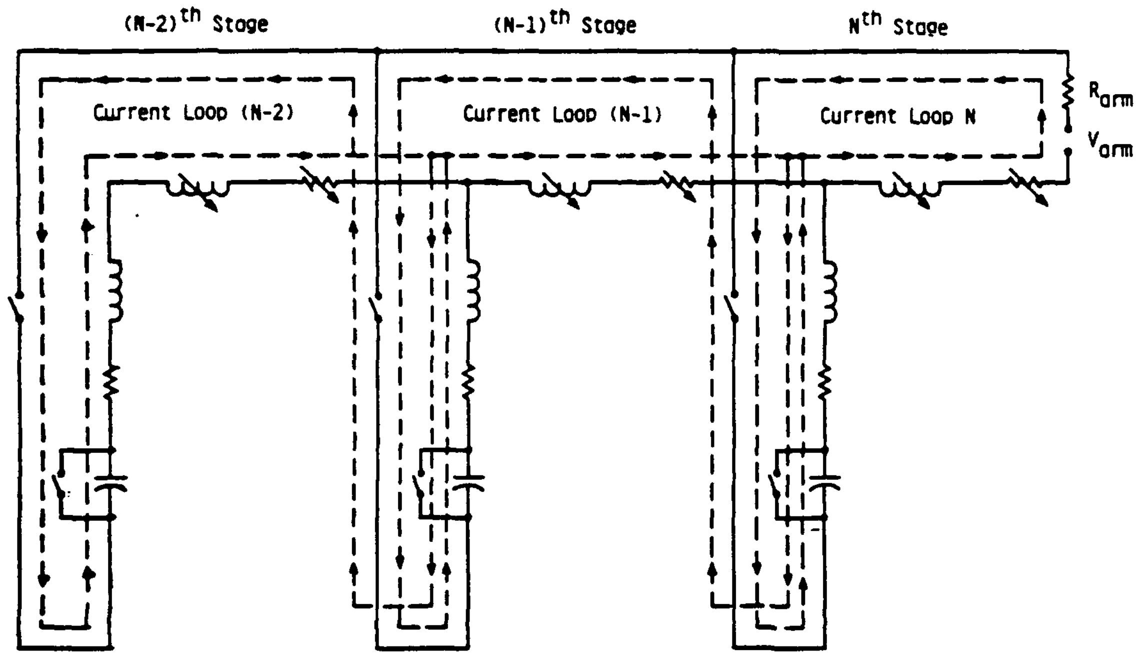

Figure 3. Multi-stage railgun circuit, shown without augmentation.

The governing equations for the circuit are derived by applying Kirchhoff's Second Law to each of the current loops as they are defined in Figure 3. Then, including equations for Joule losses in the rails and bus, one obtains eight first-order Ordinary Differential Equations (ODEs) for each stage of the gun, i.e., we have one ODE for each of the following circuit variables, for each activated stage:

I_{rail} = Current in Firing Rails

I_{bus} = Current in Bus Line

I_{aug} = Current in Augmentation Rails

Q_{rail} = Joule Losses in Firing Rails

Q_{bus} = Joule Losses in Bus Line

Q_{aug} = Joule Losses in Augmentation Rails

V_{cap} = Voltage Across Firing Capacitors

V_{aug} = Voltage Across Augmentation Capacitors

In addition, there are six first-order ODEs which must be written for the Nth stage of the railgun; the Nth stage is the stage in which the projectile is located. These ODEs govern the mass, motion, and joule losses of the projectile and armature. One ODE is written for each of the following variables:

m = Mass of the Payload (Projectile + Armature)

x = Position of the Projectile Along the Barrel Length

v = Velocity of the Projectile

E_{arm} = Energy Dissipated in the Armature

E_{drag} = Energy Dissipated by Frictional Drag

E_{inert} = Energy Dissipated by Inertia Forces

Thus, for an N-stage gun there are a total of (8 * N + 6) first-order ODEs to be solved simultaneously. Because these equations are coupled to each other, a back-substitution algorithm is employed at each time step. The equations are then integrated using a fourth-order Runge-Kutta scheme. Both the back-substitution and Runge-Kutta subroutines have built-in convergence checks. Output of PARATRANS can be presented in both text and graphic format.

The use of PARATRANS has been successful in predicting the performance of EMLs both at the Westinghouse STC and other laboratories. The required coefficients, such as the ablation and frictional drag terms, are well established. The code is well qualified for conducting analyses in the operational regime being considered for this BRL study.

2.1.2 Selection of Parameters for the Launcher

Based on scoping analyses conducted first with a simplified model as described in Section 1 and then with a more detail computer code analysis, a barrel having a length of 5 m and a bore diameter of 5.6 cm has been selected. Although power is only delivered to the rails at the breech, the delivery is staged in order to optimize the current profile and hence the driving-force profile. It has been found that four stages are adequate. The total energy storage required in the four capacitor banks to meet the BRL requirements is 10 MJ. Two engineering constraints were applied in conducting this analysis: 1) the peak driving force per unit area was kept $\lesssim$ 350 MPa, and 2) the current per unit rail height was kept $\lesssim$ 40 kA/mm.

A list of the capacitor-driven EML system parameters is given in Table 2. Note that it has been assumed for all the analyses that the projectiles are preaccelerated to a velocity of 0.5 km/s before entering the breech of the EML.

In conducting the analyses, three types of armatures were considered, viz., solid, transitional, and plasma armatures. The masses of the projectile packages for these three types of armatures are given in Table 3 for high density ($\simeq$ 17 g/cm^3) penetrators of masses 65 g and 200 g. The assumptions which were used in calculating the armature

Table 2

CAPACITOR-DRIVEN EML SYSTEM PARAMETERS

Parameter	Value
Railgun Bore Length	5 m
Bore Diameter	56 mm
Inductance Gradient of Rails	0.4 μH/m
Resistance Gradient of Rails	0.14 mΩ/m
Peak Current per Unit Rail Height	40 kA/mm
Projectile Injection Velocity	500 m/s
Total Capacitor Energy	10 MJ
Number of Capacitor Banks	4
Capacitor Voltage	22 kV
Energy in First Bank	6 MJ
Energy in Each Remaining Bank	1.4 MJ
Circuit Resistance per Bank	1 mΩ

Table 3

PROJECTILE EXAMPLES FOR EML

Solid Al Armature/Hybrid

Penetrator	65 g	200 g
Armature	125 g	125 g
Cup-Rider Sabot	175 g	175 g
TOTALS+	365 g	500 g

Average voltage drop across armature, V ≃ 50 V
Varies from 20 V with mechanical contacts to 80 V with plasma contacts

Transitional Copper Armature

Penetrator	65 g	200 g
Armature	40 g → 46 g*	40 g → 46 g*
Cup-Rider Sabot	175 g	175 g
TOTALS+	280 g → 286 g*	415 g → 421 g*

Average voltage drop across armature, V ≃ 200 V
Varies from 40 V (mechanical contacts) to 100 V (plasma contacts) to 200 V+ (full plasma armature)

Plasma Armature

Penetrator	65 g	200 g
Al Fuse Armature	12 g → 26 g*	12 g → 26 g*
Cup-Rider Sabot	175 g	175 g
TOTALS+	252 g → 266 g*	387 g → 401 g*

Average voltage drop across armature, V ≃ 200 V

---

*Due to ablation
+Must also add mass of air that is accelerated from bore and injector

masses are given in Table 4. Note in Table 3 that during transit down the bore the mass that is accelerated increases for two reasons. For the transitional and plasma armature, material will be ablated from the surface of the bore materials by the high temperature arc and increase the mass of the armature. Also, there is 15 g of air under standard conditions in the bore of the EML. Since the average molecular velocity is $\simeq$ 0.5 km/s, every fast-moving projectile will drive the air in front of it to a high velocity while creating a shock wave (speed of sound $\simeq$ 0.35 km/s). If a light-gas gun is used to preaccelerate a projectile, air in this gun's barrel that lies in front of the projectile would be a third source of additional accelerated mass.

2.1.3 Presentation of Results

Numerous calculations were conducted varying the external circuit inductances and the time delays before injecting currents into the breech from three of the capacitor banks. The first capacitor bank was always assumed to be fired when the projectile armature had moved 20 cm down the bore from the breech. Table 5 shows the sets of parameters obtained for yielding optimum current profiles; the parameters for the four capacitor bank stages are given in Table 6.

For the parameters chosen, Figure 4 shows the current profile that is obtained when accelerating the 500-g projectile package with the solid armature. The current rises abruptly (0.37 ms) to 2 MA. The armature has reached a distance of 0.45 m down the bore at this time. The current is maintained in a range of 1.9 MA $\pm$ 10% for 1.5 ms (during which time the projectile has moved to a distance of 3.2 m down the bore) before the current decreases and reaches a value of 1 MA as the projectile leaves the muzzle.

Figure 5 shows the current flow in the four different phased circuits during the acceleration of the projectile. None of the currents is driven negative.

The pressure driving the projectile which results from the current flow is shown in Section 5, Figure 56. The peak driving

Table 4

ASSUMPTIONS ON WHICH THE ARMATURE MASSES WERE BASED

- Solid/Hybrid Armature

  Armature reaches the melting point due to Joule heating as it exits the muzzle. Mechanical contacts with rails transition to plasma contacts.

- Transitional Armature

  Transit time down the bore equals twice the time interval required to vaporize the armature. For a significant portion of the transit time, the armature is in a molten state as it vaporizes. Characterized by lower plasma temperature and less bore damage.

- Plasma Armature

  Solid fuse vaporizes and forms plasma arc near the breech. A plasma armature drives the projectile for essentially the entire trip down the bore.

Table 5

RESULTING INDUCTANCES, TIME DELAYS, AND DISTANCE DOWN BORE AT CURRENT INJECTION FROM SYSTEMS CALCULATIONS+

Armature Type	Phase No.	Circuit Inductance (μH)	Time Delay (ms)	Distance Down Bore (m)
Solid (Al) (200-g Penetrator)	1	2.25	0	0.2
	2	4.5	0.616	0.7
	3	3.0	1.04	1.4
	4	1.8	1.41	2.2
Transitional (65-g Penetrator)	1	2.25	0	0.2
	2	4.5	0.533	0.7
	3	3.0	0.88	1.4
	4	1.8	1.19	2.3
Plasma (65-g Penetrator)	1	2.25	0	0.2
	2	4.5	0.525	0.7
	3	3.0	0.856	1.4
	4	1.8	1.16	2.3

+The projectiles are injected into the breech of the EML at 500 m/s by a light-gas gun

Table 6

PARAMETERS FOR STAGED CAPACITOR BANKS

Total Stored Energy of All Banks, E (MJ)	10
Phased Energy Injection, E_i (MJ)	6.00, 1.40, 1.40, 1.40
Capacitances of Phased Sources, C_i (mF)	24.79, 5.78, 5.78, 5.78
Number of Capacitors* in Phased Sources, N_i	120, 28, 28, 28
Capacitor Voltage, V (kV)	22

*Based on Maxwell Laboratories, Inc., Capacitor No. 32349, 206 μF, 50 kJ at 22 kV.

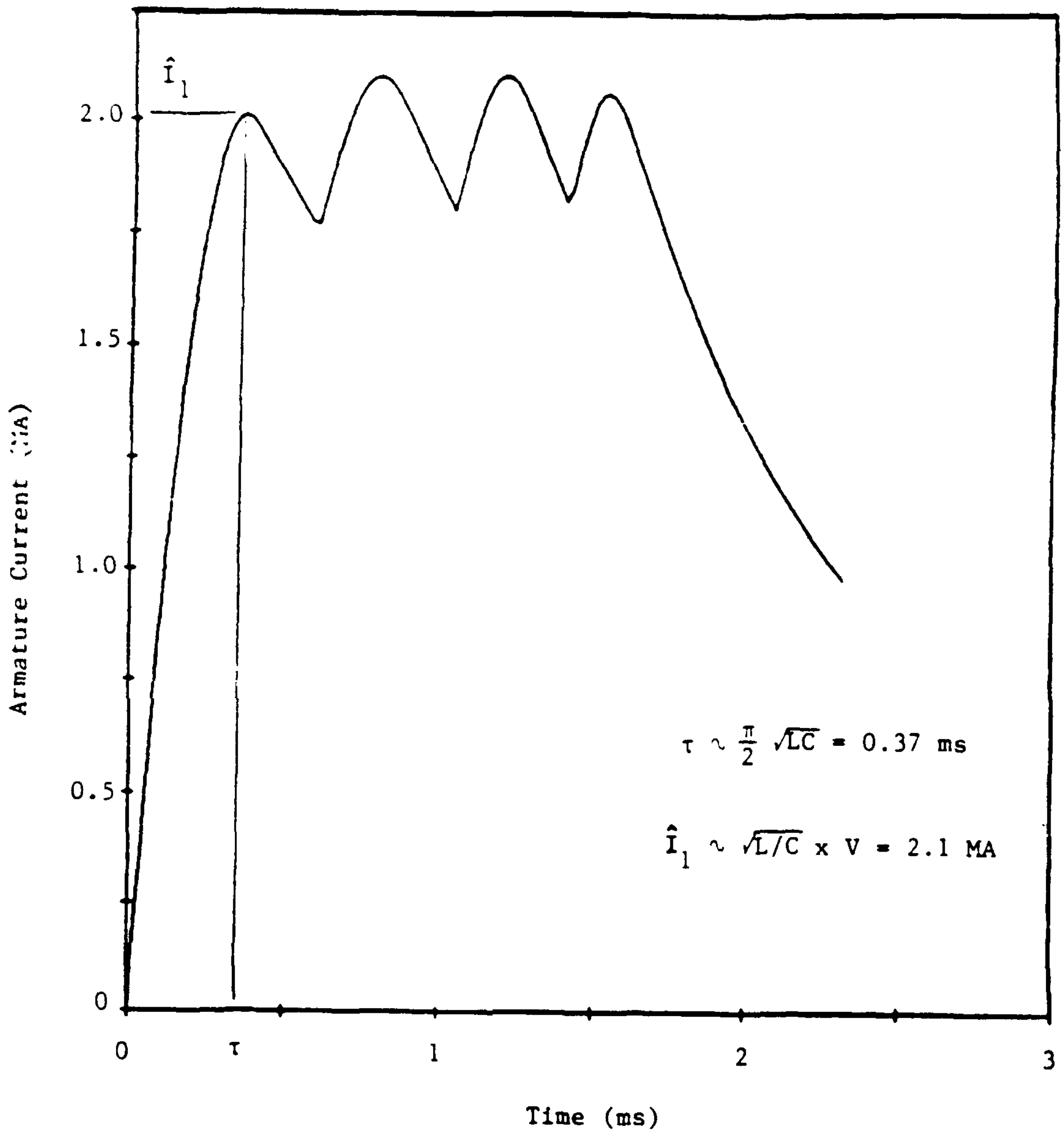

Figure 4. Current profile for solid armature (Al) and a projectile mass of 500 g.

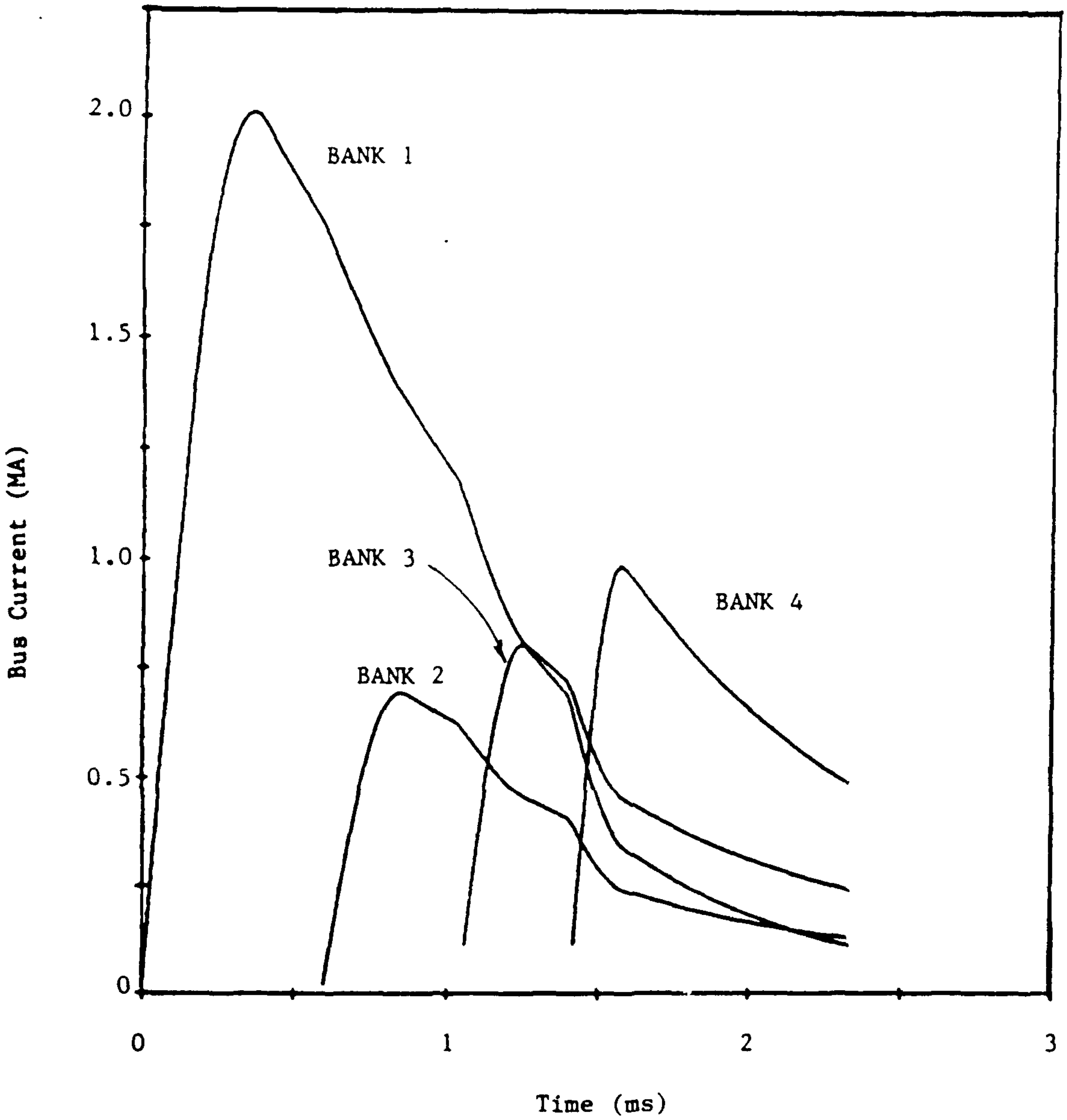

Figure 5. Composition of current profile for solid armature. Projectile mass = 500 g.

pressure is 353 MPa whereas the pressure as the projectile exits the muzzle is only 70 MPa. The average pressure as the projectile moves down the bore is 220 MPa which gives a piezometric ratio of $\hat{P}/\bar{P} = 1.60$.

Figure 6 demonstrates that the armature current profile, as a function of distance down the bore, does not vary appreciably for the different projectile packages under consideration. This means that the average driving pressure is approximately the same for the different projectiles and therefore the kinetic energies of the projectiles as they exit the muzzle should be approximately the same (see Section 1.2). (Of course, the transit time of the projectile down the bore is shorter for the less massive projectiles, see Figure 7.)

Figure 8 shows that indeed for each position down the bore a projectile has a given kinetic energy independent of its mass for the projectiles that have been considered. The kinetic energy of a projectile package at the muzzle is 2.8 MJ. This means that 28% of the 10 MJ of energy expended is converted to kinetic energy. Of course, the kinetic energy of the penetrator is only a fraction of this total kinetic energy, viz., 1.1 MJ for the 200-g penetrator and 0.63 MJ for the 65-g penetrator.

The 500-g projectile is accelerated to a velocity of 3.3 km/s, see Figure 9, and the 280-g projectile is accelerated to 4.4 km/s. Note from Figure 9 that the projectile is moving with a velocity of 500 m/s when the first capacitor bank is fired and that the projectile accelerates uniformly for 2.3 ms to 3.3 km/s. The acceleration does decrease for the last $\simeq$ 0.3 ms as the current decreases significantly.

Some of the important quantities which were obtained from calculations of launches which used different types of armatures are summarized and compared in Table 7. The energy distributions for the same cases are shown in Table 8. About half the available 10 MJ is expended as Joule heating in the rails and phased circuits. Roughly 20% is dissipated in the armature and muzzle arc and the remainder appears as kinetic energy of the projectile package. In addition to the 10 MJ stored in the capacitor banks, energy is also introduced into the system by preaccelerating the projectile to 500 m/s. However, this kinetic

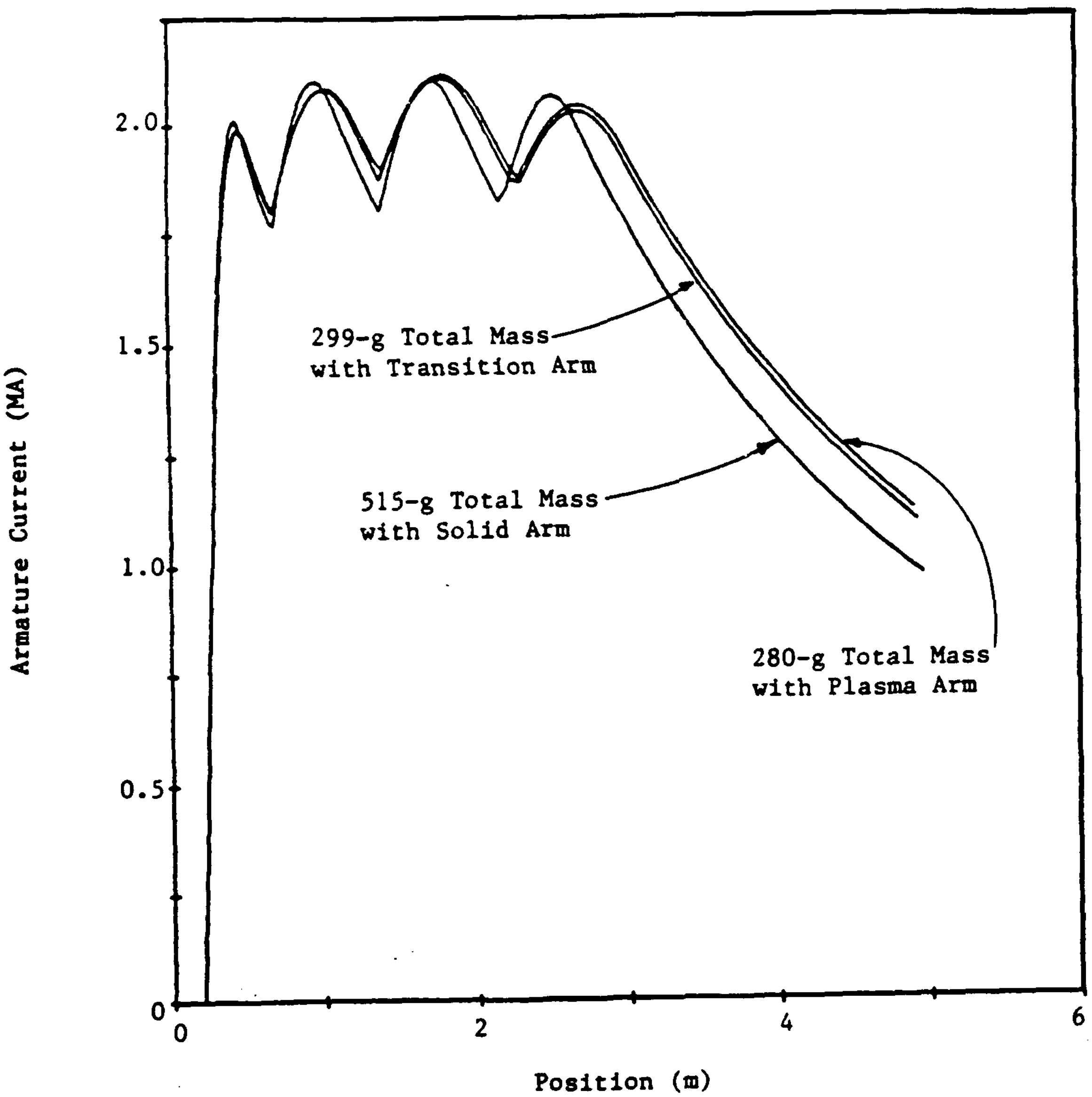

Figure 8. Comparison of current profiles for capacitor-driven EML options.

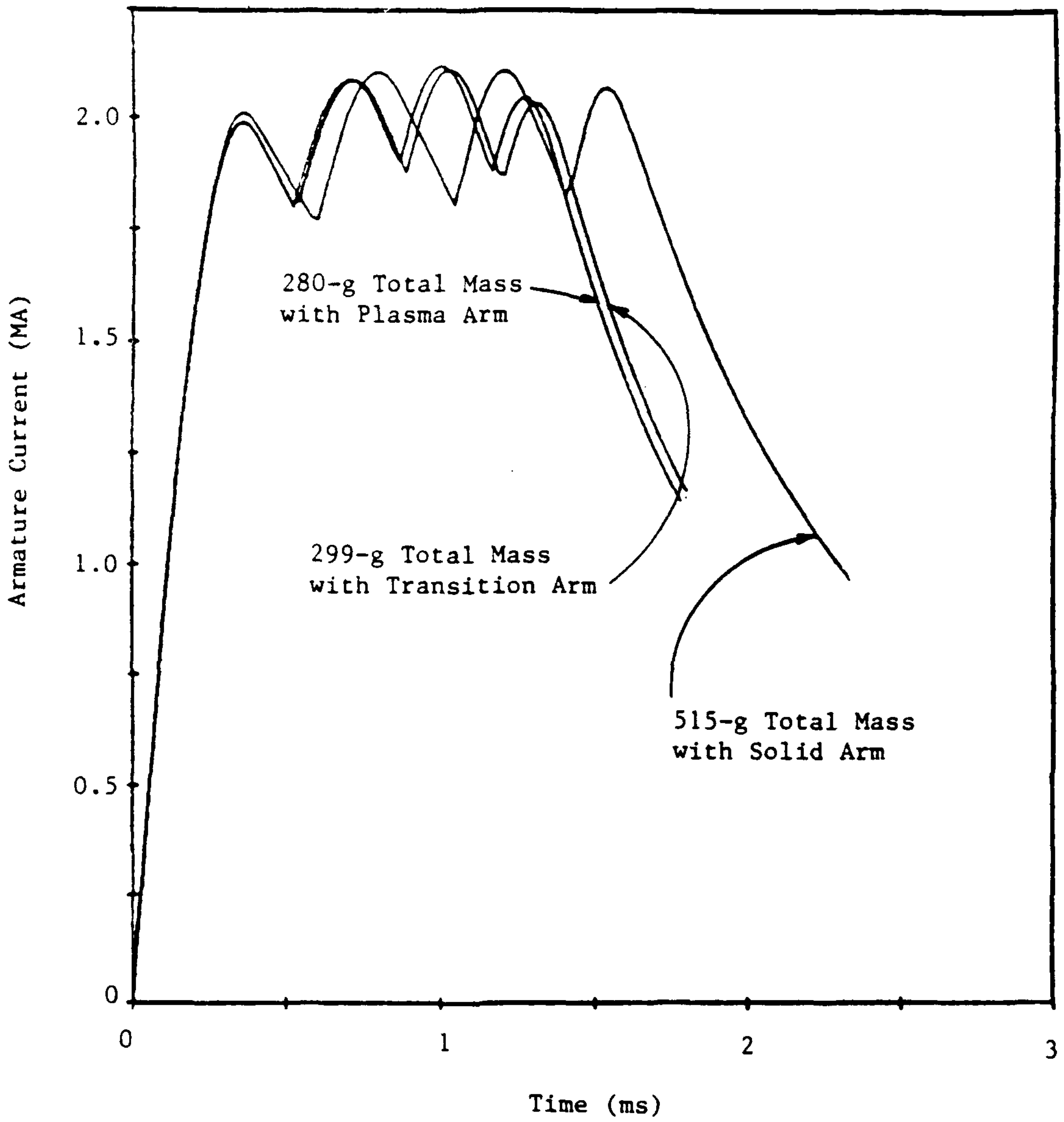

Figure 7. <u>Comparison of current temporal profiles for capacitor-driven EML options; armature current as a function of time.</u>

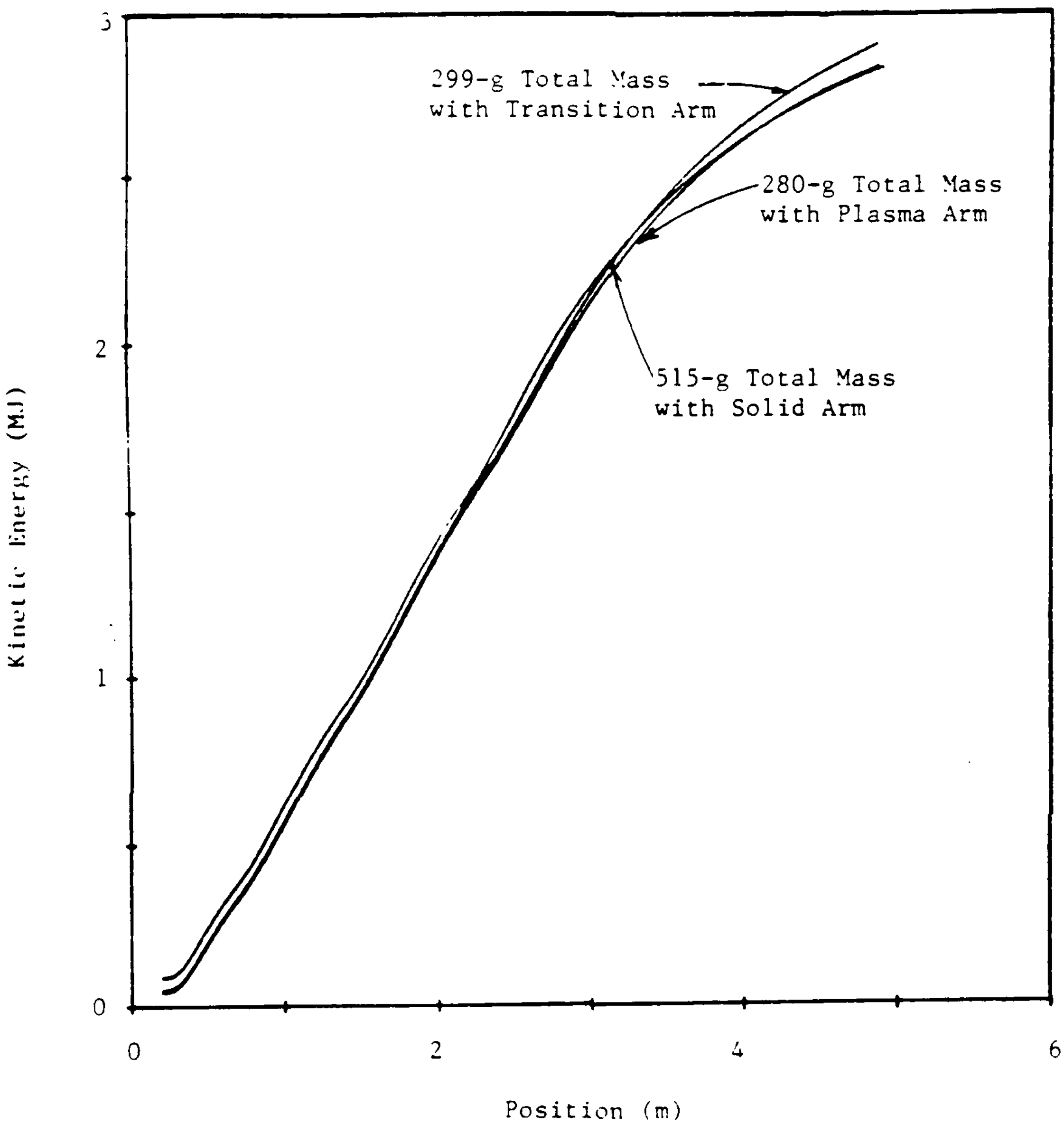

Figure 8. Projectile kinetic energy as a function of distance down the barrel.

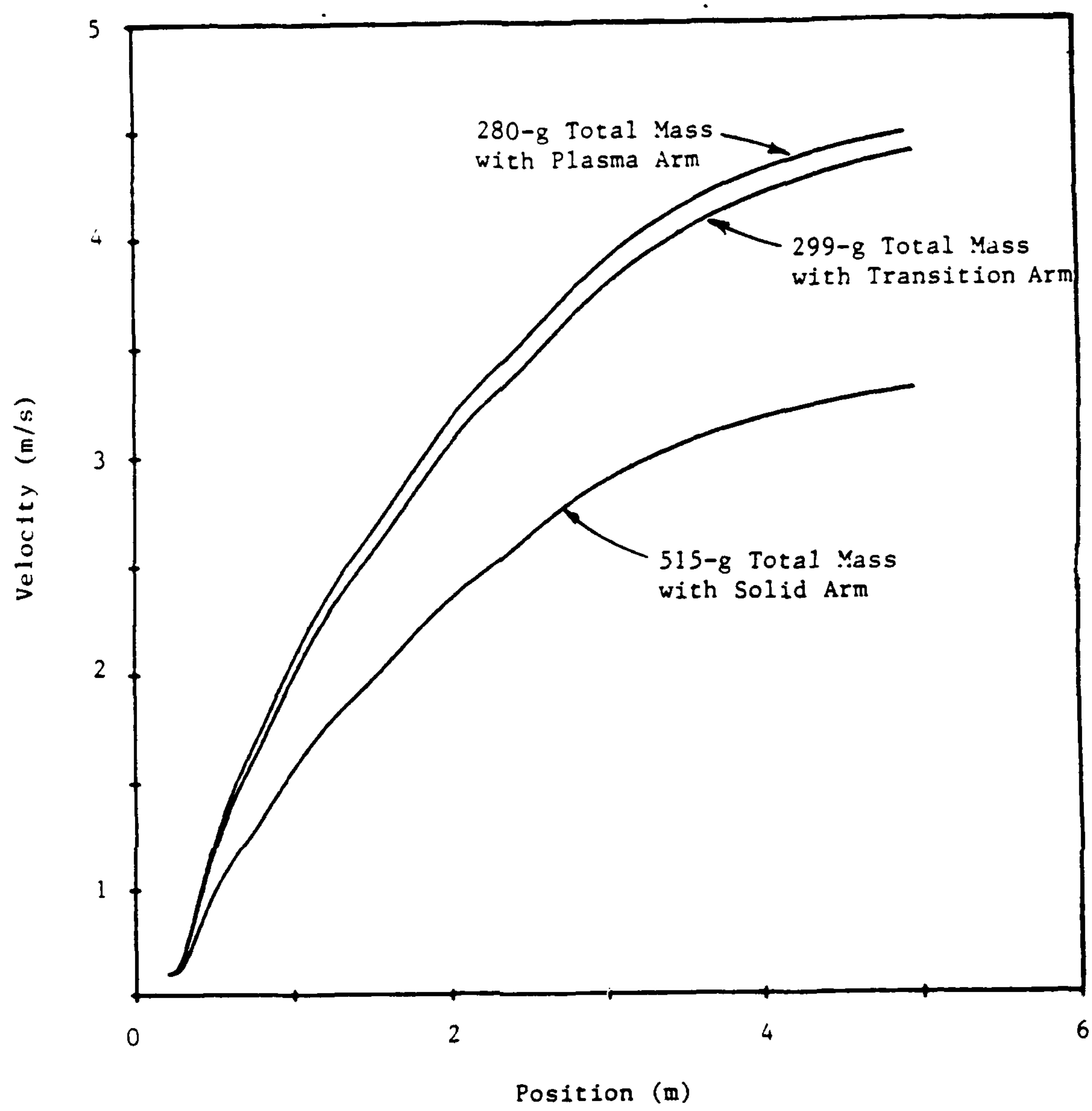

Figure 9. Variation in projectile velocity as a function of time during acceleration for various armature options.

Table 7

COMPARISON OF RESULTS FOR CAPACITOR-DRIVEN EML SYSTEM

	Armature Type		
	Solid	Transitional	Plasma
Mass of Penetrator, g	200	65	65
Total Projectile Mass at Muzzle, g	515	299	280
Muzzle Velocity, km/s	3.3	4.4	4.4
Projectile Kinetic Energy, MJ	2.8	2.9	2.8
Penetrator Kinetic Energy, MJ	1.1	0.63	0.63
Current Rise Time, ms	0.36	0.36	0.36
Peak Armature Current, MA	2.1	2.1	2.1
Peak Driving Pressure, MPa	350	340	335
Current as Armature Exits, MA	0.96	1.1	1.1
Pressure as Armature Exits, MPa	69	78	62
Current During "Flat-Top" Portion of Current Profile, MA	1.9 ± 10%	1.95 ± 8%	2.0 ± 10%
Time Interval of "Flat-Top" Portion of Current Profile, ms	1.5	1.25	1.2
Total Width of Current Pulse, ms	2.3	1.9	1.8

Table 8

COMPARISON OF ENERGY DISTRIBUTIONS
FOR CAPACITOR-DRIVEN EML SYSTEMS

	Armature Type		
	Solid	Transitional	Plasma
Projectile Mass at Muzzle, g	515	299	280
	MJ	MJ	MJ
Kinetic Energy of Projectile	2.83	2.91	2.84
Joule Heating:			
Rails	1.73	1.52	1.43
Phase 1 Circuit	2.89	2.49	2.44
Phase 2 Circuit	0.28	0.21	0.20
Phase 3 Circuit	0.30	0.23	0.23
Phase 4 Circuit	0.48	0.37	0.36
Muzzle Arc	1.38	1.60	1.66
Dissipation in Armature	0.20	0.67	0.84
TOTALS	10.	10.	10.

energy is less than 1% of the 10-MJ electrical energy which is input to the system.

Figure 10 summarizes the results of a number of calculations conducted with the PARATRANS code. The muzzle velocity is shown for each curve to vary inversely with the square root of the projectile mass. If the muzzle velocity were plotted as a function of the total projectile mass at the muzzle, the two curves in Figure 10 would lie closer together since the mass of the plasma armature increases during the acceleration process.

2.1.4 Optimization of Barrel Dimensions

As discussed earlier, by means of analytical and computer analyses, a 5-m barrel with a 5.6-cm diameter bore has been selected for the purpose of meeting the requirements set by the Army Ballistic Research Laboratory. Reasons for selecting these particular dimensions have been obtained from the analyses and are presented below:

- in order to accelerate a 200-g penetrator to > 3 km/s, the total mass that must be accelerated will be ≃ 500 g including the sabot and armature
- a 5-m long barrel with a bore having a cross sectional area of 25 cm^2 can accelerate a 500-g mass to a velocity > 3 km/s while meeting the engineering constraints, viz., $I < 40$ kA/mm, $P < 350$ MPa
- this barrel design effectively couples with a total capacitive energy storage of 10 MJ; optimum current (and pressure) profiles result
- increasing the length of the barrel while keeping everything else fixed does not result in a significant increase in the projectile velocity; the piezometric ratio, $\hat{P}/\bar{P}$, increases
- higher velocities could be achieved with a longer barrel if a larger energy source were also employed
- reducing the bore cross sectional area while keeping the barrel length and driving pressure constant will result in a smaller projectile velocity since the accelerated mass will not decrease proportionally

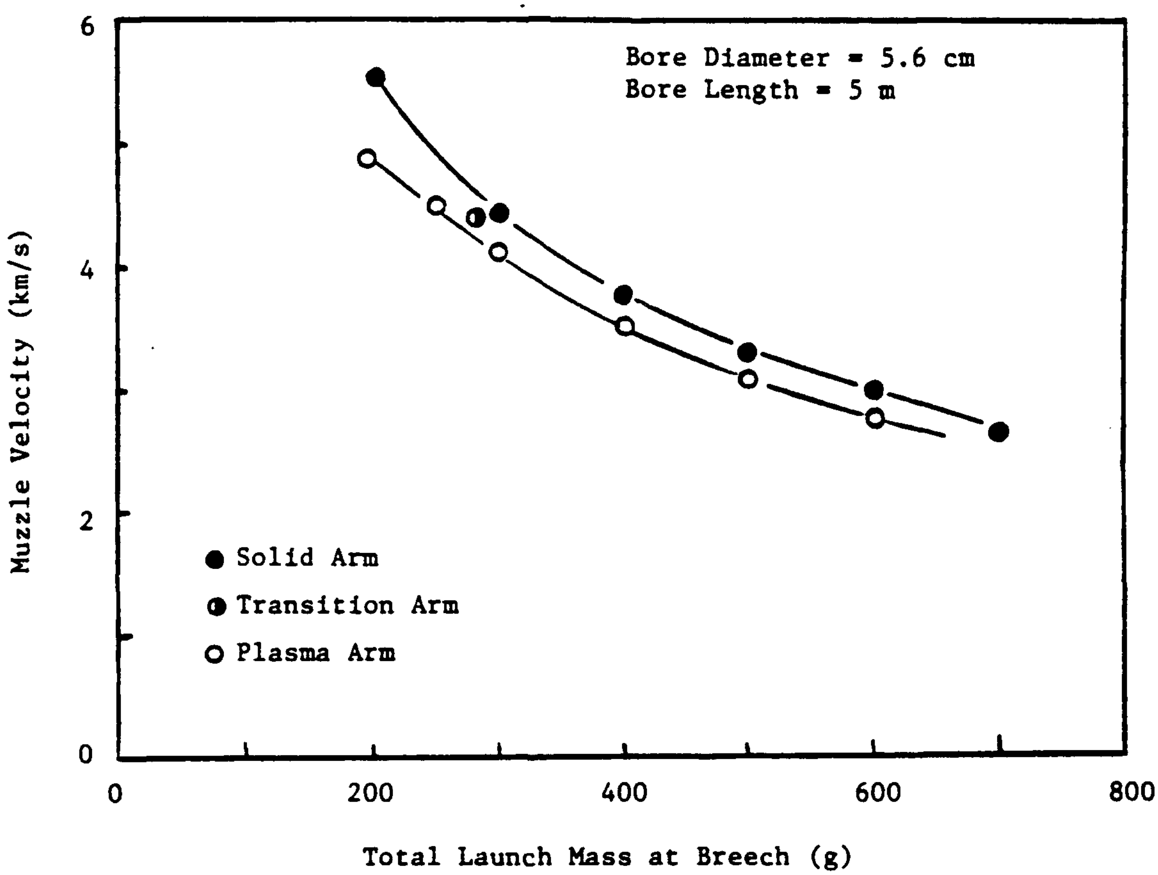

Figure 10. Muzzle velocity vs initial projectile mass.

- increasing the bore cross sectional area while keeping the barrel length and driving pressure constant will result in higher velocities, but additional energy is required and the process is less efficient, i.e., more energy is expended accelerating more massive sabots and armatures (furthermore, higher velocities are not required)
- reducing the bore cross sectional area and increasing the barrel length could result in the same final velocity, but a more complex (rail joints), less maintainable design results

2.2 DESIGN OF COMPONENTS

The modeling for the capacitor-driven EML systems has been completed and performance predictions have been made. The parameters selected for the various options are discussed in Section 2.1. For a complete range of armature and penetrator masses, a single point design has been identified for the railgun and power supply systems which would provide muzzle velocities in the range from 3 km/s to 4.5 km/s. The key system parameters are given in Table 9. The corresponding total starting launch payload masses (including armature, sabot, and penetrator) are in the range from 500 g to 250 g, respectively. The main performance parameters for this system are given in Table 10. In the following subsections, the conceptual design for the railgun, the power supply, and the I&C/DAS systems are provided.

2.2.1 Railgun System

The railgun system consists of a light-gas gun injector, the main railgun barrel, and associated breech and muzzle sections. The point design is based on specific features developed from a combination of design activities on this study as well as on a wealth of design activities on previous projects where considerable detailed engineering occurred. The selection of specifics, e.g., a round bore instead of a square bore, is somewhat arbitrary and will require further attention as the design evolves and as both cost and technical issues become more clearly defined. The following is a description of the components making up the railgun system.

Table 9

CAPACITOR-BASED EML FOR LETHALITY TESTING

Subsystems	Parameter Values
Railgun	
Barrel Length	5 m
Bore Diameter	56 mm
Rail Current	2 MA
Power Supply	
Total Cap. Energy	10 MJ
Number of Banks	4
Max. Operating Voltage	22 kV
Injector (Gas Gun)	
Injector Length	1.0 m
Injection Velocity	500 m/s
System Performance	
Velocity Range	3.3-4.4 km/s
Final Total Kinetic Energy	2.8 MJ

Table 10

PERFORMANCE FEATURES OF
CAPACITOR-BASED EML SYSTEM

- I = 40 kA/mm
- P_{ACCEL} = 350 MPa (50 ksi) maximum
- ΔT_{RAIL} < 900K (maximum rail surface temperature rise)
- Time at Peak Current = 1.25 ms - 1.5 ms
- Several Armature Options
  - For 250-g Projectiles
    v_{MUZ} = 4.4 km/s
    E_{PENE} = 0.63 MJ
  - For 500-g Projectiles
    v_{MUZ} = 3.3 km/s
    E_{PENE} = 1.1 MJ

Light-Gas Gun Injector

The main features of the injector that is able to accelerate masses from 200 g to 500 g to 500 m/s are given in Table 11. The reference gas is helium and the bore has a 56-mm round cross section which is the same as that for the railgun barrel. The operating pressure of 52 MPa (7500 psi) was selected to provide an overall design geometry consistent with the gun barrel to provide a total length of less than 7 m (for barrel, injector, fast valve, and pressure reservoir). This operating pressure does not represent a difficult design criterion, except possibly for the fast valve used to release the pressure and start the launch. Current technology is available for valves operating up to 52 MPa. The basic design is similar to that for the SUVAC II* injector, see Figure 11, which has been successfully operated for hundreds of tests.

Railgun Barrel

The barrel on the capacitor-driven EML has a 56-mm round bore and is 5-m long with the following features:

- bolted construction
- copper rails
- G-9 insulators

For the EMLs, we have chosen a circular bore (consistent with the ETL) rather than a square bore. However, both bore shapes are viable options. The square bore has the following advantages:

- easier to manufacture/machine
- easier to assemble and meet tolerances
- easier to clad the rails
- the projectile, particularly the armature, orientation is maintained
- it is less costly

---

* SUVAC II is a capacitor-driven EML located at the Westinghouse STC. It has a 5.6 MJ distributed energy source. The bore is 2 cm in diameter, and 10 barrel segments, each 2 meters in length are available.

Table 11

LIGHT-GAS GUN INJECTOR PARAMETERS

Parameter	Value
Injector Length	1.0 m
Injector Diameter	56 mm
Maximum Gas Pressure	69 MPa
Volume of Pressure Reservoir	12 ℓ
Diameter of a Spherical Reservoir	30 cm
Mass Range to be Accelerated	200-700 g
Nominal Velocity at Railgun	500 m/s

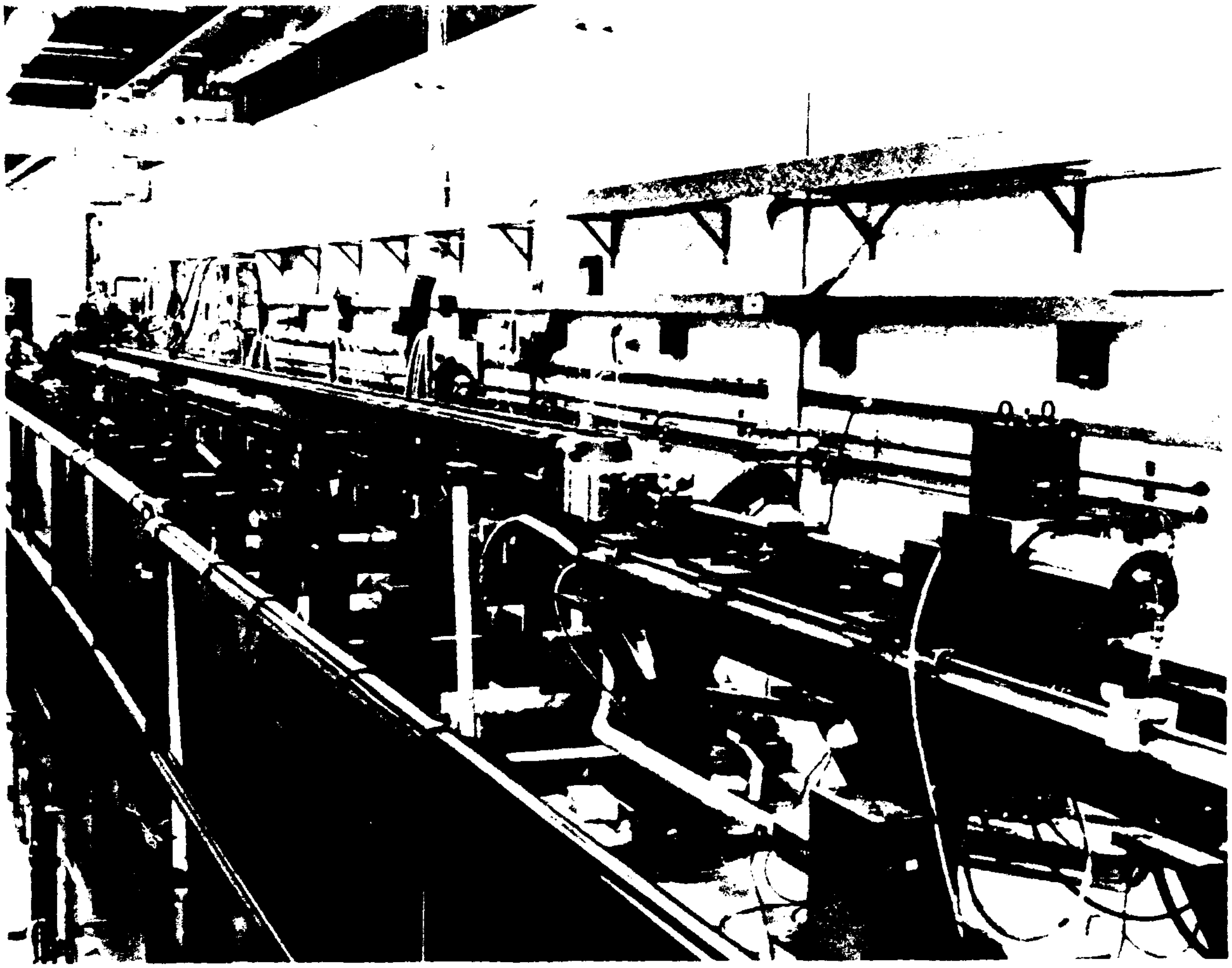

Figure 11. SUVAC II injector

The circular bore has an advantage in that it is easier to maintain better bore/projectile seals (no corners), but the overriding advantage is the ability to ream the bore. Being able to ream the bore alleviates the difficulty of meeting tolerances in the fabrication of circular bore barrels. More importantly, maintenance of the bore becomes much easier. After a number of shots the bore can be reconditioned by a honing machining procedure. It is expected that ~ 50 shots can be fired before the bore will have to be rebuilt due to ablation, pitting, and gouging of the rails and insulation. Since the bore will be reamed, cladding will not be used in general on the surfaces of the bore materials. For special tests, cladding would be used to enhance performance. Although it is not a significant consideration, the circular bore is compatible with conventional projectiles.

The assembly is a bolted pre-stressed configuration made up with a continuous set of rails such that there are no rail-to-rail joints. The containment provides a high bore stiffness and good plasma sealing with locking bore components, see Figure 12. The basic features of the design are consistent with a manufacturable, reliable, and maintainable assembly. There are no technical limitations associated with providing the 5-m feature. Bare copper rails can be obtained in lengths of 5 meters. However, the maximum insulator length that can be fabricated is 3 m; joints in the insulator should not be a problem. Joints would also be required for cladded rails, e.g., cladding by the HIP (hot isostatic press) process can only be done for rail lengths $\lesssim$ 3 m.

The inner bore elements include a pair of 90° arc segments of rails separated by 90° arc segments of insulators. The rails are not actively cooled since the testing will occur on a single shot basis. The insulator materials are made from a manufacturable structure with good mechanical properties, a high dielectric strength for many shots, and ablation characteristics favorable to the operation of the gun. Candidate materials for the bore elements are copper (e.g., GLID COP, AL-60) and G-9 (i.e., a glass, melamine formaldehyde composite). Depending on actual operating conditions, these candidate materials may not provide adequate protection against performance limitations due to secondary arcs, unfavorable ablation, etc. In such situations, the

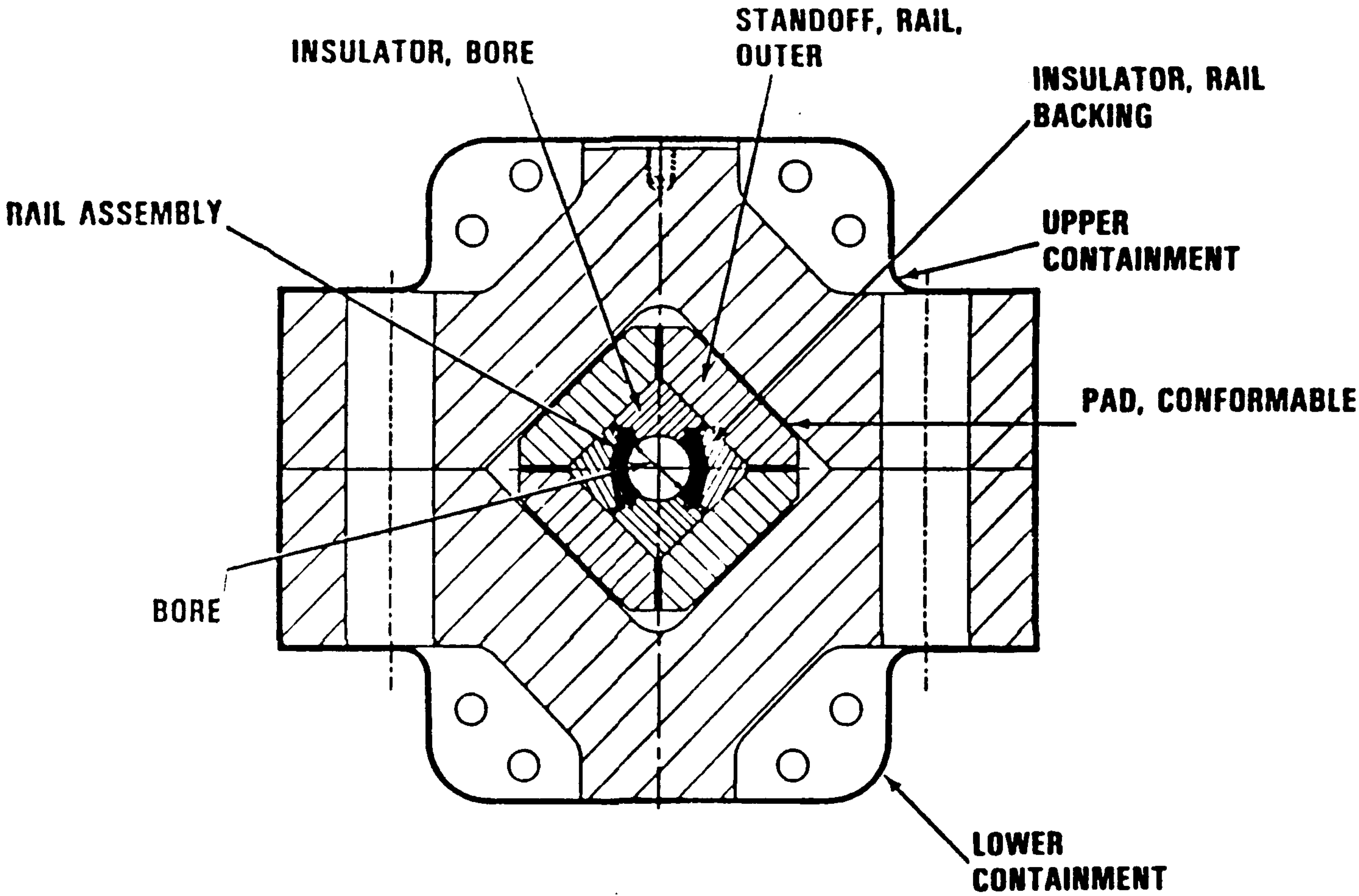

Figure 12. Cross section of railgun barrel.

barrel design may require changes in the form of a cladding on the rails and/or a sleeve on the insulators. For example, Mo-clad rails and an epoxy/alumina sleeve in the G-9 insulators are under current study in SUVAC II (see the footnote on page 35). For the main barrel parameters see Table 12.

Muzzle and Breech

The barrel muzzle has a massive arc horn to allow the rail current in the barrel following projectile exit to dissipate with a minimum of damage to the muzzle end of the rails. To localize the current path, it may be necessary to design the arc horn with graphite rods assembled with short gaps. With this arrangement, the current (or most of the current) crosses in the gap causing most of the damage to occur in the rods which can be replaced. See Figure 13 for such a design.

The barrel breech interfaces with the injector and the busbars carrying the current from the power supply. Because the launch package is preaccelerated, the damage at the breech should be minimal and comparable to that for the remainder of the barrel surfaces. To provide for the electrical isolation of the injector, the connection to the breech is via an assembly constructed of insulator materials. The current feeds into the rails consist of a single pair of busbars which fan out to provide connections to each of the individual LRC circuits. Due to the large forces associated with the current feeds, the structural design of the breech section requires special attention so that current continuity throughout the launch period is maintained without any potential for external electrical breakdown between busbar sections.

2.2.2 The Capacitor Bank Energy Source

The approach to the design development of this power supply is guided by the perception that the customer wants to obtain a reliable tool in the conduct of his investigations, and that he does not want a power supply which itself is in a developmental stage. Wherever

Table 12

RAILGUN BARREL PARAMETERS

Parameter	Value
Barrel Length	5 m
Bore Diameter	56 mm
Volume of Bore	12.3 ℓ
Mass of Air Filling Bore (STP)	15 g
Rail Angle	90°
Rail Height	5 cm
Rail Thickness	1.3 cm
Total Mass of Copper Rail Pair	58 kg
Inductance Gradient	0.4 μH/m
Resistance Gradient	0.14 mΩ/m
Current/Rail Height	40 kA/mm
Peak Accelerating Pressure	345 MPa
Peak Heat Flux to Rails	100-200 kW/cm^2
Peak Rail Surface Temperature Rise	500-900K
Projectile Injection Velocity	500 m/s
Projectile Position at Start of Current	0.2 m

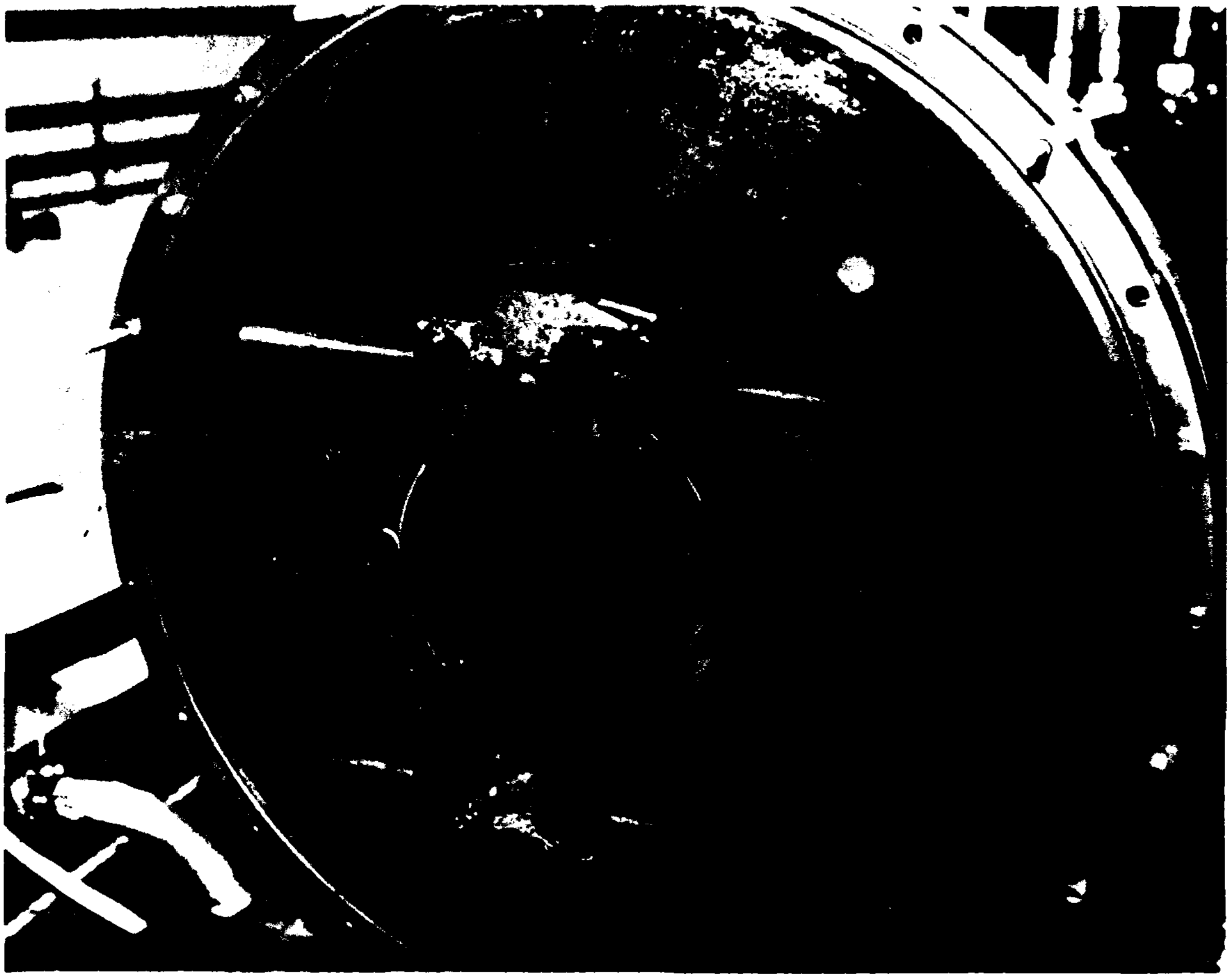

Figure 13. Arc horn at muzzle for a Westinghouse STC railgun.

possible components were selected that are off-the-shelf, of proven reliability, are readily maintainable, and can be obtained at a reasonable cost. Specifically, this led to the use of ignitrons for switching, rather than solid state thyristors and diodes or rotating arc spark gaps. The key design features for the power supply are given in Table 13.

The capacitor bank energy source consists of the capacitor banks, the charging system, the switching system, the pulse-forming inductors, and the cabling between components. The point design is based on the same system providing the current requirements for the full range of operating assumptions. The 10 MJ of stored energy is supplied by a set of four parallel LRC circuits. All the associated currents are breech-fed with time delays between bank discharges in order to tailor the rail current as a function of both time and armature position. Each LRC circuit is crowbarred for maximum energy transfer as well as to avoid reversal of currents in the circuits.

The design of the energy source is based on providing a rail current with the following characteristics:

- rapid rise in current during the start of the launch
- an extended peak current level at a relatively constant value over most of the launch period
- a reduced current at the time of mass exit to minimize forces on the launch package at the muzzle

With this current profile, the efficiency of the system is high. The maximum acceleration is extended over most of the launch, and as a result the peak acceleration and bore pressure are reduced from that associated with a single pulse of current. The pulse-forming inductors and the time delays between discharging the banks were selected to minimize the magnitude of the dI/dt ripple and its duration over the period of peak current. A sample current profile is shown in Figure 14.

Table 13

DESIGN FEATURES OF THE POWER SUPPLY FOR THE CAPACITOR-BASED EML SYSTEM

50-kJ Capacitor Units (cans)
4- and 8-Can Subassemblies
Ignitron Switching
Simple Pulse-Shaping Inductors
Breech-Fed Tailored Currents
Minimum Peak Currents
Reliable and Maintainable
Cost Effective

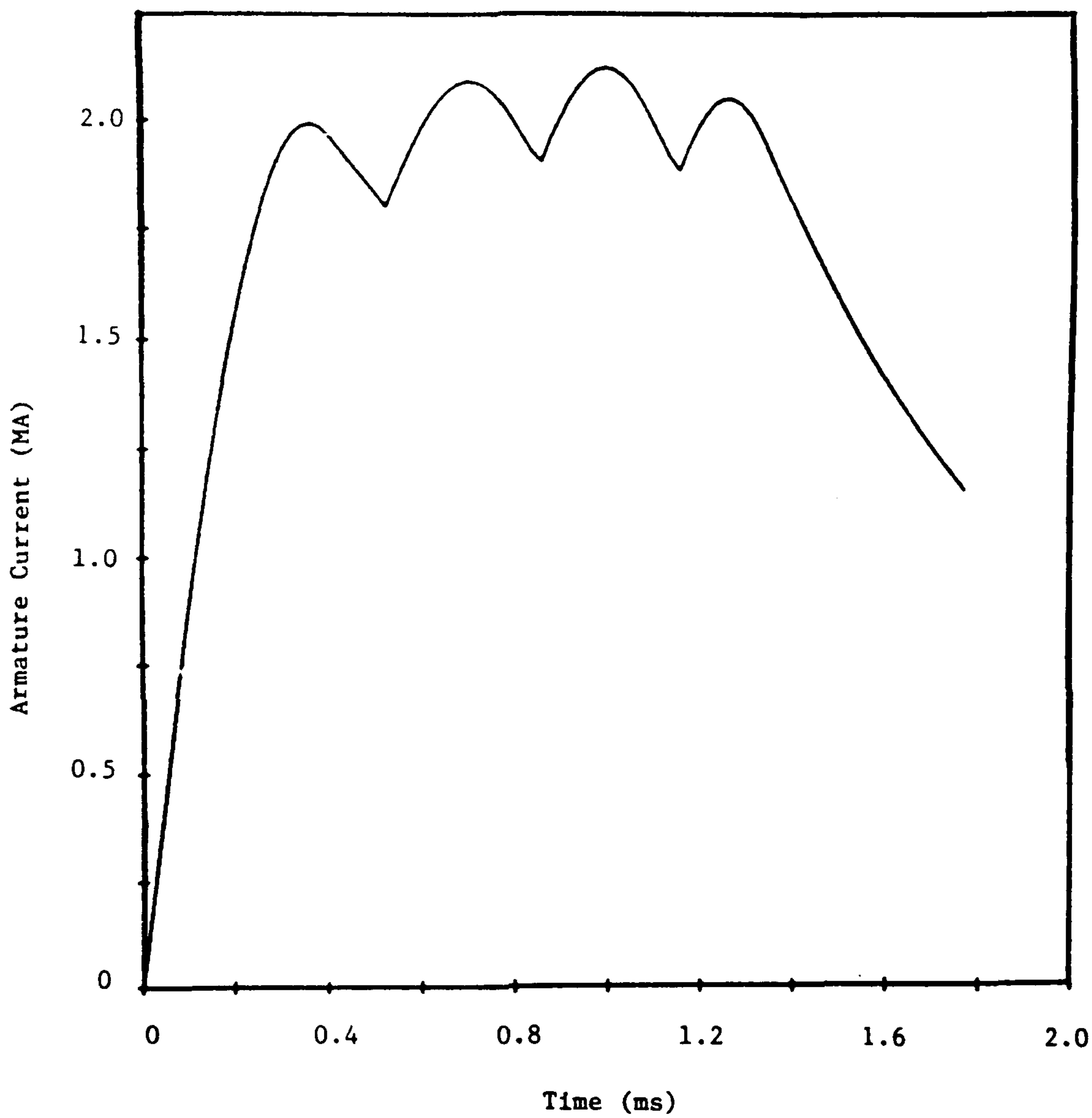

Figure 14. Typical rail current vs time profile for capacitor-driven EML.

Operating Circuit

A schematic of the electrical circuit made up of the railgun and the elements external to the barrel is shown in Figure 15. The circuit parameters are given in the schematic as well as in Table 14. The distribution of capacitors and the values for the various inductors were determined based on the three design characteristics given above. The values for the railgun electrical characteristics are consistent with values obtained in previous design activities involving detailed engineering and analyses. The circuit resistance of 1 mΩ in each bank circuit is a nominal value and consistent with previous design analyses. By varying the time delays in firing of Banks 2, 3, and 4, relative to Bank 1, this circuit will provide a good rail current for all launch packages of interest.

Capacitor Bank

The basic unit making up the capacitor bank has characteristics given in Table 15 and is shown in Figure 16. There are a total of 204 units or cans providing a total capacitance of 0.042 F and when charged to 22 kV, a total stored energy of 10 MJ is provided. Except for the first bank, the banks are configured in a modular arrangement with the same number of units per bank. The resulting distribution of energy is 6 MJ in Bank 1 (at 22 kV) and 1.4 MJ in the remaining banks. The corresponding number of capacitor cans is 120 and 28, respectively. The individual cans are arranged in a subassembly; four cans per subassembly and seven subassemblies make up a 1.4-MJ bank. For the first bank, a subassembly of eight cans, total, arranged with 15 subassemblies make up the 6-MJ bank. An individual can has the characteristics given in Table 16.

Charging System

The charging circuit for all four banks consists of a single power supply that will energize the capacitors to 10 MJ in one to two minutes. The charger is rated at 22 kV and 10 A. The supply is connected through relays and charging and dump resistors to each bank. The basic circuit is shown in the schematic in Figure 17.

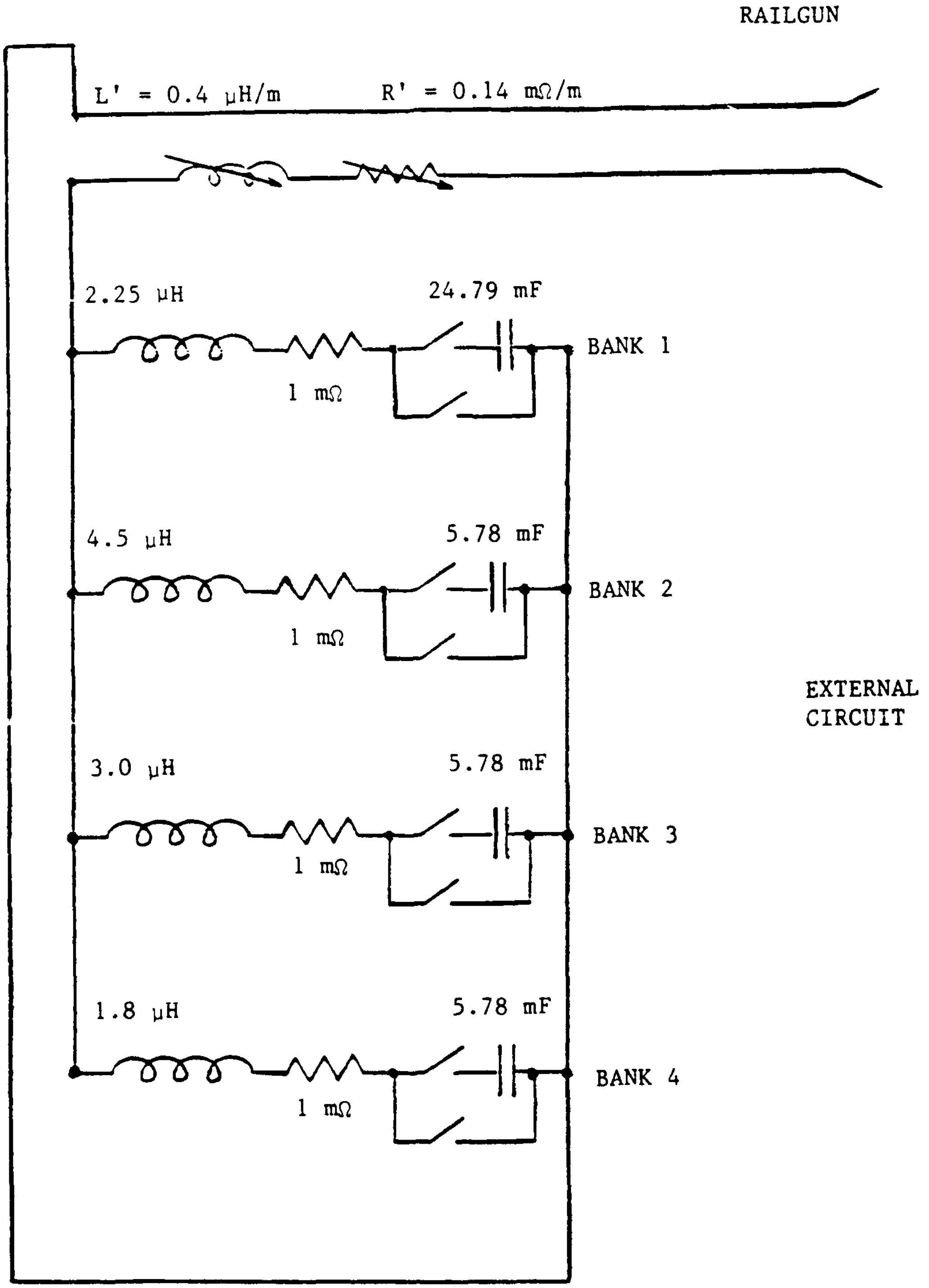

Figure 15. Schematic of electrical circuit for capacitor-driven EML system.

Table 14

CIRCUIT PARAMETER FOR CAPACITOR-DRIVEN EML SYSTEM

Parameter	Value
Total Stored Energy	10 MJ
Peak Capacitor Voltage	22 kV
Peak Operating Current	2 MA
Capacitance - Bank 1	24.79 mF
- Banks 2, 3, 4	5.78 mF
Inductance - Bank 1	2.25 μH
- Bank 2	4.5 μH
- Bank 3	3.0 μH
- Bank 4	1.8 μH
Resistance - Each Bank	1 mΩ (nom)
Rail Inductance Gradient	0.4 μH/m
Rail Resistance Gradient	0.14 mΩ/m
Losses in Armature	0.20 MJ
Losses in Rails/Bus During Launch	5.71 MJ
Energy in Inductance at Egress Time	1.29 MJ
Kinetic Energy in Launch Package	2.80 MJ

Table 15

CAPACITOR BANK PARAMETERS

Bank 1

Peak Current	2.0 MA
Capacitance	24.79 mF
Stored Energy	6.00 MJ
Number of Units	120

Banks 2, 3, and 4

Peak Current	1.0 MA
Capacitance	5.78 mF
Stored Energy	1.40 MJ
Number of Units	28

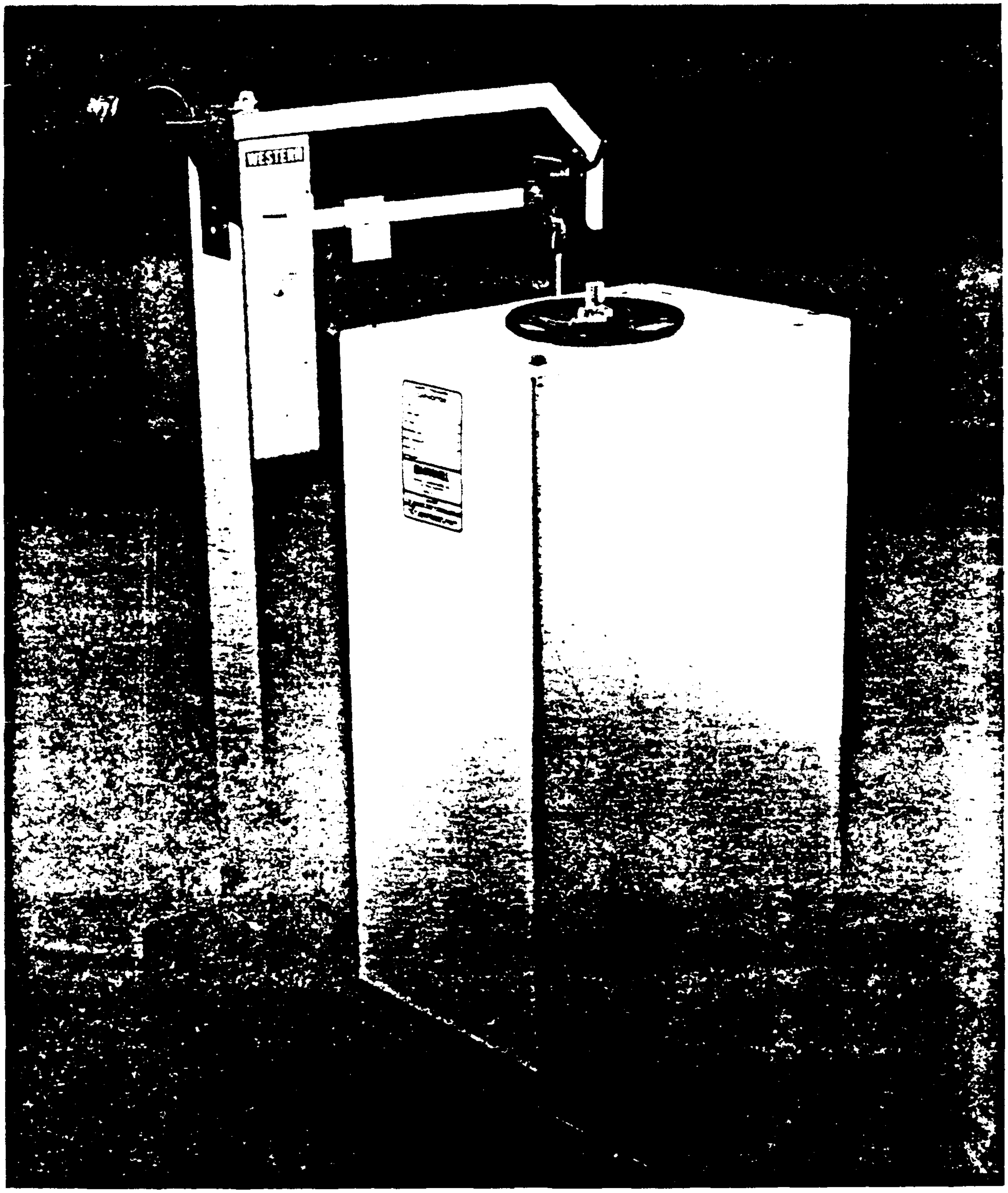

Figure 16. 50-kJ Capacitor Unit Manufactured by Maxwell Labs.

Table 16

CAPACITOR UNIT CHARACTERISTICS

Capacitance	206.6 μF
Maximum Operating Voltage	22 kV
Maximum Energy Storage	50 kJ
Can Dimensions	0.3 m x 0.25 m x 0.7 m
Mass Per Can	140 kg

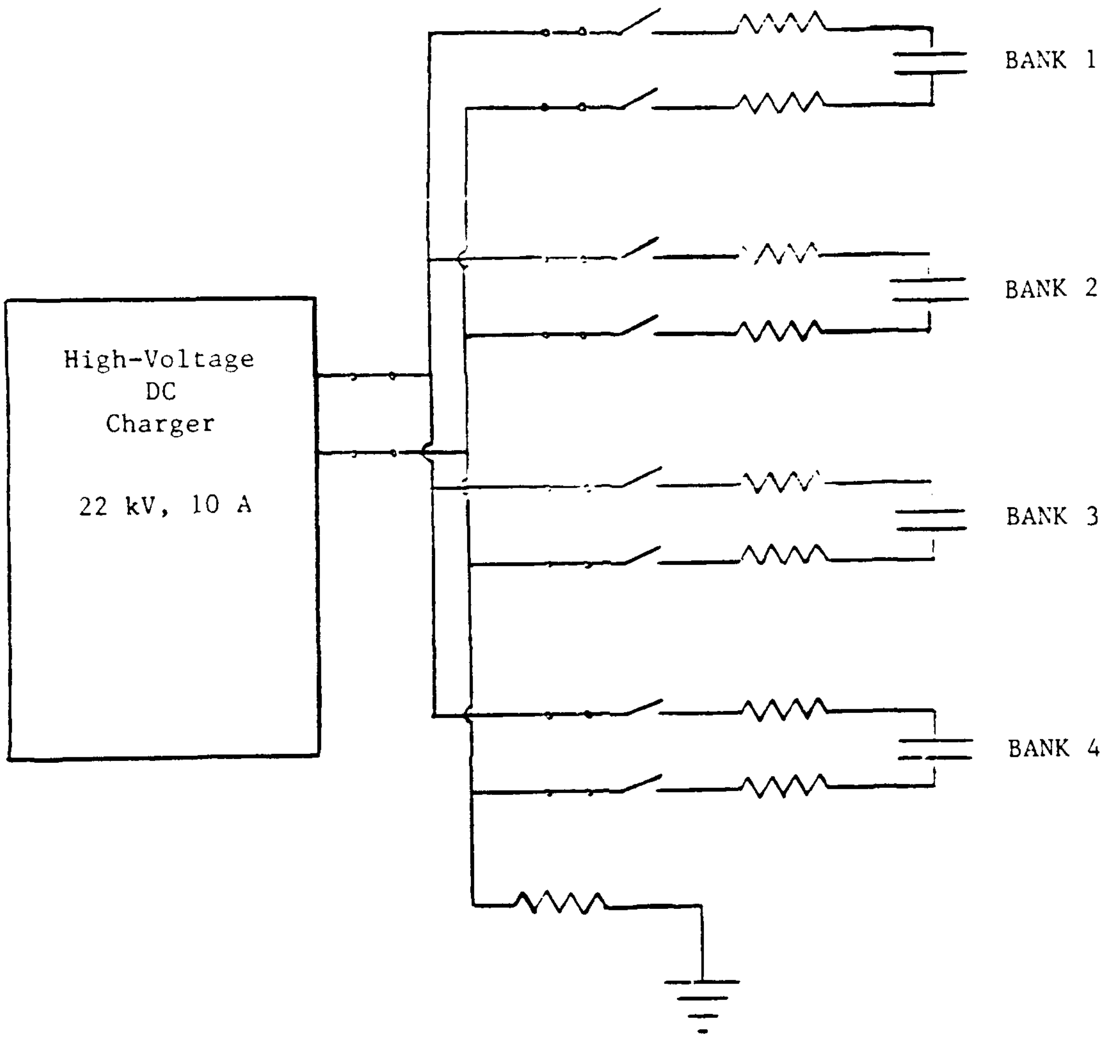

Figure 17. Charging circuit for capacitor banks.

Closing Switches and Crowbars

There are two switches for each of the four phased driving circuits. There is a series closing switch that initiates the current flow from the capacitors through the pulse-shaping inductor and railgun. When the current flow reaches a maximum value, the voltage across the capacitor goes to zero, and approximately all of the energy that was stored in the capacitor bank has been transferred to the inductor. At this time, the crowbar switch closes, essentially removing the capacitor bank and the series closing switch from the circuit.

Sparkgap switches, solid state thyristors, and ignitrons were considered for the series closing switches. Sparkgaps were not chosen for two reasons: (1) at the present time, sparkgap switches are not "off-the-shelf" items and will require considera'le development work before they can be reliably used in the quantities required for this application, and (2) they require complex voltage adjustments. It has been found that triggered sparkgaps function reliably if the gap spacing and pressures are set such that they would spark-over naturally (without a trigger pulse) at twice the set voltage. This means that operational voltage changes are difficult to achieve both in terms of effort and reliability.

In Table 17 a comparison is made between the number of solid state thyristors and ignitrons required for a peak current flow of $\simeq$ 150 kA and a peak voltage of 25 kV. The capital costs are also compared. It is shown that the capital cost of the thyristors is 7.7 times the cost of ignitrons.

Based on a peak current of 2.25 MA for the phase 1 driving circuit and 1.05 MA for phases 2, 3, and 4, ~ 36 units of the type displayed in Table 17 are required to be used in parallel for the series switches. This means the total capital cost of thyristors for the series closing switching would be $\simeq \$2.5 \times 10^6$ as compared to $\$3.2 \times 10^5$ for sufficient ignitrons.

Although the reliability of solid state switches is higher and maintenance requirements are lower than for ignitrons, ignitrons are chosen as the series switches because of the major cost savings. Note

Table 17

COMPARISON OF SOLID STATE THYRISTOR AND
IGNITRON SWITCHING CONFIGURATIONS AND COSTS

Quantity	Thyristor	Ignitron
Peak Current, kA	150	150
Peak Voltage, kV	25	25
Units in Parallel	4	1
Units in Series	8	2
Total Units	32	2
Cost/Unit, $	2,000*	2,000+
Cost of Units, $	64,000	4,000
Cost of Controls, $	5,000	5,000
Total Cost, $	69,000	9,000

*Based on Westinghouse cost data.

+Based on a combination of D-size and E-size manufactured by EEV.

also that 1152 thyristors would be required as compared to 72 ignitrons. If proper thermal management is applied to the ignitrons together with the monitoring of the ignitor resistances, reliable operation can be achieved.

We have considered solid state diodes and ignitrons for the crowbar switches. A comparison is made in Table 18 of the number of diodes and ignitrons required for a peak current of 150 kA and a peak voltage of 25 kV. The capital costs are also compared; the diode cost is 2.9 times the cost of ignitrons. Similar to the method described above for the series closing switch, 36 of the units displayed in Table 18 would be required. The total capital cost of the solid state diodes required for crowbarring in all four of the driving circuits would be $\$5.1 \times 10^5$ as compared to $\$1.7 \times 10^5$ for ignitrons.

Passive solid state diodes are attractive; however, because of the large number required (1260) and their cost, and also the fact that ignitrons were selected for the series closing switches, ignitrons have been chosen for the crowbar switches.

Because of recent problems experienced with power supplies which were switched with ignitrons, and a premature assignment of the cause of these problems to the ignitrons, a perception has been developed by many in the pulsed power community that ignitrons cannot be used as reliable switching devices. In reviewing our experience at Westinghouse, and in particular our experience and findings in connection with our own difficulties with the SUVAC II power supply, we believe that perception is not warranted. We can conclusively state that none of the misfirings observed with the SUVAC II power supply was due to the ignitrons themselves. Those that have occurred can be traced to a design weakness in the ignitor switching circuits. This weakness has been corrected, and no further problems are anticipated.

For both the closing switches and crowbars, ignitrons provide a reliable, high current, and high charge transfer system. Depending on the configuration of the various subassemblies of capacitor units, either the "D" size or the "E" size ignitron may be used. See Figure 18 for a "D" size unit. The transfer capabilities for the two different

Table 18

COMPARISON OF PASSIVE SOLID STATE DIODE AND
TRIGGERED IGNITRON SWITCHING CONFIGURATIONS AND COSTS

Quantity	Diode	Ignitron
Peak Current, kA	150	150
Peak Voltage, kV	25	25
Units in Parallel	7	1
Units in Series	5	2
Total Units	35	2
Cost/Unit, $	400*	2,000+
Cost of Units, $	14,000	4,000
Trigger System, $	100	800Δ
Total Cost, $	14,100	4,800

*Based on ABBC cost data.

+Based on a combination of D-size and E-size manufactured by EEV.

ΔAssumes six units are triggered by one trigger module.

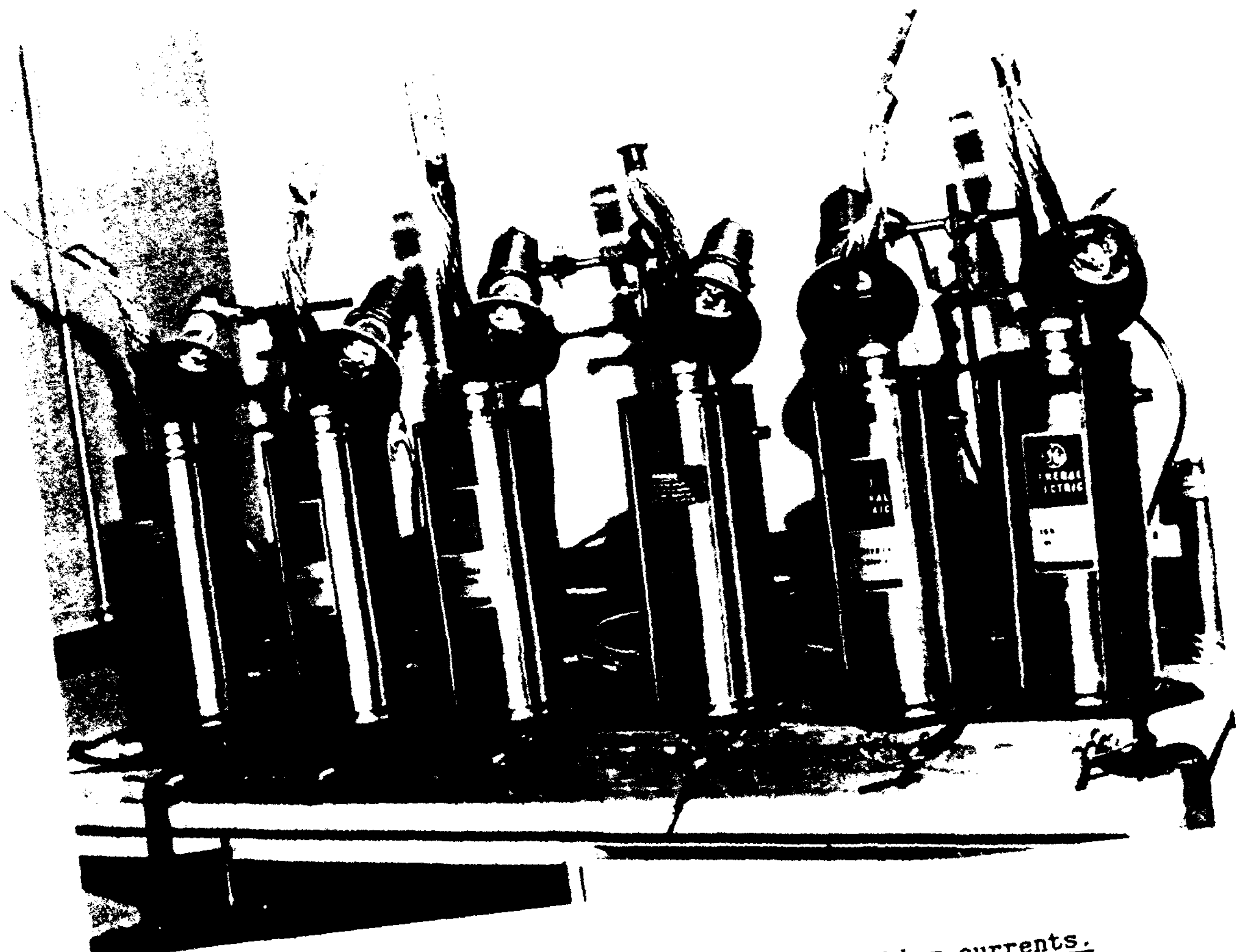

Figure 18. "D" size ignitrons for switching currents.

sizes are 116 C and 260 C, respectively. Both are capable of conducting currents to 150 kA. For each subassembly (either the 8-can or the 4-can), two ignitrons in series for each of the closing switches and the crowbars are required. In total, 144 ignitrons are required and a tabulation of the system is given in Table 19. The two-in-series feature provides the voltage withstand capability.

Pulse-Shaping Inductors

The pulsed-shaping inductors are provided to tailor both the magnitude of the rail current and the variation (i.e., dI/dt) in the current during the launch. By delaying the firing of subsequent banks, the profile of the rail current will be at the 2-MA level for most of the launch period. The design details of the inductors are such that each will be characterized by an inductance, a resistance, and an energy capacity. Configuration options available for the construction of the inductors include solenoidal, toroidal, and coaxial. There exists a fundamental difference between the requirements for the inductor of a homopolar-generator-driven power supply and that used for the pulse shaping in the capacitor-driven supply. In the homopolar system, the inductor is charged by the homopolar generator during a relatively long time. The energy dissipated in the inductor resistance must be kept to a minimum. Therefore, it is desirable to keep the inductor resistance to as low a value as possible. This resistance is typically on the order of 10 micro-ohms. This minimization process is enhanced by the choice of a toroidal inductor configuration, in which for a given length of conductor the inductance is larger than for a solenoidal configuration of the same conductor length. This is mainly due to the elimination of end-effects. The conclusion of these considerations is that there exist no compeling reasons to require that the inductors for the two power supplies be of the same generic configuration. For our purpose, a solenoidal inductor constructed in a "jelly roll" manner has been selected because of ease of manufacture and of low cost. A "jelly roll" inductor refers to a solenoid that is spiral wound from wide sheets, one sheet being a conductor and the second an insulator. Inductors have been made with this design using steel as the conductor

Table 19

SWITCHING SYSTEM

Parameter	Value
Bank 1	
Current - Peak in Circuit	2.0 MA
- Switching Capability	2.25 MA
Charge Transfer	
- Peak in Series Leg	500 C
- Switching Capability+	1740 C
- Peak in Crowbar Leg*	1600 C
- Crowbar Capability*	3900 C
Action Integral	
- In Series Leg	7.5×10^8 A^2s
- In Crowbar Leg	21×10^8 A^2s
Bank 4 (similarly for Banks 2 and 3)	
Current - Peak in Circuit	0.9 MA
- Switching Capability	1.05 MA
Charge Transfer	
- Peak in Series Leg	120 C
- Switching Capability+	812 C
- Peak in Crowbar Leg*	660 C
- Crowbar Capability*	1820 C
Action Integral	
- In Series Leg	8.4×10^7 A^2s
- In Crowbar Leg	4.0×10^8 A^2s

+Based on a D-sized unit.
*Based on an E-sized unit.

so that an additional structure is not necessary. White neoprene rubber is a satisfactory insulator. There is a conductor terminal on the inside and outside of the coil. The inductors will be fabricated with a fiberglass overwrap. The inductance and resistance is a function of the number of turns as well as the coil diameter and length. The inductor resistance is the primary component making up the 1-mΩ circuit resistance in each of the banks. Such a structure provides its own mechanical support.

<u>Buswork/Cabling</u>

The elements making up the capacitor bank energy source are connected via a system of coaxial cables. The final connections to the railgun are made with busbars. The coaxial cables provide a low reactance between elements as well as a means to reduce EMI and EM forces. The cables provide flexibility in terms of accommodating placement of units as well as making future design changes, if required. Depending on the current in each circuit, a set of coaxial cables in parallel is required where each cable can carry up to 200 kA. In order to balance currents each cable in a given set is made to the same length as the other cables.

The busbar connections between the barrel breech sections and the power supply are contained in a structure providing mechanical support to withstand the large forces developed which tend to separate and bend the individual conductors. In addition, electrical insulation is provided to prevent electrical breakdown outside the barrel.

2.2.3 Instrumentation and Controls, Diagnostics, and Data Acquisition System

The key systems supporting the operation of the EML are the instrumentation and controls (I&C), the diagnostics, and the data acquisition systems (DAS). These systems provide the capability to conduct and evaluate tests. The following is a description of these systems.

Instrumentations and Controls

The I&C consist of a remote control room with monitoring and controlling instrumentation, electrical and fiber optic connections to lab equipment, and trigger boxes, relays, interlocks, and cameras located at or near the railgun and power supply. The control room equipment includes a programmable logic controller, video monitors, and electrical interface hardware for charging the capacitor banks and for operating the pre-accelerator gas supplies and fast valve, (see Figure 19.) The trigger boxes provide the electrical circuitry to fire the ignitors on the various ignitrons. There are eight trigger circuits, i.e., two circuits on each bank to trigger the closing switches and the crowbar switches, separately. The closing switches on a given bank are triggered by a pre-set timing signal (different for each bank) and the crowbars are automatically triggered at the time that the bank voltage goes through zero. The various relays provide control features during the charging of the high-pressure gas systems on the injector, the charging of the capacitor banks, and the setting of the trigger circuits. The I&C is capable of data logging from the start of facility preparation to test completion. With this capability, the various operational features such as interlock status, relay status, voltage levels, current levels, and gas pressure levels will be recorded for later analyses.

Diagnostics

Diagnostics are provided which are sufficient to operate the system, to characterize the system performance, and to detect faults if they should occur. The various types of sensors and the measured quantities recommended for diagnostics are given in Table 20. The total number of each type of sensor installed will depend on the specific tests under study as well as the surfacing of any unexpected problems. The list tabulated could be expanded depending on the testing to include other diagnostics. For example, diagnostics to measure bore pressure, spectroscopic data, or position of the projectile could be added.

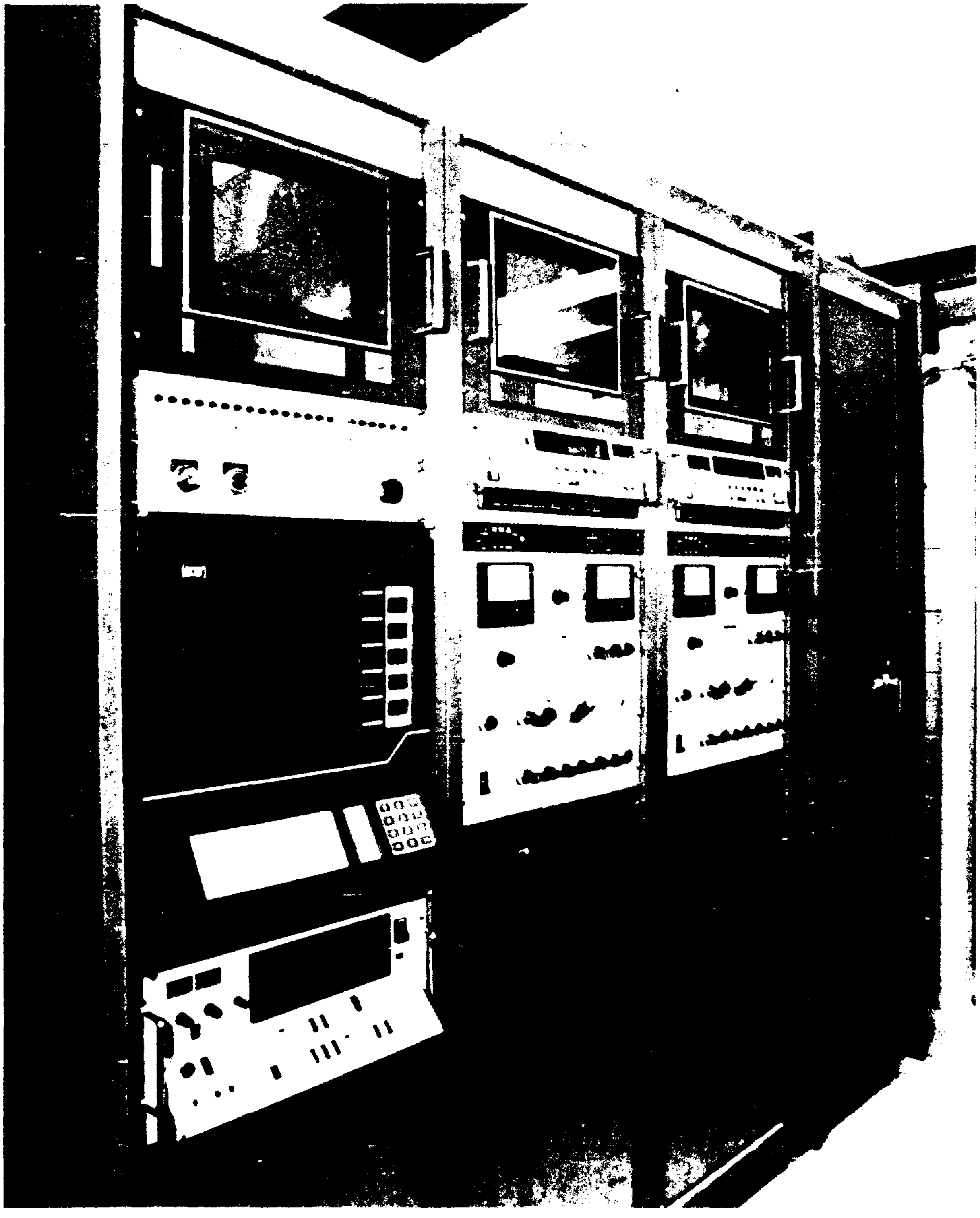

Figure 19. Control, instrument panels in railgun control room.

Table 20

DIAGNOSTICS FOR EML

Sensor Type	Quantity Measured	Number of Sensors
Armature B-Dot	Armature Current	4-10
Rail B-Dot	Rail Current	4-10
Barrel Voltage Divider	Breech and Muzzle Voltage	1-2
Capacitor Voltage Divider	Capacitor Bank Voltage	4-16
Rogowski Coil	Bus Circuit Current	5-10
Optical Velocity Station with LEDs	Injection Velocity	1 set
Breakwires	Muzzle Velocity	2-4
X-Ray Velocity Station	Muzzle Velocity	1 set

These diagnostics are more difficult to incorporate and are generally associated with factors of risk by reducing the gun performance (since additional penetrations into the bore are required). For example, for a plasma armature in-bore pressure measurements can be made with a piezoelectric transducer which is located at the end of a short channel in the insulator separating the rails of the gun. Strain gauges have also been used. However, EMI is a problem and care must be taken to keep the noise to an acceptable level.

Data Acquisition System

The instrumentation associated with collecting and recording the data from the sensors is contained in a shielded room, an example is shown in Figure 20, to provide EMI/RFI isolation. The requirements on the construction, connector panels, floor isolation, air conditioning, voltage regulation, grounding, etc., demand careful design to minimize noise in the low-voltage signals acquired. The specific instrumentation includes transient recorders and trigger-actuating pulse generators. The data collection is computer-controlled with a dedicated personal computer (PC) which activates the recorders, controls settings, and records data. Both low level signals, e.g., B-dot data, as well as high-voltage signals, such as bank voltage data, are acquired by the same DAS and require various design features for the cable connections for the different types of signals. See Figure 21 for a typical collection system.

2.2.4 Facility Design

In addition to the hardware associated with the railgun, power supply, the I&C, sensors, and the DAS, the facility provides a number of other key features.

Catch Tank

Down range from the railgun muzzle a catch tank stops the accelerated masses. The kinetic energy associated with the existing mass will be as high as 2.5 MJ and the penetrators will have a high lethality. The catch tank also provides the capability to determine the muzzle velocity and kinetic energy (e.g., a ballistic pendulum), to prevent the sabot from impacting the target under study, and to interface with any lethality diagnostics.

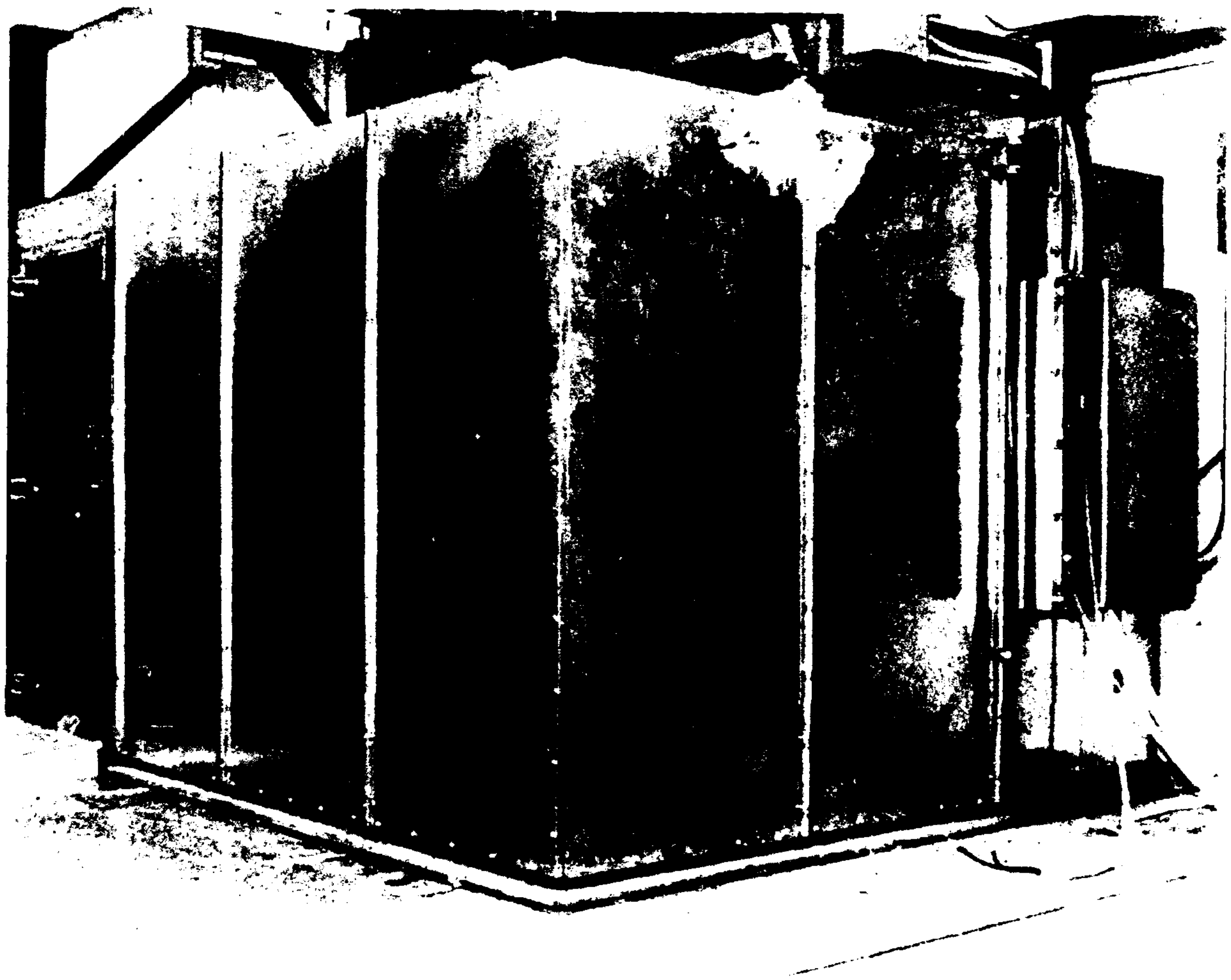

Figure 20. Shielded room to isolate DAS from EMI/RFI.

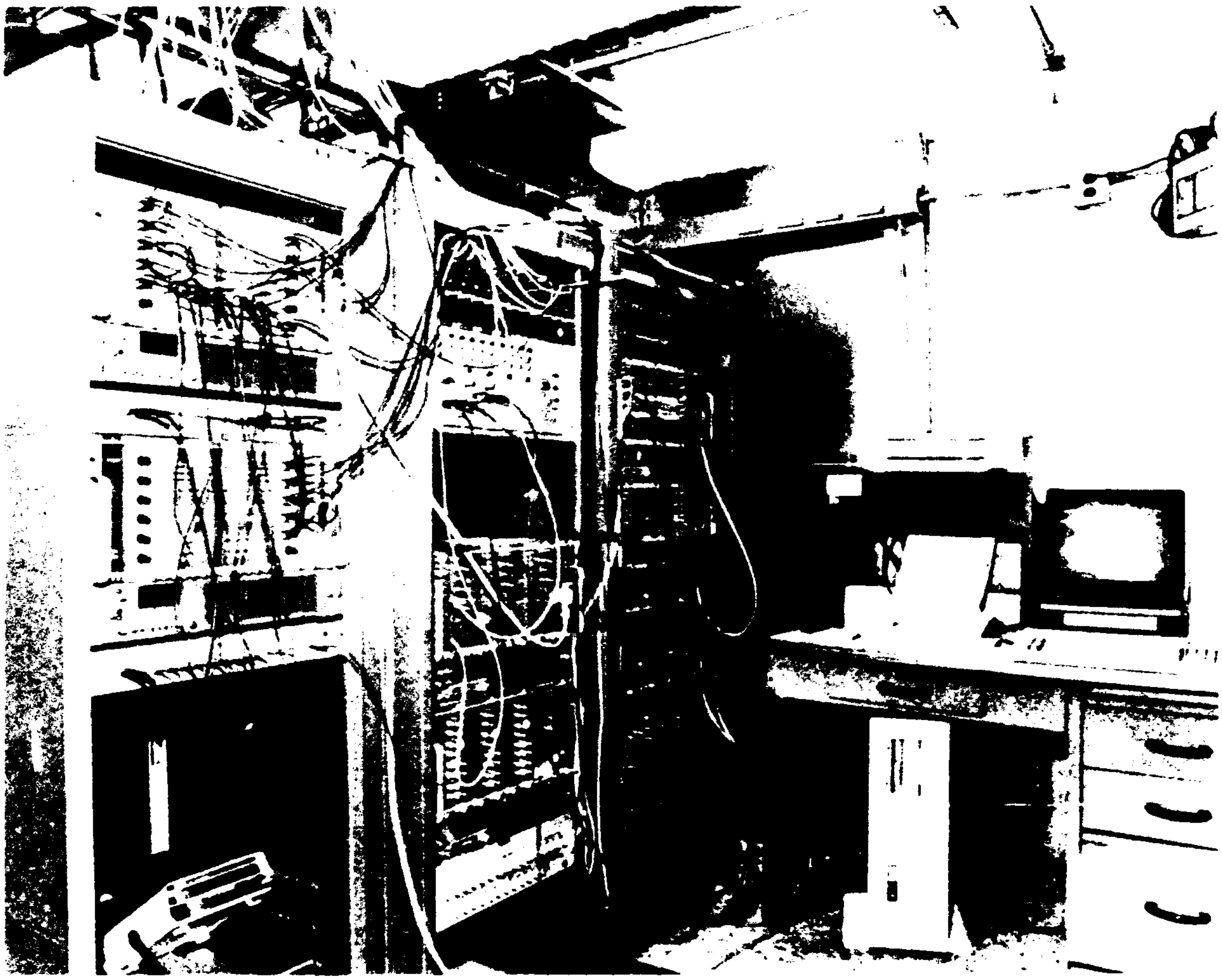

Figure 21. Data collection and triggering electronics for the computer-controlled railgun DAS.

Mechanical Supports

The railgun system, including injector and catch tank, has a total mass of approximately 15,000 kg. The structures for mounting this system support this mass as well as absorb the launch recoil forces of approximately 800 kN. Alignment features are required to connect the injector to the barrel. The structures provide the capabilities for a movable gun.

The capacitor banks and associated system have a total mass of approximately 50,000 kg. Structures support the capacitor bank subassemblies, the inductors, and the circuit cabling system.

Facility Services

To service the railgun, a number of features are required. One or more cranes are needed to assemble and maintain the system. High-pressure helium for the injector operation is required. An interface is required to connect the gun to the power supply and to the various I&C/DAS components. Both water and gas lines are required for general servicing, air-operated tools and features, etc.

Facility Safety

The safety features of the facility protect personnel and equipment. The key hazards include: high voltage, high magnetic fields, x-rays, high pressures, and toxic products. Safety interlock switches, klaxons, and warning lights provide safety features to protect personnel. Various abort and dump features are incorporated to protect equipment.

Facility Layout

The building facility required to accommodate the railgun, power supply, control room, and DAS screened room is shown in the floor plan, Figure 22. The spaces allocated for the various systems are based on existing railgun facility designs and include floor area for access, maintenance, and walkways. The actual dimensions expected for the

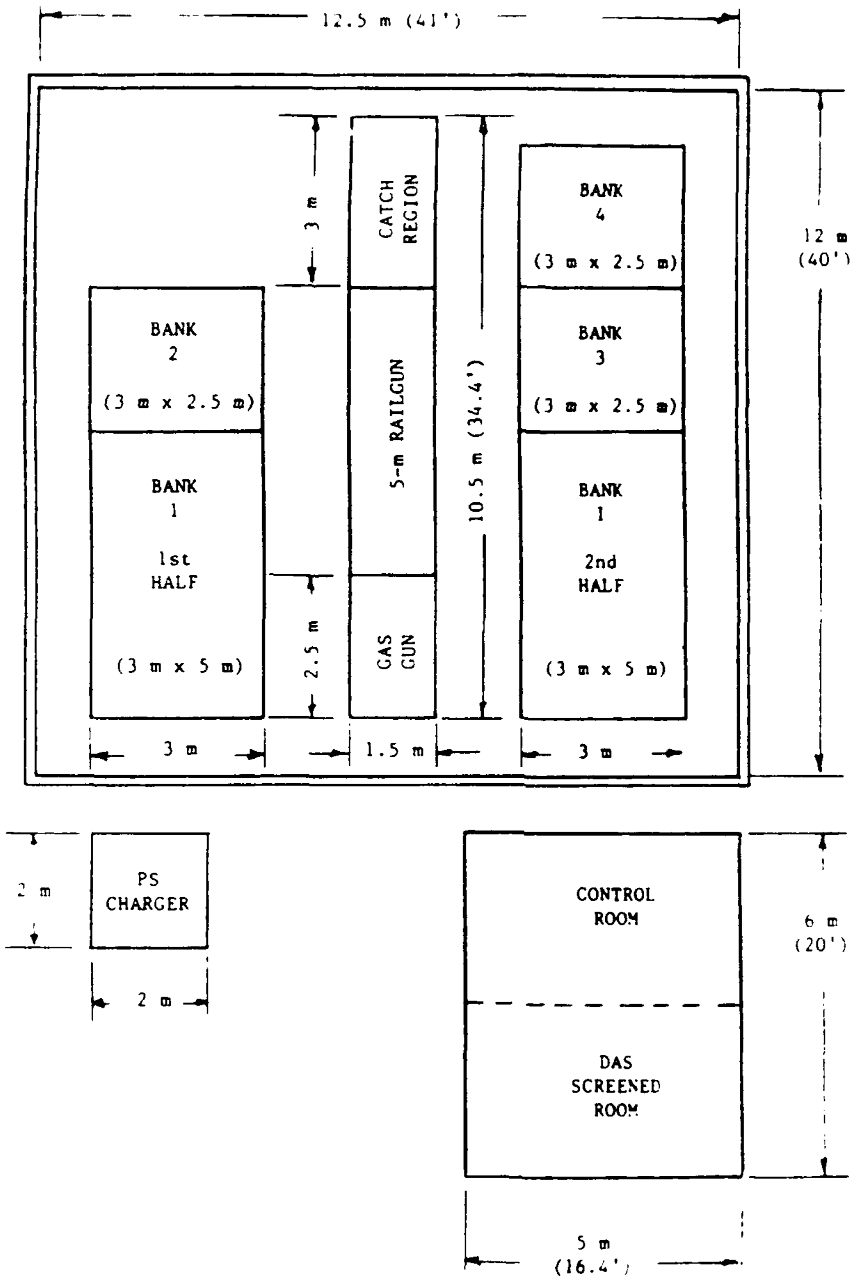

Figure 22. Capacitor-driven EML facility layout.

various hardware were considered when taking spacial requirements into account. Assuming a 10-ton overhead crane, the building for the railgun and power supplies would be ~ 8-m high. The ceilings in the control room and screened room would be of normal laboratory height.

2.3 COST ESTIMATE SUMMARY

A summary of the total equipment cost for the capacitor-driven EML facility (not including buildings) is estimated to be $3.163 M. A tabulation according to the main subsystems is provided in Table 21. This breakdown includes a spare barrel, an installation cost, and a 15% contingency.

The base cost of equipment is $2 M. The power supply systems make up 59% of that cost, while the railgun (including a spare) makes up 22% of the base cost. The remaining 19% is associated with a catch tank, controls, data acquisition, and safety components. The installation cost which adds an additional 37% to the $2 M base equipment cost, accounts for the labor intensive effort required to assemble the power supplies. This system consists of four independent banks and includes 204 capacitor cans, 144 ignitrons, 4 large inductors, and many lengths of 200-kA coaxial cabling connecting the various components.

2.4 ADVANTAGES AND DISADVANTAGES OF THE CAPACITOR-DRIVEN EML

The application of a capacitor-driven EML to advanced lethality studies and target data acquisition has the promise of providing a much needed enhancement in the lethality area. There are a number of practical considerations requiring attention for this application of EML. The results of this study strongly indicate the potential for EML in lethality, but since the technology is not fully developed or tested, there are a number of issues which must be addressed. In general, these areas are related to the railgun bore, railgun manufacturing, rail current profiles and magnitudes, the armature physics, the interaction of the launch package with the railgun, and the diagnostic requirements. A test program to address these issues is presented in Section 8.

Table 21

COST ESTIMATE SUMMARY FOR
THE CAPACITOR-DRIVEN EML FACILITY

Cost of Equipment

Item		Cost Estimate ($K)
Primary Power/Charging System		635
Power Conditioning Equipment		77
Switching/Triggering Circuitry		364
Cabling & Buswork		101
Barrel & Mechanical Structure		317
Spare Barrel		130
Catch Tank		15
Screen Room & Data Acquisition System		248
Control Room Equipment/Safety		123
	Subtotal	2010
Installation Cost		
Engineering (1.8 person years)		306
Technician (5.1 person years)		434
	Subtotal	740
Contingency (15%)		413
Total		3163

From the considerations resulting in the various trade-off studies and conceptual designs developed in this program, we are able to provide a set of lists allowing a comparison to be made among the various options for a lethality facility. A listing of the key advantages and disadvantages of the capacitor-driven EML system relative to the two other concept systems is given in Table 22. For the capacitor-driven EML concept the main advantages are associated with operating experience and with the low piezometric ratio. The capacitors offer more flexibility in terms of rail current tailoring and the EML system offers some advantages in terms of a simpler launch package.

On the side of disadvantages, the homopolar-generator-driven system does not have many of the complexities associated with a multi-bank capacitor-based system. For the barrel systems, the key disadvantages result from the complexities associated with the EML barrel design relative to the simple, more conventional barrel for an ETL.

The overall picture resulting from the comparisons provides key input which allows recommendations to be made. This input, along with discussions of other factors resulting in a recommended option, are provided in Section 5.

Table 22

ADVANTAGES AND DISADVANTAGES OF
THE CAPACITOR-DRIVEN EML SYSTEM

Advantages

Relative to HPG-Driven EMLs

More experience and more operating systems

Rail currents can be more easily tailored, especially at the breech and muzzle

Lower piezometric ratios can be achieved for low stored energy

For the same performance goals, the barrel is shorter

Circuitry requires only closing switches

Circuitry does not require low resistances

Capacitor banks can be adapted for use by ETLs

Relative to ETLs

Operating experience on ETLs is very limited, especially at the higher velocities

The launch package is simpler and less costly

The power supply is somewhat simpler, e.g., no diodes required

Lower piezometric ratios can be achieved

No capillary chamber required

Launch package loading operation is relatively simple

Disadvantages

Relative to HPG-Driven EMLs

Muzzle damage is more of a problem, due to voltage breakdown across the rails after projectile exits

Closing switch technology is limited to ignitrons unless both added costs and technology development are included

Efficient systems involve complex multi-bank operations, including staged or phased current injection

Relative to ETLs

Gun barrel is complex and heavier

Gun barrel cross section is larger

EMLs require an armature as part of the launch package

Bore damage is more serious

Bore sealing is more complex

3. DESIGN OF THE HPG-DRIVEN EML

3.1 TRADE-OFF STUDIES

3.1.1 General Description of the HPG-Driven EML

The circuit model for the HPG-driven EML is shown in Figure 23. The main components are the HPG, inductor, busbars, opening switch, barrel, projectile, and muzzle resistor. A single firing is comprised of four events:

1) HPG spin-up
2) Inductor charging
3) Projectile acceleration
4) System decay

In a single shot system, all the energy is initially stored in the rotational inertia of the HPG rotor. During the HPG spin-up, an electric motor is used to accelerate the HPG to the desired speed, or energy level. In the EML circuit, S_1 is open and S_2 is closed during this time. This phase typically lasts a few minutes, depending on the desired energy level, and the power of the drive motor.

At the end of the HPG spin-up, the drive motor is turned off and the HPG is left in a coast mode. The next event, inductor charging, starts when the HPG brushes are actuated onto the rotor surface. Brush actuation is represented in the circuit schematic by the closing of S_1. After S_1 closes, the voltage output of the homopolar generator is placed across the inductor and busbars, and current starts to flow through the circuit. Inductor charging is essentially an energy transfer from mechanically stored energy in the HPG to electrically stored energy in the inductor. This electrically stored energy is given by

$$EIND = 0.5(LE)(I1)^2$$

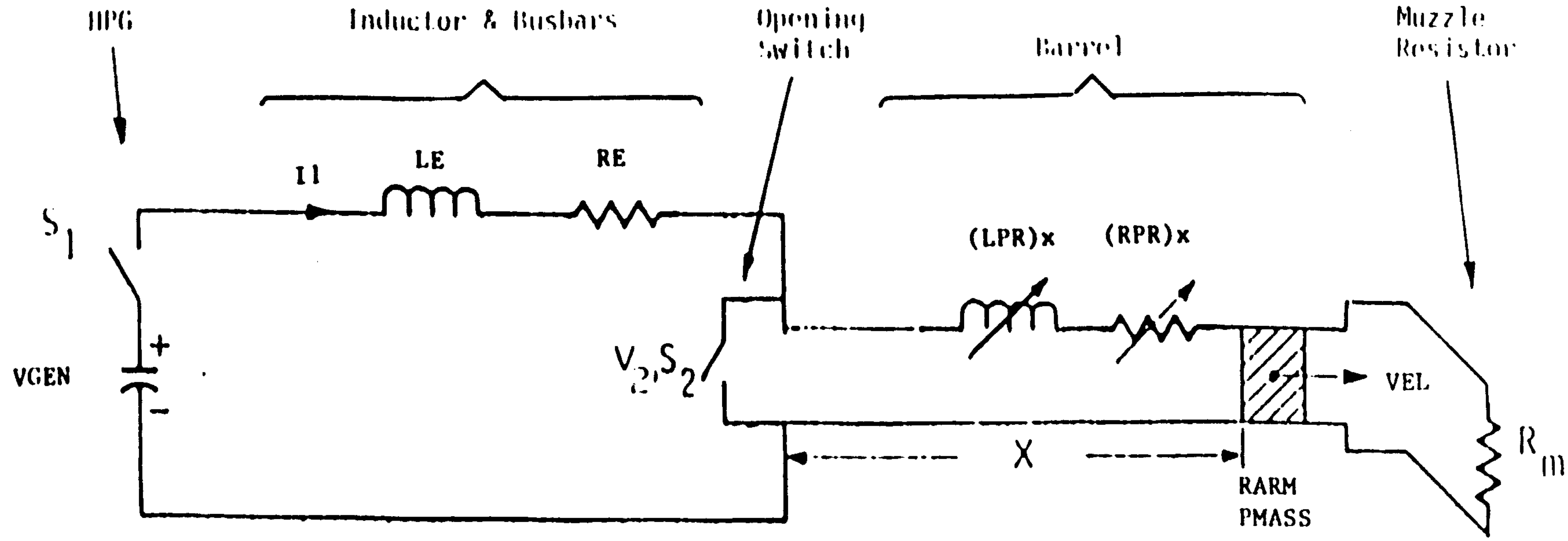

Figure 23. <u>**Circuit model for HPG-driven EML**</u>

where

EIND = electrically stored energy (J)
LE = charging circuit inductance (H)
I1 = charging circuit current (A)

When the current in the charging circuit reaches the required level, the inductor charging phase is terminated by opening S_2. By opening S_2, the charging circuit is interrupted, and the current is commutated into the barrel breech and projectile. The projectile begins to accelerate when the current is switched into the barrel. The projectile acceleration can also be described as an energy transfer. In this case, the electrically stored energy in the inductor is transferred to kinetic energy in the projectile. As the current falls, the projectile velocity rises.

The fourth event, system decay, starts when the projectile exits the muzzle of the barrel. The system current is then commutated into the muzzle resistor. The remaining stored energy, including rotational energy in the rotor and inductively stored energy in the circuit, is dissipated in resistive heating of all the circuit elements. Most of this energy dissipation takes place in the muzzle resistor.

3.1.2 Description of the HPGC Computer Code

The HPGC code is written in Fortran and runs on an IBM PC. The program solves the simultaneous differential equations of the launcher circuit, using a Runge-Kutta solver. The program is set up to simulate single or multi-shot firings. Various types of HPGs can be modeled, such as air-and iron-cored machines. The excitation current can be constant, variable by a predetermined function of time, or variable by a function of the launcher circuit current.

Table 23 shows the inputs and outputs of the HPGC code. The input values describe the final baseline system in which a 515-g projectile is accelerated to 3500 m/s. The program models the inductor charge and the projectile acceleration.

Table 23

INPUTS AND OUTPUTS FOR HPGC SIMULATION CODE

Symbol	Definition (units)	Value
Inputs		
LE	Charging circuit inductance (H)	5.43×10^{-6}
RE	Charging circuit resistance (Ω)	33.0×10^{-6}
LPR	Barrel inductance gradient (H/m)	0.4×10^{-6}
RPR	Barrel resistance gradient (Ω/m	140×10^{-6}
RARM	Armature resistance (Ω)	200×10^{-6}
PMASS	Projectile mass (kg)	0.515
BO	HPG magnetic field (T)	1.60
K	Rotor radius x active length (m^2)	9.75×10^{-2}
JGEN	Rotor inertia (kg-m^2)	3.34×10^{2}
WO	Initial rotor speed (rad/s)	5.59×10^{2}
IFIRE	Peak firing current (A)	2.10×10^{6}
Outputs		
Time (s)		
I1	Current (A)	
X	Projectile position (m)	
VEL	Projectile velocity (m/s)	
ACC	Projectile acceleration (m/s^2)	
VGEN	HPG output voltage (V)	
OMEGA	HPG rotor velocity (rad/s)	
TGEN	Electromagnetic rotor torque (N-m)	
TTURB	Mechanical shaft torque (N-m)	
CHG-L	Charge circuit resistive losses (J)	
RAIL-L	Rail resistive losses (J)	
ARM-L	Armature resistive losses (J)	

The charging of the inductor starts with the HPG coasting at the desired speed of WO. The excitation field in the HPG is assumed to be of a constant flux density, BO, over a particular axial length of rotor. This length is referred to as the active length. Outside the active length, the flux density is assumed to be zero. The launcher circuit current, I1, is assumed to flow in an infinitely thin sheet on the surface of the rotor. The active length, flux density, and radius of current flow are assumed constant during the inductor charging and projectile launch. The code solves the three governing equations of the charging circuit, which are

$$\mathrm{VGEN} = (\mathrm{K})(\mathrm{BO})(\mathrm{OMEGA})$$

$$\mathrm{VGEN} = d/dt\ (\mathrm{LE})(\mathrm{I1}) + (\mathrm{RE})(\mathrm{I1})$$

$$d/dt\ (\mathrm{OMEGA}) = \mathrm{I1}(\mathrm{BO})\mathrm{K}/\mathrm{JGEN}$$

The code simulates the inductor charging until the predetermined firing current, IFIRE, is reached. During the charging, the circuit parameters, LE and RE, are assumed constant. RE is the sum series resistance of the busbars, inductor, HPG, and switch. When IFIRE is reached, the opening switch, S_2, is assumed to open instantaneously with no loss of energy. After S_2 opens, the projectile and barrel become part of the circuit. The effect of the barrel on the overall circuit response is given by the following equations:

$$\mathrm{ACC} = 0.5\ (\mathrm{LPR})(\mathrm{I})^2/\mathrm{PMASS}$$

$$V_2 = (\mathrm{I})(\mathrm{RPR})(\mathrm{X}) + (\mathrm{I})(\mathrm{LPR})(\mathrm{VEL})$$

The simulation code has several simplifying assumptions. The net effect of these assumptions would affect the final results by approximately 10%. It was judged that this error was small enough so that the code could still be used effectively to specify an optimum baseline system. These assumptions were then compensated for during the

were then compensated for during the design of the individual components. The performance capabilities of the individual components were increased as needed. The simplifying assumptions, in order of importance, were as follows:

1) constant flux and load current distribution in HPG
2) 100% efficiency in opening switch
3) no friction between projectile and barrel bore
4) no friction and windage losses in HPG
5) no preacceleration of projectile

The first assumption forces the HPG to behave according to the two equations given earlier. Under these conditions, the voltage output is directly proportional to the rotor speed, and the angular deceleration of the rotor is directly proportional to the load current. These proportional relationships remain constant throughout the pulse. Under these conditions, the HPG acts as a capacitor, and the following equations hold true;

$$C = JGEN/K^2(BO)^2$$

$$EGEN = 0.5\ JGEN\ (OMEGA)^2 = 0.5\ C(VGEN)^2$$

where

C = effective capacitance of HPG (F)
EGEN = energy stored in HPG (J)

The baseline HPG design utilizes a solid steel rotor. As the inductor charging begins, the relatively small circuit current flows very close to the surface of the rotor. As the time and current increase, the current moves inward, away from the rotor surface. This changing distribution of load current within the HPG magnetic circuit causes a decrease in magnetic flux density in the active length. This causes eddy currents, and a "droop" in the output voltage, relative to ideal behavior. This phenomenon was analyzed for the EMACK system, and

was found to cause a 5-10% reduction in the peak current produced in that particular system.[1,2] This factor has been accounted for by designing the HPG to produce a peak current, under ideal conditions, of 2.35 MA, or 12% over the 2.1 MA that is required.

The efficiency of the opening switch is predicted to be 92%. This was accounted for by increasing the inductively stored energy by a factor of (1/0.92). The code predicted that an inductive energy store of 5 μH and 2.1 MA would produce the desired performance. After applying the correction factor, the specifications for the inductive energy storage were changed to 5.43 μH and 2.1 MA.

The simulation code does not account for projectile friction and the initial projectile velocity provided by the gas gun injector. These two energies are estimated at approximately 60 kJ, and have a cancelling effect.

Brush frictional losses average about 12 MW during the inductor charging, and produce a total energy loss of 1.7 MJ over this period. This is about 3% of the initial stored energy in the HPG. This loss has not been accounted for in this simulation, but it could easily be incorporated into the final design of the system. Bearing and windage losses are approximately 50 kW, and have a negligible effect.

3.1.3 Presentation of Results

A system has been designed which will meet the nominal performance goals of a 515-g projectile, and a 3500-m/s muzzle velocity. The system consists of an HPG, busbars, inductor, opening switch, gas gun injector, barrel, muzzle resistor, and projectile. The injector, barrel, and projectile are very similar to the components used in the

---

1. "DC Electromagnetic Launcher Development, Phases II and III," D. W. Deis, et al., ARDEC Contract DAAK-79-C-0110 Final Report February 20, 1984.

2. "An Analysis of the Effects of Load Current Flowing in the Rotor of the Upgraded EMACK HPG," D. Pavlik, Westinghouse R&D Report 87-8J6-ARDEC-R2, May, 1987.

capacitor-driven EML system described in Section 2. These three components are fairly generic to both EML systems. The detailed discussion from Section 2 applies to the HPG-driven system as well. The only difference is in the barrel length. The HPG-driven system requires a longer barrel, because the current pulse supplied to the breech of the barrel is less optimal than that of the capacitor-driven system.

The velocity and driving pressure of the projectile are shown in Figure 24.

3.1.4 Selection of Parameters for Launcher

The 56-mm round bore barrel, with a 515-g projectile, was selected as the baseline accelerator subsystem for the HPG-driven EML system. This is the same accelerator described in Section 2. Thus, the following parameters were held constant during the parametric study:

Barrel Inductance Gradient (LPR) = 0.4×10^{-6} H/m
Barrel Resistance Gradient (RPR) = 140×10^{-6} Ω/m
Armature Resistance (RARM) = 200×10^{-6} Ω
Projectile Mass (PMASS) = 515 g

With these parameters defined, the next step was to define what combinations of barrel length, peak current, and charge circuit inductance would provide the desired performance. A series of HPGC runs was performed in which barrel lengths of 5, 7, and 9 meters were considered, and inductance values of 2-9 μH were used. For each combination of barrel length and inductance, HPGC runs were performed to determine what values of peak current (IFIRE) were needed to produce muzzle velocities of 2.5, 3.0, and 3.5 km/s. The results are shown in Figure 25. In each of the nine curves shown in the figure, the muzzle velocity and active barrel length are constant. Each curve shows various combinations of inductance and peak current that are required to reach the noted velocity within the noted barrel length.

It should be noted that the inductively stored energy, as defined by LE and IFIRE, is the only useful energy available for

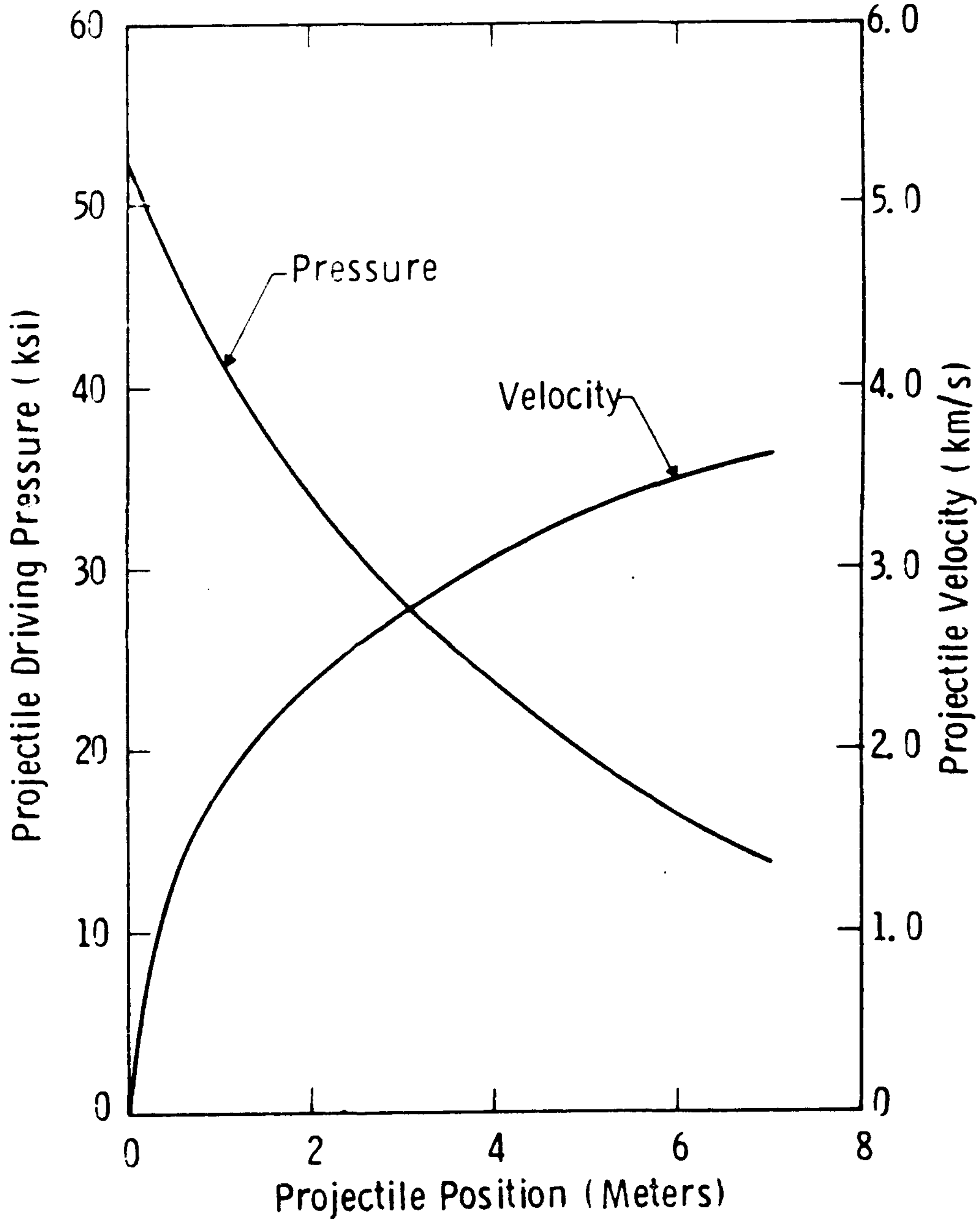

Figure 24. Projectile base pressure and velocity as a function of projectile position in bore for an HPG-driven EML. Peak current = 2.1 MA. Bore diameter = 56 mm. Projectile mass = 515 grams.

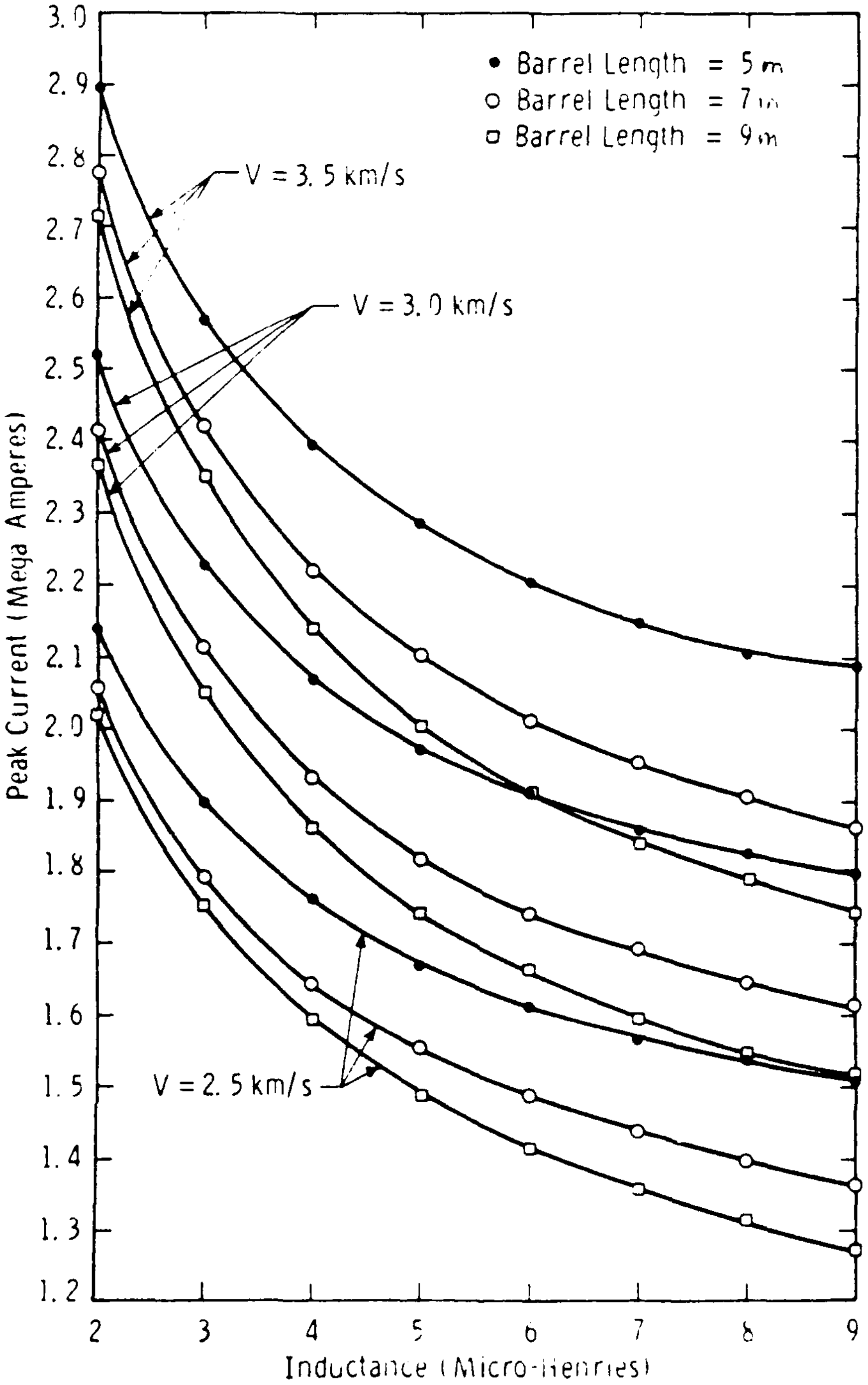

Figure 25. Launch parameter relationships for an inductively driven launcher with a 515-g projectile.

accelerating the projectile. For given values of LE and IFIRE, the projectile acceleration is relatively unaffected by the HPG parameters. This is because the voltage output of the HPG is small relative to the voltage at the barrel breech during acceleration. Also, the HPG rotor inertia is too great to allow any significant energy transfer during the 3-ms duration of the projectile acceleration. Because of this, defining the overall power supply becomes a two-step process. First, the inductive energy store must be defined. Then, an HPG must be designed that is capable of charging the designated inductance up to the required current.

The design point of the system is on the 3.5-km/s, 7-m curve in Figure 25. This is the second curve from the top. This curve shows that at a peak current of 2.1 MA, an inductance of 5 μH is required. This point was chosen for several reasons. The 2.1-MA level is a practical limit for a low-risk, reliable system. This current level produces a high, yet acceptance I' current density on the barrel rails, and is a reasonably low extrapolation of Westinghouse experience in HPG design and operation, as shown in Figure 26. With a peak current of 2.1 MA, the 7-m length appears optimal. Figure 25 shows that extending the barrel to 9 m gives a small inductance reduction to 4.3 μH, while cutting the barrel down to 5 m requires a much larger inductance increase to 8.5 μH. Therefore, the preliminary nominal parameters were chosen as follows:

Barrel Length = 7 m
Velocity = 3.5 km/s
Inductance (LE) = 5 μH
Peak Current = 2.1 MA

After correcting for opening switch losses, the inductance requirement was boosted to 5.43 μH. Also, an extra meter of barrel length was added to account for some inactive length at the breech and muzzle. With these corrections, the major parameters become:

- Maximize Current, Maintain Acceptable Risk
- Limit Current to 2.1 MA
  - Westinghouse Experience

EMACK:	Design 1.5 MA Operation 1.6 MA
EGLIN:	Design 1.5 MA Operation 1.0 MA
ROCKETDYNE:	Design 2.0 MA No Operation to Date

  - Greater Currents Will Increase Bore Size and Parasitic Launch Mass
- 56 mm. Barrel, Eight Meter Length

Figure 26. Selection of parameters for HPG-driven EML.

Barrel Length = 8 m

Velocity = 3.5 km/s

Inductance (LE) = 5.43 μH

Peak Current = 2.1 MA

The tradeoffs in selecting current and inductance are also illustrated in Figure 27. The current vs. inductance curve is the same as the 3.5-km/s, 7-m curve from Figure 25. This curve shows how increasing inductance decreases peak current, and therefore technical risk. However, the figure shows how increased inductance produces a less efficient system with a bigger, more costly HPG.

As shown in Figures 25, 26, and 27, the best way to balance cost, energy, and risk is to operate at the highest current level possible, while maintaining an acceptable level of risk. For this system, a value of 2.1 MA has been chosen.

3.1.5 List of Required Components and Their Specifications

Based on the main parameters selected in Section 3.1.4, the remainder of the system was designed in accordance with these parameters. A complete list of component specifications is listed in Table 24.

3.2 DESIGN COMPONENTS

3.2.1 Barrel System

Preaccelerator

The preaccelerator for the HPG-driven EML is identical to that used in the capacitor-driven EML system described in Section 2. The preaccelerator will accelerate a 515-g projectile to 500 m/s in a length of approximately 1 meter. The preaccelerator is powered by a 7500-psi helium reservoir and a single fast-acting valve. The pressure of 7500 psi was chosen because it represents the current state-of-the-art in commercially available, fast-acting opening valves. The predicted performance of the preaccelerator is shown in Figure 28.

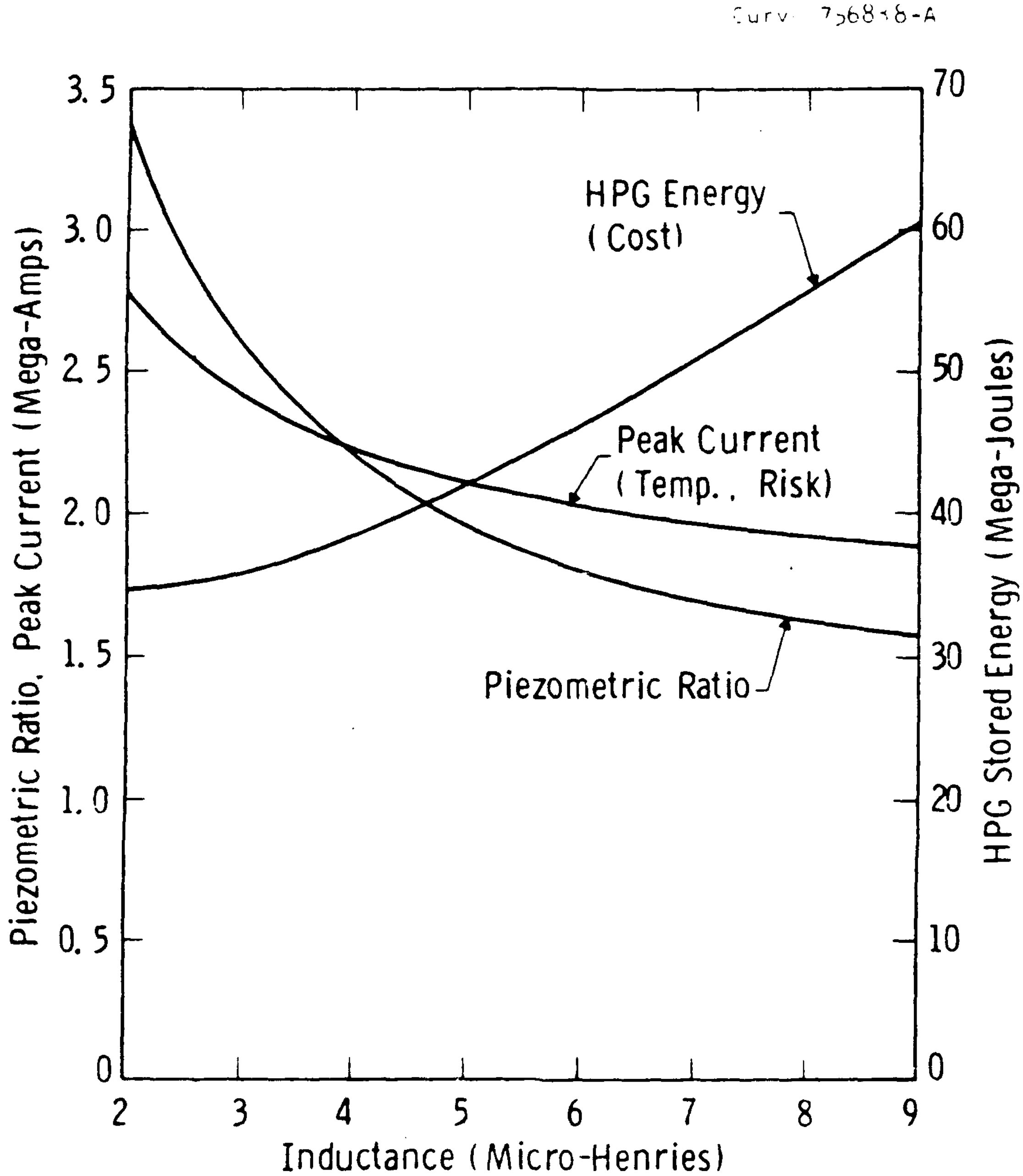

Figure 27. System parameters as a function of inductance. Power supply is modeled as a series LCR circuit, C = 6321 F, R = 2.85 (LE) + 18 $\mu\Omega$. Active barrel length = 7 m, velocity = 3.5 km/s.

Table 24

COMPONENT SPECIFICATIONS

Parameter (units)	Value
Velocity (m/s)	3500
Barrel Bore (mm)	56
Barrel Length (m)	8
Proj. Mass (g)	515
Peak I (MA)	2.1
Inject Vel (m/s)	500
Inject Length (m)	1
Switch Type	Explosive
Charge Action (A^2s)	3.5×10^{11}
Inductance (μH)	5.43
Charge Resistance ($\mu\Omega$)	33
Ind.	15
Bus	11
HPG	5
Switch	2
Muzzle Resistor	
Res. ($\mu\Omega$)	2000
Heat Cap. (MJ)	52
HPG Energy (MJ)	52

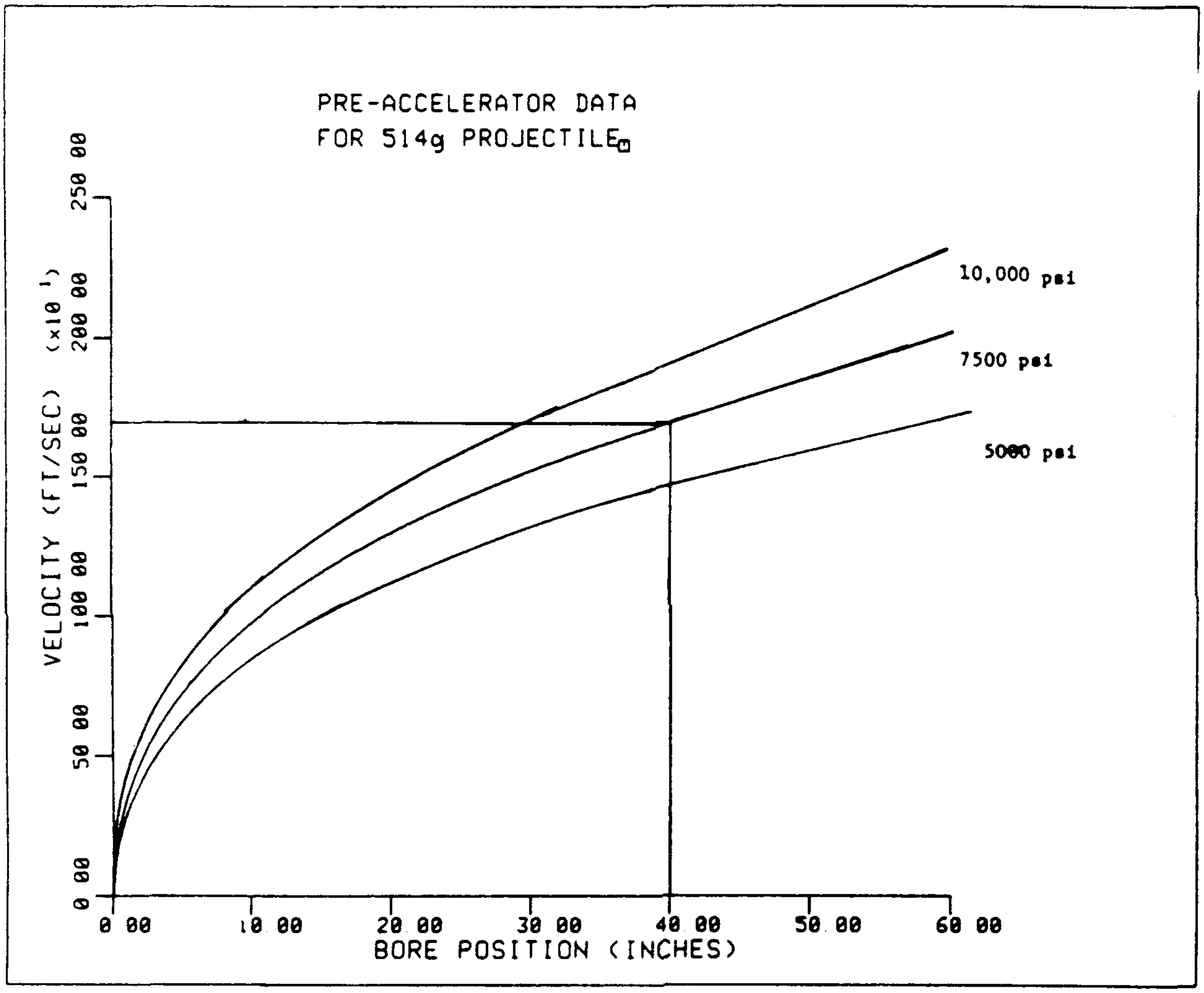

Figure 28. Preaccelerator performance for three different pressures. 7500 psi is the design pressure.

Rail System

The rail system is similar to the one described in Section 2. The only difference is that the HPG-driven system has an 8-m barrel, which is 3 meters longer than that of the capacitor-driven system. The barrel cross sections are identical.

Muzzle

The muzzle is slightly more complex in the HPG-driven system. A muzzle resistor is needed to safely dissipate the energy remaining in the system after the projectile exits the muzzle. This quantity of energy is significant, as shown in Table 25, which shows the energy balance of the system. Note that a total of 36.4 MJ remains to be disposed of after the projectile exits.

Table 25 ENERGY BALANCE

Time (s)	HPG Energy (MJ)	Inductive Energy (MJ)	Losses (MJ)	Kinetic Energy (MJ)
0.0	52.2	0.0	0.0	0.0
0.140	32.1	12.0	8.1	0.0
0.143	31.6	4.8	12.6	3.2
30.0	0.0	0.0	49.0	3.2

If there were no muzzle resistor, the 4.8 MJ of inductively stored energy would be dissipated rapidly by arcing between the rails. Some damage would result, depending on how effectively the arcing could be controlled. More important, however, is that the arc would extinguish when the inductive energy was dissipated, and only the HPG voltage would be left to sustain the arc. At this time, the HPG would still be storing close to 30 MJ, but would only be producing about 100 volts. After the arc extinguished, the launcher circuit would be opened, and no current would flow. This would leave brush friction as the only means of decelerating the HPG. Overheating of the brushes would result.

With a muzzle resistor in the system, a closed circuit exists whenever the HPG brushes are down. Therefore, current will flow, and an electromagnetic decelerating torque will exist, as long as the HPG is spinning and creating voltage. The muzzle resistance value should be large enough so that it does not draw significant current from the projectile. The resistance value should be small enough to make a reasonably small RC decay time constant. For this system, a muzzle resistance of 2 mΩ has been chosen. This value is 10 times the projectile armature resistance of 0.2 mΩ.

The muzzle resistor would be similar to the muzzle resistor of the EMACK launcher, shown in Figure 29. There are two blocks of stainless steel bolted across the rails. The overall size is dictated by heat capacity and temperature rise. The desired resistance is obtained by adding saw cuts to produce a convoluted current path. Two blocks are preferable to one, because symmetry can be maintained. The EMACK muzzle resistor shown in Figure 29 has a heat capacity of 15 MJ. The system currently under study would require a resistor approximately 3.5 times larger.

<u>Breech</u>

The barrel breech is the interface between the barrel rails and structure, busbars, preaccelerator, and opening switch. The breech of the HPG-driven system is similar to that of the capacitor-driven system.

3.2.2 Power Supply

<u>Homopolar Generator</u>

For this system a 52-MJ, 129-V, 2.1-MA homopolar generator has been conceptually designed. This design uses many of the concepts and features used in developing the EMACK and EGLIN machines. The EMACK machine was originally operated at 17 MJ, and is presently being upgraded to 30 MJ. It is presently in operation at ARDEC in Dover, NJ. The EGLIN machine, designed and operated at 10 MJ, is at EGLIN AFB, Florida.

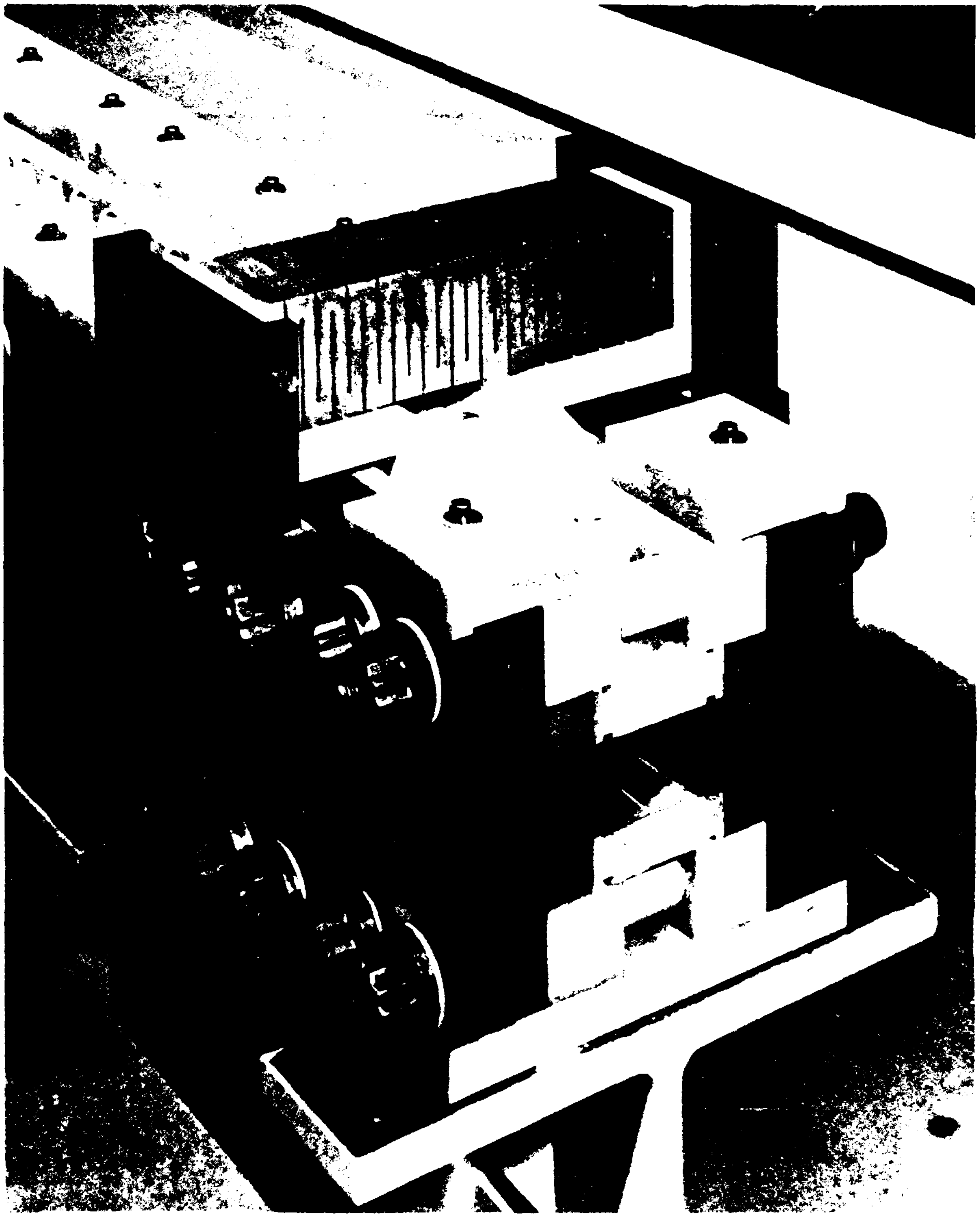

Figure 29. The EMACK muzzle resistor has a heat capacity of 15 MJ. The bore is 2 in. x 2 in.

The EMACK HPG is shown in Figure 30. This photo shows the rotor, stator structure, and brush actuation cylinders. The design of the 52-MJ HPG is similar to EMACK. The two designs are compared in Table 26.

The 52-MJ HPG design consists of a rotor with a copper-plated surface. This design gives high energy density, ruggedness, and low brush contact drop at the surface. The center section of the rotor is a solid steel cylinder with a diameter of 90 cm (35 in.) and a length of 68 cm (27 in.). This steel cylinder provides the bulk of the rotor's inertia (334 kg-m^2) and energy storage capability. The non-driven end of the rotor shaft passes through an oil seal, and rides on a hydrodynamic, tilted pad bearing. The driven end of the shaft rides on a combination hydrodynamic journal and thrust bearing. There is an oil seal on each side of the drive-end bearing

The outer ends of the 68-cm long rotor cylinder serve as current collector rings. These collector rings are each 12.7-cm (5-in.) wide, and have an area of 3,591 cm^2 (556 in^2). Current is collected from the rotor surface by monolithic sintered copper graphite brushes that are identical to those used in the EMACK and EGLIN machines. Each brush measures 12.7 mm (0.50 in.) by 3.2 mm (0.125 in.), and there are seven axial brush rows per collector ring, with 396 brushes per row. This results in 2,772 brushes, and 1,118 cm^2 (173 in^2) of total brush area per collector ring. The maximum current density in the brush is 1,878 A/cm^2 (12,118 A/in^2), which is 10% less than EMACK. Brush current density is a key indicator for heating of the brushes and rotor surface.

A second important parameter with regard to brush design is the rotor tip speed, for this affects frictional losses, and therefore heating of the brushes and rotor surface. EMACK operates at 225 m/s, and the 52-MJ machine operates at a slightly higher value.

The thermal behavior of the brush rotor interface is the most critical part of HPG design. The parameters that have the most effect on this thermal behavior are the brush current density, rotor tip speed, and rotor surface material. In comparing the 52-MJ machine with the proven EMACK design, one sees from Table 26 that the 52-MJ design has

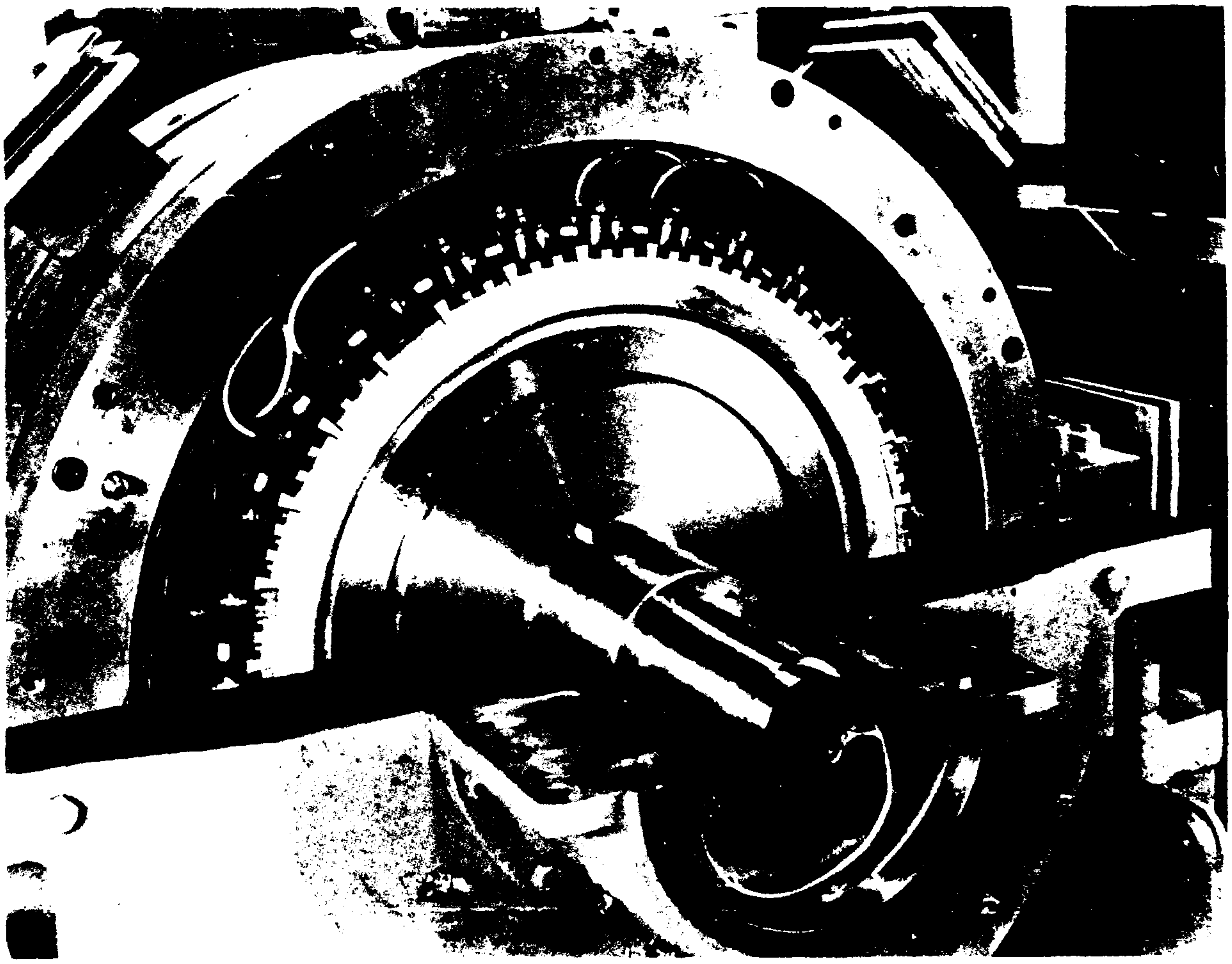

Figure 30. EMACK homopolar generator.

Table 26

COMPARISON OF EMACK AND 52-MJ HPGs

Parameter (units)	EMACK	52-MJ HPG for BRL	Selected Δ
Current (MA)	1.5	2.1	+40%
Rotor Rad. (cm)	32.0	45.0	+40%
Rotor Lgth. (cm)	62.0	68.0	+10%
J (kA/cm^2)	2.06	1.88	-10%
Tip Speed (m/s)	225	250	+11%
Speed (rad/s)	705	559	
Voltage (V)	105	129	
C (F)	3200	6321	
Energy (MJ)	17.6	52.0	
Inertia ($kg\text{-}m^2$)	71.0	334	
Surface	Cu. Pl. Alum	Cu. Pl. Steel	

10% less current density, 11% greater tip speed, and a similar rotor surface. Therefore, the 52-MJ machine should exhibit acceptable thermal behavior and reliability at its rated output of 2.1 MA.

One disadvantage of the HPG-driven system is its poor efficiency in the single shot mode. As a result of this poor efficiency, there are relatively high amounts of stored energy, both before and after the shot. The main reason for this poor efficiency is that a conventional, steel core HPG is inherently a low voltage machine, and therefore takes a long time to charge up the inductor.

There is another type of HPG that is fundamentally different from the steel core, so-called conventional HPG. It is a self-excited, air-core (SEAC) HPG. The Westinghouse STC has designed a SEAC HPG on an ARDEC contract.[3] This type of machine has two main features that increase its voltage output and efficiency. One feature is that the magnetic flux resides in air, so that higher flux densities can be obtained. Secondly, the excitation coils are part of the charging circuit, so that the excitation current, flux density, and voltage output all increase as the inductor charges. This results in a more rapid and efficient inductor charging.

Although the SEAC HPG technology is very promising, it has yet to be successfully demonstrated. Therefore, it was not chosen for this design, since the design philosophy is to select proven, low risk technology.

The HPG rotor is accelerated to its design speed of 5340 rpm by an electric drive system. This drive system utilizes a 320-hp dc motor coupled to a speed increasing gear box and an over-running clutch. The over-running clutch protects the speed increaser during rapid rotor deceleration that normally occurs with each test. The over-running clutch couples the HPG rotor to the high-speed output shaft of the gearbox. The clutch is manufactured by the Hilliard Corporation, Elmira, New York. The clutch disengages when there is no shaft torque.

---

3. "Self-Excited Air Core (SEAC) Homopolar Generator Concept Design," D. W. Ohst and D. Pavlik, ARDEC Contract DAAA21-85-C-0214, September 30, 1986.

This disengagement occurs automatically, without any control signal. In a normal shot scenario, the drive motor would be turned off when the HPG reaches its desired speed. This loss of drive torque would disengage the clutch. The drive motor and gear box would quickly come to a stop, while the HPG rotor remained coasting at speed. With the rotor uncoupled, the high rotor deceleration experienced during launching would not be transmitted into the gearbox and drive motor. The clutch also facilitates the ability to reverse the drive components prior to firing, further protecting the speed increaser in the event that a potential fault condition, such as rotor reversal, occurs. This drive system will take approximately 10 minutes to reach the design speed.

Opening Switch

A homopolar-driven EML needs a switch that can efficiently conduct high currents in the closed position, rapidly open during peak current, then remain open while standing off the barrel breech voltage during projectile acceleration. When the opening occurs, the projectile must be located in the breech of the gun. Therefore, the opening switch and the preaccelerator must be well synchronized. If opening occurs before the projectile reaches the breech, then the arc will continue to dwell in the switch and potentially damage it. If the opening occurs after the projectile has entered the breech, then the inductance and resistance through the projectile will be greater because it is farther away. This will result in a slow, inefficient commutation of current into the projectile. The opening switch requirements are as follows:

Closed Position	
Resistance	2 $\mu\Omega$
Action	3.5×10^{11} A^2s
Current	2.1 MA
Opening (commutating) Function	
Commutation Time	500 μs max
Peak Commutation Voltage	2 kV
Actuation Jitter	0.1 ms, max
Open Position	
Standoff Voltage	1.5 kV

Two general types of switches were considered. These are metallic interrupting switches, and semiconductive opening switches. Semiconductive devices were ruled out because development is needed to meet the closed position conducting requirements of 3.5 x 10^{11} A^2s and 2.1 MA. Metallic interrupting switches have been made and demonstrated at peak currents approaching 2 MA. This approach was selected because the technology exists today, and it was judged to be the low risk approach.

Two types of metallic interrupting switches were considered. These were a mechanical rail switch, and an explosive switch. A rail switch, similar to the EMACK rail switch, would meet all the above requirements with the exception of the actuation jitter time. The jitter time of a rail switch would be about 2 ms at best, or about 2000 times greater than what it needs to be to obtain proper synchronization with the preaccelerator. The jitter time is defined as the uncertainty in predicting the time interval from when the switch actuation command is given to when the commutation actually occurs.

An explosive opening switch design was chosen because the jitter time of 0.01 m/s is very low. In this time interval, the preaccelerated projectile, with a velocity of 500 m/s, only moves 5 mm. This is a negligible amount, from the standpoint of commutation circuit geometry and overall commutating efficiency. The explosive actuation time of 50 μs is quite low, and is therefore another attractive feature of the explosive opening switch. In this time interval, the preaccelerated projectile moves only 25 mm. Therefore, the explosive switch can be actuated by a sensor that is very close to the end of the preaccelerator. The explosive switch basically consists of two parallel copper plates that are bolted onto the busbars so that they are a series element in the HPG-inductor charging circuit. This plate assembly is also connected in parallel with the barrel. The plates are each machined in two places in order to weaken them. Shield mild detonating cord (SMDC) assemblies are placed in the machined grooves. The explosion causes the plates to fracture at the machined grooves, so that

two series arcs are formed in each plate. The plates and SMDC assemblies would have to be replaced with each shot.

The Westinghouse STC has built and tested this type of switch at approximately 100 kA. The concept can be easily scaled up to 2.1 MA.

Pulse Shaping Inductor

The baseline system design calls for a 5.43-μH, 15-$\mu\Omega$, 2.1-MA inductor. Additional desirable features are:

1) Variable inductance
2) No external magnetic fields
3) Magnetic fields reside mainly in air instead of conductor
4) Inexpensive

A coaxial design has been selected that meets all these requirements and desired features. The outer coaxial inductor has a nominal outer diameter of 2 m (79 in.). The outer conductor is 13-mm (0.5-in.) thick aluminum. The inner conductor is a copper tube with an outside diameter of 23 cm (9 in.) and an inner diameter of 16.5 cm (6.5 in.). This configuration has an R' of 1.47 $\mu\Omega$/m, and an L' of 0.52 μH/m. The required length is 10.5 m.

A practical embodiment of the design is shown in Figure 31. The entire conductor consists of three stages that are each 3.6-m long. This size is convenient from the standpoint of material availability, and ease of handling. The outer conductor is formed by bolting eight aluminum plates onto an octagonal steel skeleton. There would be no close tolerance machining or critical assembly processes involved. The aluminum plates could be sawcut to size, and then match marked and drilled at assembly. At the end of the inductor, busbars connect the center flange to the outer aluminum plates. If inductance changes were anticipated, then the center conductor could be made with several flanges spaced along its length, and the outer aluminum plates could have corresponding hole patterns to accept the busbars. With these

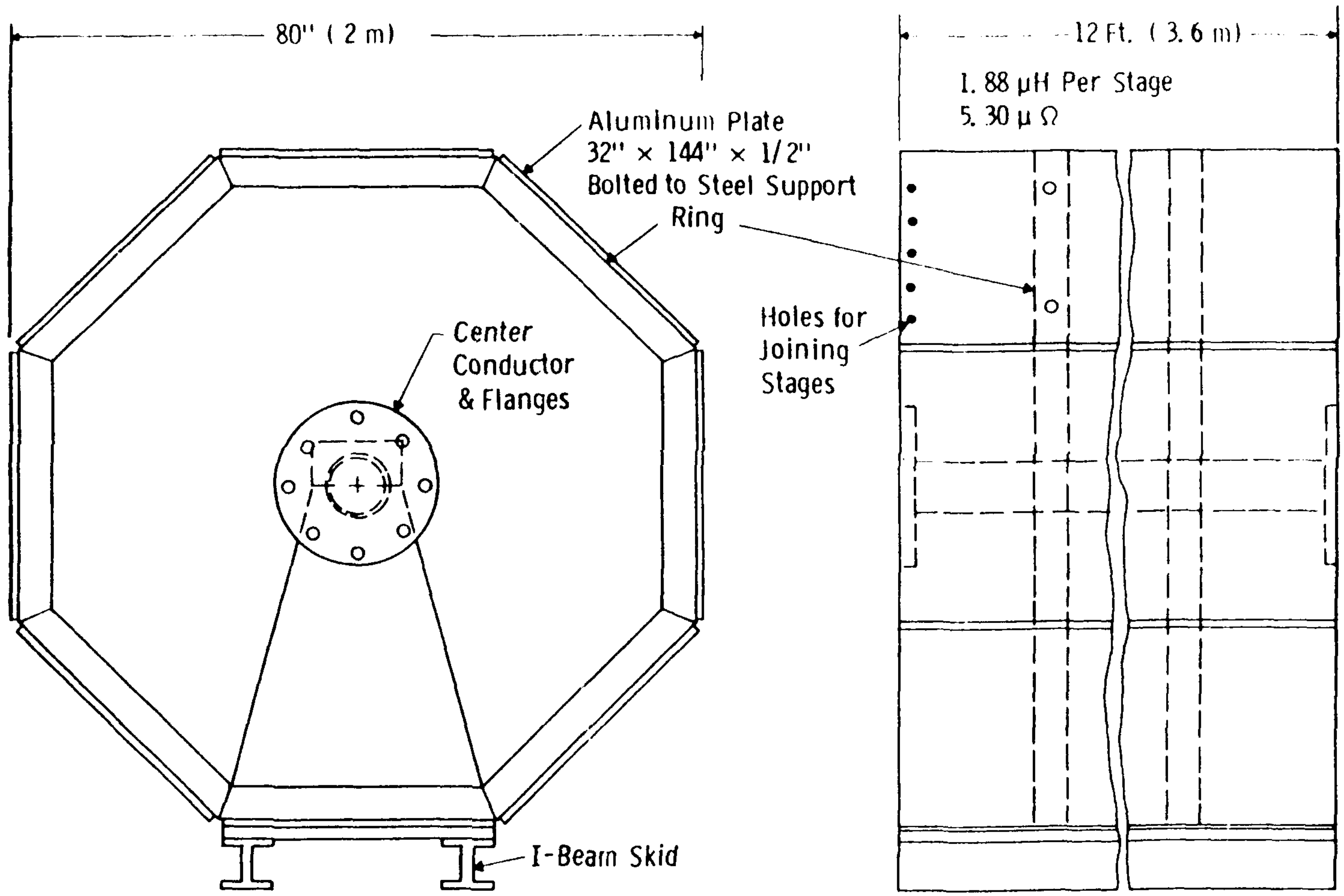

Figure 31. Coaxial inductor stage.

accommodations built in, inductance changes become a simple matter of moving the busbars to a different flange.

Buswork/Cabling

Buswork is required to join the HPG, inductor, barrel breech, and explosive opening switch. The buswork consists of copper bars and plates, typically 1-1.5 in. thick. The total resistance is 11 $\mu\Omega$. The HPG contains eight pairs of output terminals. These eight pairs of terminals are spaced 45° apart on the axial center plane of the HPG. Each pair contains a negative terminal and a positive terminal. Eight copper bars join the positive HPG terminals to the aluminum plates on the inductor. This is a short, straight run because the HPG and inductor are coaxial, and spaced closely together, as shown in the facility layout in Figure 32.

The current travels down to the end of the inductor, where it is bussed into the center copper tube. The current then travels back to the HPG end of the inductor. The center flange of the inductor is bolted onto the positive feeder plate that runs to the barrel breech and switch. Current travels back from the breech through the negative feeder plate. The feeder plate pair is spaced closely to minimize inductance and space. The feeder plates are each 3.81 cm (1.5 in.) thick by 45.7 cm (18 in.) tall x 2.9 m (113 in.) long. The negative feeder plate is connected to the negative HPG terminals via eight copper bars. All bars connected to the HPG terminals have a cross section of 2.54 cm (1 in.) x 20.3 cm (8 in.).

All bus joints are bolt lap joints. Contact areas are silver plated to minimize corrosion and contact resistance. Each joint has a minimum of one 0.75-10 grade eight bolt for every 75 kA passing through it.

3.2.3 Instrumentation and Controls, Diagnostics, and Data Acquisition

Instrumentation and Controls

The I&C consist of a remote control room with monitoring and controlling instrumentation, electrical and fiber optic connections to

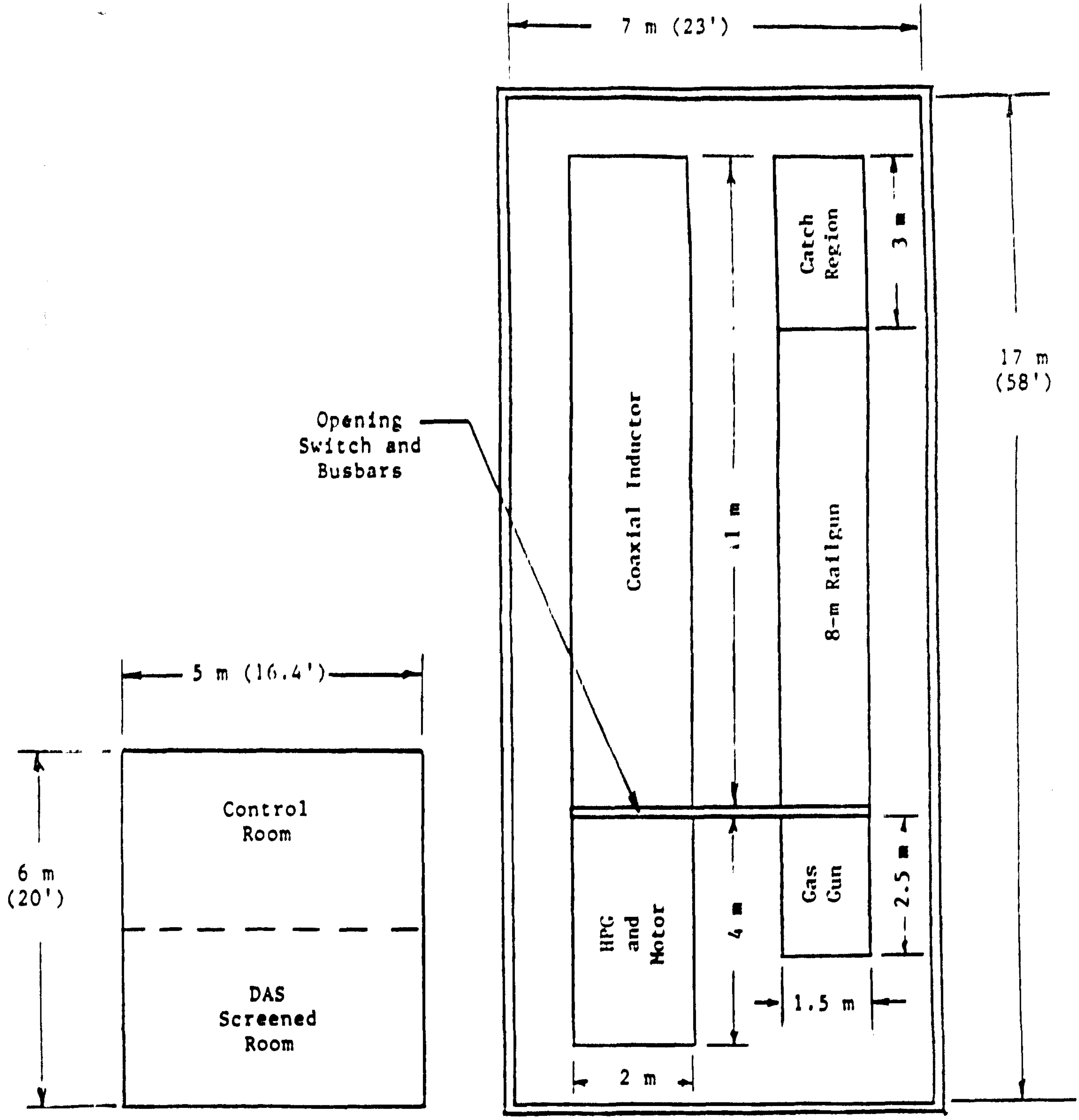

Figure 32. Homopolar-driven EML facility layout.

lab equipment, a trigger box, relays, interlocks, and cameras. The control room equipment includes a programmable logic controller, video monitors, and electrical interface hardware for operating the HPG drive motor, preaccelerator fast valve, HPG excitation power supply, and HPG brush actuation. The trigger box provides the electrical circuitry to fire the detonation card in the explosive opening switch. The I&C is capable of data logging from the start of facility preparation to test completion. With this capability, the various operational features such as interlock status, relay status, voltage levels, current levels, shaft speeds, and gas pressure levels will be recorded for later analyses.

Diagnostics

The gun related diagnostics are similar to those discussed in Section 2. Diagnostics unique to the HPG-driven system are listed in Table 27.

Data Acquisition System

The data acquisition system is similar to that described in Section 2.

3.2.4 Facility Design

The catch tank, barrel, and barrel mechanical supports are similar to those described in Section 2. Other facility features, unique to the HPG-driven system are described here.

Facility Services

One or more cranes are needed to assemble and maintain the system. The HPG weighs approximately 15 tons, and is the heaviest single component. Maximum flexibility would be obtained by installing a cr^ne capable of lifting the HPG. However, this would not be absolutely necessary, since the HPG could be installed using jacks, dollys, and forklift trucks. The rotor weighs 3410 kg (7500 lb), and will have to

Table 27

DIAGNOSTICS FOR HPG-DRIVEN EML

Sensor Type	Quantity Measured	Number of Sensors
RTD	Muzzle resistor temp	2
HPG Encoder	HPG rotor speed	1
Motor Encoder	Drive motor speed	1
Pressure Transducer	Switch chamber pressure	1
Excitation Shunt	Excitation current	1
Pressure Transducer	Brush manifold pressure	4
Insulated Brush	Rotor voltage	4
Hall Probe	HPG flux density	4
Rogowski Coil	HPG terminal current	8
Accelerometer	HPG vibration	4
Accelerometer	Gearbox vibration	4
RTD	Bearing temp	8

be removed, inspected, and dressed periodically. To perform this operation a crane of sufficient capacity and fine manual control would be preferable.

The HPG bearings and the gearbox each have a closed loop oil system. House water would be needed to cool the oil in both systems. A third coolant system is needed for the HPG excitation coils. This should be a closed loop system with deionized water. Helium should be available for HPG cover gas, and dry nitrogen is needed to clean and purge the HPG after tests. The lube oil pumps uses 220-V, 3-phase power, and the drive motor uses 440-V, 3-phase power. A portable 5-kW gasoline generator should be available to keep the lube pumps running in the event of a power failure.

Facility Safety

The key hazards involving the HPG-driven system are the rotational energy of the HPG and drive system, and the explosives used in the switch. Generic EML problems include magnetic fields, barrel bore pressure, x-ray diagnostics, and projectile kinetic energy. Safe practices for storing and using the shield mild detonating cord are well established. Protection of personnel and equipment requires thorough recording and scrutiny of all data. Any damage to the generator would likely be foretold by trends in HPG data such as vibration, bearing temperatures, etc. All HPG sensors would trigger the appropriate abort action in the control system.

Facility Layout

The facility layout is shown in Figure 32.

3.3 COST ESTIMATE SUMMARY

The cost estimate for the HPG-driven EML is shown in Table 28.

Table 28

COST ESTIMATE SUMMARY
FOR THE HPG-DRIVEN EML FACILITY

Cost of Equipment

Item		Cost Estimate ($K)
Primary Power/Charging System		1637
Power Conditioning Equipment		166
Switching/Triggering Circuitry		203
Cabling & Buswork		225
Barrel & Mechanical Structure		412
Spare Barrel		169
Catch Tank		15
Screen Room & Data Acquisition System		248
Control Room Equipment/Safety		123
	Subtotal	3088
Installation Cost		
Engineering (0.33 person years)		56
Technician (0.5 person years)		43
	Subtotal	99
Contingency (15%)		478
	Total	3665

3.4 ADVANTAGES AND DISADVANTAGES OF THE HPG-DRIVEN EML

Advantages

- Meets performance requirements
- Proven technology, low risk
- Simple, relatively few components

Disadvantages

- Low efficiency and high stored energy
- Explosive switching is required
- Higher stored energy creates additional safety and energy management issues
- Energy cannot be distributed to the barrel with time-phased switching. This results in a longer barrel and a higher piezometric ratio.

4. DESIGN OF THE ELECTROTHERMAL LAUNCHER

An electrothermal launcher contains the basic elements indicated in Figure 33. There is a capillary chamber in which a plasma arc is struck. The electrical power comes from a pulsed power supply and the arc material is supplied by the ablation of paraffin or a similar hydrocarbon lining the capillary walls. The highly ionized, high velocity arc gases enter the fluid mixing chamber, rapidly heating the liquid contained in it. The arc is powered in such a way that the fluid is rapidly vaporized within a few hundred microseconds to a high initial pressure and temperature. During this rapid vaporization, the volume of the fluid which is in contact with the back of the projectile has not changed very much due to the projectile's inertia. The arc power is then adjusted in such a way that the high initial pressure in the mixing chamber is maintained constant for a certain holding period while the expanding gases drive the projectile down the barrel. The power is then turned off and the gases continue to expand adiabatically until the projectile leaves the barrel.

This brief description of the operating principal of the electrothermal launcher or electrothermal gun (ET-gun) is given by way of introduction and to put in perspective the discussion of the individual components which follows.

4.1 TRADE-OFF STUDIES

4.1.1 Description of Computer Codes

There are two separate computer codes which describe the processes occurring in the capillary chamber and the fluid mixing chamber. One of these, CAPIL, models the gas dynamics within the capillary chamber, including Joule heating, ablation of the wall material, and mass flow out of the chamber. Another program, ELTARC, models the gas dynamics within the mixing chamber and gun barrel,

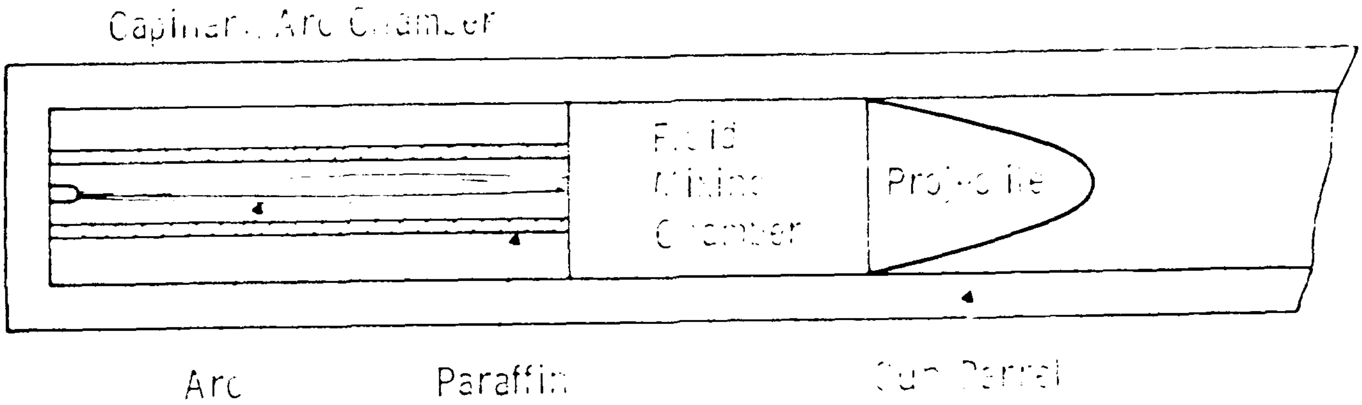

Figure 33. <u>Schematic of ET-gun and operation.</u>

including the projectile motion. Both of these codes are compressible gas dynamics codes which use MacCormack's method to solve the Navier-Stokes equations.[4] They are both 1-dimensional, transient codes. The results of these codes have been calibrated against data from an ET-gun built and operated by GT Devices. By adjusting one parameter, a wide variety of experimental data could be fit.

4.1.2 Presentation of Results

Many trade-off studies were performed using the above-mentioned codes. Certain constraints relating to barrel limitations need to be satisfied in the final design. These include keeping pressures below

4. R. W. MacCormack, "A Numerical Method for Solving the Equations of Compressible Viscous Flow," Paper 81-0110 at the AIAA 19th Aerospace Sciences Meeting, St. Louis, MO, Jan. 12-15, 1981.

about 100 ksi and gas temperatures in the barrel under 3500K. Because there is a pressure gradient in the capillary, being lowest at the end in contact with the mixing chamber, it was necessary to keep the mixing chamber pressure below about 75 ksi in order that the pressure at the opposite end of the capillary remain within bounds. The barrel diameter was set at 56 mm as a result of many trade-off studies. The mixing chamber fluid was chosen to be water because of its relatively low molecular weight and ease of handling.

The first step in the analysis was to run the barrel code, ELTARC, in order to see whether the design objectives could be met. We wished to accelerate a 65-g and a 200-g penetrator to velocities of 2.5-3.5 km/s. For the 56-m bore, we estimate that the sabot will weigh about 175 g. If we include the 15 g, or so of air ahead of the projectile in the mass to be accelerated, the gun needs to accelerate total effective masses of 255 g and 390 g, corresponding to the two penetrators. Results of ELTARC calculations for the heavier mass and for a pressure hold-time of 1 ms in the mixing chamber are shown in Figures 34 to 37. The barrel length was fixed at 5 m since the velocity curve begins to level off beyond this length.

Note in Figure 34 how the pressure directly behind the projectile drops off rather precipitously from the hold value in the mixing chamber. The ripple in this curve is due to compression and expansion pressure waves in the barrel which are well known phenomena. This pressure drop off leads to a rather high piezometric ratio for an ET-gun.

The gas temperature versus time profiles for the mixing chamber and near the base of the projectile are shown in Figure 35. The highest temperature is reached in the mixing chamber and it would also appear in the gas just outside the mixing chamber. The highest temperature is reached at the end of the hold time.

The mass flow out of the mixing chamber into the gun barrel is shown in Figure 36. The starting mass of water was 1 kg and this, in vapor form, is nearly all inside the barrel by the end of the shot.

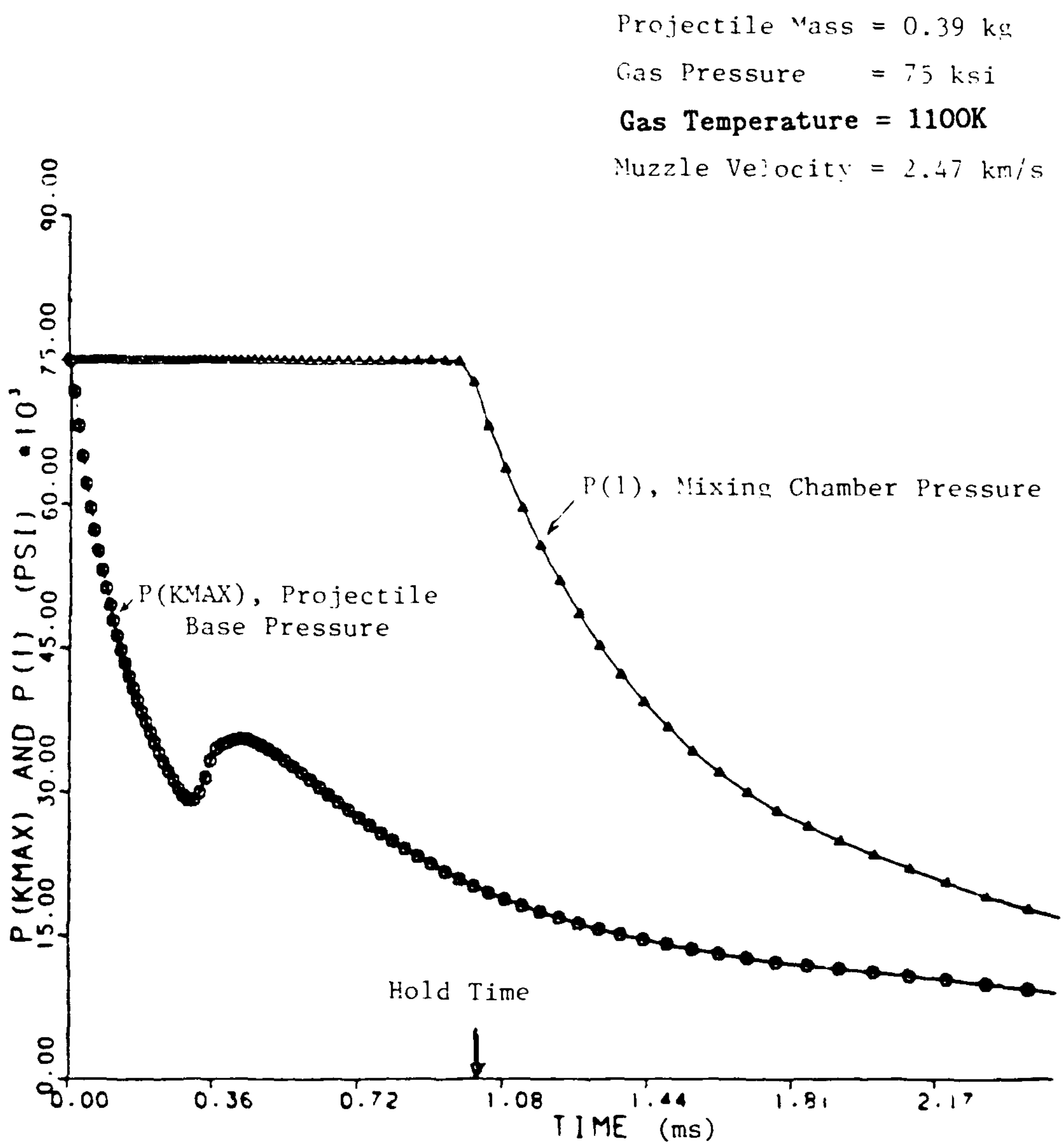

Figure 34. Comparison of projectile driving pressure and mixing chamber pressure.

Projectile Mass = 0.39 kg
Gas Pressure = 75 ksi
Gas Temperature = 1100K
Muzzle Velocity = 2.47 km/s

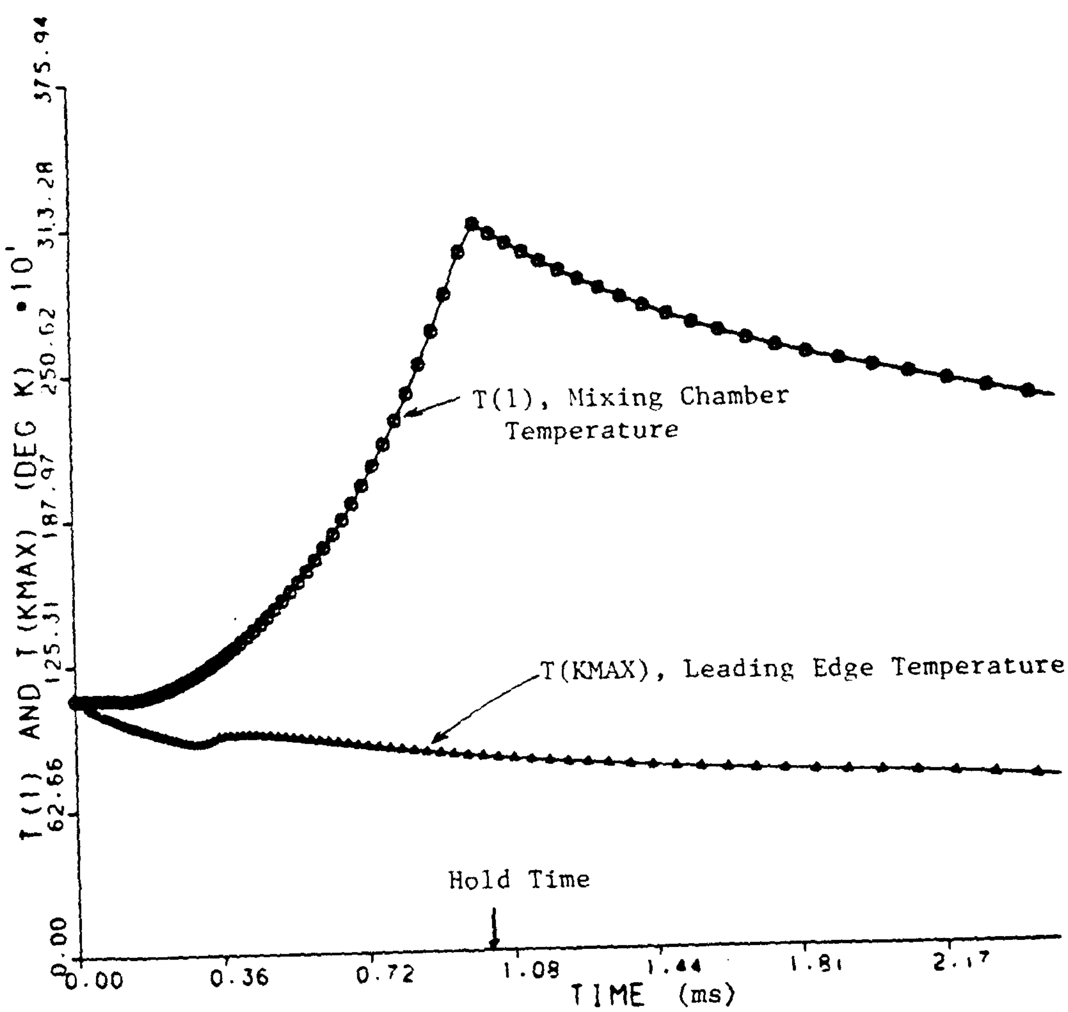

Figure 35. <u>Comparison of propellant temperatures in the mixing chamber and at the base of the projectile.</u>

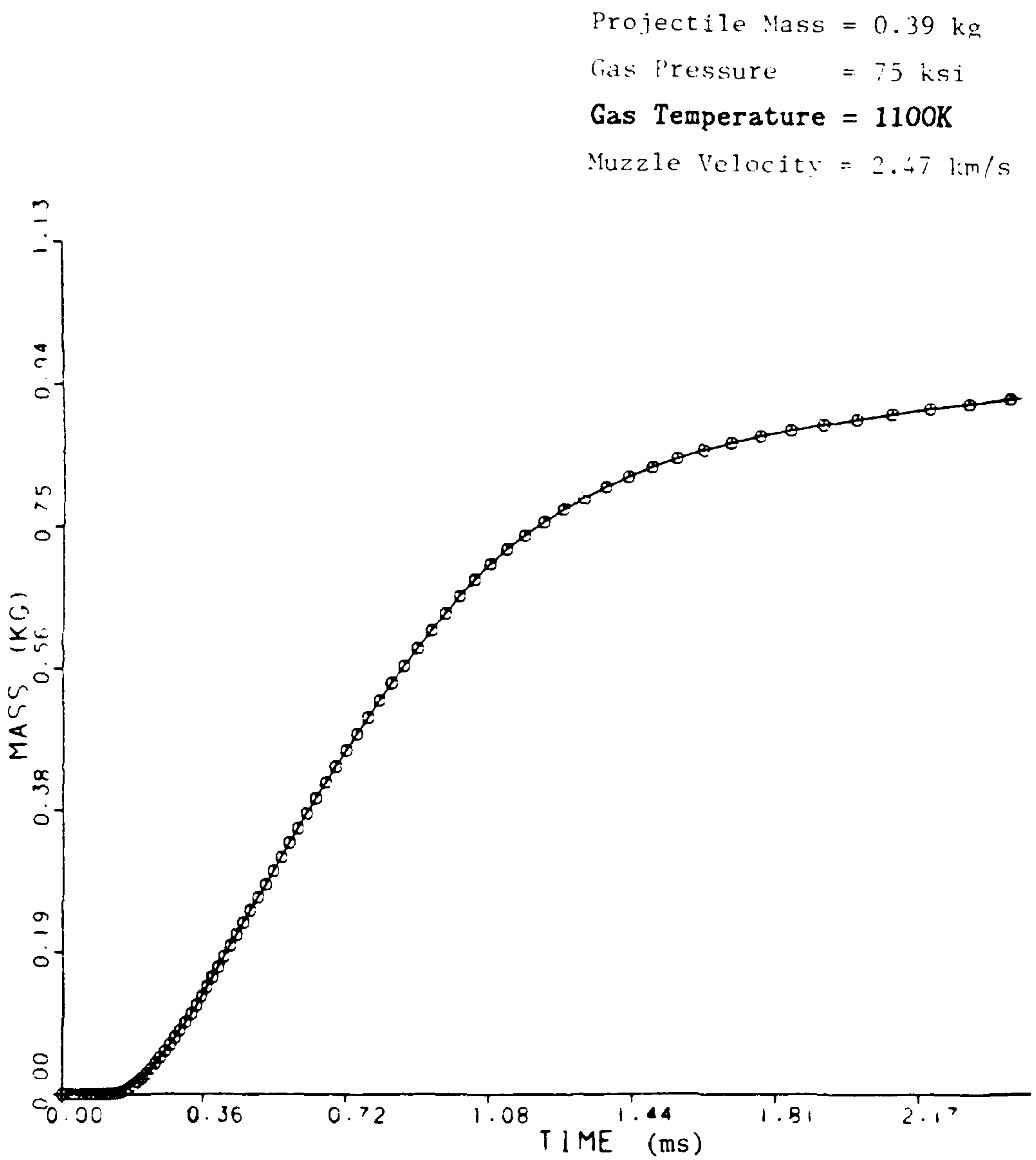

Figure 36. <u>Propellant mass flow into the bore of the gun.</u>

The velocity-time profile is shown in Figure 37. No frictional force was included in the calculation but this is not expected to be large for these guns. The velocity barely reaches 2.5 km/s. Since the velocity is leveling off towards the end of the shot, increasing the barrel length will not provide very much additional velocity.

The next step is to run the program CAPIL to simulate the performance of the capillary chamber. The program ETLARC calculates the input power to the mixing chamber needed to accelerate the projectile. In addition to this, the energy needed to bring the liquid water up to the holding pressure is needed. Assuming this energy is delivered over 300 μs determines the input power required for the vaporization phase. The powers needed in the vaporization and acceleration phases of the shot must be converted to a current input requirement to the capillary based on the capillary resistance and the number of capillaries. This is an iterative process since the capillary resistance is a function of the current. Figure 38 shows this dependence for a capillary chamber 1.5 cm in diameter and 30-cm long. These capillary dimensions were arrived at through trade-off studies, and the number of capillaries required is five.

For the highest current in the capillary, Figure 39 shows the pressure profile along the capillary tube. Note the gradient going from 95 ksi at the closed end to about 75 ksi at the end which opens into the mixing chamber. Figure 40 shows the temperature profile in the capillary which is essentially uniform at about 35,000K. Figure 41 shows the velocity profile of the hot gases along the capillary tube. It is important that this remain below Mach 1 at the exit to avoid choke off. Although the scale cannot be seen on the figure, the exit Mach number is below 0.5. Figure 42 shows the mass flow out of the capillary. For the total time the arc is on, viz., a couple of milliseconds, the total mass of paraffin leaving the capillary is a few grams.

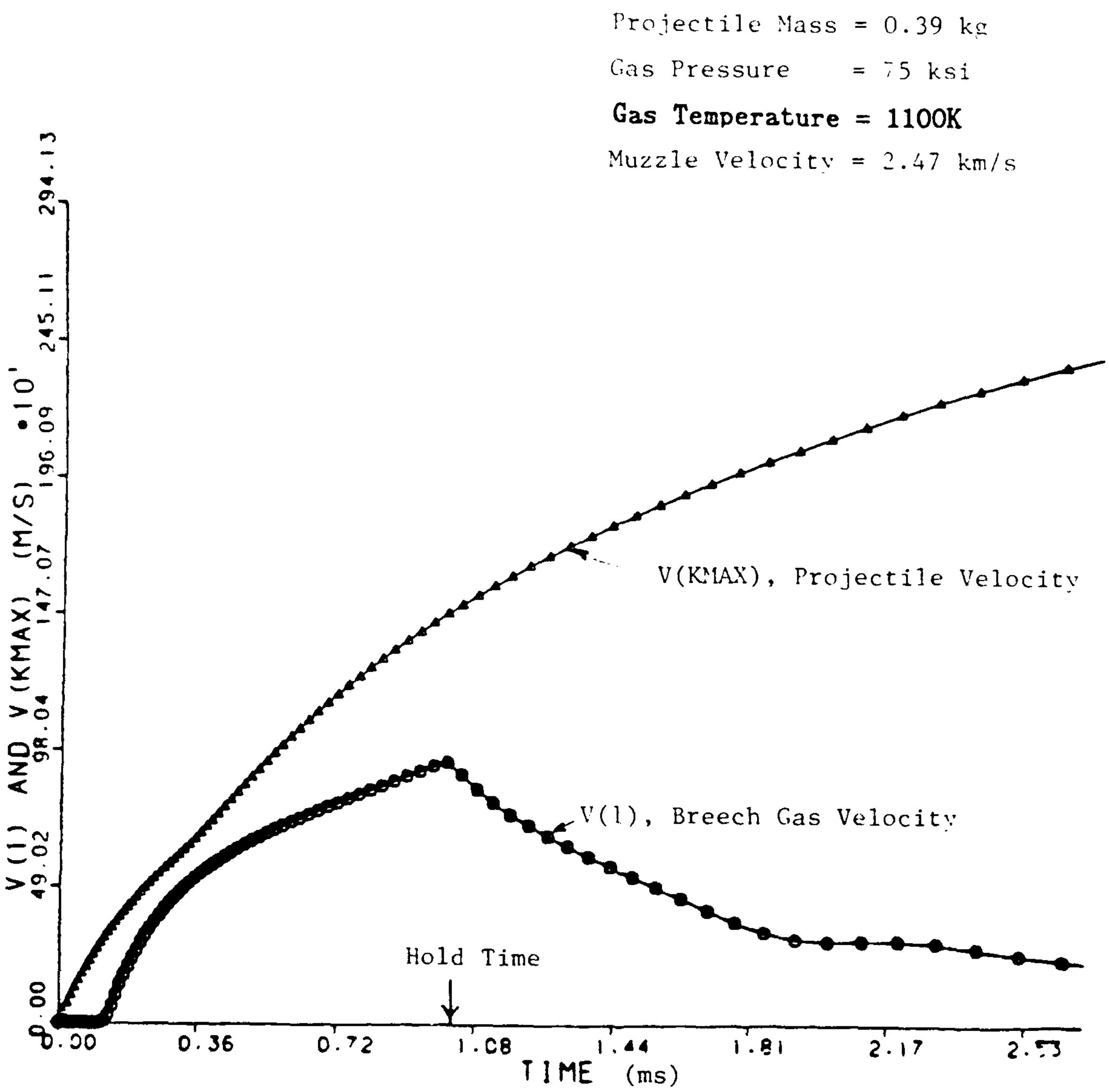

Figure 37. Comparison of propellant velocity at the breech of the gun with the projectile velocity.

Curve 757?8-A

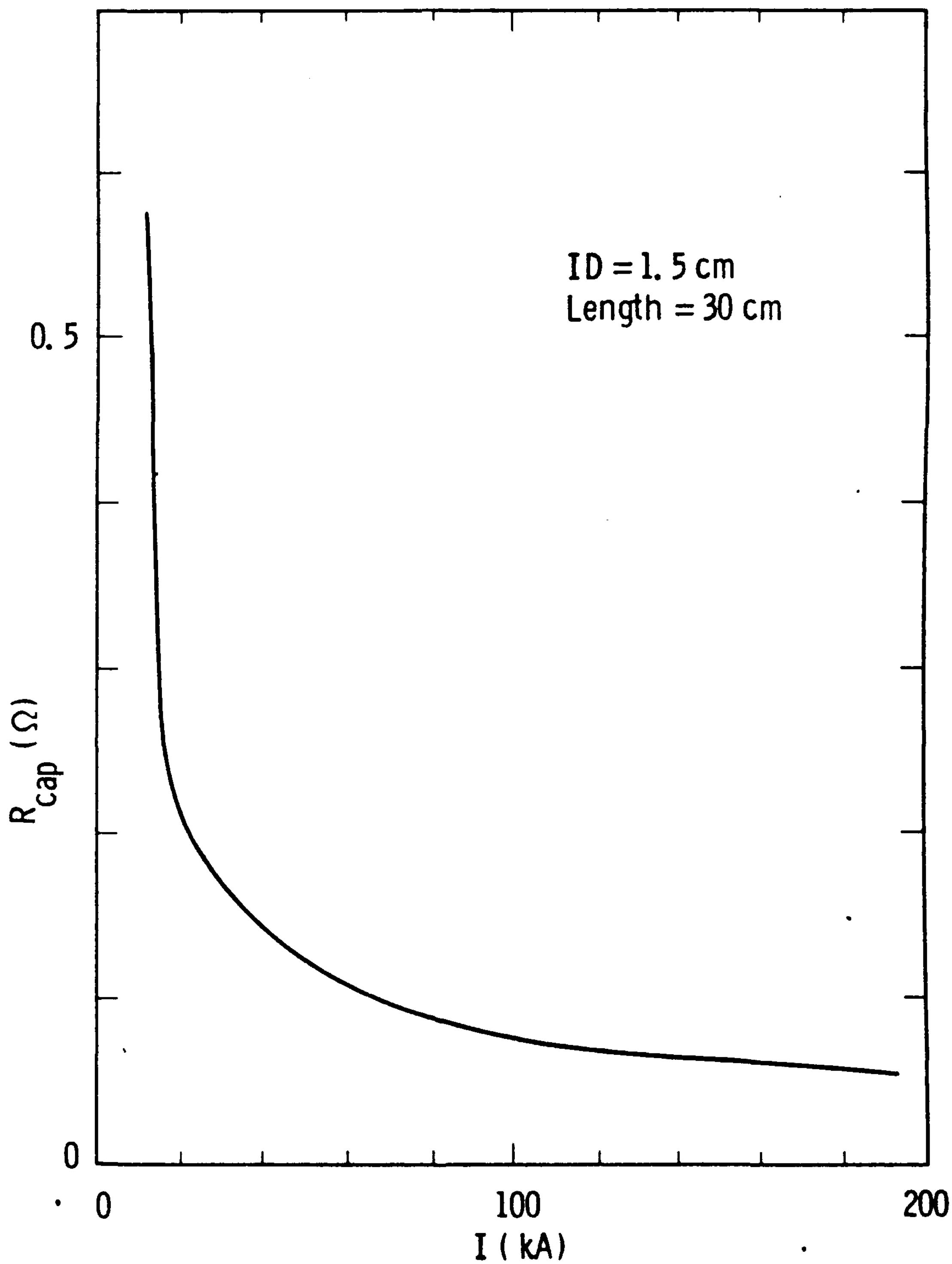

Figure 38. Capillary resistance as a function of the current flow.

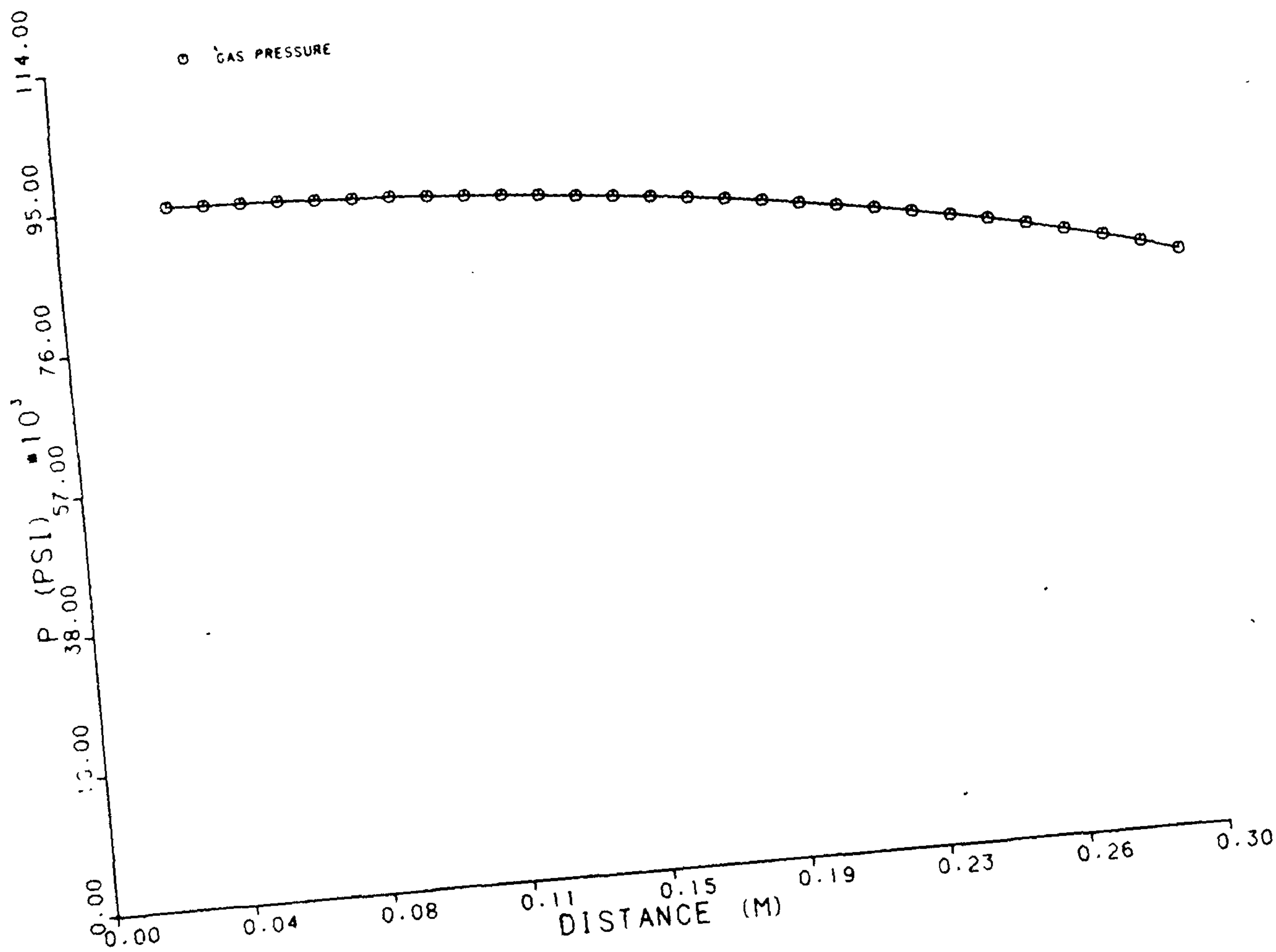

Figure 39. Pressure profile along a capillary tube (length = 30 cm; diameter = 1.5 cm).

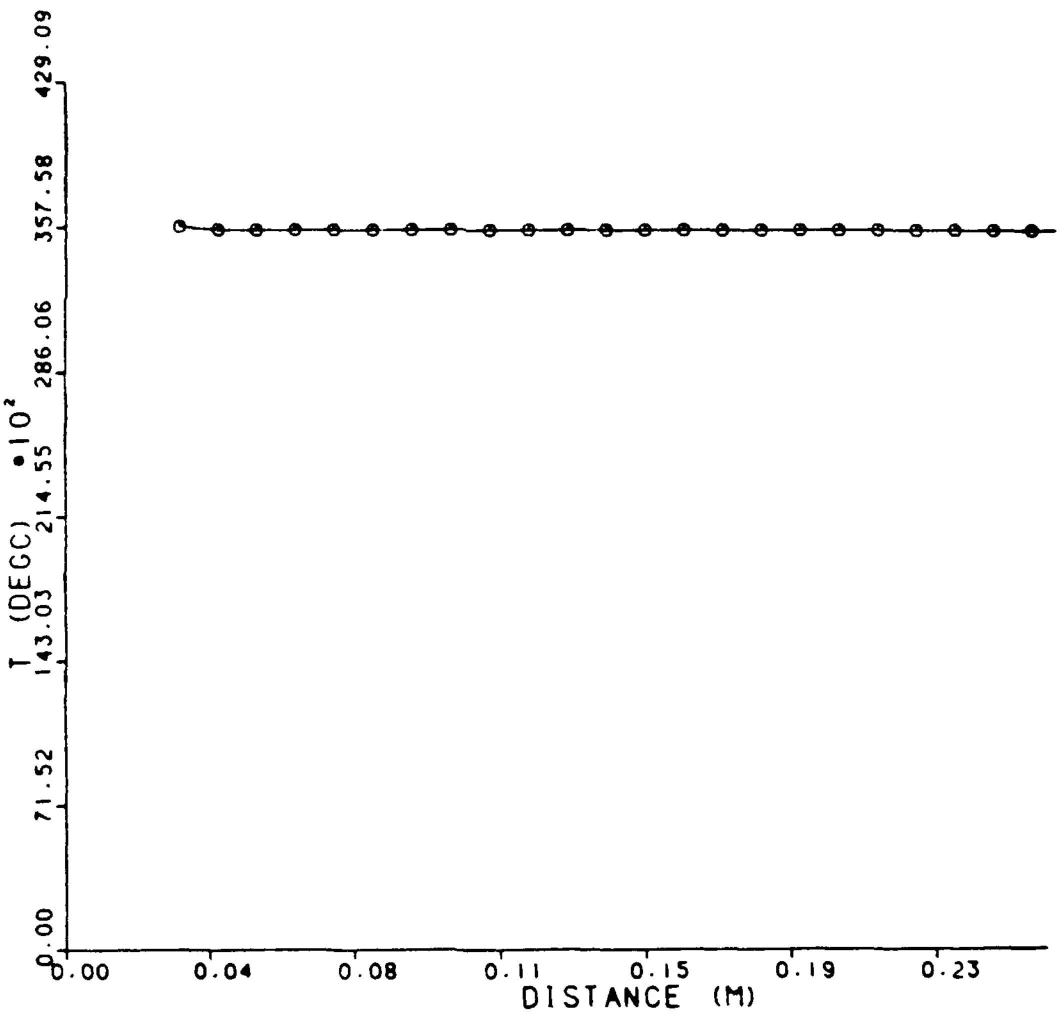

Figure 40. Plasma temperature profile along a capillary tube.

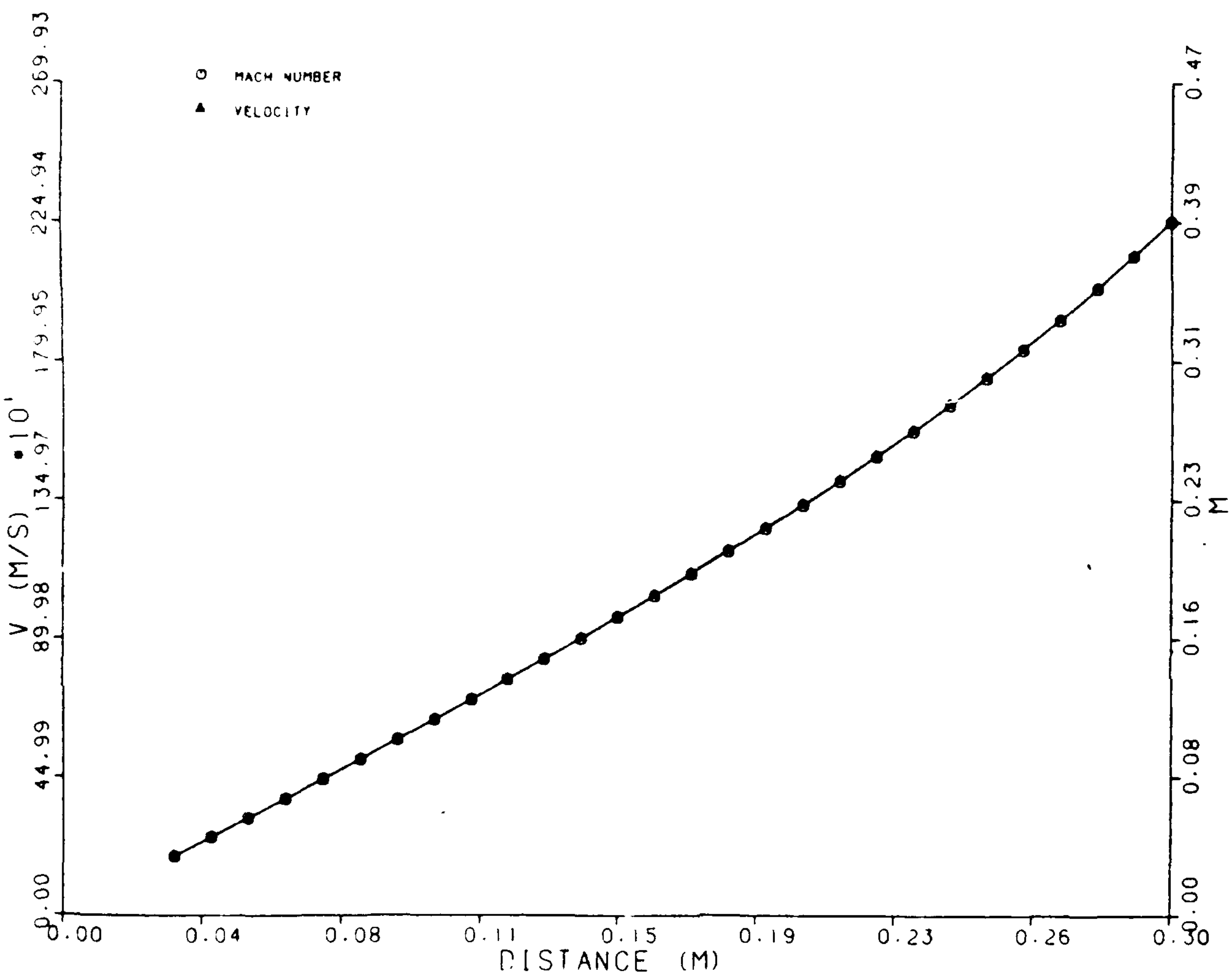

Figure 41. Velocity profile along a capillary tube (length = 30 cm; diameter = 1.5 cm).

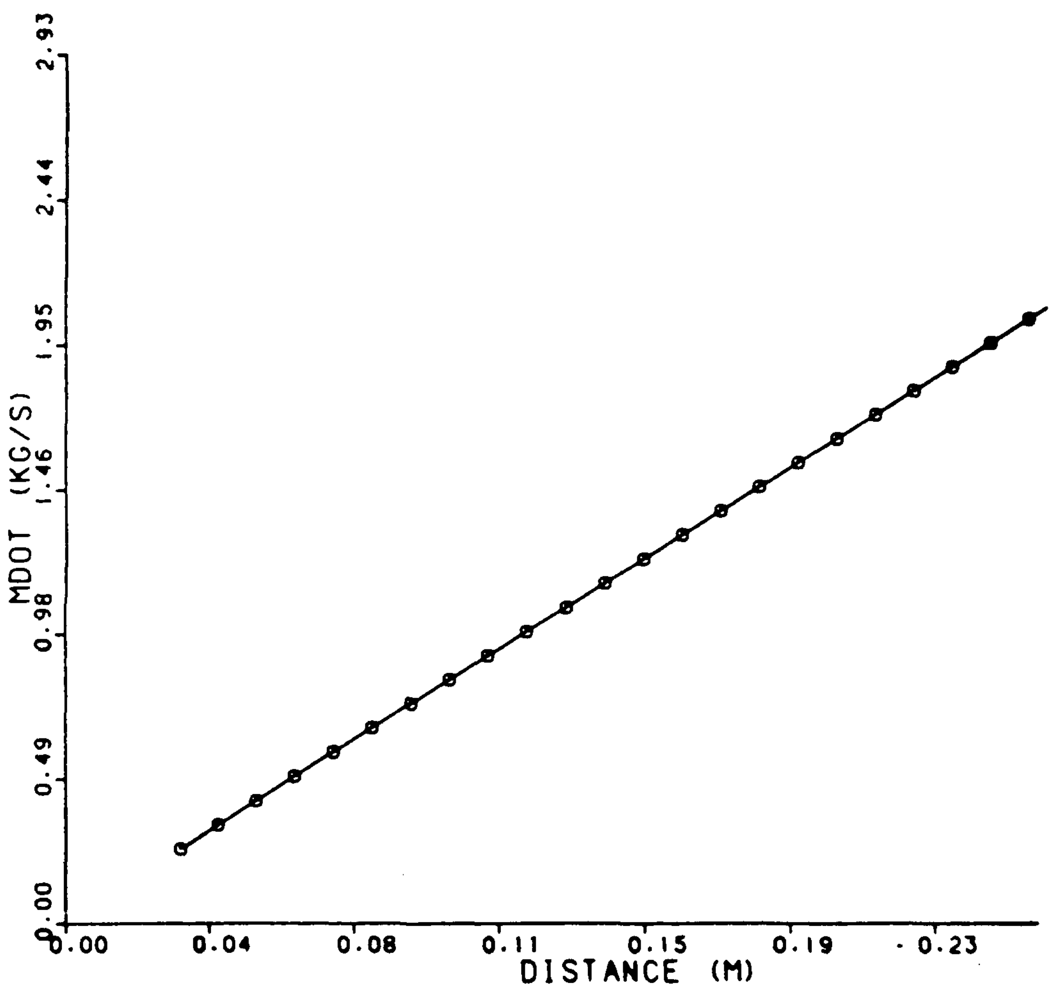

Figure 42. <u>Mass flow rate out of capillary.</u>

4.1.3 Selection of Parameters for the Launcher

Many trade-off studies were performed, such as varying the mixing chamber mass, the hold time, and other variables to a more limited extent. Results are presented in Table 29. Note that as the mass of water decreases, the maximum gas temperature increases as expected but the velocity increase is only marginal. For a given water mass, the maximum temperature increases as the hold time increases with only a slight increase in velocity. Even with longer barrels and higher holding pressures, the table indicates that the slightly higher velocities are achieved at the expense of unacceptably high gas temperatures.

As a result of these and similar trade-off studies, we arrived at the gun parameters in Table 30. We could only achieve about 2.5-km/s exit velocities for both penetrators. This limiting velocity is a function of the fluid selected in the mixing chamber and might be improved with a different choice. The pressure at the base of the projectile can be sustained at a higher level for a propellant in which the sound speed is higher at the working temperature. Therefore, low atomic mass molecules are desirable. Hydrogen gas would be a good choice, except it is not practical to achieve the required density. The explosive nature of the exhaust gas could also be a problem. Propellants composed of molecules that would dissociate into molecules of smaller mass at the high operating temperatures could be attractive, e.g., lithium hydride. However, the reactive lithium could be a problem. More tests need to be conducted to evaluate the propellant options. For tests that have been conducted with fluids such as methanol, no clear advantage has been seen over the use of water.

Chemically reactive propellants such as hydrogen peroxide, H_2O_2, have an advantage in that less electrical power is required to raise the temperature and pressure of the propellant in the mixing chamber to their operating values. However, the reactions occur predominantly in the mixing chamber and therefore are not effective in increasing the

Table 29

TRADE-OFF STUDY

Projectile Mass = 0.39 kg
Bore diameter = 56 mm
Barrel length = 5 m
Holding pressure = 75 ksi

Mass-water [kg]	Hold-time [ms]	Temp-max [deg-K]	Final vel [km/s]
1.0	1.0	3130	2.45
0.75	1.0	4670	2.52
0.5	1.0	>10000	2.59
1.0	1.5	8570	2.50
0.75	1.5	>10000	2.69
0.75	1.1	6120	2.58
0.75	1.2	8150	2.88 (a)
0.75	1.0	7180	2.83 (b)

(a) Barrel length = 8 m
(b) Holding pressure = 90 ksi

Table 30

FINAL DESIGN PARAMETERS

Bore diameter = 56 mm
Barrel length = 5 m
Holding pressure = 75 ksi
Holding time = 1 ms
Water mass = 1 kg

MIXING CHAMBER & BORE

Penetrator mass	200 g	65 g
Max gas temp [deg-K]	3130	3406
Exit velocity [km/s]	2.45	2.59

CAPILLARY CHAMBER (5 capillaries)

	(Worst Case)
Plasma Temperature [deg-K]	35300-35700
Plasma Pressure [ksi]	75-95

pressure driving the projectile. Therefore, the efficiency is improved, but the piezometric ratio is not.

Based on the information available today, water represents the best choice for a propellant for a test facility.

4.1.4 List of Required Components and Their Specifications

Based on our trade-off studies, the ET-gun will consist of a gun barrel 5-m long which has a 56-mm diameter bore and which is of nearly conventional design. The capillaries, mixing chamber, and projectile can be designed as a cartridge package which inserts into the breech of the gun barrel and is ejected after the shot. The electrical connections must be relatively easy to make and break. There will be five capillaries, 1.5-cm ID and 30-cm long connected in parallel to the current supply. They will be lined inside with a paraffin casing, thick enough to not vaporize through to bore metal during the shot. The volume of the mixing chamber is 1 liter and is filled with water. There is a diaphragm between the capillaries and mixing chamber which will break when sufficient pressure is built up in the capillaries. This is to prevent water from entering the capillaries before the shot. A wire fuse will connect the anodes and cathodes of the capillaries and will be designed to quickly vaporize, initiating the arc.

The power supply must deliver an initial burst of power within 300 μs to vaporize the water and bring it up to the holding pressure of 75 ksi. This will require 2.3 MJ of energy and a peak current of about 700 kA which divides equally among the five capillaries. After this initial burst of energy, a gradually increasing input power is required to maintain the holding pressure in the mixing chamber as the projectile moves down the bore. That is, the density of vapor decreases in the mixing chamber and therefore the temperature must increase to maintain the pressure. The total energy required in this phase is 3.5 MJ. The current in the individual capillaries should not be permitted to fall below ~ 20 kA or the arc resistance will get too high (Figure 38) and the arc will extinguish. Thus the power supply must have sufficient

capacitive storage to supply the required power bursts and the buswork must be able to handle the required currents for the 1.3 ms that the arc is on.

In addition to these basic components of an ET-gun, a complete system will have sensors and monitors to control its operation and data acquisition facilities to evaluate the results. This will require a screened room, data loggers, a small computer, and appropriate wiring. There will also be a catch tank, a mechanical support structure for the gun barrel and its recoil, and appropriate facilities for repair and maintenance.

4.2 DESIGN OF COMPONENTS

4.2.1 Barrel System

The barrel must be designed to withstand 100 ksi at the breech end, gradually tapering to 75 ksi at the mixing chamber and even lower pressures further down the bore. The bore is circular with a 56-mm ID along most of its 5-m length. The capillaries, mixing chamber, and projectile can be packaged as a cartridge as shown in Figure 43. The bore diameter increases in the mixing chamber and capillary section of the cartridge. The shape and size of the cartridge is very similar to conventional brass cartridges.

A cross-section through the cartridge in the capillary region is shown in Figure 44. There are five capillaries, symmetrically placed. They are embedded in an aluminum block which is insulated from the capillaries and from the outer brass shell. The aluminum provides the return path for the current and also withstands the high pressures developed in the tubes. A cross-section through the lines indicated in Figure 44 is shown in Figure 45. Here the mechanism by which electrical power is delivered to the capillaries is indicated as is the spring loaded connect and disconnect mechanism. The full current is delivered to the hot leads and it is subsequently shared among the capillaries.

Table 31 shows the cost breakdown for the barrel and cartridge. Note that the cost of the first cartridge depends on whether it is made

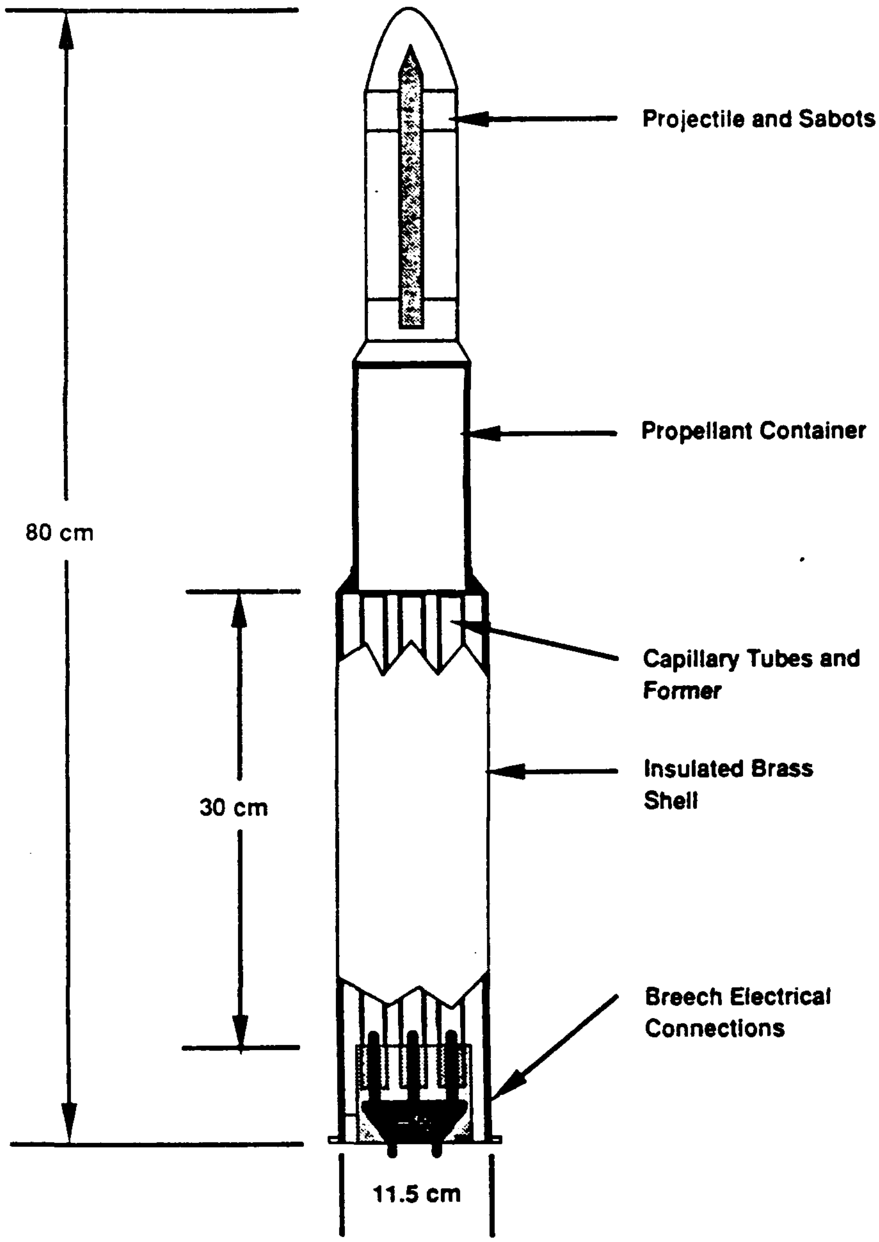

Figure 43. ET gun cartridge concept.

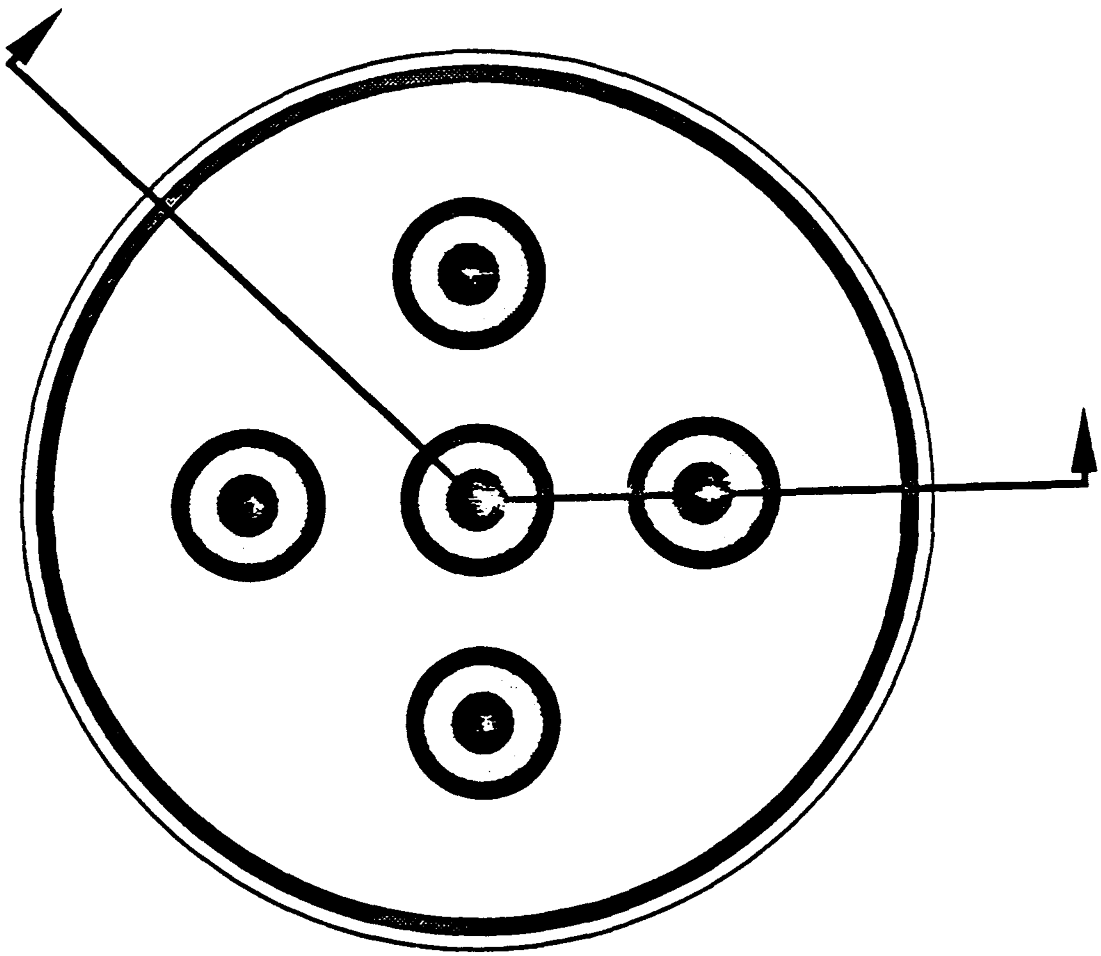

Figure 44. Cross-section through capillaries.

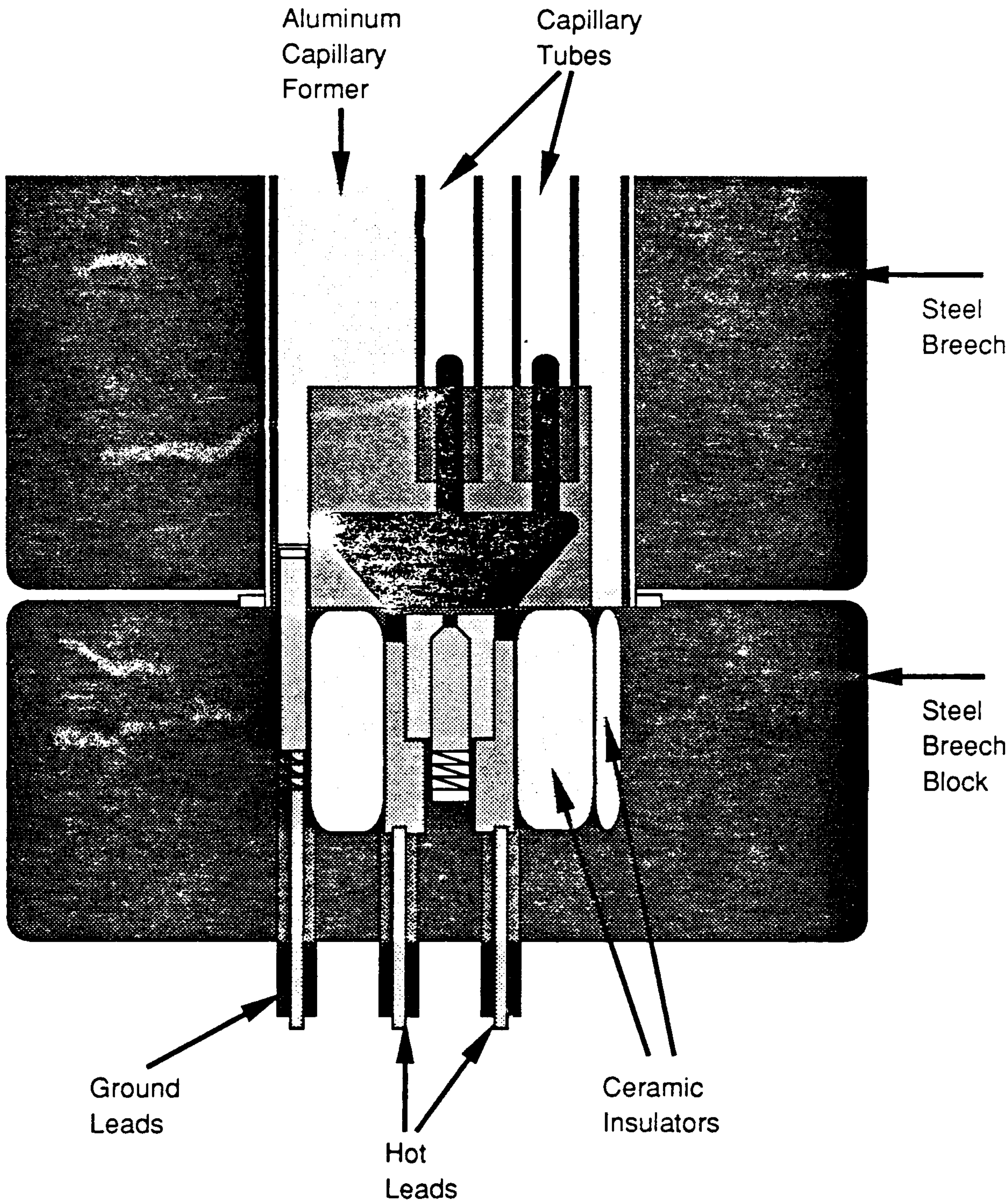

Figure 45. ET-gun breech design - cartridge concept.

Table 31
APPROXIMATE COSTS OF CARTRIDGES (Dollars)

(Materials & Manufacture)

Item	Method	1st part	100th part	1000th part
Alum former	Extrude & machine	10100	200	110
Electrode assy	Forge+weld+machine	10000	200	110
	(Machine+weld)	(1000)	(400)	(400)
Water tank	Extrude & glue	5000	100	20
	(Machine & glue)	(1000)	(500)	(200)
Capillaries	Cutoff & glue	400	20	10
Brass case	Deep draw	10000	120	20
Potting	Mat'l & labor	300	100	50
Projectile	Machine	1000	200	200
Sabot	Die cast	10000	100	10
	(Machine)	(600)	(200)	(200)
Assembly	Labor	500	50	50
		------	------	------
Costs When Planning for Multiple Cartridges		47300	1090	580
Costs Based on Limited Production		(24900)	(1790)	(1240)

COST OF BARREL AND ATTACHMENTS - 50000

in such a way as to facilitate the manufacture of subsequent cartridges. A high cost for the initial cartridge and its tooling results in cost savings for additional cartridges. The barrel manufacture is conventional.

4.2.2 Power Supply

The dotted line in Figure 46 shows the desired total current profile feeding the capillaries. It is based on a constant capillary resistance which is a fairly good approximation for the current levels involved. The solid line in the figure shows the current profile actually achieved with the circuitry to be described later. The code WATAND[5] was used to analyze the circuits. It permits the use of switches as circuit elements.

PFN for Vaporization Pulse

Figure 47 shows the pulse forming network used to create the initial 300-μs vaporization pulse. It consists of capacitors, inductors, and ignitron switches. These latter serve not only to discharge the capacitors but to crowbar them to keep the voltage from going negative. This latter precaution is necessary for the high power density capacitors which will be used (50-kJ, 22-kV rating). The capacitors will be operated at 21 kV and the capacitances as well as inductances required are shown in the figure. In addition, parasitic resistances and inductances were also modeled in the WATAND analysis. These are indicated in the figure, but the numerical values are omitted. An isolating diode is also required to prevent current from the circuitry used to produce the longer hold time pulse from feeding back. This diode must be sized to carry the required forward current and to withstand the back EMF. It will consist of series and parallel combinations of available power diodes. The load resistor indicated in

---

5. Code WATAND developed by the Dept. of Electrical Engineering, University of Waterloo, Waterloo, Ontario, Canada.

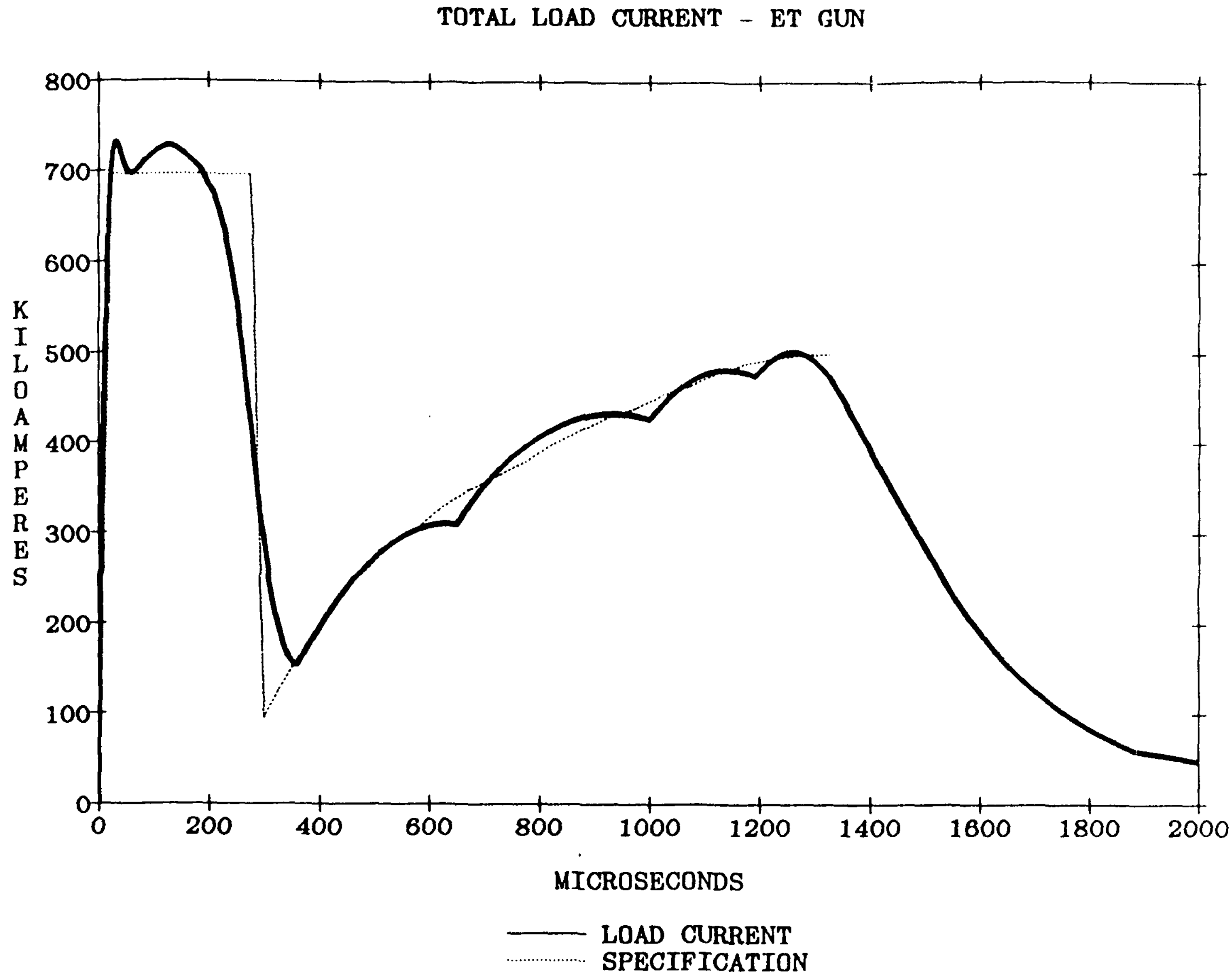

Figure 46. Comparison of capillary current profile that is obtained with the circuitry vs. the specified profile.

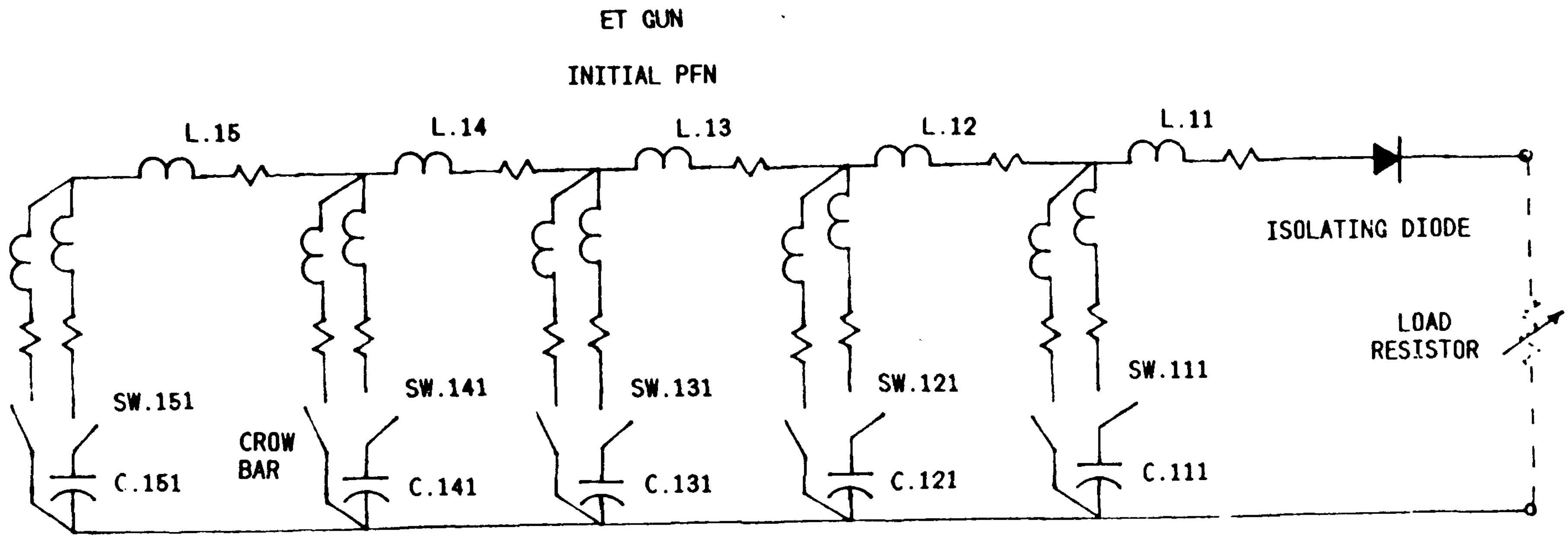

C.111	1236 uF	L.11	0.328 uH
C.121	1236 uF	L.12	0.265 uH
C.131	1648 uF	L.13	0.276 uH
C.141	2060 uF	L.14	0.325 uH
C.151	3296 uF	L.15	0.459 uH

Figure 47. Pulse forming network for providing vaporization current pulse (300 μs).

the figure is the parallel combination of capillaries and in general is variable although in this study it was modeled as a constant. All of the ignitron switches in series with the capacitors are fired simultaneously.

In addition to the net output current, currents and voltages across individual components were produced by WATAND in order to choose components of the proper size and rating for the actual circuit. An example of this type of output is shown in Figures 48, 49, and 50.

Phased LRC Circuits for Maintaining Pressure in Mixing Chamber

Figure 51 shows one of four circuits used to create the hold-time pulse. These are in parallel with each other and with the initial vaporization pulse network. These switches are fired sequentially to create the required rising hold time current pulse as indicated in Figure 52. These are simply LRC circuits with crowbars. Although one of these would suffice to give the required rising current pulse shape, there would be much more energy remaining at the end of the pulse and the efficiency would suffer.

The total capacitive energy stored is 5.8 MJ and for the heaviest payload the efficiency, defined as the final kinetic energy of the projectile + sabot divided by the initial stored capacitive energy, is 20%.

Table 32 presents detailed costing information for the components of the power supply. This list also includes the charging supply for the capacitors, required cabling, and dump resistors should it be necessary to dump the capacitors and abort a shot.

4.2.3 Instrumentation and Controls, Diagnostics, and Data Acquisition

The instrumentation and controls for the power supply are included in the costing information provided in the last section. Various diagnostics must be provided in order to monitor the shot. Some of these, such as x-ray cameras, may already be available on site. A shielded, screened room is needed to collect the various signals, store

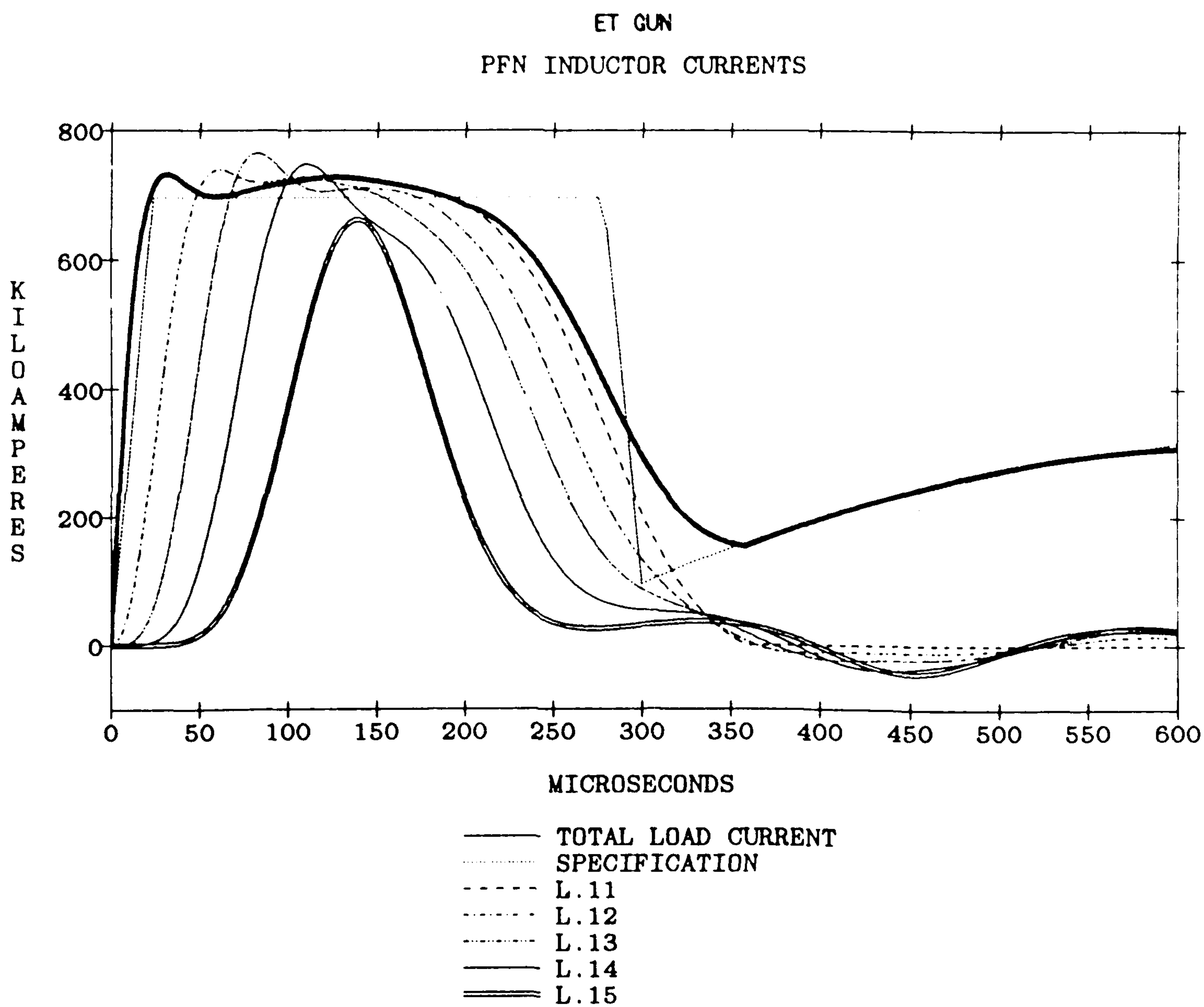

Figure 48. Currents through the PFN inductors (see Figure 47).

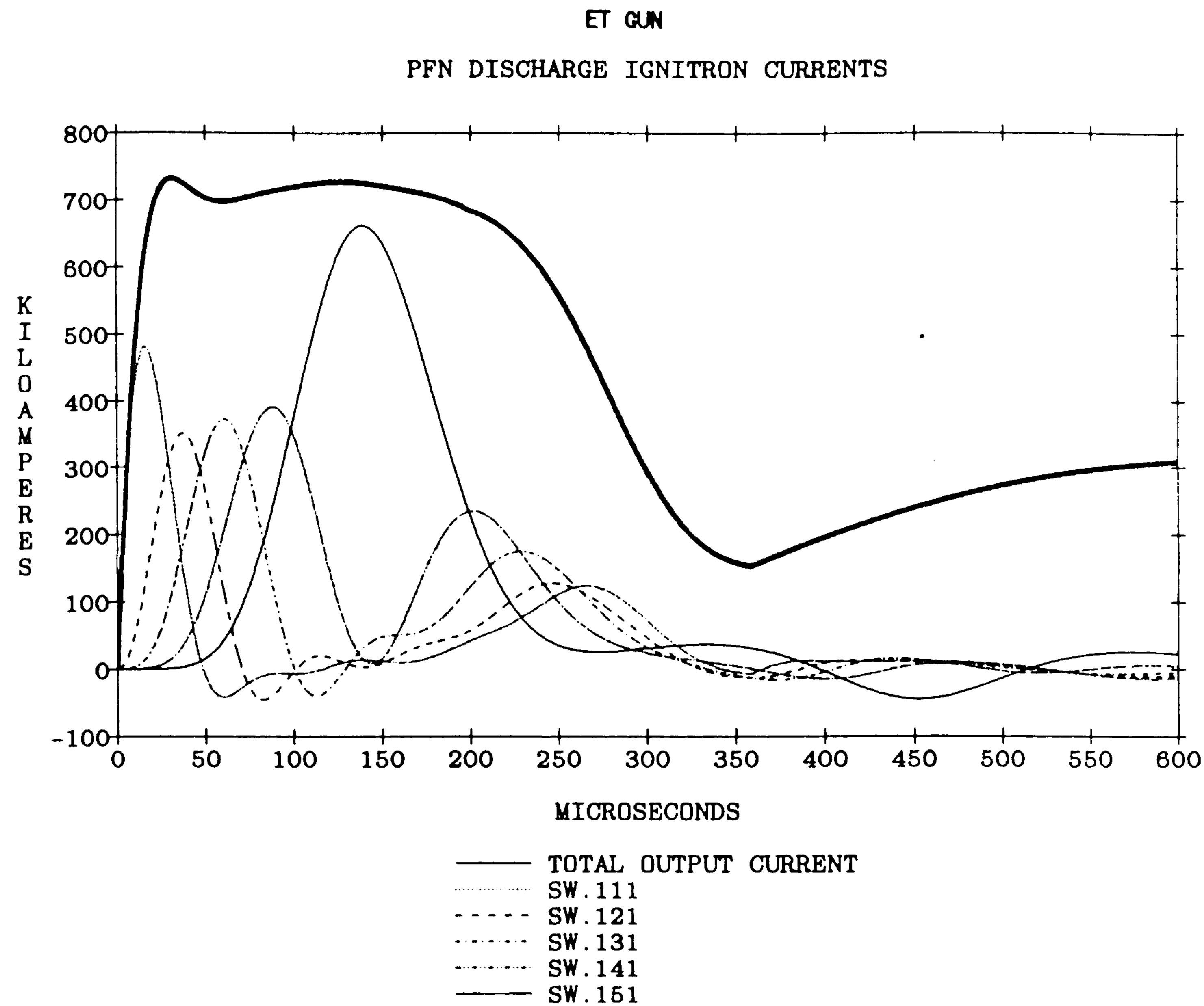

Figure 49. Currents through the PFN ignitrons (see Figure 47).

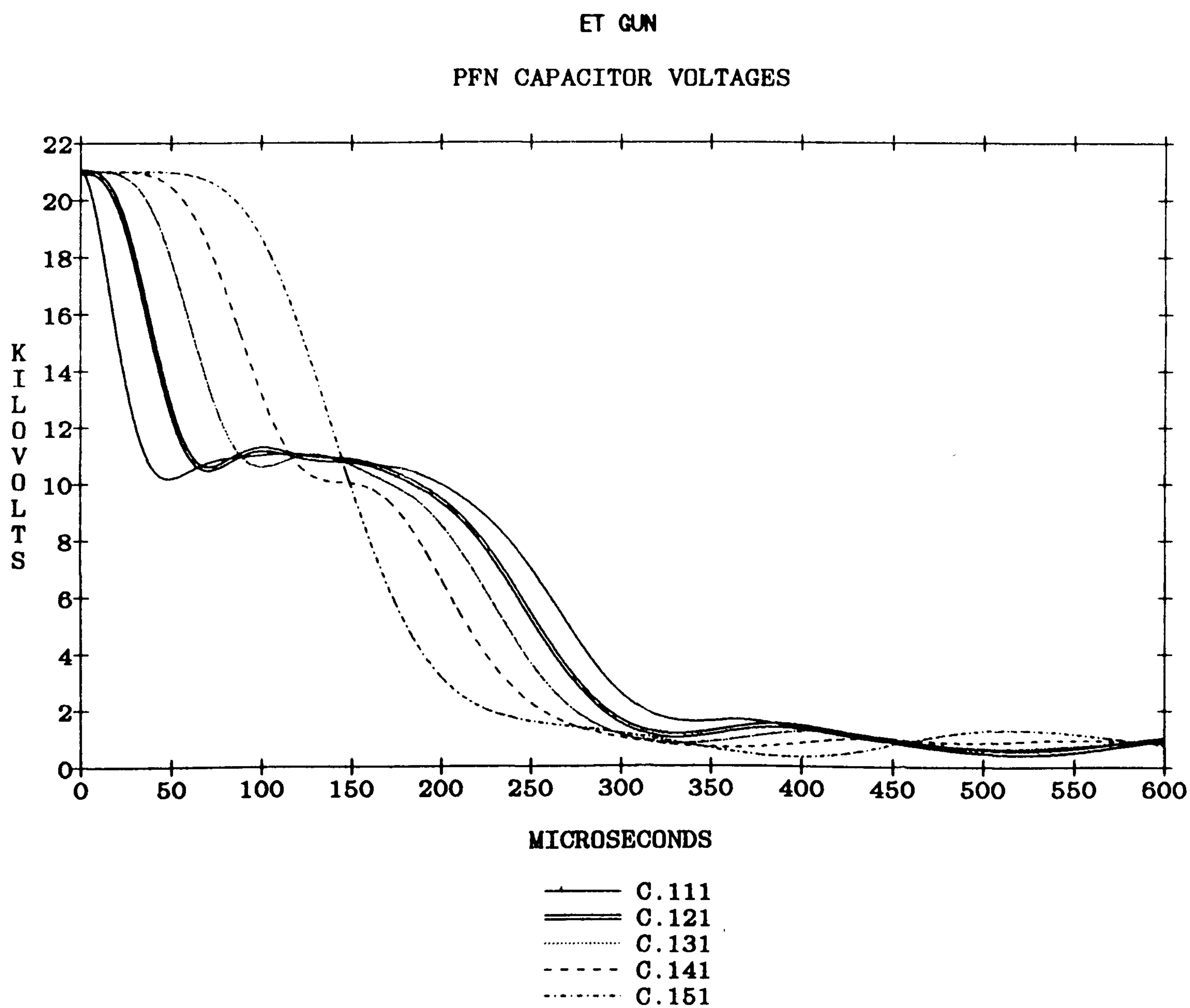

Figure 50. Currents through the PFN capacitors (see Figure 47).

ET GUN

PULSE CIRCUITS

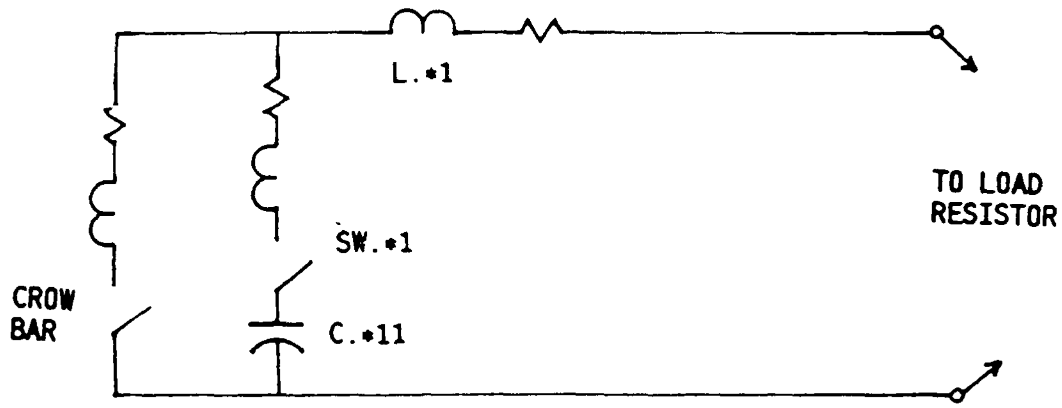

PULSE 1
C.211 4944 uF L.21 15 uH

PULSE 2
C.311 4944 uF L.31 15 uH

PULSE 3
C.411 4120 uF L.41 15 uH

PULSE 4
C.511 412 uF L.51 15 uH

* = 2, 3, 4, 5

Figure 51. Circuits used to generate increasing current profile to sustain mixing chamber pressure.

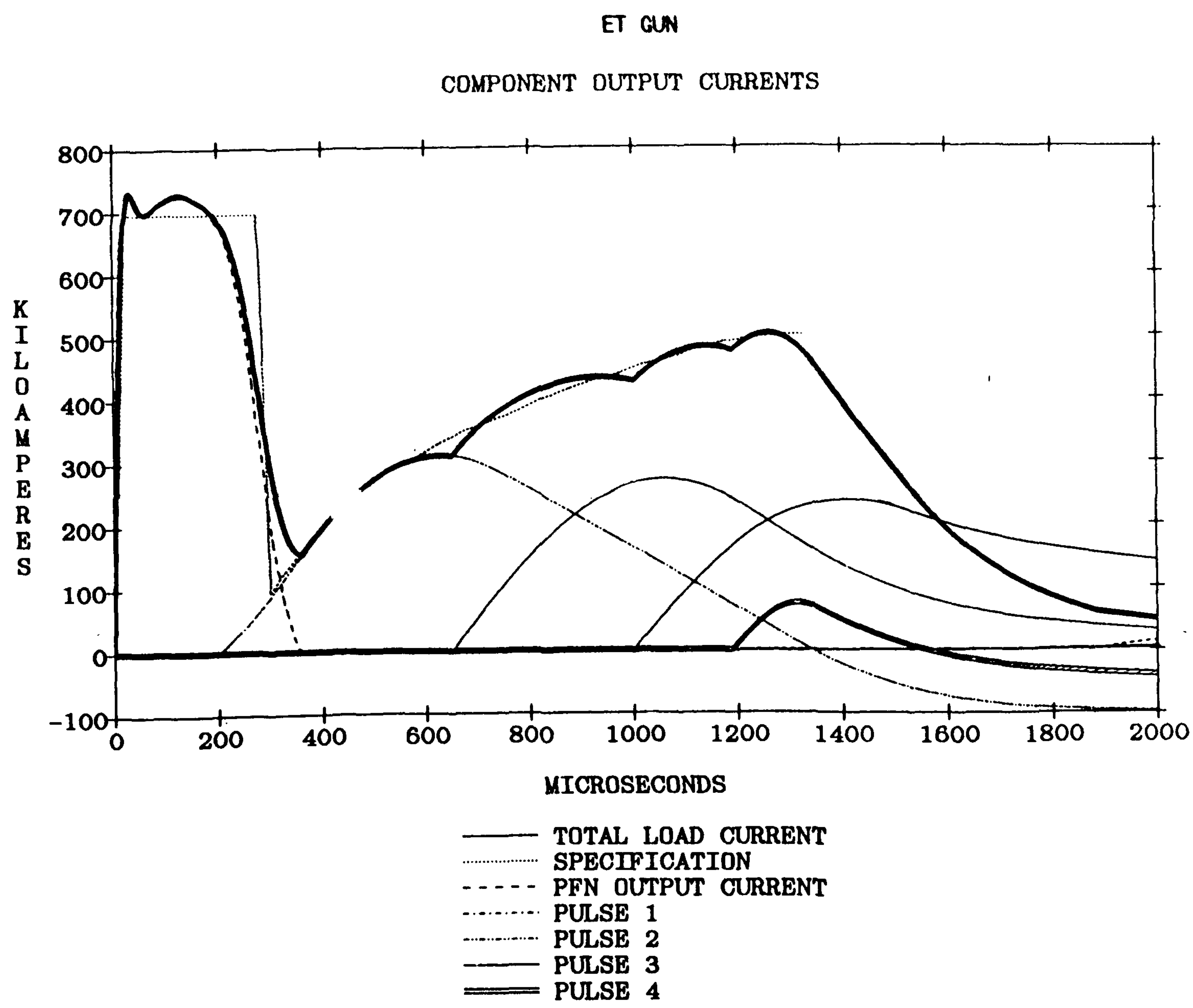

Figure 52. Composition of total capillary current profile.

Table 32

CAPITAL COST ESTIMATE SUMMARY - ET-GUN

Cost of Equipment

Item		Cost Estimate
Primary Power/Charging System		$424,900
Power Conditioning Equipment		83,100
Switching/Triggering Circuitry		290,600
Cabling and Buswork		72,350
	SUBTOTAL	$870,950
Barrel & Mechanical Structure		$100,000
Spare Barrel		50,000
Catch Tank		15,000
Screen Room & Data Acquisition		248,000
Control Room Equipment/Safety		123,000
	SUBTOTAL	$536,000
	PROJECT TOTAL	$1,406,950

BREAKDOWN OF COSTS FOR INDIVIDUAL ITEMS

Primary Power/Charging System

116	22-kV, 50-kJ Capacitors	$178,000	
20	Tubular Steel Racks	28,000	
20	Intra Rack Wiring	6,000	
20	Capacitor Shorting Switches	34,000	
116	Capacitor Shorting Cables	17,000	
232	Capacitor Shorting Resistors	12,000	
232	Sets of Resistor Hardware	3,500	
20	Rack Grounding Resistors	4,000	
20	Rack Grounding Cables	17,000	$299,500
1	HV Charging Supply (25-kV, 100-A)	60,000	
1	Ground Isolation Relay	350	
1	Charging Relay (Main)	350	
9	Charging Relays (System)	3,200	
10	Insulated Relay Enclosures	3,000	
10	Charging Cables	1,500	
116	Charging Resistors	20,000	
116	Sets of Resistor Hardware	2,300	
1	System Ground	7,500	$ 98,200
9	50 kV Dump Relays	3,200	
116	Dump Resistors	15,000	
116	Sets of Resistor Hardware	1,700	
20	Dump Relay Assy	4,000	
20	Manual Shorting Switches	3,300	$ 27,200
	PRIMARY POWER SUBTOTAL		$424,900

Table 32

COST ESTIMATE SUMMARY - ET-GUN
(continued)

Power Conditioning Equipment (Reactors)		
24	Aluminum Castings	9,600
1	Tooling	40,000
5	PFN Inductors	3,750
9	Sets Inductor Hardware	19,000
9	Sets Inductor Support Hardware	10,800
	POWER CONDITIONING SUBTOTAL	$ 83,100
Switching/Triggering Circuitry		
74	Ignitrons D Size	72,150
37	Sets Ignitron Hardware	11,000
175	Solid State Diodes	70,000
36	HV Relays	13,500
18	50 kV pulse Transformers	9,000
18	Low Inductance Capacitors	6,800
18	Ignitrons A Size	4,500
36	Sets Trigger Generator Cable	18,000
18	Switch Module Frames & Supports	18,000
5	Sets Diode Support Frames	10,000
5	Sets Diode Connections	5,000
20	Voltage Sensing Networks	5,000
18	EMI Electronic Enclosures	27,000
18	5 kV Power Supplies	11,250
116	Bias Resistors	7,800
116	Resistor Hardware	1,600
	SWITCHING SUBTOTAL	$290,600
Cabling and Buswork		
116	Capacitor Output Cables	5,000
116	Capacitor Cable Hardware Sets	5,500
79	Inductor Cables	11,850
25	Negative Switching Bus	20,000
25	Positive Switching Bus	10,500
25	Transition Bus	9,000
25	Sets EM Coil Output Hardware	10,500
	CABLING SUBTOTAL	$72,350

the information, and partially analyze it. It would be desirable to monitor the velocity of the projectile continuously by means of a laser Doppler system. This does not require any holes to be bored in the gun barrel nor any sensors to be placed on the barrel. The practicality of such a system will depend on whether radiant energy from the hot gases which may seep around the projectile can interfere with the laser light. A computerized turn key data acquisition system is desirable since it can save considerable software development time.

4.2.4 Facility

A diagram of a possible facility layout with dimensions is shown in Figure 53. The arrangement of the various components can be changed, but the total floor space will either remain the same or possibly increase. Some room has been allotted for working around the components, but additional room may be desirable for work benches and tools. The position of the screened room and power supply charger has been left unspecified and would be placed for convenience. The cartridge loading area, the barrel, and catch tank or region must be collinear as shown and will extend about 10 m. A length of about 5 m, collinear with the barrel, is needed for reaming or cleaning out. Three meters of this can come from the catch tank if it can be detached.

The capacitor bank will be configured in the same manner as discussed in Section 2, except that a smaller bank is needed. The same type of capacitors and switches will be used.

4.3 COST ESTIMATE SUMMARY

The costs for the ET-gun facility and installation are summarized in Table 33. The major facility cost is the capacitor bank and charging system. The ignitron switches also represent a major expense but solid state switches would be much more expensive. The costs for the data acquisition system, screen room, and control and safety equipment are assumed to be the same for all options.

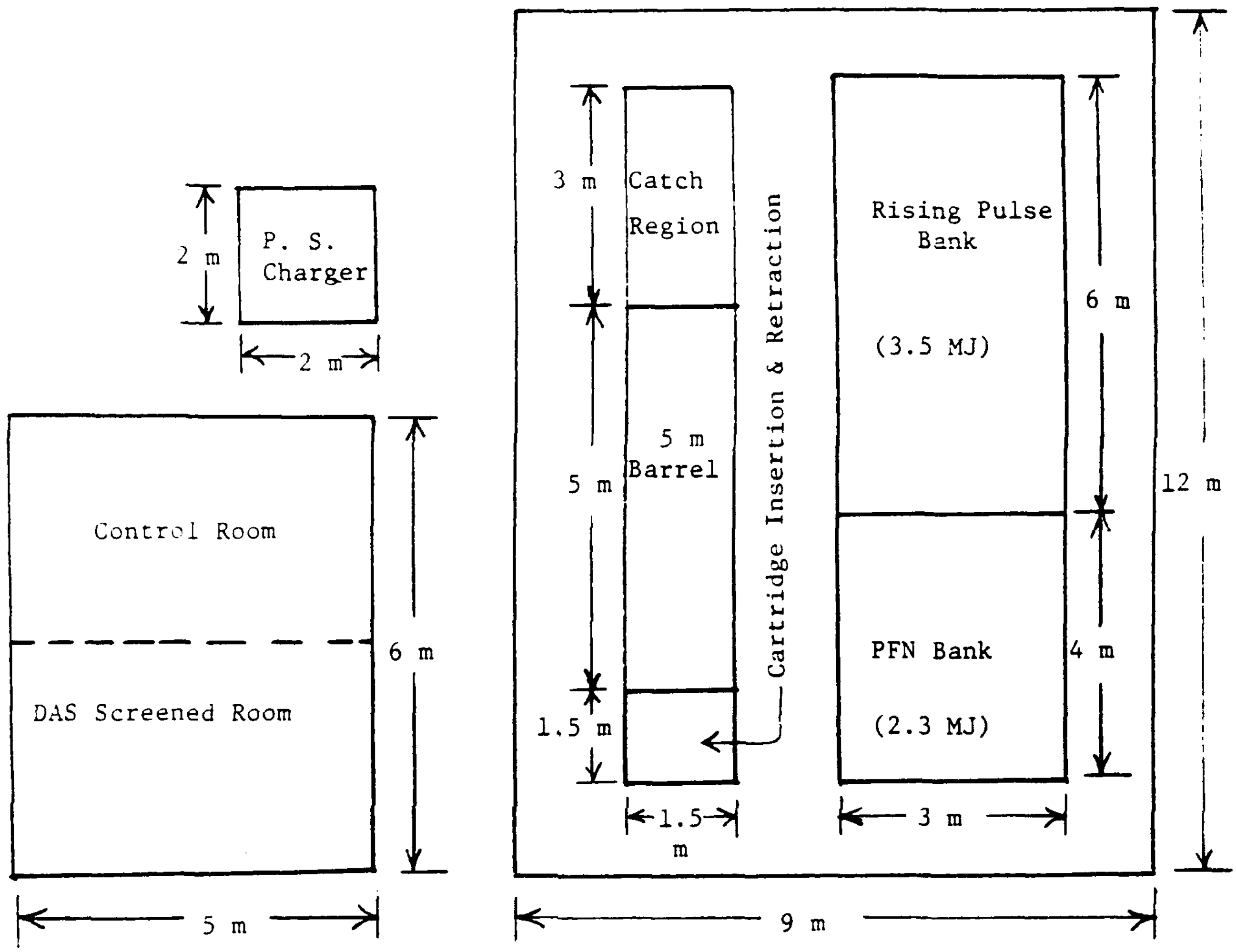

Figure 53. ETL facility layout.

Table 33

COST ESTIMATE SUMMARY FOR THE
CAPACITOR-DRIVEN ETL FACILITY

Cost of Equipment

Item		Cost Estimate ($K)
Primary Power/Charging System		425
Power Conditioning Equipment		83
Switching/Triggering Circuitry		291
Cabling & Buswork		72
Barrel & Mechanical Structure		100
Spare Barrel		50
Catch Tank		15
Screen Room & Data Acquisition System		248
Control Room Equipment/Safety		123
	Subtotal	1407

Installation Cost

Engineering (1 person years)		170
Technician (2 person years)		170
	Subtotal	340

Contingency (15%)		262
Total		2009

The total cost of about $2 M is less than the other options but the final velocity is also less and just barely falls in the range of interest.

4.4 ADVANTAGES AND DISADVANTAGES OF THE ETL

A primary advantage of the ET-gun is its similarity to conventional guns in terms of its appearance and operation. The ET cartridge can be made to look like a conventional powder cartridge and can be loaded and unloaded in a similar manner. The major difference is that the power supply leads must be attached to it and later detached. The power supply itself is also a major difference.

The ET-gun's projectile and sabot package can also look very similar to that of conventional guns since it is driven by hot gases in both cases. Thus barrel wear should be similar to conventional guns as should barrel maintenance. It should wear much better than railguns.

A disadvantage of the ET-gun is its high piezometric ratio relative to railguns. Because of this, it is difficult to get velocities above 2.5 km/s using water. Another disadvantage relative to railguns is the limited experience using ET-guns.

5. COMPARISON OF LAUNCHER OPTIONS; RECOMMENDED OPTION

The design of the three electrical-powered guns that have been considered for meeting the BRL requirements for terminal ballistic research have been discussed in the previous sections. The advantages and disadvantages of the options have been presented. In this section, comparisons are made of the three options, and one is recommended as best fitting the requirements for an advanced launch facility for BRL.

5.1 PRESSURE PROFILES

Figures 54, 55, and 56 show the pressure variations at the base of the projectiles as they move down the bore of the electrothermal launcher, the HPG-driven EML, and the capacitor-driven EML, respectively. Figure 54 demonstrates a basic limitation in the performance of an ETL. Even though the pressure in the mixing plenum is being maintained at 517 MPa (75 ksi), the pressure at the base of the projectile drops precipitously as the projectile accelerates down the bore. The ratio of the peak pressure, which is set by an engineering constraint, to the average pressure is 5.3 for a 5-m long barrel. Since the velocity achieved by the projectile varies as the square root of the average pressure behind the projectile, we would like the piezometric ratio (ratio of peak to average pressure) to be as close to unity as possible. It was found during the analysis of the ETL that making large variations in those quantities that can be changed made only small variations in the velocity achieved by the projectile. As a result, it has been concluded that it will be difficult to accelerate a $\simeq$ 390-g projectile into the specified velocity range, viz., 2.5 km/s-3.5 km/s, and that the mid to upper portions of that range will definitely not be accessible with an ETL.

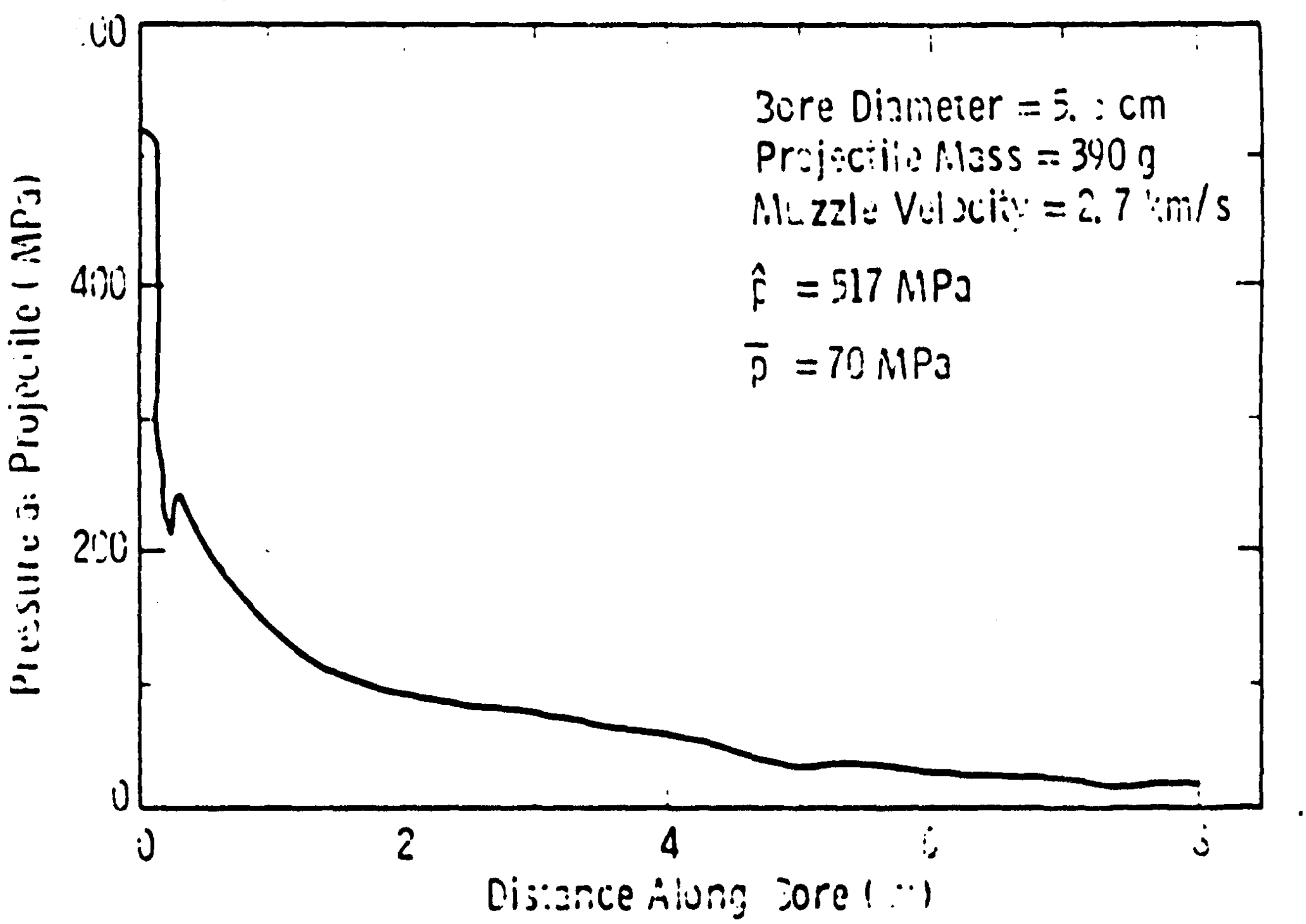

Figure 54. **<u>Pressure profile for the electrothermal laucher.</u>**
<u>Piezometric ratios: $\hat{P}/\bar{P}$ = 7.4 for L = 8 m</u>
<u>$\hat{P}/\bar{P}$ = 5.3 for L = 5 m</u>

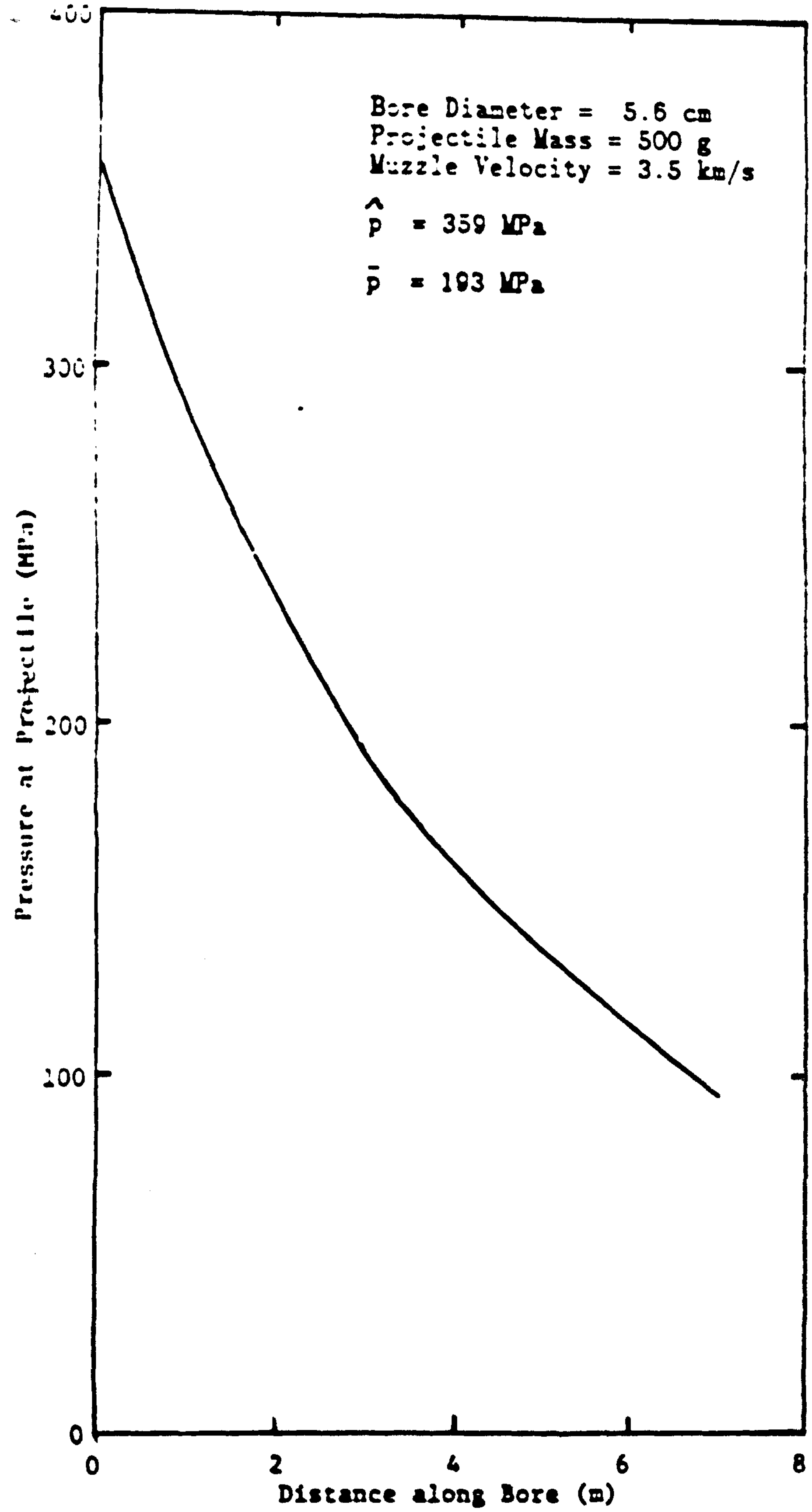

Figure 55. Pressure profile for HPG-driven EML. Piezometric ratio: $\hat{P}/\bar{P} = 1.9$.

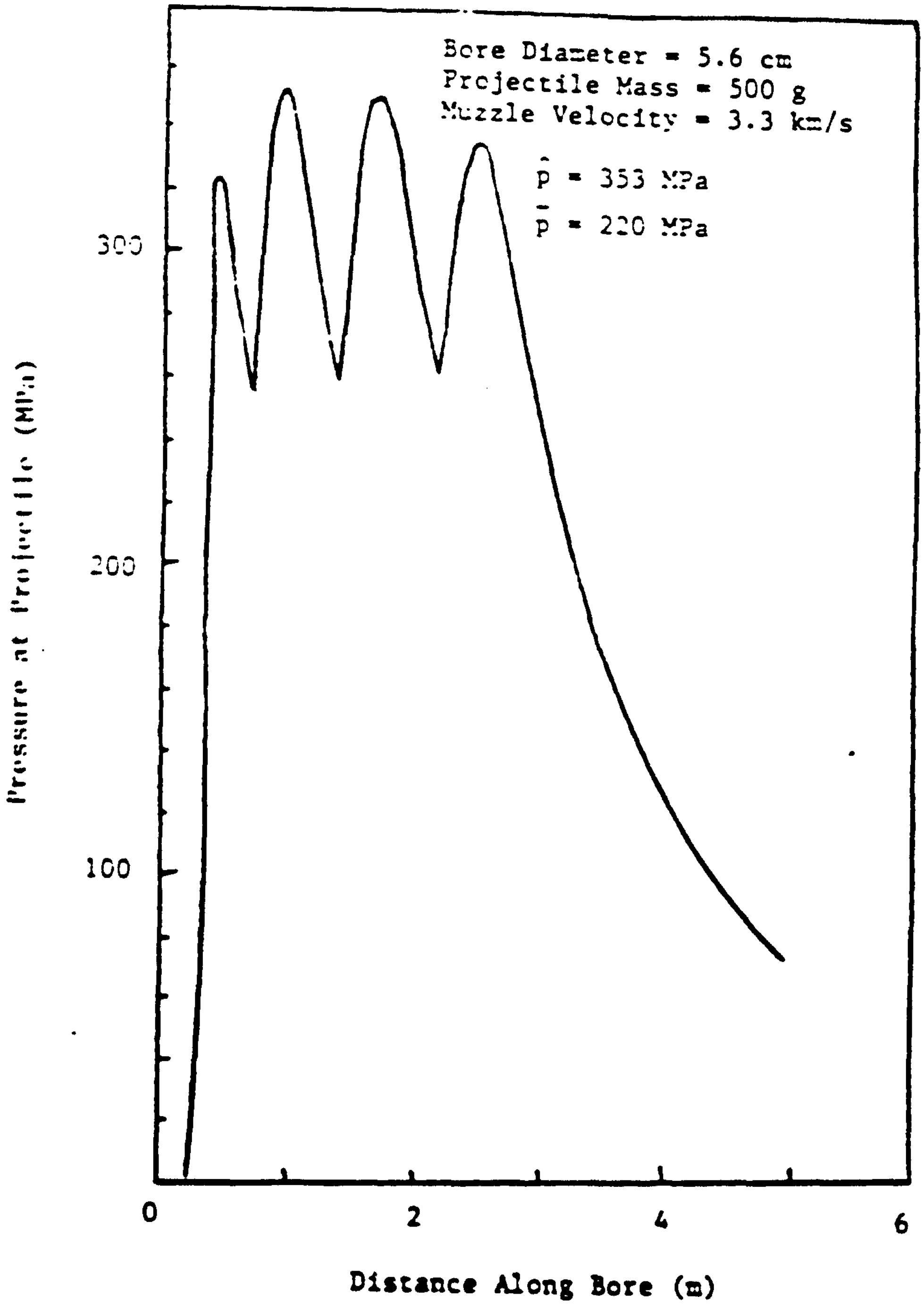

Figure 56. Pressure profile for capacitor-driven EML. Piezometric ratio: $\hat{P}/\bar{P} = 1.6$.

An electromagnetic launcher has an advantage over an electrothermal launcher in that electrical energy is coupled to the armature of the projectile package and the current directly drives the projectile via the Lorentz force. On the other hand, in an ETL the electrical energy is dissipated in a propellant which in turn drives the projectile. Figure 55 shows the pressure at the base of the projectile as the projectile moves down the bore of a HPG-driven EML. Because of the more complex bore (joints) in an EML, the peak pressure is limited to ≃ 350 MPa (50 ksi). However, the pressure driving the projectile does not decrease nearly as rapidly as for an ETL, i.e., the piezometric ratio is 1.9 as compared to 5.3 for the ETL, so that the average driving pressure is 193 MPa which is a factor of 2.8 times greater than for the ETL. There is a penalty associated with achieving this favorable pressure profile in an HPG-driven EML, viz., a large inductance is required in the external circuitry. This large inductance results in a larger time interval being required to drive the current up to its peak value, and consequently to the dissipation of more energy in the system.

The capacitor-driven EML has more flexibility than the other options in that the electrical energy can be programmed to be injected into the breech in a manner to shape the pressure profile as we want it. Figure 56 shows the pressure profile where energy is injected at four different times during the acceleration process. The peak pressure is approximately the same as for the HPG-driven EML, viz., 350 MPa (50 ksi). The pressure at the base of the projectile is driven to its peak value and maintained at approximately the peak value until the projectile nears the muzzle. At this time the pressure is allowed to decrease so that the projectile does not explode or get driven from its intended trajectory by the sudden drop in pressure it experiences as it exits the bore. The piezometric ratio is 1.6, and the average driving pressure is 220 MPa.

The capacitor-driven EML obviously has the capability of achieving the most favorable pressure profile.

5.2 COMPARISON OF PERFORMANCE

Some quantities that illustrate the performance capabilities of the three electric guns under study are summarized in Table 34. the guns all have the same bore diameter, viz., 5.6 cm; however, the HPG-driven EML was designed with a longer barrel, 8 m, as compared with the other two options that have a length of 5 m. Note that the HPG-driven EML accelerates a 500-g projectile to the full velocity of 3.5 km/s.

The electromagnetic launchers require a peak current, 2.1 MA, that is three times the 0.7-MA current required by the ETL. Obviously, a more massive power transmission system will be required for the EMLs and switching will be more of a problem.

There is a wide variation in the primary stored energy required for the three options. The homopolar generator must store 52 MJ or nine times the amount of energy stored in the capacitors for the ETL and five times the amount stored in the capacitors for the capacitor-driven EML. Note, however, that the ETL does not achieve the velocity that the EMLs achieve. A velocity of $\simeq$ 2.5 km/s represents an upper limit for the ETL. The efficiency for converting electrical energy to kinetic energy of the penetrator is only 2% for the HPG-driven EML because of the high energy that is initially stored in the HPG. The efficiencies of the other two options are about the same magnitude, viz., $\simeq$ 10%, and about five times larger than the HPG-driven EML. The efficiency for converting electrical energy to kinetic energy of the complete projectile package is larger for the capacitor-driven EML (27%) than the ETL (21%) because of the larger mass of the capacitor-driven EML; the ETL does not require an armature.

5.3 COMPARISON OF COSTS

The cost estimates that were made during this study were based on vendor costs for the capital equipment. They did not include any costs incurred in purchasing the equipment or in the cost of capital. Estimates of the cost of installing the equipment were included in the cost estimate. It was assumed that a facility would be available; facility costs were not included in the estimates.

Table 34

PERFORMANCE COMPARISON

Quantity	CAP/EML	HPG/EML	ETL
Barrel Length (m)	5	8	5
Bore Diameter (cm)	5.6	5.6	5.6
Peak Current (MA)	2.1	2.1	0.7
Primary Energy Stored (MJ)	10	52	5.8
Peak Driving Pressure (MPa)	350	359	520
Average Driving Pressure (MPa)	220	193	98
Piezometric Ratio	1.6	1.9	5.3
Penetrator Mass (g)	200	200	200
Projectile Mass (g)	500	500	375
Velocity at Muzzle (km/s)	3.3	3.5	2.5
Efficiency/Total Mass (%)	27	6	21
Efficiency/Penetrator (%)	10	2	11

A comparison of these costs is presented in Table 35. The capacitor-driven and the HPG-driven EMLs are 60% and 80% more costly than the ETL, respectively. However, in comparing these costs it must be remembered that the ETL does not have the performance capability of the EMLs. To reflect the performance capability, the last column in Table 35 gives the capital cost (including installation) per Joule of kinetic energy achieved by the penetrator. This quantity is approximately the same for all three options, viz., 3.0 ± 7% \$/J.

On a performance basis, none of the options has a capital cost advantage.

The capital cost estimates were made in considerable depth, e.g., see the Appendix. In comparison, only crude estimates were made of operating costs. Table 36 is a summary of these costs. It was assumed in obtaining these estimates that a total of 100 shots would be conducted per year. This is based on the gun being available for operation 50% of the time, and obtaining four shots per week when it is available.

The operating costs for the power supply and the gun (mechanical) were based on experience and include the costs of reconditioning equipment and replacing worn-out components. The power supply costs for the HPG-driven EML are high due to the need to recondition the generator. It was assumed that for the EMLs the bore materials would be replaced after 50 shots.

The costs for the operating personnel were based on the equivalent of two E&S and two technicians full time, and it was assumed that the costs for operating personnel would be the same for all three options.

The estimated yearly operating costs fall in the range of \$860 K ± 14%, and this translates to average values of ≃ \$10K per shot and ≃ \$20K per week of operating costs.

5.4 COMPARISON OF SPACE REQUIREMENTS

A comparison is made in Table 37 of the test cell dimensions for the three options. The capacitor-driven EML requires about 40% more

Table 35

COST ESTIMATE SUMMARY

Device	Cost Estimate ($M)	Ratio	$\frac{\text{Cost}}{\text{Penetrator K.E.}}$ $\left(\frac{\$}{J}\right)$
Electrothermal Launcher	2.0	1.00	3.2
Capacitor-Driven EML	3.2	1.60	2.9
HPG-Driven EML	3.7	1.80	3.0

Table 36

ESTIMATED OPERATING COSTS

	Yearly Costs* ($K)		
	ET	CAP/EML	HPG/EML
Power Supply	40	60	220
Mechanical	50	60	60
Projectiles	150	200	200
Subtotal	240	320	480
Operating Personnel	500	500	500
TOTAL	740	820	980

Operating Cost/Shot = $7.4-10 K/shot.

Operating Cost/Week = $15-20 K/week.

*Based on a total of 100 shots/year (~50% availability and ~ four shots per week when available).

Table 37

SPACE REQUIREMENT COMPARISON

Device	Test Cell Dim. (m)	Area Ratio
Electrothermal Launcher	12 x 9 x 8	1.00
HPG-Driven EML	17 x 7 x 6	1.10
Capacitor-Driven EML	12.5 x 12 x 8	1.39

floor space area than the others because of the two-hundred, 50-kJ capacitors that must be located within the cell.

The height of the room required for the capacitor-driven EML and the ETL is greater than that of the homopolar-generator-driven EML because it is assumed that the capacitors are stacked to a height of 3.3 m. A space of 1.7 m was allotted above the capacitors for inductors, and an additional 3 m for the operation of a crane.

Each launcher system would also require space for a control room and screened room for the data acquisition system. These rooms together would require an area of $\simeq 30\ m^2$. Furthermore, a work area would be required to lay down components, e.g., barrels during maintenance work. There would also be need for access through a wall to allow reaming of the bore of the barrel.

BRL has not identified a specific test cell at their laboratory as a potential site for an electric gun test facility. However, provided that the required area and height that has been identified are available in an existing cell, we should have sufficient flexibility in locating the components to fit them into that cell.

5.5 RECOMMENDED OPTION

Each of the three potential launchers for the advanced Terminal Ballistic Research Facility for the U.S. Army's BRL have been discussed in depth in Sections 2, 3, and 4. Technical issues have been identified and advantages and disadvantages delineated. Based on the analyses that have been conducted we feel that a clear choice can be made.

We recommend that a capacitor-driven EML be chosen as the best option for meeting BRL's needs. The three major reasons for selecting this option are:

- projectiles having the required mass can be accelerated to all velocities within the desired velocity range
- it is a flexible system that allows a low piezometric ratio and a high efficiency to be achieved
- it is a proven system

The fact that the capacitor-driven EML requires more floor space than the other options is not considered a sufficiently negative factor to alter this decision.

Two major reasons for not choosing the electrothermal launcher are:

- projectiles having the required mass cannot be accelerated to the desired velocities because of the poor piezometric ratio that is achieved
- there is a high risk due to the limited experience with ETLs regarding performance, reliability, and maintenance

Two major reasons for not choosing the HPG-driven EML are:

- a homopolar generator having a high stored energy is required in order to obtain a satisfactory piezometric ratio and this results in a low efficiency and consequently high energy deposition in the system
- explosive opening switches are required

6. DESIGN REQUIREMENTS FROM A FACILITY OPERATIONAL VIEWPOINT

The task to be addressed for the commissioning/test program is to define a plan aimed at reducing costs and technical risks associated with the operation of the Electromagnetic Launcher, consisting of a power supply and a rail system. Such a plan would involve the identification and analysis of those elements, which have a significant impact on these costs and risks and the identification of those methods that would reduce or eliminate the effects of these elements.

For the purpose of being able to concretely focus on the objectives of this task, we have assumed that the term technical risks has reference to the probability that the objectives of the test program will not be achieved for reasons associated with the Electromagnetic Launcher. From the perspective of the power supply and the rail system, this would mean that the equipment is not performing as planned, thus preventing the satisfactory completion of the test program.

Performance of the power supply is measured by how well it produces the specified current waveforms into a proper load repeatedly a specified number of times. Rail system performance is related to obtaining the specified velocity in the presence of the specified power input. The plan to reduce costs and risks in regard to rail system performance, as defined here, is not part of this section. This section restricts itself to considerations relating to the power supply portion of the Electromagnetic Launcher only.

In regard to the power supply, we believe that the technical risks are always associated with a failure of some sort, be that catastrophic or in the nature of a gradual degradation, that will prevent continued operation at the design levels of voltage or current and thus jeopardize the completion of the test program. In addition to

the "cost" of an unscheduled test program termination, there will be the cost associated with downtime and repair in terms of manpower and materials. These costs can be substantial as compared with the overall cost of normal day to day operation.

From the foregoing, it is clear that any plan aimed at reducing costs and risks is one that has as its prime goal the design, fabrication, and construction of a highly reliable, maintainable, and repairable piece of equipment. Such a plan would consider that incurring some extra initial expenses associated with the acquisition and validation of these characteristics is a small price to pay for the long-term savings of costs associated with downtime and repairs.

To achieve the desired characteristics in the final product, they must be the objective in all the phases of design, component acquisition, construction, assembly, and testing. In particular for this power supply to be a reliable and dependable tool in the performance of a test program, it will be necessary to design these qualities in from the beginning. It will be difficult and costly to add them later.

In the approach to the design of the power supply, the design philosophy must include three major considerations, i.e., maintainability, failure prevention, and failure damage minimization. These three considerations are reflected in the design requirements as specified in the next sections.

6.1 DESIGN REQUIREMENTS

6.1.1 Maintainability

6.1.1.1 Modularity

As far as feasible, a modular approach to the entire system construction is desirable from the perspective of being able to quickly remove and replace a substructure, which contains an element which has failed and which is an integral part of that substructure. We visualize a "module" to consist of all those elements associated with one set of series and crowbar ignitrons. Modules would then be assembled into "racks," racks into banks and the sum of the banks would constitute the power supply.

6.1.1.2 Component Testing in Place

Provision should be made to perform tests on various components without major disassembly. This applies particularly to the ignitrons. For the ignitrons, it would include the ability to perform a bi-polar "hipot" test and "recondition" them in place should tests indicate that it is desirable.

6.1.1.3 Component Replacement

Provisions should be made for the rapid exchange of components such as ignitrons without major disassembly.

6.1.1.4 Prefire Datalogging

To enable some diagnosis of a prefire failure, during a charging cycle, it will be necessary to record and store values of all bank voltages, module currents, crowbar currents, and external load currents for the complete charging cycle.

6.2 FAILURE PREVENTION

The failure most commonly encountered in a system such as this is an electrical failure usually accompanied by the destructive dissipation of large amounts of energy. These failures can be prevented as described below.

6.2.1 Derating the System

By operating the capacitors and ignitrons somewhat below their recommended ratings, their life is greatly extended and the probability of failure greatly reduced. By operating capacitors at 20 kV, which are rated at 22 kV, an operating safety margin is obtained, and the cost in performance will be more than offset by the savings in downtime and repair costs.

6.2.2 Voltage Stand-Off Capability

The minimum test voltage stand-off capability, with a dc hipot tester, shall be at least three times the rated maximum value, at all locations where this voltage might appear in the system.

6.2.3 Insulation

In addition to satisfying the condition under Section 6.2.2 above, all exposed nonuniform field electrodes, such as nuts and bolts,

should be completely enclosed with insulating materials, such that any discharge path will be extremely tortuous and confined. This is particularly important in regard to positive electrodes where corona inception is most likely to occur.

6.2.4 Thermal Management

Thermal management should be applied to all ignitron tubes, regardless of duty cycle or duty severity. The management system should be activated after final installation, immediately after a final ignitron tube conditioning.

6.2.5 Igniter Resistance Monitoring

A system should be incorporated to constantly monitor the igniter resistances of all ignitrons. Sudden or dramatic changes in these values have been known to coincide with internal ignitron deterioration in regard to voltage stand-off capability. Minimum values of these igniter resistances are needed to insure reliable triggering.

6.2.6 Wiring Color Coding

In a system where large bundles of wires are present, the likelihood of an erroneous connection is finite. The interchange of a series tube igniter wire with that of a crowbar tube in the same module can have disastrous effects. Appropriate color coding can reduce the probability of occurrence of such human error.

6.3 FAILURE DAMAGE MINIMIZATION

Should a failure occur at which time large amounts of energy must be dissipated, it will be desirable to minimize the damage done to various system components. The component most vulnerable to damage is the ignitron tubes in the crowbar function. To minimize excessive overload currents during failures, the following design features should be considered.

6.3.1 Distributed Loading

Rather than having multiple modules feeding the same load inductor, the bank inductance required should be distributed over the modules or racks. This will isolate them from each other by some reasonable level of impedance, reducing the magnitude of short circuit currents in any one crowbar.

6.3.2 Mutual Crowbar Triggering

Provision should be made for a system that will trigger all crowbar tubes in any one stage as soon as one of them begins to carry current. This will distribute the total available short circuit current over all the crowbar tubes, rather than all modules feeding into one crowbar tube.

6.3.3 Capacitor Fusing

Capacitors should be provided with a fus[illegible] protect against overcurrents.

7. COMMISSIONING PROGRAM

The commissioning program for the capacitor-driven EML is described in detail in the following subsections. At the systems level there are several considerations which require attention so that the various subsystems are contributing to a fully-integrated facility which can be commissioned in an efficient manner. Those considerations include the interfacing of the subsystems, the key steps in the commissioning process, and the identification of critical operating data that must be obtained.

The various subsystems which must interface to provide a complete test facility are given in Table 38. The details of the interfaces must be developed in a manner consistent with the detailed final system design of the facility. An iterative procedure would provide a reasonable approach since the design requirements and the interface requirements must be integrated. As a starting point, consider the tabulations shown in Tables 39 to 42 which provide some details for key interfaces. Of course, more specifics are required for a complete description, but these details will be design dependent. A block diagram of the EML facility from a systems interface point of view is provided in Figure 57.

During the commissioning there is a need to operate in a team manner so that all members of the operating staff are aware of as many of the facility activities as possible. It is important that the overall facility goals provide the focus of all activities, and that subsystem operational needs be primarily concerned with the system needs. Individual task leaders must be responsible for identifying and meeting the various interface requirements associated with his system. Finally, the transition from assembly to operation should be carefully planned and all procedures documented.

Table 38

SUB SYSTEMS OF THE EML TEST FACILITY

Launcher Barrel
Preaccelerator
Mechanical Systems
Electrical Power Supplies
Control Systems
Data Acquisition System
Gun Sensors/Diagnostics
Catch Tank and Associated Diagnostics
Test Systems
Safety Systems
Spares/Supplies and Assembly Systems

Table 39

INTERFACES INVOLVING THE RAILGUN BARREL

Subsystems	Interfaces
Power Supply	Busbar Connections
Mechanical Systems	Barrel Supports Recoil Structure Bore Alignment Facility Cranes
Gas Gun Injector	Connecting Flange Bore Alignment
Catch Tank	Arc Horn Tank Flange Exhaust System
Gun Sensors/Diagnostics	Bore Inspection System B-Dot Sensors Voltage Probes

Table 40

INTERFACES INVOLVING CONTROL SYSTEMS

Subsystems	Interfaces
Power Supply	Capacitor Charger Control Logging Pre/Post Shot Data Video Cameras Trigger Generator Monitoring
Gas Gun Injector	Gas Supplies Injector Fast Valve Velocity Sensors
Test Systems	Procedures Bank Voltage Settings Helium Gas Setting Video Cameras
Safety	Interlocks Procedures Crane Operations Assembly Operations X-Ray Operations

Table 41

INTERFACES INVOLVING DATA ACQUISITION

Subsystems	Interfaces
Control Systems	Communication Links Shot Initiation Link DAS Armed Indication Injector Velocity Sensors Muzzle Velocity Sensors
Power Supply	Bank Current Sensors Bank Voltage Sensors Bank Trigger Generators
Sensors	Cabling/Patch Panels Velocity Measurements Gun Voltage Dividers B-Dot Sensors
Test Systems	Time Delays Timing Windows Computer Links Computer Software System Readiness Indicators System Trouble Indicators

Table 42

INTERFACES INVOLVING SAFETY

Subsystems	Interfaces
Test Systems	Procedures Inspections Aborts Safety Officer Communication Links Readiness Indicators
Mechanical Systems	Lab Exhaust Fire Protection Warning Lights Klaxons
Power Supply	Ignitron Readiness Indication

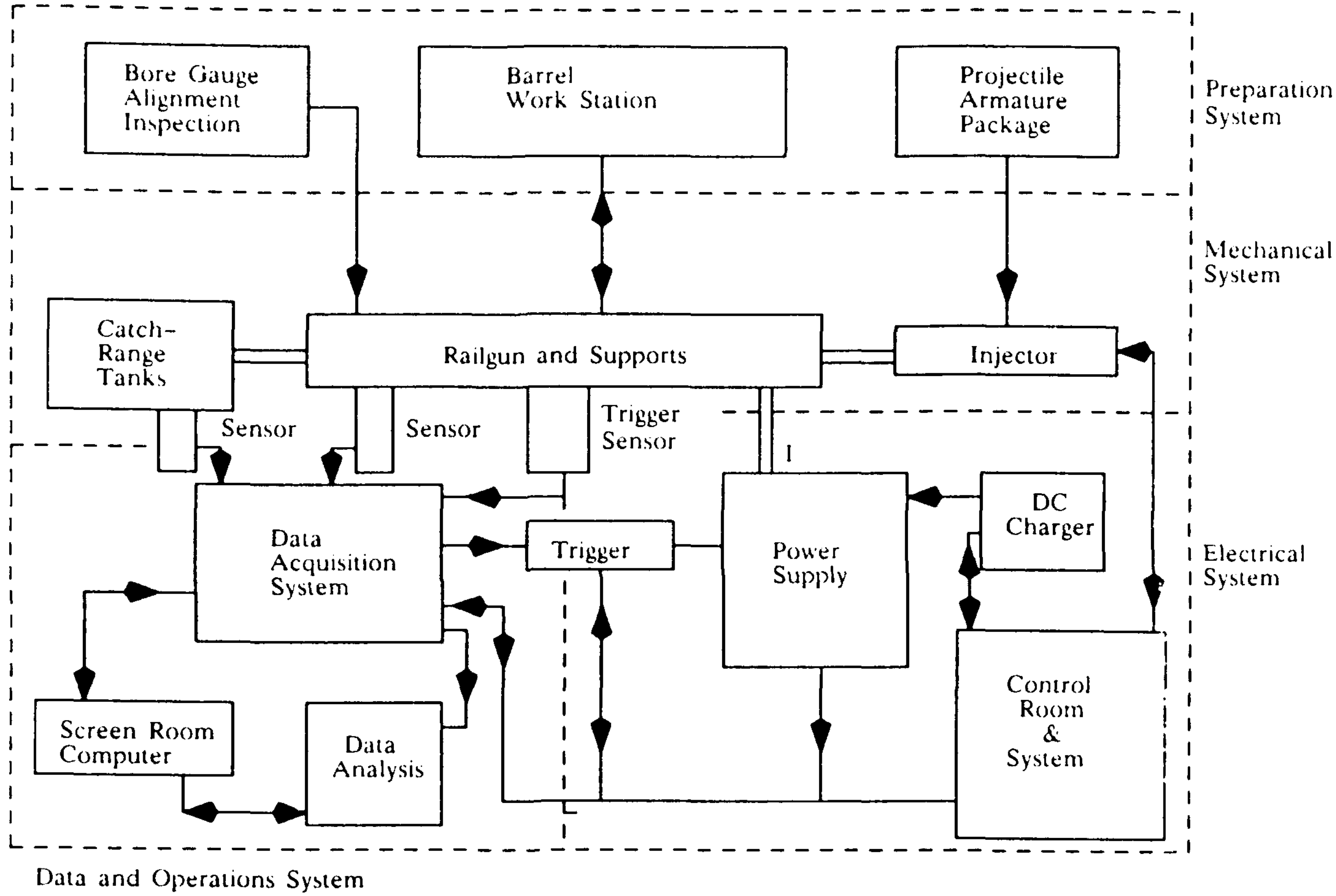

Figure 57. <u>Systems Interface Block Diagram</u>

As part of the documentation, the accumulation of critical operating data which provides the basis for future testing and facility maintenance is important to have available as data logging files, see Table 43. During the initial testing period, the data will provide critical information allowing key system unknowns to be determined. See Table 44 for a listing of the type of information that must be generated during the commissioning and testing of a new EML facility.

7.1 POWER SUPPLY COMMISSIONING

The testing to be conducted can be divided into two parts. One part consists of electrical tests, which are concerned with the discharge characteristics of the equipment and involves the measurement of electrical quantities such as voltages, currents, and magnetic fields, both in their magnitude and time dependence. These measured quantities are then to be compared with results obtained from mathematical simulations to ascertain that the electrical behavior is as expected and meets the specifications. The second part of the testing involves the evaluation of the physical condition of the power supply. This involves the mechanical integrity of the components in the presence of large electromagnetic forces generated during its operation, and the integrity of the insulation. In particular, the state of the ignitrons in terms of voltage breakdown, leakage current levels, and igniter resistances are of interest.

The final phase of the commissioning of the power supply consists of a full power discharge test into a dummy load. Successful completion of this test, both electrically and mechanically would signal customer acceptance of the equipment.

7.1.1 Component and Sub-Assembly Tests

In addition to the standard quality assurance and/or acceptance tests on manufactured or purchased parts or components, the following items are worthy of special attention.

Table 43

CRITICAL OPERATING AND PERFORMANCE DATA

For Operation:

- Rail/Insulator Surface Conditions
- Triggering of Stages
- Rail-to-Rail Resistance
- Rail Joint and Rail/Insulator Seam Conditions

For Performance:

- B-Dot Data
  - Position vs Time
  - Signal Profiles
- Armature Composition Effects
  - Launch Efficiency
  - Breech Damage
- Muzzle Ballast Effects
  - Component Damage
  - Breakwire Operation
- Launch Velocity vs Distance Profiles
  - Performance Evaluation
  - Data Integration
  - Prediction Capabilities
- Muzzle and Breech Voltages

Table 44

KEY INFORMATION GATHERED DURING COMMISSIONING/TEST PROGRAM

- Number of Shots per Bore Assembly Change-Out and Replacement.
- Lab Operations and Interface Problems.
- Type and Frequency of Failures.
- Validity of Performance Calculations at the Higher Velocities.
- Rail Design Capabilities at Full Energy and Full Current.
- Rail Assembly and Replacement Time.
- Lab Personnel Requirements.

Capacitors

Check for specifications and physical characteristics (size and bolt hold arrangement and location). Electrical tests should be conducted as follows:

** Measure Capacitance and dissipation at 1 and 1000 Hz.

** +22 kV one-minute voltage tests and electrical leakage tests.

Inductors

Check for value and mechanical integrity and connector mechanisms.

Joints and Connectors

Evaluate the various connector schemes and joint configurations with high current tests.

Ignitrons

Check Voltage standoff and leakage currents. Condition the ignitrons if necessary. Also, check values of igniter resistance.

Develop and apply test program to HiPot any subassemblies.

Build and test Inductors and Load Resistors for module, rack, bank and commissioning tests.

7.1.2 Power Supply Tests

In order to conduct the power supply tests, the following must be in place:

1. High voltage charging supply.
2. Control and firing system.
3. Data logging and acquisition system.
4. Load inductors and resistors.
5. Thermal management system.

Assuming that this equipment is available and operational, the Power Supply tests can be performed.

Module Tests

A module consists of a subassembly of all the circuit elements that are controlled by one discharge ignitron assembly (series tube) and one crowbar ignitron assembly (there are two ignitrons in series per assembly).

- Discharge tests

Test the module at low voltage to verify the data acquisition, charging and firing systems. Ascertain that the proper wave forms are obtained for the given circuit parameters. Increase the test voltage until operation at rated voltage and current is obtained.

- **Module state tests. (Typical)**

After each electrical test measure the characteristics of the ignitrons in terms of voltage stand-off, leakage current and igniter resistance. Inspect for mechanical damage.

- **Module life tests. (Typical)**

Conduct a multiplicity of discharge tests at rated voltage. Determine module state after each test. Vary time between tests. Determine if deterioration of any aspect of the module takes place.

Rack Test

A rack consists of a number of modules assembled into one physical, movable unit, which may be the building block of a bank or a stage.

- Discharge tests

Test the rack at low voltage. Verify the data acquisition, simultaneity of module firing, charging circuit, and discharge firing. Carefully ascertain that the characteristics of the waveform in magnitude and time dependence are consistent with the circuit parameters. Compare with results of simulations. Increase test voltage until rated voltage and current are obtained.

- **Rack state test**

After each test measure the characteristics of the ignitrons as described above. Inspect the system for mechanical and insulation integrity. Examine for slight physical distortions such as bent cables or bus bars.

Bank Tests

The bank would consist of the appropriate number of racks, all connected in parallel to the bank inductor and the bank dummy load resistor. The effect of the connecting cabling on the circuit inductance must be accounted for in the determination of circuit parameters.

The electrical and physical bank tests follow identically those for the racks.

Power Supply Commissioning Test

For this test each stage must be connected to a dummy load resistor, capable of absorbing the energy and withstand the forces. Through the control system the stage timing should be set such that stage firing times are measurably different. The complete power supply should be charged to 40% of rated voltage and discharged. Current waveforms and voltage waveforms should be checked for each stage, as well as firing time for each stage and compared with those expected. Test should be repeated at 80% and 100% of rated voltage.

After each test the power supply should be inspected for its physical state.

7.2 PREACCELERATOR COMMISSIONING

For commissioning and testing purposes, the light-gas gun injector consists of the following components:

- gas supply systems
- controls and diagnostics
- fast valve
- gun barrel

The gas supply systems include both the helium gas used to preaccelerate the launch package and the nitrogen gas used to operate the fast valve. The controls and diagnostics provide capabilities to remotely charge the gas systems, fire the fast valve, measure velocities, and monitor the system for safety and shut-down. The fast valve is assumed to be an

item manufactured by Seco-Dyn, Rancho Cucamonga, CA and is able to be operated to 7.5 ksi (510 atm) of helium. The gun barrel includes the projectile loader, velocity sensors, and connecting flanges for attachment to the railgun.

Upon the completion of the injector assembly, the individual components should be tested, one at a time. For example, the gas supplies should be pressurized and dumped over the full range of operating conditions. The controls and diagnostics can be tested without pressurizing the gases or actually accelerating a projectile. The fast valve should be operated for many cycles (~50) to clear the oils used in assembling the gun at the factory. The loader and velocity sensors should be tested with simple procedures to be sure that all problems are eliminated.

Operating with a simple projectile, e.g., a lexan cylinder in the mass range from 250 to 500 g, tests over the full range of helium pressures (starting at low pressures) can be conducted. It is important to record operating conditions and measured velocities. Based on calculations, the expected velocities as a function of the injection parameter $p_o\, x_L/m_t$ are given in Figure 58. The factors in the injection parameter are the initial helium pressure, p_o, the length of acceleration x_L, and the total projectile mass, m_t. For $x_L = 1$ m, and $p_o = 510$ atm (7.5 ksi), the expected velocity for $m_t = 250$ g is 660 m/s and for $m_t = 500$ g is 525 m/s. Since the curve in Figure 58 is based on formulas derived after a number of simplifying assumptions (see Siegel[6]), the actual velocities will be somewhat different. For example, in SUVAC II (see footnote on p. 35), calculated velocities in the range from 900 to 1300 m/s were found to be low by ~100 m/s when compared to measured experimental velocities.

---

6. A. Seigel, Theory of High Muzzle Velocity Guns, Presented at the AIAA, October 1978, U. of Maryland.

Curve 757365-A

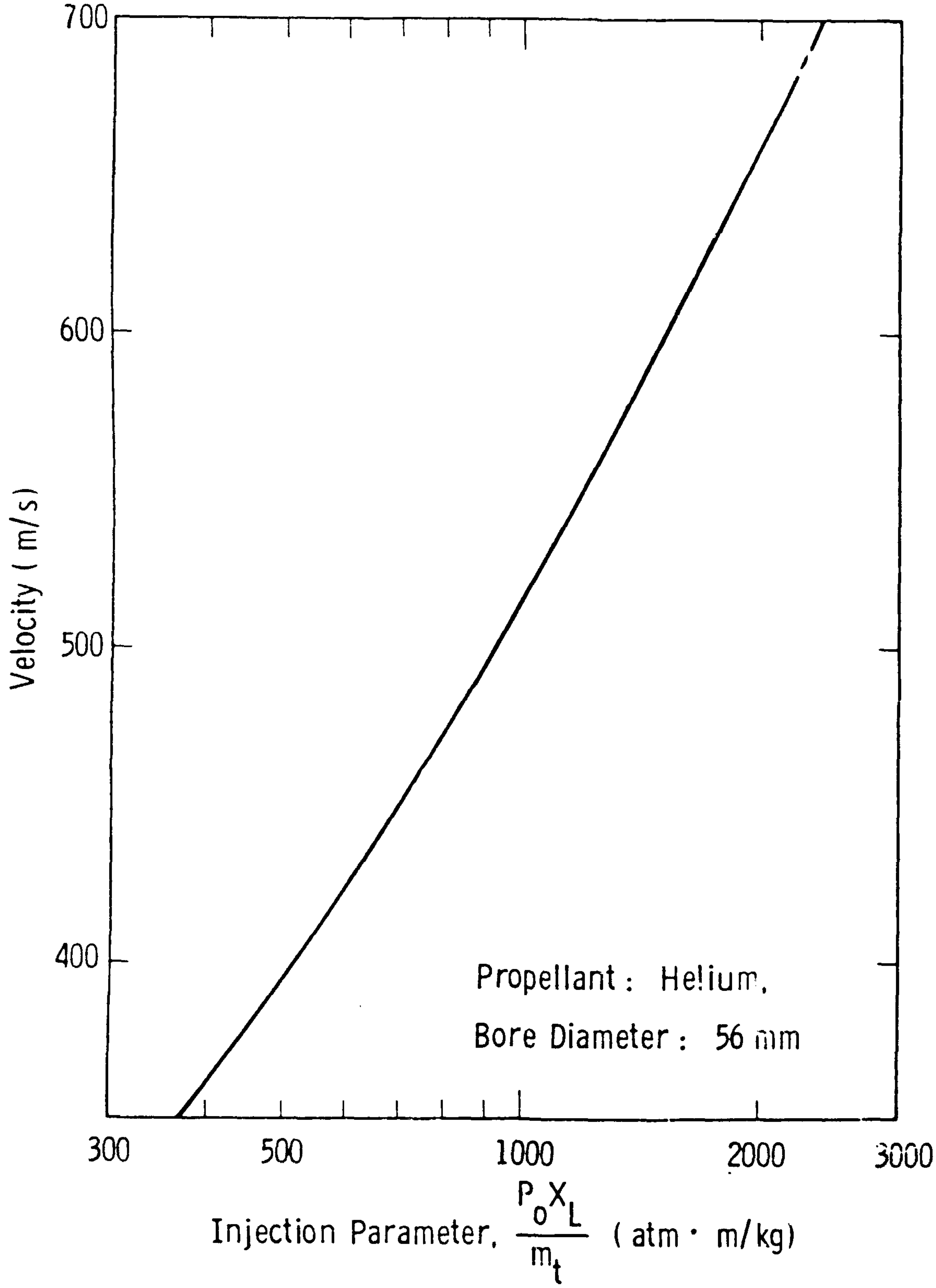

Figure 58. Theoretical Performance of the Preaccelerator as a Function of the Operational Parameters.

7.3 INTEGRATED EML SYSTEM COMMISSIONING

The full commissioning of the integrated launcher can begin after the completion of the commissioning of the power supply and the preaccelerator. The number and type of tests should be based on criteria which simultaneously allows a number of accomplishments to be achieved, including:

- meeting interface requirements
- determining actual operating parameters
- establishing performance curves
- developing modeling and predictive capabilities
- developing testing procedures
- establishing operating and maintenance schedules

By conducting these tests, operating experience and data can be accumulated to optimize the capabilities of both the facility and the staff running the launcher.

The sequence of shots should allow the facility to be brought on-line in a simple and straightforward manner so that troubleshooting will be efficient and conditioning of the systems will progress smoothly. Recommended shot sequences are provided in Table 45. The emphasis, as indicated in the comments listed for each shot sequence, is to quickly establish a capability with a low risk of jeopardizing the schedule and of equipment damage.

The commissioning shot sequence will involve between 10 and 20 test shots where each capacitor bank is brought into operation, one at a time, and is initially operated at low and moderate voltages. Such a sequence will satisfy the various conditions indicated above while minimizing potential equipment damage. For these initial shots, a simple launch package which is expected to cause only low-level damage to the gun barrel wall surfaces is recommended. A teflon projectile with a solid metallic armature or transitional metallic armature are the likely candidates.

Table 45

SHOT SEQUENCES FOR THE COMMISSIONING OF THE LAUNCHER

Sequence Number	Number of Shots	Number of Banks Used	Bank Voltage	Comments
1	3-5	0	0	Operate injector with no current to rails to check launch package survivability, velocity diagnostics, and performance parameters.
2	1-2	1-4 (into dummy load)	low	Check projectile triggering of capacitor banks and verify the timing delays between banks.
3	3-5	1	7-15 kV	Operate gun with low values of rail currents to check in-bore diagnostics, bore surface wear, and performance.
4	1-2	2	15 kV	Operate gun for 2-bank current injections at moderate currents to verify systems and accumulate performance data.
5	2-4	3-4	15 kV	Complete moderate current operations, verify systems, and accumulate performance data.
6	1-2	4	18-20 kV	Operate gun at near maximum currents to fully commission system, accumulate performance data, and obtain bore surface and pressure sealing data.

Key to the successful commissioning of the gun is the acquisition of data of actual velocities as well as B-dot sensor and barrel voltage data. The direct velocity data is clearly important to obtain so that predicted performance can be verified. The B-dot and voltage data are needed to understand the launcher's internal dynamics for purposes of optimizing performance velocities as well as to help in troubleshooting if problems occur. From the B-dot data, position vs time profiles can be obtained. With this data, velocities and accelerations can be calculated so that effects due to drag can be evaluated. With this information, the selection of starting armature characteristics and capacitor bank voltages and time delays can be determined which provide the required performance velocities.

The barrel voltage data, including both breech and muzzle voltages, are important to obtain for several reasons. Since injection of the launch package at an initial velocity is required to minimize breech damage, the position of the package at the start of current is critical. The timing of this current should allow the package to travel beyond the current feed point, but not to travel too far such that the full length of the barrel cannot be fully used in the acceleration. The barrel voltage data provides the clearest indication of the time associated with the start of the current, and with additional data from a bore inspection the position of current start can be obtained. In addition, the voltage values throughout the launch can be used to characterize the armature in terms of its composition (due to ablation products) and its state (solid, transitioning, or plasma). Finally, the voltage properties can be used to select the timing delays for the firing of the various banks. With the adjustment of the delays, the barrel voltage can be optimized to allow for increased launch efficiency. The commissioning sequence outlined in Table 45 will yield steadily increasing kinetic energies at the muzzle. In the final shots, when almost all of the capacitor bank energy is used, the muzzle

velocity should be over 3000 m/s with a 500-g launch package. The test sequence is one in which the launcher can be brought on-line with velocities in the appropriate range and which allows the various subsystems to be incorporated in a simple sequential manner.

8. TEST PROGRAM

Even after the facility has been fully commissioned, there are additional technical issues that must be addressed before the facility can be operated in a reliable, efficient, cost-effective routine manner to conduct terminal ballistic studies. These issues can be best addressed by further tests.

Four separate test programs are described here. These programs and their objectives are as follows:

1. Launcher Tests: Conduct a series of shots while incrementally increasing the capacitor energy. Verify that the launcher works properly and predictably throughout its operating range, and that desired amounts of kinetic energy can be achieved at the muzzle.
2. Armature Tests: Conduct a series of shots to determine the optimum armature design. The optimum armature has minimal mass, causes minimal bore damage, and can be interfaced with the projectile package.
3. Projectile Package Tests: Conduct a series of shots to determine the optimum launch package design. This is a design in which the desired penetrator is consistently delivered to the target with the required trajectory, orientation, and velocity.
4. Bore Reconditioning Tests: Develop bore evaluation and reconditioning tests that minimize operating cost and maximum the availability and performance of the facility.

Although all four test programs can be conducted in parallel, a certain amount of prioritizing should take place. As suggested by the list, the launcher tests should be emphasized initially. During the first few tests, when the capacitor banks are incrementally brought on

line, it would be best to stick with a simple armature and launch package design, so that each new test does not incorporate too many variables. As resources and crew expertise permit, variations of armature and launch package design can be worked into the test program.

8.1 LAUNCHER TESTS

In order to establish a data base for this particular gun that will guide the selection of those quantities that are preset prior to a firing, additional tests of the launcher beyond the commissioning tests will be required. However, they will be conducted under the guidelines established for the commissioning plan, i.e., to increase the number of capacitor banks used, and to increase the energy stored in the capacitors as more confidence is gained in the performance of the gun. Tables will be generated of the velocity achieved for a given projectile mass as the number of capacitor banks, the voltage of each bank, and the time delays following the entrance of the projectile into the rail gun prior to firing the different banks is varied. This information will be generated for various projectile masses. Obviously, this data will be augmented by the data obtained during the tests to establish a standard armature and projectile package.

During these tests, experience will be gained in obtaining and interpreting the output of the sensors used in the diagnosis of a shot such as B-dot signals, rail current, breech and muzzle voltages,and x-ray signals. The output of the sensors will be correlated with the performance of the gun.

Some statistics on failure modes will also be generated during the course of these tests and methods of operation will be identified that will minimize the number of failures.

8.2 ARMATURE TESTS

The launcher tests described for the commissioning of the facility are based on using a launch package which is relatively simple

and will allow the commissioning to occur without directly addressing all the many armature design issues. After the launcher is commissioned, armature tests should be conducted in a manner allowing the quick selection of a few options which provide a degree of flexibility in the ballistic research program to cover the range of muzzle velocities of interest. With some analytical and design activities conducted before the actual testing of armatures, the optimization of the various designs can be completed with only a few tests. In the following section, armature design is discussed in some detail, followed by consideration expected in the testing and commissioning of practical armatures.

8.2.1 Armature Features

The function of the armature is to provide a continuous low resistance current path between the EML device rails while accelerating a given projectile to the required velocity. The armature may be a separate entity or an integral part of the projectile. The armature interfaces intimately with the rails and insulation in the bore of the device, and the driving electrical circuitry.

The armature should function in a manner such that:

- No debris is left behind the armature as it moves down the rails. Debris can provide current paths between the rails which results in a reduction of the final velocity.
- There is limited damage (ablation, sputtering, melting, chemical erosion, material deposition) to the bore of the EML device so that a specified number of launches can occur before maintenance is required.
- The integrity of the armature is maintained throughout the acceleration, e.g., solid armatures should not melt, arc armatures should not become massive due to ablation. The length of an arc armature must be limited and the arc must be continuous so that forces are effectively transmitted.
- The length-to-bore diameter ratio and design of a solid armature/projectile package should be such that there is no

mechanical binding or tilting as the armature/projectile package moves down the bore.

- For high efficiency, the mass of the armature must be small compared to the mass of the payload projectile unless it is an integral part of the projectile. If it is an integral part of the projectile, it should not impact on the kinetics of the projectile motion in a detrimental manner. The armature voltage must be low to minimize electrical losses.

We have considered three basic categories of armatures for the EML:

1) solid conducting armatures
2) plasma-arc armatures
3) hybrid or transitioning armatures (both an arc and a metallic mass conduct current)

There are many variations within each category, e.g., solid armatures may be fabricated from different conductors such as copper or aluminum, and they may consist of multi-leaf chevrons or multifibers; arc armatures may be formed by vaporizing foils of different materials including propellants and seed materials that have low ionization potentials.

The solid armature has the following advantages over the arc armature:

- The voltage drop (as measured across the rails at the muzzle) is small and therefore there is low power dissipation in the armature and less damage due to radiative power deposited in the rails and insulators.
- Current flow is confined to a small axial distance which allows efficient use of distributed energy systems for introducing power to the rails.
- Probability of secondary arc formation is minimized.
- Change of phase of a portion of the armature represents a heat sink that can limit temperature excursions of the armature and reduce mass requirements.

- The solid armature can be designed to shield the insulators which separate the rails.

The arc armature has the following advantages over the solid armature:

- Smaller mass and therefore higher overall efficiency.
- More flexibility, mass-wise, in the design of the projectile.
- Electrical contact with the rails is insensitive to bore expansion.
- Smaller current densities.

In practice, for high-powered EML devices, a solid armature will naturally tend to become a hybrid armature at high velocities. Early in the acceleration process, electrical contact is made by metal-on metal and later in the launch with arcs at the rail-armature interfaces. The hybrid is a combination of the above two types and if designed properly will have a combination of the advantages listed for each of these types.

8.2.2 Design of Solid Armatures

There are three aspects to the design of solid armatures:

- Design of the bulk of the armature to assure that the armature retains its integrity under the ohmic heating and Lorentz force to which it is exposed while moving down the full length of the bore of the gun,
- Design of the sliding contact regions of the armature to reduce the contact resistance sufficiently that melting and arcing at the interface is minimized throughout the period of acceleration, and
- Integration of the armature into the projectile package.

<u>Bulk Armature Design</u>

It is preferable to have uniform ohmic heating throughout the armature to avoid damage and to minimize the armature mass. Accounting for the skin effect in the design of the armature should improve its performance. Multileaf chevron or fiber brush designs of solid

armatures allow a more uniform field penetration and consequently uniform current density. However, at high velocities the velocity skin effect can still affect the current distribution in the armature. Near the projectile, the current flows on the surface of the rails and fans out from all the rail surfaces in order to flow through the armature. When the armature moves at high velocities, the current tends to flow through the rear of the armature, since the fields have inadequate time to diffuse into the rails near the leading edge of the armature. In order to combat the velocity skin effect, transposed armature conductors can be used. A transposed armature consists of conducting filaments that are twisted so that a filament that is at the leading edge of the armature adjacent to one rail rotates in crossing the gap so that it is at the trailing edge of the armature at the second rail. Although this design minimizes the velocity skin effect, the resistivity and consequently the ohmic heating of the armature will be increased because of the longer path length for the current. Other drawbacks of a transposed design are increased cost and complexity, and decreased packing density of the fibers.

Care must be taken in the design of projectile packages when they are driven by a solid armature down a circular bore so that no rotation occurs which will result in contact-points being off the rails. Preacceleration of the projectile package so that it enters the railgun with a velocity ≥ 500 m/s is important for minimizing rail damage near the breech of the gun. Operation of electromagnetic launchers has clearly demonstrated the importance of preacceleration.

When the armature is properly designed for uniform heating, the maximum bulk temperature of the armature due to ohmic heating, will be determined by the cross-sectional area of the armature conductor. The two most practical conductors, aluminum and copper, have adiabatic action-to-melt values of 2.7×10^8 and 8.6×10^8 A^2s/cm^4, respectively. These numbers take into account the variation of resistivity and heat capacity with temperature. If we divide these action-to-melt values by the material densities, we see that aluminum has a greater action-to-melt per unit mass, and is therefore a more efficient conductor.

The following equation can be used to thermally size the armature for ohmic heating;

$$A_{MELT} = \sqrt{\frac{(PA)}{(ATM)}}$$

where

A_{MELT} = conductor cross section (cm^2) at which bulk melting temperature is reached.

PA = Pulse Action (A^2s)

ATM = Action to Melt (A^2s/cm^4)

In order to avoid melting in a solid armature, the conductor cross sectional area must be greater than A_{MELT}.

In addition to meeting the thermal requirements, the armature must be designed to be structurally sound so that it does not distort to the extent that it cannot perform its function.

Sliding Contact Region

If a solid armature were constructed of a single piece of conductor there would be contact at only several points with the rails corresponding to the high spots or asperities on the surfaces. The current must constrict to pass through these spots and this constitutes one component of the contact resistance viz the constriction resistance. The constriction resistance equals the average resistivity of the two contact materials divided by the effective diameter of a circle having the area of the sum of the areas of the contact points. The area of contact is given by the ratio of the contact force to the hardness of the softer of the two materials in contact. This expresses the fact that at the actual contact points the localized applied pressure exceeds the yield point of the softer material and it plastically deforms, increasing the contact area, until the applied pressure equals the hardness. For sliding contacts, the hardness must be modified to account for shearing mechanisms in addition to the static pressure

affecting the contact area. An additional resistance term must be added to account for any surface films. The expression for the total contact resistance shows that for given contact materials the contact resistance is only a function of the applied force. For a given available total force, it is better to subdivide the available area into many separate independent contacts in order to reduce the contact resistance. There is, however, a limit to the number of independent contacts based on mechanical considerations.

In order to prevent arcing at an interface the voltage drop across the interface should be kept below ~ 0.5 V. Substituting this critical value of voltage into the expression for the contact resistance yields a minimum value that is required for the contact force. As a rule of thumb, this force is typically one gram force per ampere of current. The frictional force and amount of wear are also proportional to the contact force.

The power dissipated at the sliding surface is the sum of that due to frictional heating and ohmic heating caused by the contact resistance. The heat generated will go partially into the rails and partially into the armature. The heat generated will not penetrate deeply into the armature during the short acceleration time interval. The surface temperature of the rails and armature can be calculated from the power dissipation.

Control of the normal force acting on the fiber or finger tips is important for achieving reliable armature performance. This force will be determined by the mechanical design of the contact arms, and by the current profile of the launch. For most designs, the electromagnetic force is used to produce the normal force.

8.2.3 Design of Plasma Armatures

Railgun launches using plasma armatures have been successful in achieving velocities up to 6 to 7 km/s since the late 1970s. Based on these experiments, the understanding and associated technical issues needed to apply plasma armatures to accelerating railgun projectiles is well developed and comprehensive. The following discussion indicates

the basic elements associated with the development of plasma armatures for low and moderate velocity launches.

Testing activities, which are directly applicable to this application, have resulted in plasma armature designs with the following features:

- light-gas gun injected launch packages
- launch packages which minimize breech damage to the bore walls
- initial armature fuse configurations which smoothly transition into fully-formed plasma arcs
- armatures with good low- and moderate-velocity launch dynamics
- armature calculated parameters which have been anchored to experimental launch data (i.e., B-dot signals and railgun voltage signals) over a wide range of rail currents and operating conditions

From the test data and associated analyses, the issues which are the most critical in terms of providing efficient launches are the following:

- controlled rail and insulator ablation
- reduced arc viscous drag effects
- minimization of performance limiting effects due to secondary arc formation and to instabilities in the acceleration dynamics
- stiffened bore assemblies to minimize bore leakage
- sufficient diagnostics to characterize each launch

The provision of the proper launch characteristics is via model calculations to aid in the determination of the railgun operating parameters, i.e., rail currents, timing of staged currents, and initial parameters for starting launch packages.

The modeling of the physics of railgun armatures requires the development of equations involving a number of overlapping analytical areas and disciplines. Approaches which have been successfully applied

involve both design and data analysis activities as shown in Figure 59. As indicated in the figure, a set of input parameters characterizing a design or test are supplied to a number of physics and engineering models which self-consistently interface with each other. The resultant solution, obtained in an iterative manner, provides calculated results which account for a full range of physical phenomena associated with a railgun launch. The discussions which follow indicate a number of key areas in which the physics modeling is critical to understanding how plasma armatures behave and efficiently accelerate projectiles.

One of the key operating parameters is the pulsed pressure associated with the plasma arc. This pressure is a function of the time-dependent rail current and of the axial pressure profile associated with the armature region behind the projectile. For example, the peak pressure at any point in a launch is expected to be immediately behind the projectile and the volume-averaged pressure within the plasma is less by factors of 1.5 to 2.5 than the peak, depending on the actual length of the plasma.

Another area is the modeling of the plasmas power balance conditions. The power balance determines the plasma temperature and thus affects the arc voltage. In addition, the plasma atomic composition and total arc mass is a function of the rate of the wall ablation which is determined by the power balance conditions. Since wall ablation can result in performance limiting effects on the launch dynamics, the complete modeling of the armature power balance is important to provide.

A third area important to understanding the plasma physics is the arc voltage. Compared to solid armatures, plasma armatures have large voltage drops which can result in launch inefficiencies, bore surface damage, and long, massive plasmas late in the launch. These plasmas are characterized by arc temperatures and particle densities resulting in a partially-ionized plasma which has a resistivity determined by the atomic composition of the arc. As a result, ablation processes and arc voltages are strongly inter-dependent so that the

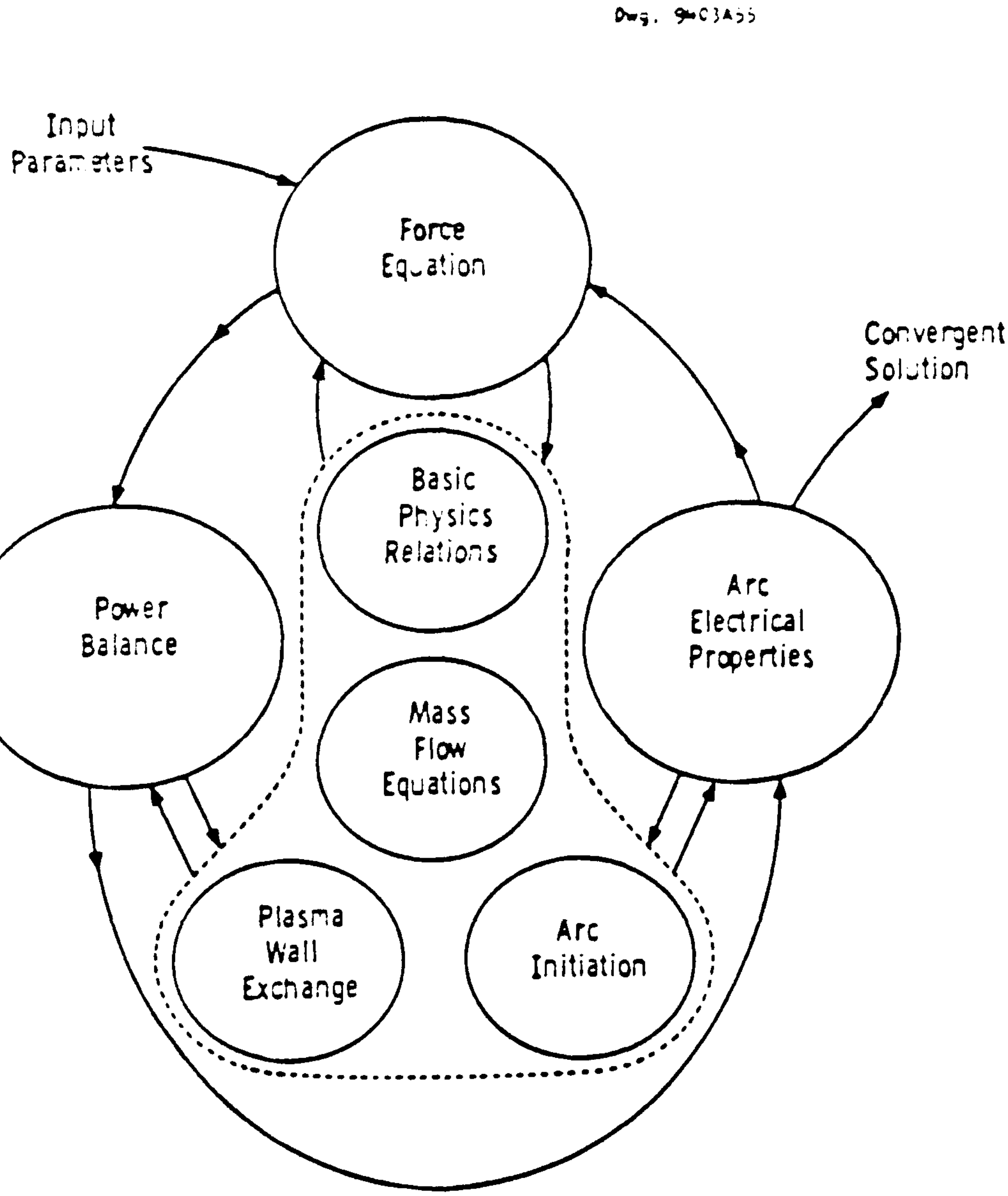

Figure 59. Schematic representation of the general approach to railgun physics.

design of the initial armature package must be carefully completed with the optimization of the launch dynamics in mind. For velocities in the range from 2 km/s to 4 km/s, we have both analytical and experimental results providing a strong basis for such a design. Key to this design are calculations which indicate launcher performance based on bore materials, rail currents, launch accelerations, and projectile masses. From such calculations, the flow of masses into and out of the plasma region can be quantified and optimized. See Figure 60, which indicates the nature of this mass flow.

Finally, another area of importance associated with the physics of plasma armatures is the formation of the moving, plasma arc. The starting armature configuration consisting of a metallic fuse which carries the rail current for a brief period, fuses, vaporizes, and then transitions into a fully-formed plasma arc. The operating phases which occur prior to the full plasma arc are indicated in Figure 61. The resulting behavior of the arc voltage due to the formation of the plasma is shown in Figure 62. With the careful selection of initial conditions, fuses which undergo smooth transitions into plasma armatures which have atomic compositions providing low-voltage, low-mass arcs have been demonstrated in launches at the Westinghouse STC.

8.2.4 Design of Hybrid Armatures

To understand the behavior of the hybrid armature during the initial portion of the launch, a set of calculational models based on power balancing were used to quantify the vaporization during the transition period of the launch. The models include the same equations that govern the performance of fuse wires under the action of high short-circuit currents.

Inputs to the equations include the properties of the starting metallic mass as well as the rail current during a shot. The properties of this mass used in the modeling include:

- mass density of the solid material
- heat capacity in the solid state
- heat capacity in the molten state

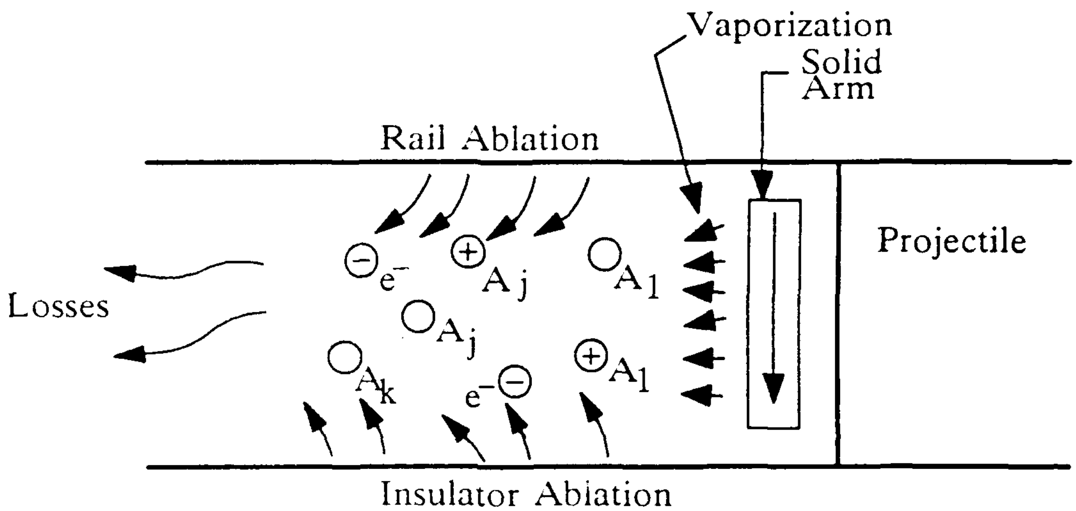

$$m_{ARC} = \sum_{i=1}^{k} m_{A_i}$$

Figure 60. Schematic of the armature mass flow indicating a multi-component plasma and vaporizing solid.

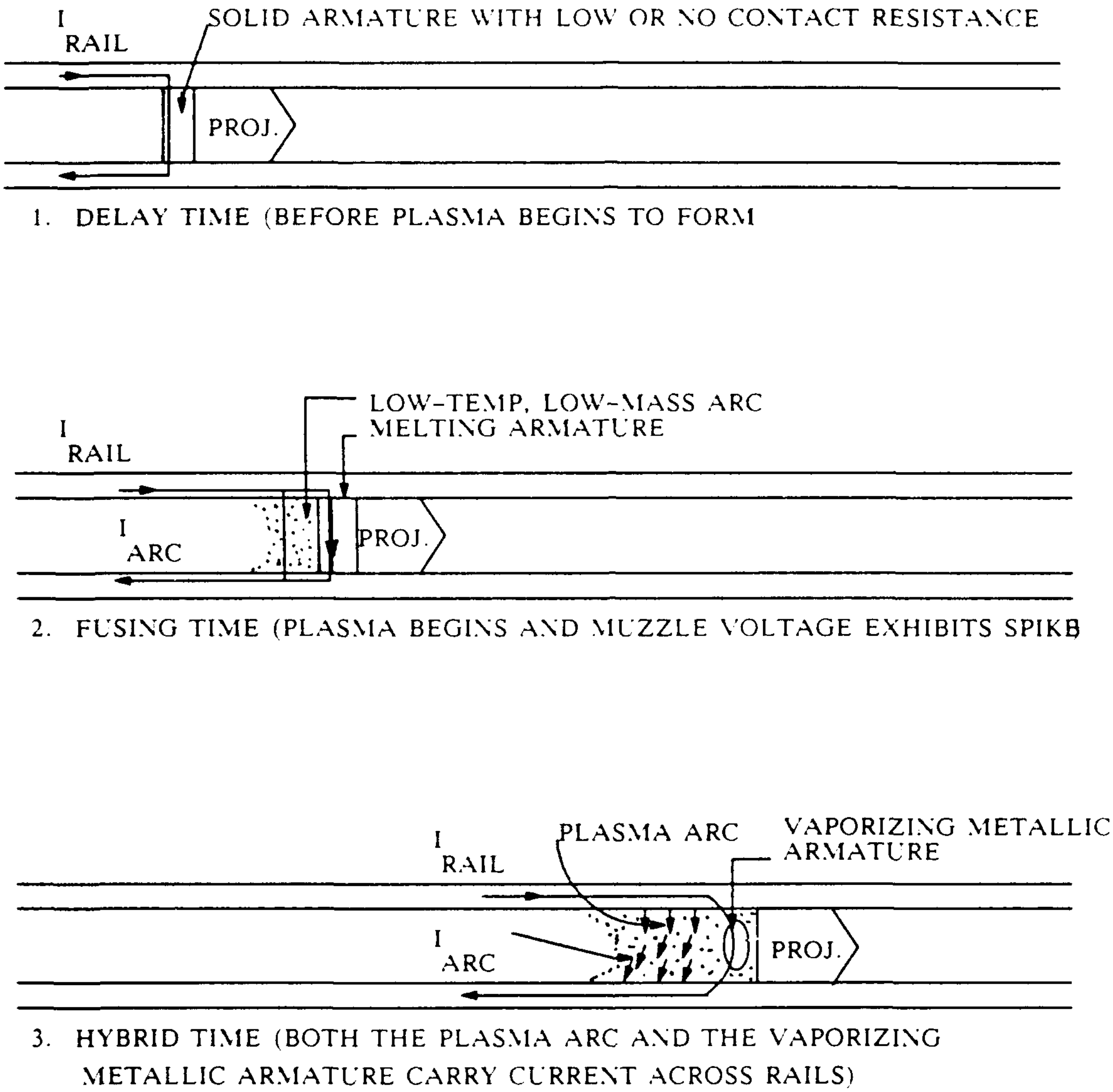

Figure 61. Three periods of arc formation using a metal fuse.

Curve 757366-A

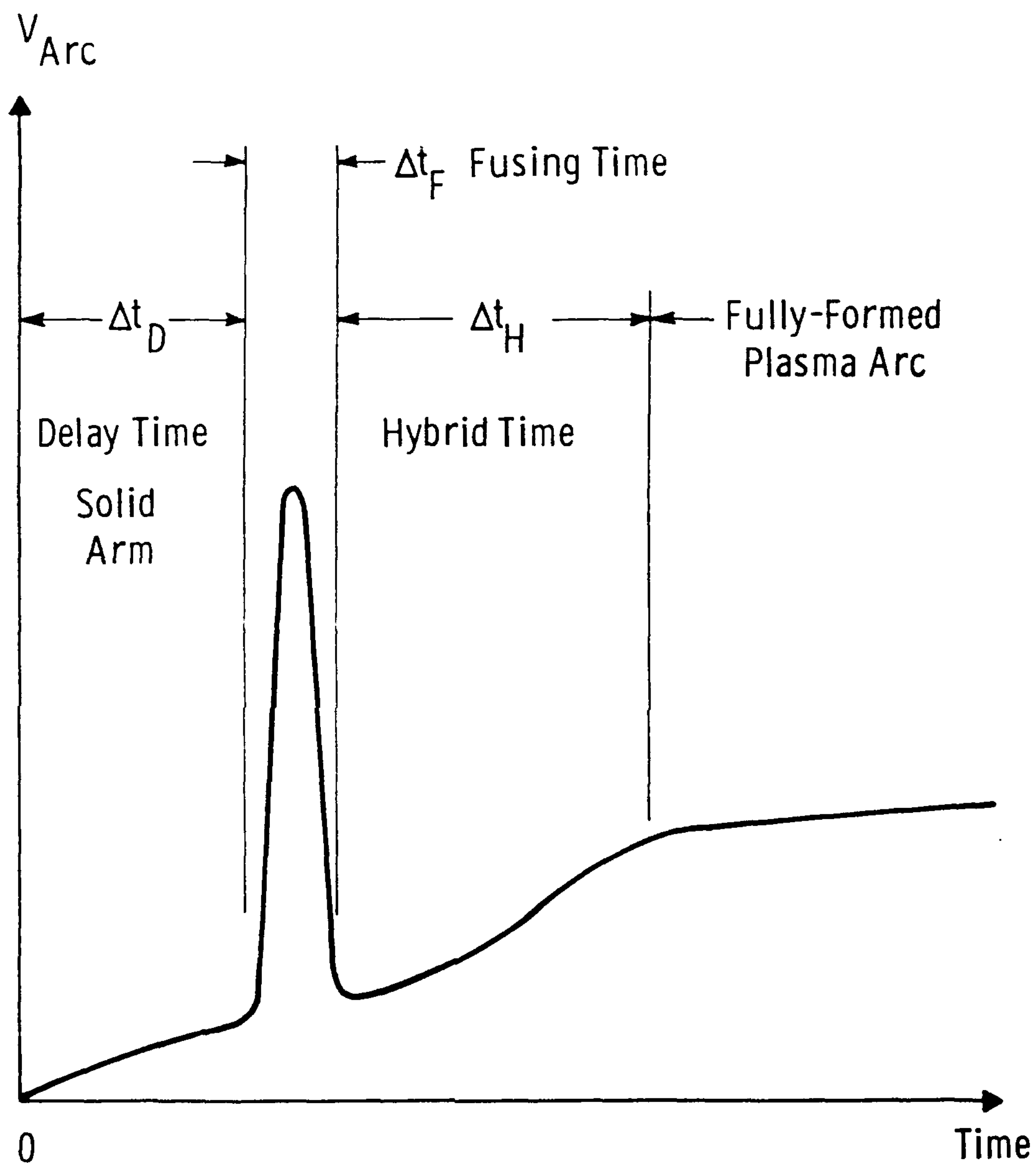

Figure 62. Characteristic arc voltage on SUVAC II.

- temperature-dependent electrical resistivity
- heat of fusion
- heat of vaporization
- melting temperature
- vaporization temperature

The fuse design characteristics used include:

- armature starting cross sectional area
- armature starting thickness
- armature starting mass
- armature starting length

The model equations allow values to be determined for the following:

- time period before vaporization begins
- time period over which the armature fuses
- vaporization rates during the fusing period
- vaporization rates during the hybrid phase

The equations are a function of the material properties, armature characteristics, railgun operating parameters, and the effective fraction of rail current vaporizing the metal. The instantaneous vaporization rate at each point in the launch is given by the equation

$$\dot{m}_{VAP} = m_{ARM}/\tau$$

where m_{ARM} is the remaining mass of the metal at that point in the launch and τ is a characteristic decay time given by

$$\tau^{-1} = \frac{(f_H\ I_{RAIL})^2\ R_{ARM}}{m_{START}\ \Delta h_{ARM}}$$

where f_H is a multiplier (≤ 1) on the rail current I_{RAIL} and represents an average of the fraction of the total current that flows through the metallic portion of the armature, R_{ARM} is the armature resistance which is a temperature-dependent function for the particular armature geometry used, m_{START} is the starting metallic armature mass, and Δh_{ARM} is the enthalpy required to vaporize a unit mass (e.g., Δh_{ARM} = 10.31 MJ/kg f r

aluminum). For SUVAC II data, the value of f_H was determined from the time interval that the hybrid exists (see Δt_H in Figure 62), and also from B-dot data, and was found to be $\simeq$ 0.5 for the three shots studied. From the vaporization rate equation, one can see that the $\dot{m}_{VAP}$ contribution to the plasma can be controlled through I_{RAIL} and m_{START} and that, with an optimum value of m_{START}, the value of $\dot{m}_{VAP}$ and the duration of the hybrid phase can be predetermined for an efficient launch. Thus, a transitioning metallic armature can provide a source of atoms supplying the arc portion of the armature. With this source, ablation of the rails and insulators can be effectively reduced, and the net increase in total armature mass and length slowed during the hybrid phase of the launch.

The application of the hybrid armature to SUVAC II testing has proven to be an important part of that program. This is the case because we have been able to identify specific performance advantages of the hybrid when it is compared to the more conventional plasma-only arc armatures. Based on both experimental and analytical results, the advantages which were discovered include the following:

- plasmas are strongly ablation-controlled while hybrids are only weakly controlled by ablation since the metallic fuse provides a second source of arc atoms
- hybrids provide stabilization against armature current disintegration by having a low-resistance current path through the non-arc portion of the armature
- data and analysis show that the armature voltage is lower during the hybrid period of a launch
- data and analysis also show that the arc portion of the hybrid has a lower mass and a shorter length when compared to a plasma-only armature, especially late in the launch
- experiments have demonstrated that with preacceleration the heavier starting armatures provide additional protection against damage to the bore walls in the breech region for the reasons given above.

From these results, we feel that the hybrid option represents a viable armature for achieving good velocity performance in the BRL system.

8.2.5 Selection of Armatures

Based on the previous discussions, and on experience at Westinghouse and throughout the EML community, seven specific armature options are presented for consideration in the BRL test program. They are:

1. Solid - monolithic metallic block.
2. Solid - straight fibers.
3. Solid - transposed fibers.
4. Plasma - metallic fuse.
5. Hybrid - monolithic metallic block.
6. Hybrid - straight fibers.
7. Hybrid - transposed fibers.

Note that the three basic types are all represented, and that the solid and hybrid designs each have the same three subgroups. The solid and hybrid designs (2 and 6, for example) could be the exact same armature. In this case, the difference between a solid and hybrid would be the level of energy used. A 50-g aluminum fiber armature would be classified as a solid armature at low energy, because bulk melting would not be expected. However, at full energy this same armature would be expected to undergo bulk melting late in the launch, and would therefore be classified as a hybrid.

Design #2, a solid armature with straight aluminum fibers, is proposed for the initial launcher commissioning tests. The armature is shown schematically in Figure 63. The contact areas subtend 90° arcs on a 5.6-cm bore. This produces an average fiber length of 5.09 cm. The total cross-sectional area of the armature fibers is 5.78 cm^2, which will produce bulk melting from even ohmic heating at a pulse action of 9×10^9 A^2s. The pulse action is calculated from the following equation;

$$PA = \frac{2\ M\ V}{L'}$$

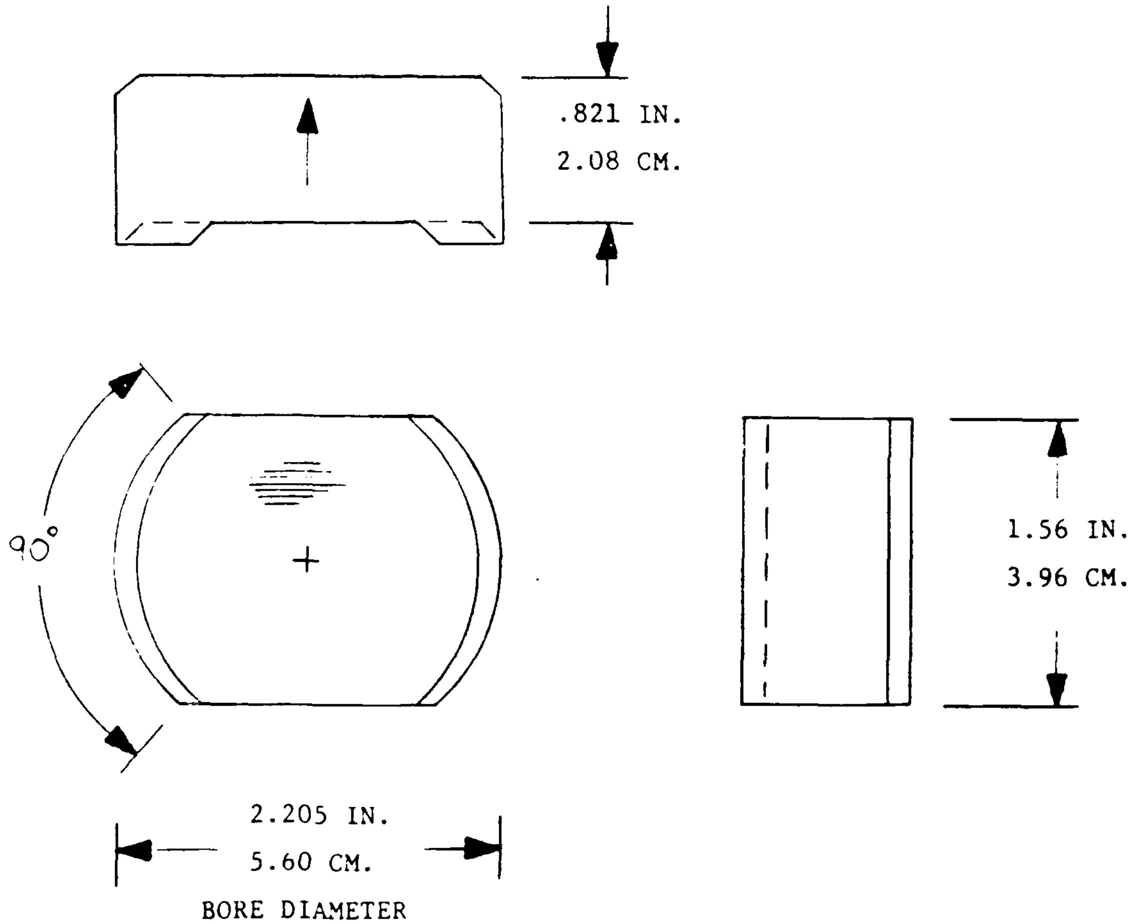

Figure 63. This is an aluminum fiber armature with the overall dimensions as shown. This armature contains 80 grams of aluminum and 17 grams of epoxy. This is the baseline armature to be used in early commissioning of the BRL launcher.

where PA = Pulse Action (A^2s)

M = Launch Package Mass (0.515 kg)

V = Muzzle Velocity (3,500 m/s)

L' = Inductance Gradient (0.4 μH/m)

This equation holds true for a square current pulse, and if the injection velocity is zero. The armature contains 79.8 grams of 0.51-mm diameter aluminum fiber, with a packing density of 70%. The remaining 30% is filled with 17.2 grams of epoxy, thus giving a total armature mass of 97 grams.

This armature should remain solid at the lower energy levels, but should show signs of melting as higher energy levels are reached. At what level melting occurs, and its affect on performance, are difficult to predict. These questions can be answered during the test program. If performance is not satisfactory, this baseline design could be improved by changing the mass or by transposing the fibers. As discussed earlier, transposing the fibers results in a more uniform current flow and consequently more uniform heating in the armature.

Initial tests could utilize a launch package similar to that shown in Figure 64. This 350-g launch package consists of an aluminum body containing an 88-g aluminum fiber armature and a lexan sleeve. This launch package was designed and built by Westinghouse for use in a 50 mm round bore gun at ARDEC.

A second promising armature design is design #5. This type of armature has been used successfully on SUVAC II at Westinghouse. This armature is shown in Figure 65. It is the same approximate size and weight as the 97-g fiber armature, but is cheaper and easier to integrate into the launch package. Initially, it is a truncated aluminum cone. The base of the cone is the leading edge. It makes edge contact with the rails. The edge quickly ablates and generates a plasma that fills the small gaps between the rails and the aluminum cone. The voltage drop is kept fairly low due to the short arc lengths. This armature can also be reused, as long as a new fuse foil replaces the ablated edge.

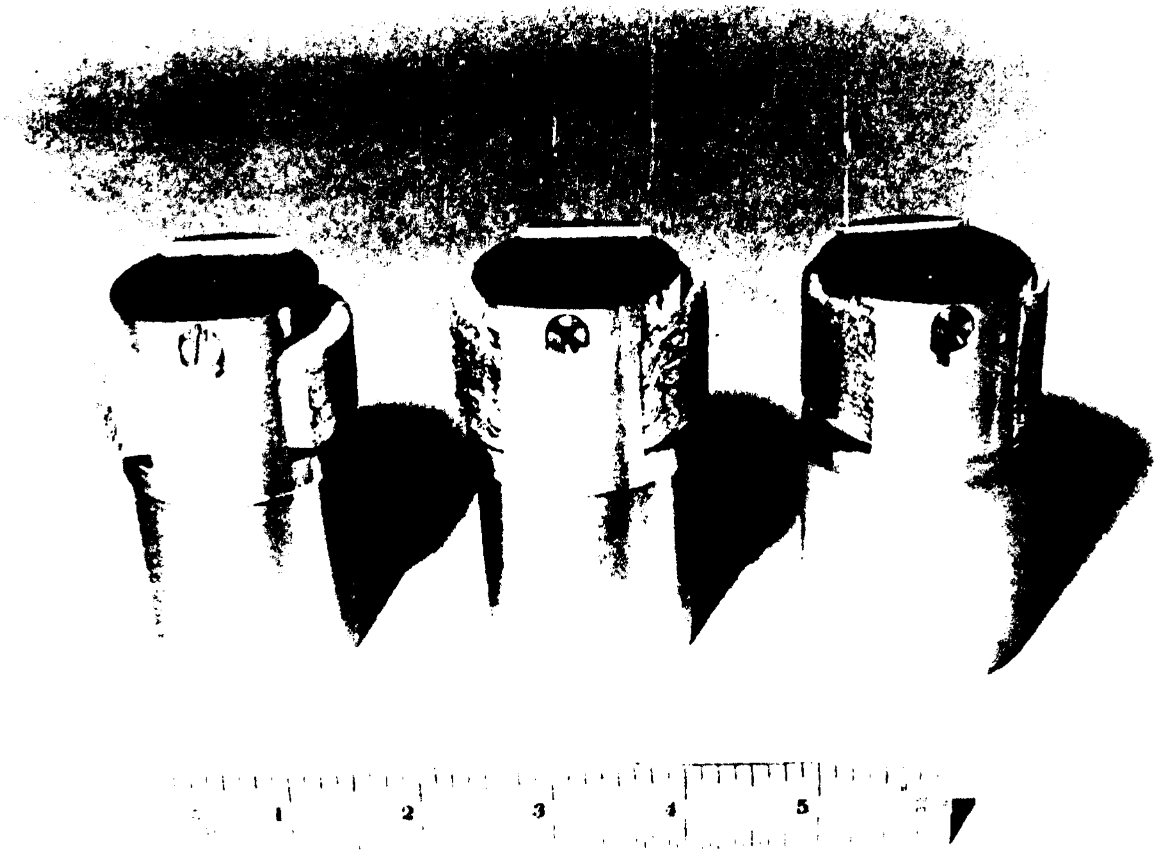

Figure 64. This photo shows the 3 final stages of fabrication of a 50-mm aluminum fiber armature and launch package for ARDEC. The right view shows the finished package, with the fibers swept back and machined, and a lexan sleeve added to the body. This launch package would be similar to the one used in the initial commissioning of the BRL system.

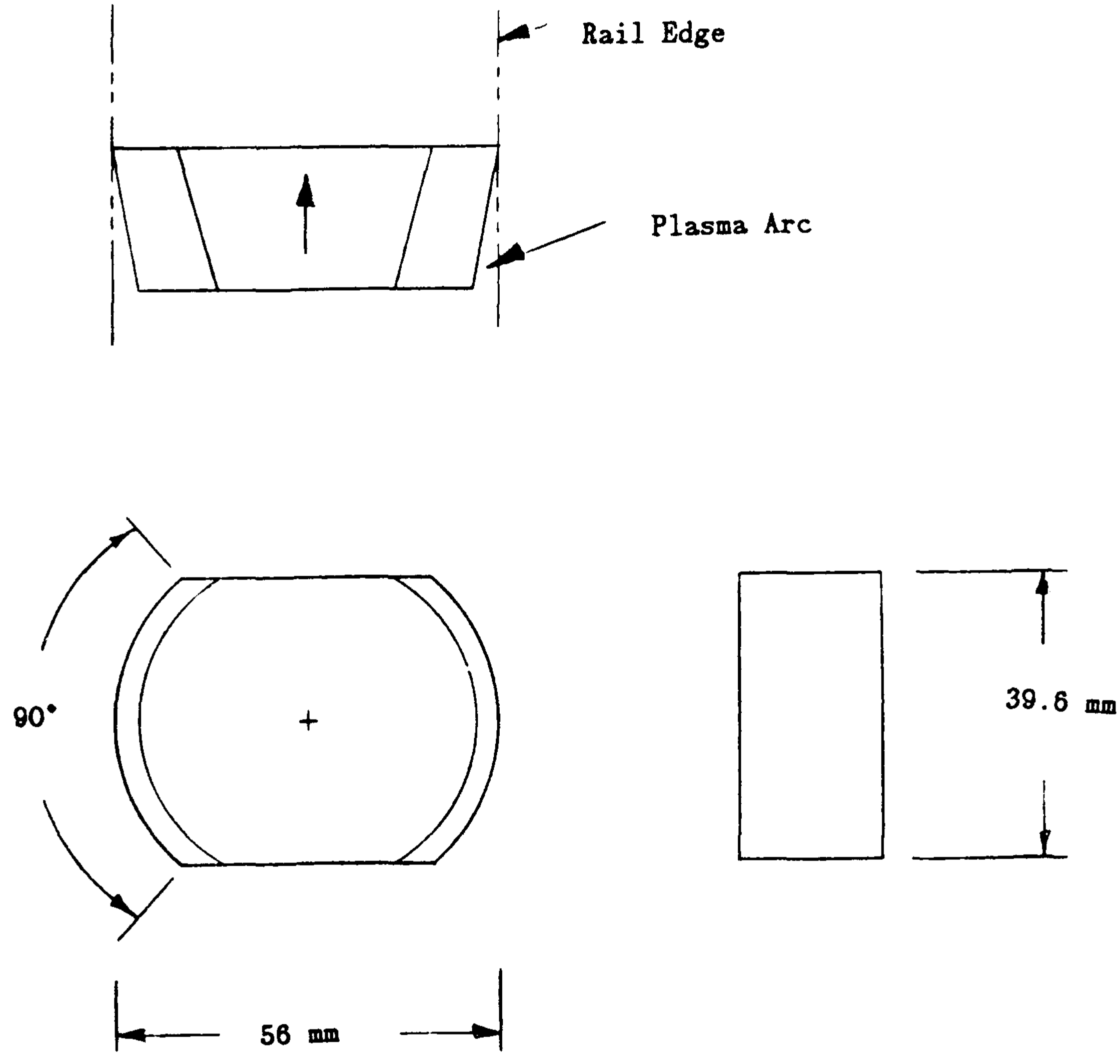

Figure 65. This shows armature design No. 5, which is a truncated aluminum cone. The base edge of the cone makes initial contact with the rails and acts as a fuse. The plasma forms and dwells in the small gaps between the armature and rails.

8.3 PROJECTILE PACKAGE TESTS

The goal of these tests is to successfully launch meaningful projectiles at desired velocities, thereby achieving the ultimate goal of making the launcher an effective terminal ballistics facility. The projectile package test sequence would begin when the simple slug shown in Figure 64 is first replaced with a saboted penetrator. It would end when a launch package, containing an optimized armature and saboted penetrator, is repetitively delivered to the target successfully. We recognize that BRL personnel are experts in the design of obturator/sabot/penetrator packages. Consequently we have not done any in-depth analysis or design for this study. However, some conceptual designs are presented below to indicate how these packages can be integrated with their armatures.

Theoretically, these projectile package tests could be done in parallel with previous tests. However, if faced with limitations in manpower, expertise, or any other resource, it is probably best to concentrate first on the launcher tests (Section 8.1) and then on the armature tests (Section 8.2) before firing more complex and costly launch packages.

A generic launch package is shown in Figure 66. A more detailed sketch of the sabot and penetrator is shown in Figure 67. From back to front, the launch package consists of a lexan helium seal, armature, lexan plasma seal, and sabot/penetrator assembly. The lexan helium seal enables the expanding helium gas to push the launch package through the preaccelerator. It must be firmly attached to the back of the armature. The armature, shown as a fiber armature in Figure 66, is a modular part of the launch package, thus enabling different armature designs to be used. The plasma seal in front of the armature provides the mechanical interface that transmits the armature accelerating force to the sabot/penetrator assembly. The total launch package contains six loose pieces. They are the armature with two seals attached, the penetrator, and four sabot petals. The total launch package mass is 500 g, and the penetrator mass is 160 g. The payload percentage could improve as the design is optimized.

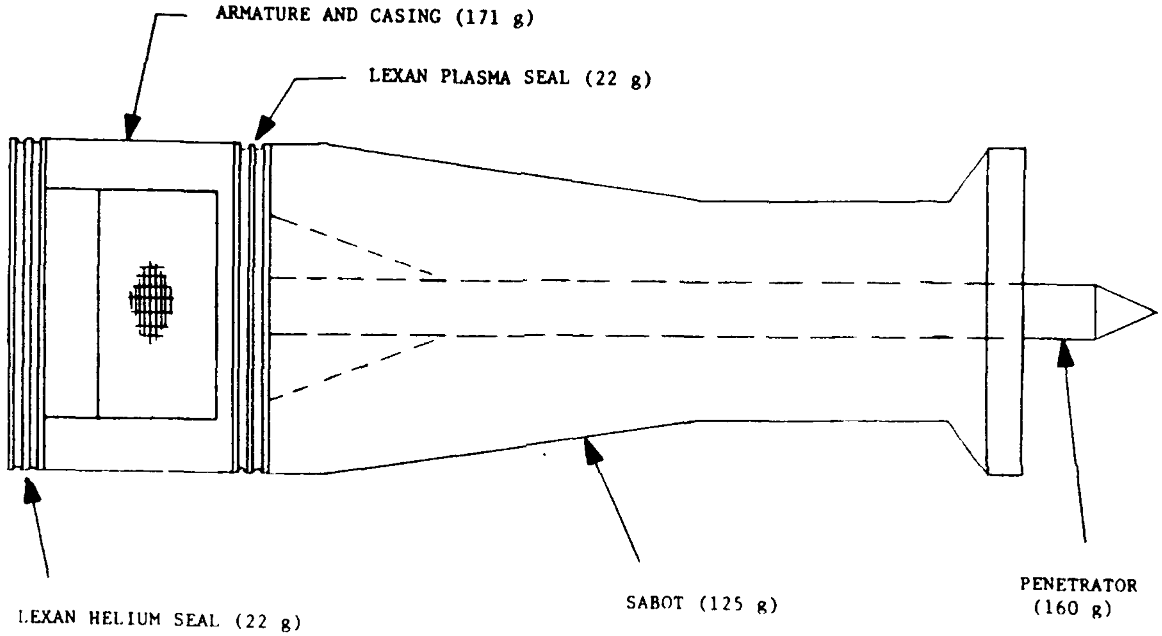

Figure 66. Complete launch package with 2 seals, fiber armature, penetrator, and 4-piece aluminum sabot. Total launch package mass is 500 grams.

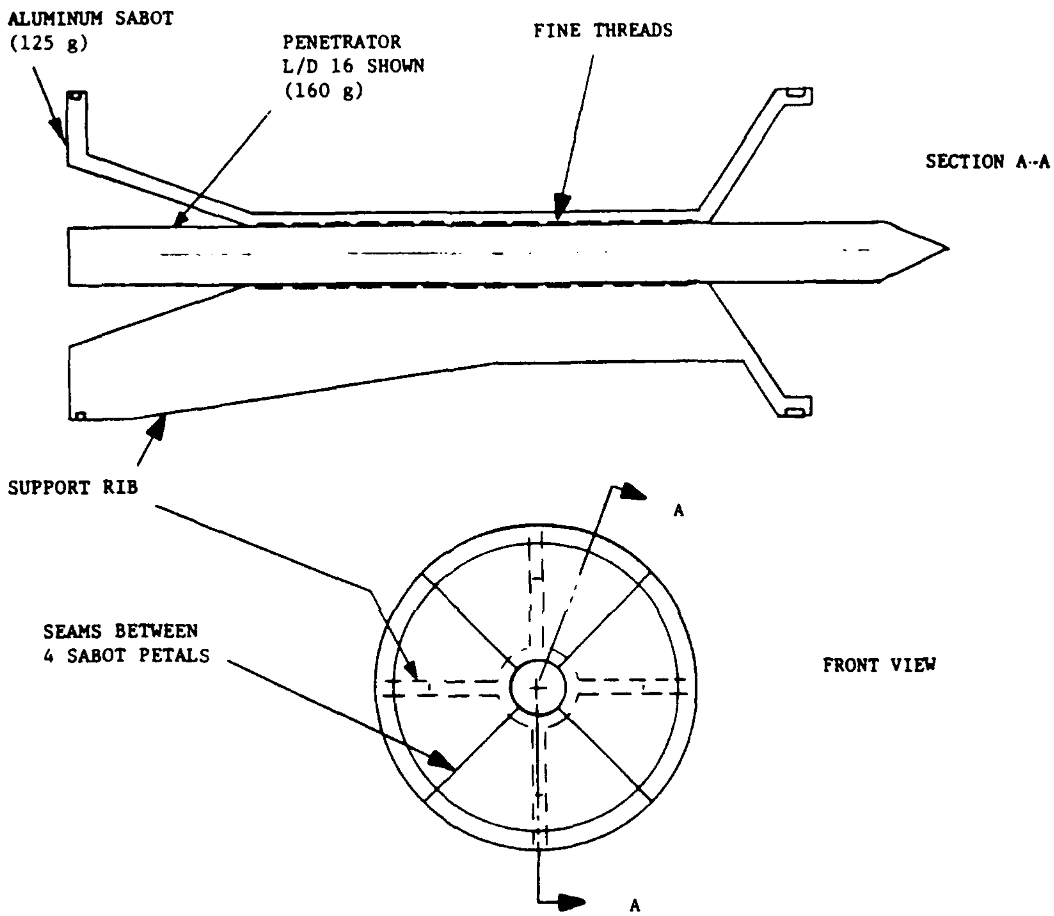

Figure 67. Sabot/Penetrator assembly with a four-piece aluminum sabot, and a tungsten penetrator. Assembly is pushed on the annular surface at the rear of the sabot. The sabot grips the rod with ridges along the rod's center section.

As shown in Figure 67, the sabot/penetrator is pushed from behind. This accelerating force is distributed to the penetrator via threaded ridges along much of the penetrator's length. At a peak current of 2.1 MA, and a total accelerated mass of 515 g, a peak acceleration of 1.71×10^6 m/s^2 is expected. The sabot/penetrator package, at 285 g, therefore requires a force of 488,000 N, or 110,000 lb, to be communicated to the sabot base. An average compressive stress of 42,000 psi is produced. The sabot is made of 7075-T6 aluminum, and the rod is made of tungsten. The average shear stress at the sabot/penetrator threaded interface is 17,000 psi.

8.4 BORE RECONDITIONING TESTS

Bore reconditioning will be a regular maintenance item to be addressed during the commissioning and operation of the facility. The two main issues regarding bore reconditioning are 1) evaluating the bore condition, and 2) taking the proper remedial action.

8.4.1 Bore Lifetime

The number of shots or the total allowable time under barrel preload before some remedial action or refurbishment of the bore is required is dependent on a number of factors. Perhaps the most important is the precision of alignment during initial assembly and application of preload. Careful placement of conformable pads, seals, reinforcement around diagnostic probes and careful mating of the ends of insulator sections are essential to assure uniform distribution of externally applied preloads. Failure to distribute the preloads properly can lead to several potential bore damaging conditions including: blow-through of unreinforced sections; premature cracking and leakage at the bore insulators; extrusion of seals into the bore leaving gaps between insulator and conducting rails; internal "steps" at insulator sections and nonuniform bore cross section dimensions at different positions along the barrel. These conditions may make it impossible to avoid leakage of a plasma armature thereby severely limiting the choice of armature until the bore is rebuilt.

Steps or offsets can severely perturb the integrity and trajectory of the projectile/armature package unless corrected. Small geometric discontinuities or "high spots" due to minor misalignment of a

a few tenths of a millimeter in segmented guns have not proven to be detrimental and can be smoothed out by firing dummy loads (plastic projectiles) using only the preinjector after initial alignment. Alternatively, a reaming operation can be performed on initial assembly as described below.

Even in the absence of dynamic loads due to firing, the high preloads required to contain a calculated peak accelerating pressure of 345 MPa will cause dimensional changes in the bore due to creep. Extensive testing of time dependent changes in bore ovality, strains (stresses) in bore conductors and insulators and in bolt tensioning has been conducted for the SUVAC II Program, for example. The amount of stress relaxation and loss of preload can be minimized by allowing the barrel to creep under partial load for a period of time at each of several successively higher load levels as shown in Figure 68. Long hold times of six months to a year under high preload, with the reference barrel design, has been observed to result in a slow transition to an elliptical cross section with 10 % to 20% difference in major and minor axes if the barrel is not reamed. The combination of startup operations involving staged preloading, boroscope examination, bore reaming and/or dummy load shots with the preaccelerator constitute initial "bore conditioning." These procedures are an integral part of the Commissioning Program.

Following barrel assembly and initial bore conditioning, bore lifetime is mainly determined by the processes of ablation, erosion, loss of dielectric properties and cracking due to dynamic thermal and mechanical loads during firing. These processess are highly dependent on the composition of the bore materials, bore diameter, nature of the armature, rail current per unit rail height, and current injection profile. Thus it is difficult to accurately predict when bore reconditioning will be required. A reasonable data base should be established during the first year of the Commissioning and Test Program. It is encouraging that larger diameter EMLs, such as the reference design proposed for BRL, show much less bore damage for a given I' than

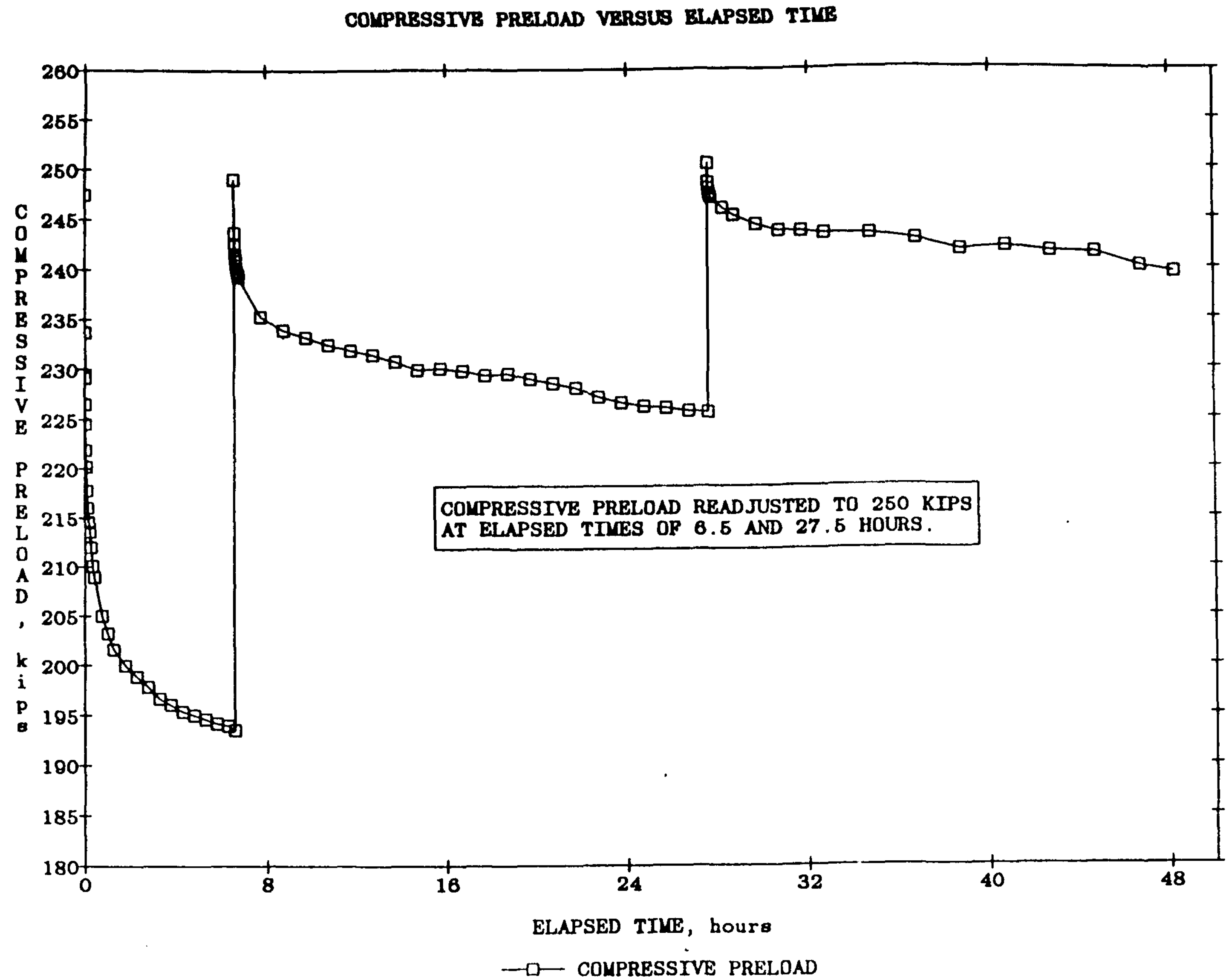

Figure 68. Application of preload with intermediate hold times for creep accommodation in SUVAC II launcher.

would be predicted on the basis of scaling effects observed in small bore diameter guns.

8.4.2 Materials Issues

Dynamic Load Effects

Assuming that the barrel has been properly assembled and aligned and that sufficient preload has been applied so that radial deflections of bore components are limited to design values, mechanical damage from multiple firings will be minimal. Copper alloys such Glidcop Al-60 possess sufficient strength and fracture toughness to withstand the peak pressure loads. The insulators are the more load sensitive components. At least four different fracture modes have been identified for G-9 bore insulators in the SUVAC II tests. Of these, delamination (cracking) along plys of the E-glass reinforcement is the most severe form of degradation leading to plasma leakage. Dynamic fracture toughness data indicate that G-9 possesses adequate resistance to cracking or fast fracture with sufficient preload. Fracture at "soft spots" in the bore generally requires replacement of bore insulators. Strain gauging of bolts and periodic measurements of bolt loads (strains) at the peak pressure region may provide an early indication of loss of preload after multiple shots. This should be conducted as part of the initial Commissioning/Test Program and a methodology for retorquing established if required.

Use of refractory metal clad copper rails or ceramic bore insulator sleeves, which may be necessary for plasma armature driven high velocity railguns, can exhibit fractures due to the combined action of mechanical and thermal stresses after multiple shots. In general, such bore components cannot be refurbished in-situ.

Thermal Effects

Calculated peak heat fluxes of 100-200 kW/cm^2 and peak rail surface temperature rise of 500-900K are sufficient to induce significant ablation and erosion of both copper alloy rails and the reference G-9 bore insulators. Although generalized melting of the

surface of the copper is not predicted, localized arc energy deposition has been observed to result in melting along arc tracks. Rapid solidification of the melted region results in entrained shrinkage porosity. In addition, mixing of gaseous ablation products from the insulator and armature with the molten metal in the arc tracks often produces gas bubbles as the molten zone rapidly cools and the gas solubility falls precipitously. Both shrinkage and gas entrainment effects result in a porous, embrittled near surface region which can be fractured or melted off by passage of subsequent projectile/armature packages leading to a roughened surface.

Alloying of the surface of the conductors by plating out of armature species is another degradation mechanism that has been observed after 40-50 shots with aluminum armatures, for example. The deposited aluminum layer can form a diffusion couple with the rail material resulting in the growth of brittle intermetallic layers. Erosion of this altered surface layer also contributes to the observed roughening of the rail surfaces.

The nitrogen linked resin and E-glass composite designated NEMA grade G-9 exhibits excellent resistance to loss of surface dielectric properties with exposure to high current arcs and/or high heat fluxes. This property plus its high compressive strength and fracture toughness have made it the bore insulator of choice for a large number of railguns. However, the retention of surface resistivity and resistance to flashover or restrike is due to the inherent high ablation rate of the resin which prevents the formation of an adherent, conducting char. Ablation of the organic resin occurs at low temperature while the glass phase resists ablation until higher temperature. The net result is the formation of a rough, glassy matted surface with successive shots. Melting and loss of the resin and glass from the insulator surface will thus increase armature drag and result in loss of bore dimensions in the peak pressure regions of the gun. After a certain number of shots it will become necessary to rebore or ream the gun.

Since these degradation mechanisms depend upon the details of rail, insulator and armature composition and projectile-armature-bore surface interactions, it is not possible to predict the extent of topological and dimensional change with successive shots. Experience and estimated ablation/erosion rates for the proposed operating conditions indicate that it will probably be necessary to ream the bore at least twice to achieve adequate performance for 50 shots.

8.4.3 Evaluation

At this time, it is difficult to predict when the bore will need reconditioning. However, once the facility is operational, the need to service the bore will become apparent, provided a complete and accurate data bank is available. Four general techniques can be utilized to evaluate the condition of the bore. These are:

1. Degraded performance, with all other experimental parameters being equal.
2. Bore diameter measurements.
3. Visual inspection with boroscope.
4. Cumulative bore surface thermal loading since latest bore servicing.

Degraded performance for no apparent reason is the strongest single indication that bore reconditioning is needed. For this reason, a control shot, or shots, with a specific set of parameters, should be selected, and repeated periodically during the commissioning phase. All variables should be kept consistent for these shots. If a strong trend of degraded performance is exhibited through three or more shots, and there is no other explanation, then bore reconditioning is probably required. After reconditioning, the control shot should be repeated immediately to see if performance has been restored to expected levels.

Bore diameter measurements should be performed routinely with every shot. Accelerated or uneven wear in the bore can signify deficiencies in the bore materials, or problems with armature design. Dimensional irregularities, in and of themselves, should not be of great

concern, if the performance is good. When bore machining is done, enough material should be removed so that the irregularities disappear.

Bore diameter measurements can also detect deposits on the bore surface, such as a solidified layer of molten aluminum from the armature. Again, this condition should not have to be remedied unless it is linked to degraded launcher performance.

Internal examination by means of a borescope during assembly and between shots can often reveal incipient flaws which could adversely affect the performance of the EML. Such examinations should be routinely performed since adjustment of peak pressure magnitude and position in the gun or bore reaming operations may significantly extend bore life without seriously degrading performance. Decisions for remedial action based on borescope observations require a significant amount of engineering judgement and experience with a given gun system. It is generally not possible to establish a priori criteria.

A fourth indicator of bore condition is the cumulative thermal loading that the bore surface has been subjected to since the latest bore servicing. A barrel's "age" could potentially be quantified by taking the breech energy during the launch, and subtracting the kinetic energy of the launch package. The remaining quantity could be called "barrel energy." Cumulative barrel energy is a possible indicator of bore condition.

8.4.4 Remedial Action

Demonstration of the ability to dress the bore with a suitable reaming tool is an integral part of the Test/Commissioning Program. Tooling and bore reaming procedures for copper rails and G-10 insulators have been developed and successfully applied to Maxwell Laboratories SSG large round bore EML. A similar approach should work well for the Reference Design BRL Capacitor-Driven EML with 56-mm (2.205-in.) bore. Modifications will include diamond tipped flutes and integral borescope for improved cutting of harder copper alloy rails such as Glidcop Al-60 and the G-9 insulators and better control of the in-bore machining

process. For purposes of discussion it will be assumed that two reaming operations will be required in a 50 shot series which increase the bore diameter to 57 mm (2.244 in.) and 58 mm (2.283 in.), respectively.

The tooling concept involves modification of standard, indexable end mill tooling to match the required diameters. The reamer would be attached to a drive mechanism with integral coolant and borescope access. A variable speed drive would permit tool rotation speeds to several hundred rpm. The optimum cutting speed would be determined during the initial boring operation after barrel assembly. Either hand or power feed could be used. A fiberoptic borescope such as the Lenox Instrument Co. Model FF896DR with 8-mm diameter head would permit inspection during cutting.

Figures 69 and 70 are schematics of the proposed tooling. The indexable milling tool could be fed through a starting bushing attached to either the breech or muzzle. The cutting medium would be a combination air blast past the tool and an inert lubricant such as a silicone oil/alcohol mixture. If required, the self-centering of the milling tool could be improved by addition of a forward pilot section suitably modified for coolant channels and borescope access. The coolant would be collected at the far end and could be filtered for reuse. The borescope would be removable for use between reaming operations

Precision ground milling inserts such as Kennametal's K68 or KD100 inserts have been used extensively by L&S Machining Co. for fabrication of hard copper alloy rails and G-9 insulators for the SUVAC II EML and are recommended for the reference BRL EML design. These are polycrystalline diamond tipped carbide tools developed for cutting nonferrous metals and abrasive composites. Choice of a specific end mill design for multiyear use will depend on the criteria and frequency of bore machining that will be established during the Commissioning/Test Program, and will be made in conjunction with a machine-tool production company.

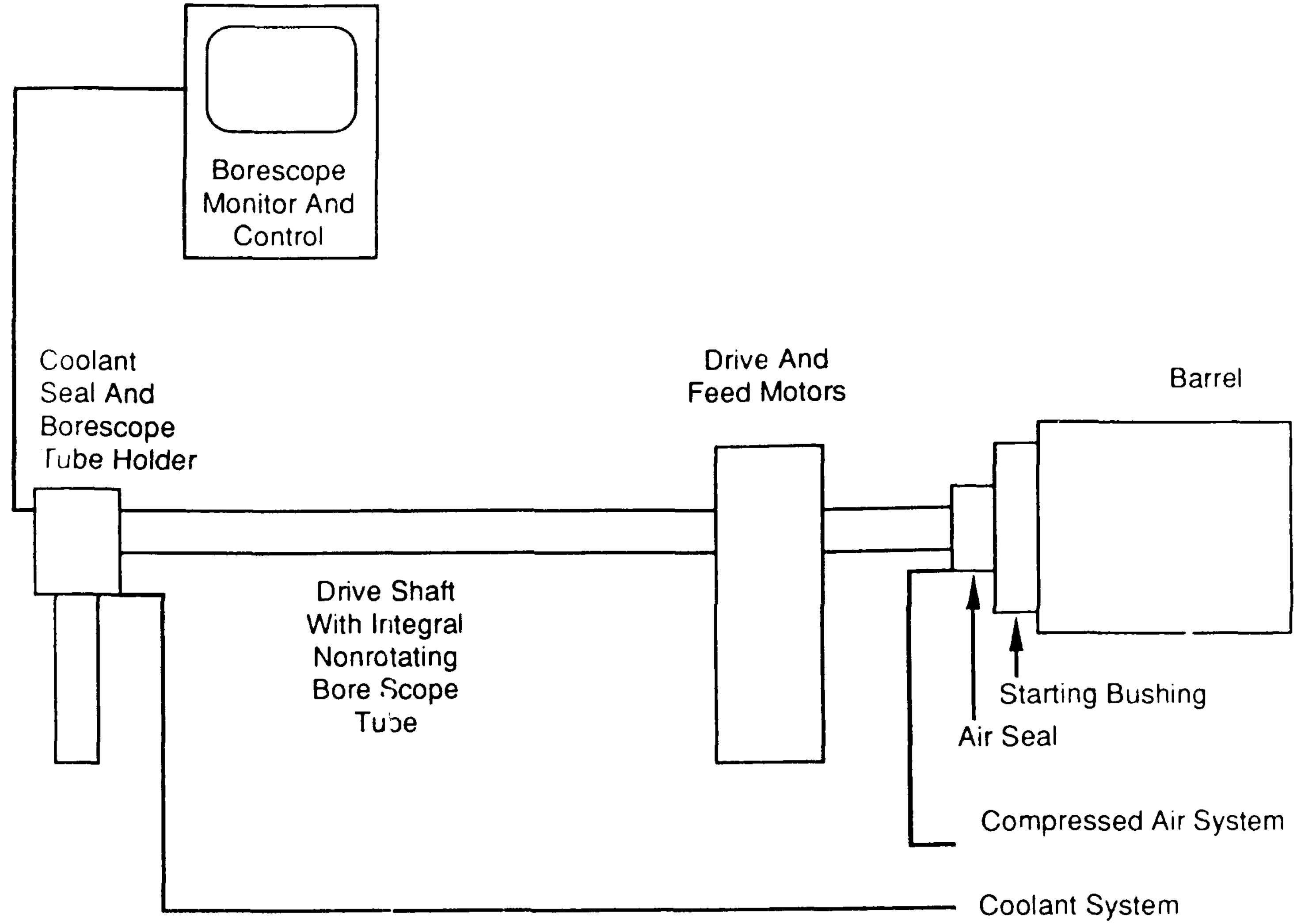

Figure 69. Schematic of proposed bore reaming assembly external to bore for either muzzle or breech indexed machining.

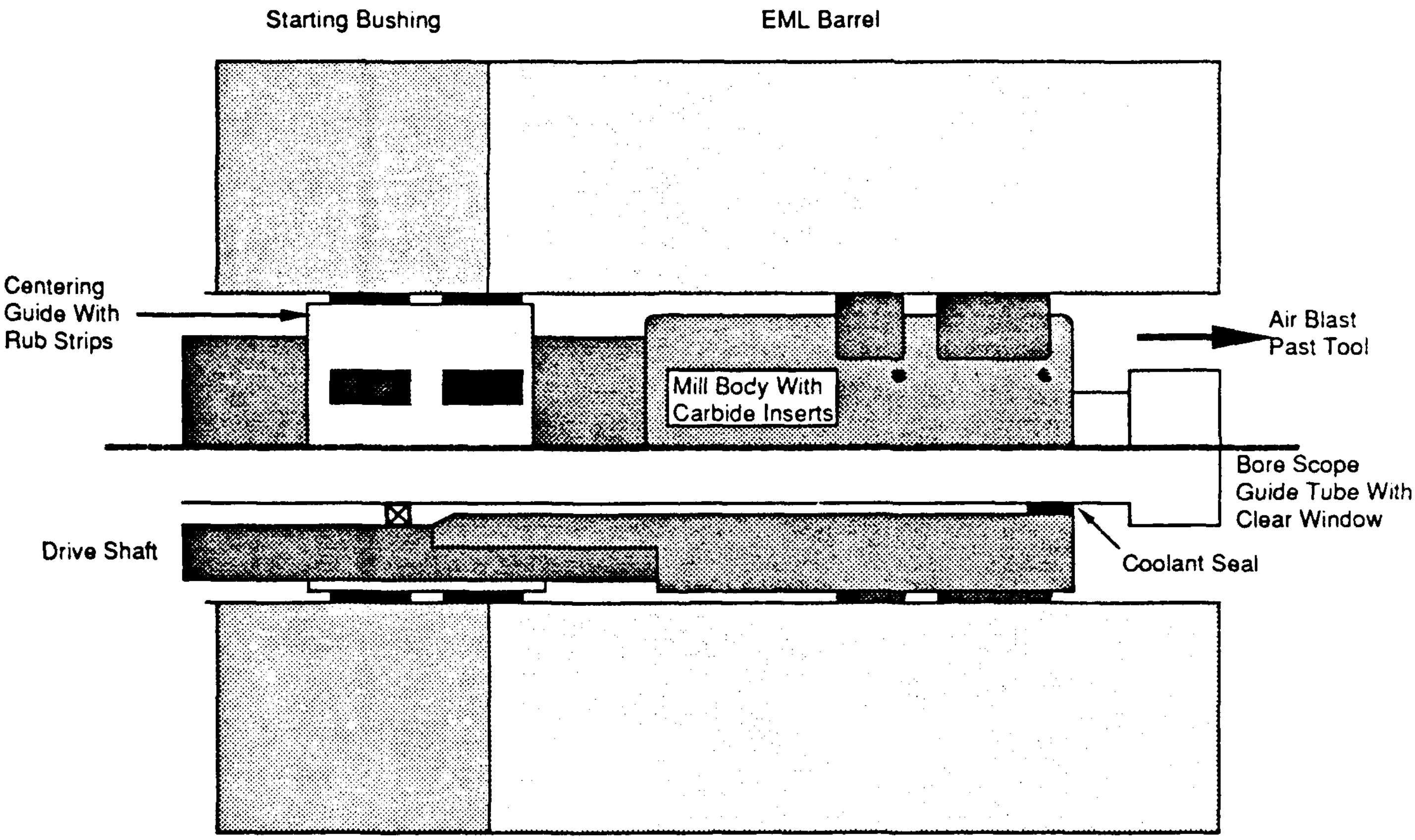

Figure 70. Cross-section schematic of starting bushing, EML barrel and reaming tool.

9. SCHEDULE AND COST ESTIMATE FOR COMMISSIONING/TEST PROGRAM

The Commissioning/Test Program schedule is shown in Figure 71. The total program will require about one year; the first six months will be devoted to commissioning the facility and the remaining six months to conducting the test program. However, planning and design work for the test program would commence early in the year during the commissioning of the facility. For example, the design, engineering, and fabrication of projectile packages would occur prior to the initiation of the test program.

As stated in the Introduction, it is assumed that the equipment is fully assembled in the test cell at the time the commissioning commences. The schedule shown in Figure 71 does not allow any time for this activity.

During the first six months, i.e., during the commissioning of the facility, the EML will suffer a small amount of bore damage since the power supply and preaccelerator will be commissioned without firing the rail gun and only two full power shots are required to commission the full EML. Each of the test series to develop a standard armature and standard projectile package will require about 15 shots. The integrated EML system test series will require about 18 shots. The total of ~50 shots should be obtained without replacing the bore materials, but will require reconditioning (reboring) the barrel as needed. The damaged barrel used for the test program will be replaced by the spare barrel prior to initiating the terminal ballistic research program.

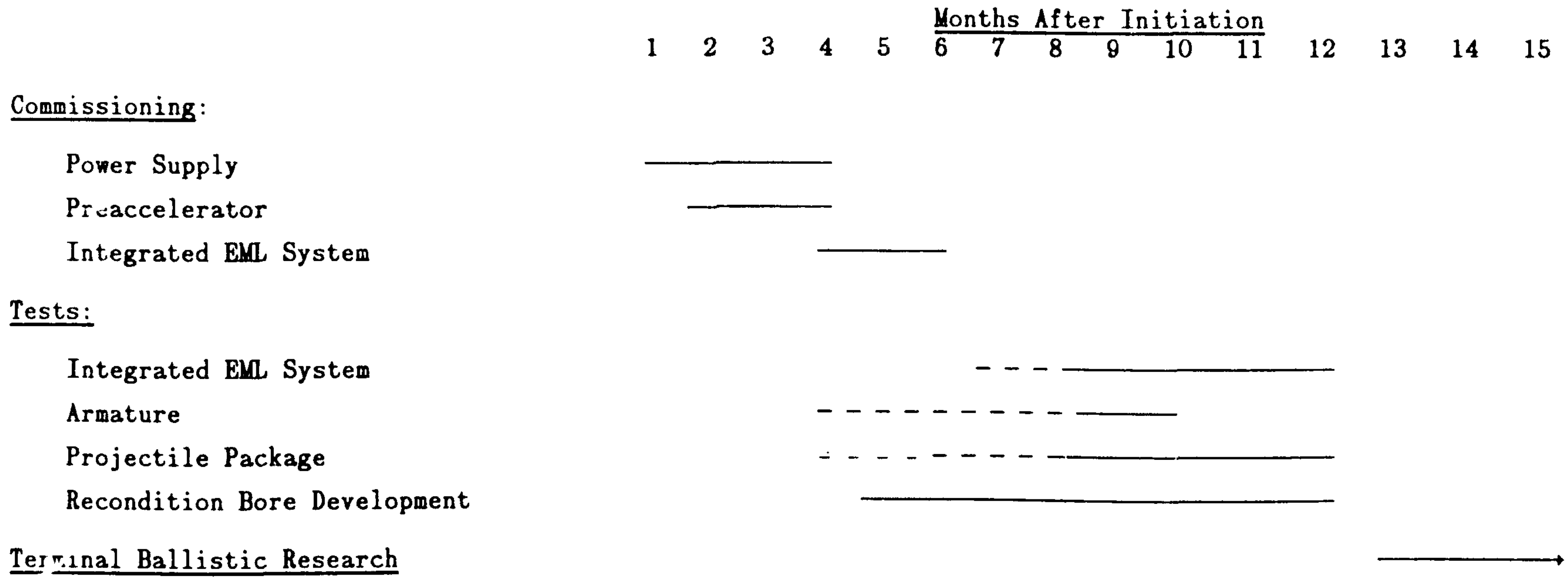

Figure 71. Commissioning/Test Program Schedule.

The estimated operating costs during the one-year Commissioning/Test Program are presented in Table 46. It is estimated that the equivalent of two engineers/scientists (E/S) and two technicians will be required throughout the year for the Commissioning/ Test Program. At times, during the commissioning for example, one E/S will suffice, but additional technicians will be required. At other times, when data is being analyzed, when components such as the projectile packages are being designed, and when tests are being planned, additional E/S will be required. The total operating costs for the one-year commissioning/test program are estimated to be $\simeq$ \$730K.

Table 46. Estimated Operating Costs for the Commissioning/Test Program

	K$
Power Supply	50
Mechanical	30
Projectiles	150
Material Subtotal	230
Operating Personnel	500
TOTAL	730

10. SUMMARY AND CONCLUSIONS

Conceptual designs for three electric launchers have been developed that could serve as advanced gun facilities for conducting terminal ballistic research. The types of launchers considered were capacitor-driven electromagnetic launchers (EMLs), homopolar-generator-driven EMLs and electrothermal launchers (ETLs). The optimized designs for these three options were evaluated on the basis of technical risks and capital costs. The capacitor-driven EML is the best option for satisfying the criteria set down by the Army's Ballistic Research Laboratory for an advanced test bed, viz., to accelerate rod-type penetrators having masses in the 60-200 g range and length-to-diameter ratios in the 10-40 range to velocities in the 2.5 - 3.5 km/s range.

A major reason for selecting the capacitor-driven EML over the homopolar-generator-driven EML is its flexibility. The projectile can be driven by a relatively uniformly high pressure during its transit down the bore by programming the application of different portions of the capacitor bank across the rails at the breech of the gun. This allows a low piezometric ratio (ratio of peak-to-average projectile driving pressure) and a high efficiency to be achieved. The homopolar-generator-driven EML does not have this flexibility and achieves a low piezometric ratio only at the expense of poor efficiency. The required energy storage for the homopolar-generator-driven EML is approximately five times that of the capacitor-driven EML.

A major reason for selecting the capacitor-driven EML over the electrothermal launcher is its ability to meet all of the performance criteria established for the advanced test facility. The electrothermal launcher cannot drive the projectiles to the desired velocities, i.e.,

it cannot drive a 200-g penetrator into the 2.5 - 3.5 km/s velocity range.

Another fact that entered into the decision is that the capacitor-driven EML is a proven system for the operating conditions required for this test facility.

It is worth noting that there may be other possible gun options outside the scope of this study that may satisfy the requirements for the BRL test facility. In particular, a multistaged light-gas gun might meet the requirements, but a detailed study would be required to verify it and to compare it with the selected electric gun.

The test cell to house the equipment necessary for the capacitor-driven EML must have an area of 12 m x 12.5 m = 150 m^2 and be 8 m in height to accommodate a 10-ton crane. In addition, an area of 34 m^2 is required for a screened room for the data acquisition system, a control room, and a power supply charging system.

The capital equipment plus installation costs are estimated to total 3.2M$ for the capacitor-driven EML facility. This does not include the cost of purchasing the equipment, the cost of capital, or the cost of a building to house the equipment. The annual cost for routine operation of the facility is estimated to be 820K$. This includes 500K$ for operating personnel, 200K$ for the design and fabrication of projectile packages, and 120K$ for electrical and mechanical component replacements. Based on a total of 100 shots per year (~50% availability and ~4 shots per week when available), the average operating cost per shot is 8.2K$.

During the second phase of the study that has been conducted, three issues were addressed that would make the selected electric gun, if it were to be built, have less technical risk, cost less to operate, and have maximum operating time as a terminal ballistic research tool.

1. The EML power system should be designed satisfying requirements that will allow:
   a. necessary tests for verifying the conditions of components
   b. certain maintenance procedures to be easily conducted

2. A six-month commissioning program is required to verify the operational capability of the fully integrated launcher system. During the early portion of the commissioning process, the components should be operated far below their rated capability. As the equipment is conditioned and the problem areas are eliminated, the system can be driven harder and harder until maximum performance is achieved. The power supply can be commissioned by firing into dummy loads; the rail gun itself does not have to be fired. Likewise, the preaccelerator can be commissioned without firing the rail gun. However, in order to fully commission the integrated EML, all systems including the rail gun, must be operated. For the commissioning, a simple projectile package can and should be used.
3. A six-month test program is required beyond the commissioning plan to assure a reliable, high performance gun for terminal ballistic research. Test series must be conducted to develop/select standard armature and projectile packages for the terminal ballistic research program. These test series plus additional tests are required to establish tables of gun performance as a function of parameters such as projectile mass, energy stored in capacitor banks, time delays before discharging capacitors, etc. In parallel with this, some statistics on failure modes will be developed. Techniques must also be developed to diagnose the state of and to recondition the bore.

During the course of developing the Commissioning/Test Program, simplistic designs were developed for potential projectile packages. The expertise of BRL personnel in the area of projectile package design would be brought into play during the test program to develop these packages. A tooling concept was also developed for reaming the bore.

All of the technical issues discussed above were addressed during the study that has been conducted and the results are documented in this report. The Commissioning/Test Program would require one year to complete, and the operating cost for that year is estimated to be $730K. At the completion of the year, BRL personnel will be thoroughly familiar with the operation of the advanced gun facility and terminal ballistic research could commence.

APPENDIX A

DETAILED COST ESTIMATES FOR THE CAPACITOR-DRIVEN EML

Table A-1

CHARGING SYSTEM

Quantity	Description	Cost ($K)
1	*HV Charging Supplies 25-kV, 100-A*	60.00
1	Ground Isolation Relays	0.35
1	Charging Relays (Main)	0.35
7	Charging Relays (System)	2.50
8	Insulated Relay Enclosure	2.40
8	Charging Cables (25 ft each)	1.20
204	Charging Resistors	36.00
204	Resistor Hardware	4.10
1	System Ground	7.50
	SUBTOTAL	114.40

Table A-2

ENERGY MODULE (RACK)

Quantity	Description	Cost ($K)
36	Tubular Steel Rack	50.00
36	Intra Rack Wiring	11.00
36	Capacitor Shorting Switches	60.00
204	Capacitor Shorting Cables	3.00
408	Capacitor Shorting Resistors	22.00
408	Sets Resistor Hardware	6.00
36	Rack Grounding Resistor	7.00
36	Rack Grounding Cables	3.00
204	22-kV, 50-kJ Capacitor	313.00
	SUBTOTAL	475.00

Table A-3

EMERGENCY DUMP SYSTEM

Quantity	Description	Cost ($K)
7	50-kV Dump Relays	2.50
204	Dump Resistors	27.00
204	Sets Resistor	3.00
36	Dump Relay Assy.	7.00
36	Manual Shorting Switches	6.00
	SUBTOTAL	45.50

Table A-4

PULSE SHAPING INDUCTORS

Quantity	Description	Cost ($K)
9	Aluminum Casting	10.00
4	Tooling (sets)	40.00
8	Sets Inductor Hardware	17.00
8	Sets Inductor Support Hardware	10.00
	SUBTOTAL	77.00

Table A-5

CABLING AND BUSES - POWER CIRCUIT

Quantity	Description	Cost ($K)
204	Capacitor Output Cables	9.00
204	Cable Hardware	10.00
36	Inductor Cables ea 14 m	10.00
36	Neg SW Bus	29.00
36	Pos SW Bus	15.00
36	Transition Bus	13.00
36	Sets EM Coil Output Hardware Load Current	15.00
	SUBTOTAL	101.00

Table A-6

IGNITRONS, TRIGGERING AND SWITCHING

Quantity	Description	Cost ($K)
72	Ignitrons E Size	179.64
72	Ignitrons D Size	70.20
72	Sets Ignitron Hardware	21.30
16	HV Relays, 50-kV	6.00
8	50-kV Pulse Transformers	4.00
8	Low Inductance Capacitors	3.00
8	Ignitrons A Size	2.00
16	Sets Trigger Gen. Cable	8.00
10	Switch Module Frames and SW Support Structures	10.00
36	Voltage Sensing Networks	9.00
8	EMI Electronic Enclosure (Modified) with 50-kV Standoff	12.00
8	5-kV Power Supplies	5.00
204	Bias Resistors	13.60
204	Resistor Hardware	2.80
	SUBTOTAL	346.54

Table A-7

IGNITRON THERMAL MANAGEMENT AND RESISTANCE MONITORING

Quantity	Description	Cost ($K)
100	2.5 in. O.D., 16 Wall CPVC Tubing	0.22
100	1 in. CPVA Ells	0.07
100	1-1/2 in. x 1 in. Tees CPVA	0.80
20	1.5 in. Long Radius Ells	0.50
25	2-1/2 in. x 1-1/2 in. Tees CPVA	0.25
12	Contactors	0.20
200	Epoxy Air Duct Casting	0.90
3	Duct Heater Enclosure	0.03
5	Simplex Blowers	2.00
3	Air Cooled Condensing Unit	1.00
3	Expansion Valve	0.08
3	Durham Bus Heat Exchanger	0.25
75	3/8 in. Refrigeration Tube	0.03
75	1/4 in. Refrigeration Tube	0.02
3	Finned Tubular Duct Heaters	1.00
150	1 in. O.D., 12 Wall CPVC	0.10
250	1.5 in. O.D., 14 Wall CPVC Tubing	0.50
144	Resistance Monitoring Circuits + Readout	10.00
	SUBTOTAL	17.50

Table A-8

INJECTOR

Quantity	Description	Cost ($K)
1	Injector (complete)	130.00
1	Transition piece	35.00
	Installation	4.00
	SUBTOTAL	169.00

Table A-9

RAILS

Quantity	Description	Cost ($K)
1	5-m Rail Section Complete	130.00
	Installation (200-h)	8.00
	Support Structure	10.00
1	Catch/Range Tank	15.00
	SUBTOTAL	163.00

Table A-10

DATA ACQUISITION

Quantity	Description	Cost ($K)
1	Shielded Enclosure	20.00
	Installation	8.00
1	Input Isolation Transformer	1.00
1	Regulating Transformer	2.00
2	Instrument Racks	0.50
2	CAMAC Crates	8.50
2	Crate Controllers	2.80
10	Differential Recorders	70.00
4	Sync Timing Generators	8.00
2	Termination Panels	1.00
2	"Stop Trigger" Signal Buffers	1.00
1	Multiplexer	2.00
1	Oscilloscope	4.00
1	Test Signal Generator	1.00
40	B-Dot Probes and cables	1.50
	Misc. Cables/Connectors	0.50
2	CW X-Ray Units	60.00
2	X-Ray Sensors	2.00
1	Flash X-Ray Unity	50.00
	X-Ray Unit Installation	4.00
	SUBTOTAL	247.80

Table A-11

CONTROL ROOM EQUIPMENT

Quantity	Description	Cost ($K)
2	Processor	5.69
4	EEPROM Module	1.24
3	I/O Chassis	1.11
3	Power Supply	1.56
3	Power Cable	0.01
2	Communication Adapter	3.36
8	24-Vdc Input Module	0.96
8	110-Vac Output Module	2.02
8	110-Vac Output Module	1.30
8	24-Vdc Output Module	1.40
7	Analog Iso. Input Module	8.74
4	TTL 8-Bit Output Module	0.53
4	TTL 8-Bit Input Module	0.53
1	Programming Software	3.50
1	Compaq Computer Hardware	5.78
1	Interface Terminal	6.00
1	Keyboard	0.38
1	Support Kit	0.40
1	Rack Mount Kit	0.13
4	Isolation/Filter	3.26
1	"Fix" Software Kit	5.50
24	Fiber Optic Passive HV Probes	12.00

Table A11

CONTROL ROOM EQUIPMENT

(cont.)

Quantity	Description	Cost ($K)
10	Timer Box	3.00
15	Sync Generator	5.30
24	Rogowski Probes	5.88
1	Instrumentation cable	1.50
3	Interlok Box	0.75
3	Controller Box	1.80
4	Power Contactor	0.17
160	Control Relay	2.03
160	Relay Socket	0.80
	SUBTOTAL	86.63

Table A-12

CONTROL ROOM ELECTRICAL ISOLATION

Quantity	Description	Cost ($K)
8	FO RS-232	4.72
16	Fiber Optic Transmitter	2.72
16	Fiber Optic Receiver	3.60
2	Status Transmitter	1.19
2	Status Receiver	1.10
4	Rack Mount	1.41
2	Fiber Optic Multimeter	0.96
30	Dual Fiber Optic Cable	6.45
40	Single Fiber Optic Cable	4.40
144	Single Fiber Optic Cable	6.62
1	Misc. Wiring Component	1.50
1	Misc. Control Wires	1.50
	SUBTOTAL	36.17

No of Copies	Organization
2	Administrator Defense Technical Info Center ATTN: DTIC-DDA Cameron Station Alexandria, VA 22304-6145
1	HQDA (SARD-TR) WASH DC 20310-0001
1	Commander US Army Materiel Command ATTN: AMCDRA-ST 5001 Eisenhower Avenue Alexandria, VA 22333-0001
1	Commander US Army Laboratory Command ATTN: AMSLC-DL Adelphi, MD 20783-1145
2	Commander US Army, ARDEC ATTN: SMCAR-IMI-I Picatinny Arsenal, NJ 07806-5000
2	Commander US Army, ARDEC ATTN: SMCAR-TDC Picatinny Arsenal, NJ 07806-5000
1	Director Benet Weapons Laboratory US Army, ARDEC ATTN: SMCAR-CCB-TL Watervliet, NY 12189-4050
1	Commander US Army Armament, Munitions and Chemical Command ATTN: SMCAR-ESP-L Rock Island, IL 61299-5000
1	Commander US Army Aviation Systems Command ATTN: AMSAV-DACL 4300 Goodfellow Blvd. St. Louis, MO 63120-1798

No of Copies	Organization
1	Director US Army Aviation Research and Technology Activity ATTN: SAVRT-R (Library) M/S 219-3 Ames Research Center Moffett Field, CA 94035-1000
1	Commander US Army Missile Command ATTN: AMSMI-RD-CS-R (DOC) Redstone Arsenal, AL 35898-5010
1	Commander US Army Tank-Automotive Command ATTN: AMSTA-TSL (Technical Library) Warren, MI 48397-5000
1	Director US Army TRADOC Analysis Command ATTN: ATRC-WSR White Sands Missile Range, NM 88002-5502
(Class. only) 1	Commandant US Army Infantry School ATTN: ATSH-CD (Security Mgr.) Fort Benning, GA 31905-5660
(Unclass. only) 1	Commandant US Army Infantry School ATTN: ATSH-CD-CSO-OR Fort Benning, GA 31905-5660
1	Air Force Armament Laboratory ATTN: AFATL/DLODL Eglin AFB, FL 32542-5000
	Aberdeen Proving Ground
2	Dir, USAMSAA ATTN: AMXSY-D AMXSY-MP, H. Cohen
1	Cdr, USATECOM ATTN: AMSTE-TD
3	Cdr, CRDEC, AMCCOM ATTN: SMCCR-RSP-A SMCCR-MU SMCCR-MSI
1	Dir, VLAMO ATTN: AMSLC-VL-D

No. of Copies	Organization
1	AEDC Aeroballistics Range Arnold AFB, TN 37389-5000
2	AEDC/DOFR ATTN: CPT N. Patnode (2) Arnold AFB, TN 37389-5000
1	AEDC Technical Library MS100 Arnold AFB, TN 37389-5000
5	Air Force Armament Laboratory ATTN: AFATL/SAH, Dr. Eugene Cottle LT Sheli Foley Mr. Billy Lucas Dr. Al Young Mr. Kenneth Cobb Eglin AFB, FL 32542-5000
2	Air Force Armament Laboratory ATTN: J. C. Foster, Jr. Gerry Winschenbach Eglin AFB, FL 32542-5434
1	AFROTC/Det 128 ATTN: CPT Jere Brown Newark, DE 19716
4	Commander US Army, ARDEC ATTN: SMCAR-FS, Dr. Thomas E. Davidson SMCAR-CCL-FA, Mr. H. Kahn SMCAR-FSA-E, Dr. Thaddeus Gora SMCAR-AEE-B, Dr. David Downs Picatinny Arsenal, NJ 07806-5000
1	Commander Armament RD&E Center ATTN: Edwin A Webster, Jr. ARDC Test Site Fort Dix, NJ 08640-5290
1	Commander USA Aviation Systems Command ATTN: AMSAV-E 4300 Goodfellow Blvd. St. Louis, MO 63120

No. of Copies	Organization
1	Commander Army Missile and Munitions Center and School ATTN: CSSD-H-QL, Mr. Stan Smith P. O. Box 1500 Huntsville, AL 35807-3801
1	Director Benet Weapons Laboratory US Army, ARDEC ATTN: SMCAR-CCB-RM, Dr. Pat Vottis Watervliet, NY 12189-4050
1	Commander, USACECOM R&D Technical Library ATTN: ASQNC-ELC-I-T, Myer Center Fort Monmouth, NJ 07703-5301
1	Director DARPA ATTN: Dr. Peter J. Kemmey Tactical Technical Office 1400 Wilson Boulevard Arlington, VA 22209-2308
1	DNA/RAEV ATTN: MAJ David Lewis 6801 Telegraph Road Alexandria, VA 22310
1	Foreign Science & Technology Center ATTN: Scott LeBeau 220 7th Street, NE Charlottesville, VA 22901
3	Director Lawrence Livermore National Laboratory ATTN: J. E. Reaugh, L-290 R. S. Hawke, L-156 Alan L. Brooks P. O. Box 808 Livermore, CA 94550

No. of Copies	Organization
5	Director Los Alamos National Laboratory ATTN: M-8, MS J960, J. W. Straight MS G787, Mr. Max Fowler MS E525, Dr. J. V. Parker Dr. William Condit MS K482, Patrick Stanley P. O. Box 1663 Los Alamos, NM 87545
1	CG, MCRDAC CODE: AWT ATTN: Carrol Childers Quantico, VA 22134-5080
2	Director US Army Materials Technology Laboratory ATTN: SLCMT-MRD, P. Woolsey SLCMT-ATL Arsenal Street Watertown, MA 02172-0001
1	NASA Langley Research Center ATTN: Mr. William Scallion SSD M/S 408 Hampton, VA 23665
1	NASA Lewis Research Center ATTN: Mr. Donald Schultz MS 501-6 21000 Brookpark Road Cleveland, OH 44135
1	Naval Surface Warfare Center ATTN: W. H. Holt Mail Code G35 Dahlgren, VA 22448
1	Commandant Naval Surface Warfare Center Special EW Systems Division ATTN: Dr. John A Copley Dahlgren, VA 22448

No. of Copies	Organization
2	Commander SDIO ATTN: SDIO/IS/T, LTC Peter Rustan MAJ M. Huebschman Washington, DC 20301-7100
1	USASDC ATTN: LTC Gary Hagan P. O. Box 1500 Huntsville, AL 35807-3801
2	SDIO/T/SK ATTN: Dr. Mick Blackledge Dr. Walt Dyer The Pentagon Washington, DC 20301-7100
1	SDIO/T/KE ATTN: LTC Roger Lenard The Pentagon Washington, DC 20301-7100
1	Aerovox, Inc. 740 Belleville Avenue New Bedford, MA 02745
1	Anser Corporation ATTN: Mr. Robert Petkewicz Suite 800 1215 Jefferson Davis Highway Arlington, VA 22202
1	Astron Research & Engineering ATTN: Charles A. Powars 2028 Old Middlefield Way Mountain View, CA 94043
1	Atlantic Research Corporation ATTN: M. K. King 5945 Wellington Road Gainesville, VA 22065
1	Auburn University ATTN: Dr. Raymond F. Askew Space Power Institute Auburn University, AL 36849-3501

No. of Copies	Organization
1	Babcock and Wilcox ATTN: Mr. John Coiner P. O. Box 10935 Lynchburg, VA 24505
1	Baldini Resource Associates, Inc. ATTN: Mr. Lou Baldini 10 Barry Lane Newton, NJ 07860
2	The BDM Corp. ATTN: Dr. Darrel Harmon Dr. Ed Wilkinson 950 Explorer Avenue Huntsville, AL 35806
1	California Research and Technology Inc. ATTN: Dennis L. Orphal 5117 Johnson Drive Pleasanton, CA 94566
1	CALSPAN Corp./AEDC Div. ATTN: John Cable VKF/AP MS440 Arnold AFB, TN 37389-9998
1	California Research and Technology, Inc. PAI Division ATTN: Hallock F. Swift 7546 McEwen Road Dayton, OH 45459
5	Center for Electromechanics The University of Texas at Austin Balcones Research Center ATTN: Dr. Harry Fair Mr. Dennis Peterson Dr. William Weldon Mr. Raymond Zowarka Mr. John Gully 10100 Burnett Road Austin, TX 78758-4497
1	EML ATTN: Dr. Henry Kolm 625 Putnam Avenue Cambridge, MA 02139

No. of Copies	Organization
3	FMC Corporation ATTN: George Chryssomallis Brad Goodell Ronald Ricci Advanced Systems Center P. O. Box 59043 Minneapolis, MN 55459-0043
1	GA Technologies, Inc. ATTN: Dr. Leo D. Holland P.O. Box 85608 San Diego, CA 92138-5608
1	General Dynamics ATTN: Dr. Jaime Cuadros P. O. Box 2507 Pomona, CA 91766
2	General Dynamics Space Systems ATTN: David Madura, MZ 92-8260 John Nakai, MZ C1-7105 P. O. Box 85990 San Diego, CA 92138
2	General Electric Company Armament and Electrical Systems Dept. ATTN: William M. Bird, Jr. Alan Wait Rd. #3, Plains Road Ballston Spa, NY 12020
1	General Electric Company ATTN: W. R. Broyles OP 43-243 100 Plastics Avenue Pittsfield, MA 01201
3	General Research Corporation ATTN: Dr. William M. Isbell Dr. Jeffrey G. Reed T. L. Menna 5383 Hollister Avenue Santa Barbara, CA 93160-6770
1	General Research Corporation ATTN: Mr. Gene Hauze 7655 Old Springhouse Road McLean, VA 22102

No. of Copies	Organization
1	Paul Gough Associates, Inc. ATTN: Dr. Paul S. Gough 1048 South Street Portsmouth, NH 03801-5423
1	Dr. Edward B. Goldman 6253 Ridgemont Drive Oakland, CA 94619
1	GT Devices ATTN: Dr. Derek A. Tidman 5705 General Washington Drive Alexandria, VA 22312
2	IAP Research, Inc. ATTN: Dr. John P. Barber Mr. David P. Bauer 2763 Culver Avenue Dayton, OH 45429-3723
1	Litton Industries ATTN: Dr. Robert M. Salter, Jr. 360 North Crescent Drive Beverly Hills, CA 90210
1	Lockheed Aeronautical ATTN: Mr. Craig Smyser Dept 1-330/Upland P. O. Box 33 Ontario, CA 91761-0033
2	LTV Aerospace and Defense Co. Vought Missiles and Adv. Pgms. Div. ATTN: Dr. Charles H. Haight Dr. George L. Jackson Mail Stop TH-83 P. O. Box 650003 Dallas, TX 75265-0003
3	Maxwell Laboratories ATTN: Dr. Rolf Dethlefson Dr. Michael M. Holland Mr. Peter Krickhuhn 8888 Balboa Avenue San Diego, CA 92123

No. of Copies	Organization
1	S-Cubed ATTN: Dr. R.T. Sedgwick P.O. Box 1620 La Jolla, CA 92038-1620
1	Olin Ordnance ATTN: Hugh McElroy Flinchbaugh Operations 200 East High Street Red Lion, PA 17356
1	Orbital Transfer Services ATTN: Bruce Roth 304 Monroe Tahlequah, OK 74464
1	Orlando Technology, Inc. ATTN: James R. Crowder P. O. Box 855 Shalimar, FL 32579
1	Parker Kinetic Designs, Inc. ATTN: James Weldon P. O. Box 26092 Austin, TX 78755
1	Pennsylvania State University Department of Mechanical Engineering ATTN: Dr. K. K. Quo 312 Mechanical Engineering Building University Park, PA 16802
1	The Rand Corporation Engineering and Applied Sciences Dept. ATTN: Dr. James L. Bonomo P. O. Box 2138 Santa Monica, CA 90401-2138
1	R&D Associates ATTN: Dr. John Barnett 301-A South West Street Alexandria, VA 22314
1	Rocket Research Co. ATTN: Mr. Allan Harvey P. O. Box 97009 Redmond, WA 78073

No. of Copies	Organization
3	Sandia National Laboratory ATTN: J. L. Wise, Div. 1534 J. R. Asay, Div. 1534 Maynard Cowan, Jr., Div. 1220 P. O. Box 5800 Albuquerque, NM 87185
1	W. J. Schafer Associates ATTN: Dr. Robert Kraus 1901 North Fort Myer Drive, #800 Arlington, VA 22209
1	Science Application International Corp. ATTN: Dr. Dan Dakin 7200 Powell Street Emoryville, CA 94608
1	Science Application International Corp. ATTN: Dr. Ed O'Donnel Suite 2400 2860 South Circle Drive Colorado Springs, CO 80906
1	Science Application International Corp. ATTN: Dr. Jad H. Batteh 1519 Johnson Ferry Road, Suite 300 Marietta, GA 30062
2	Science Application International Corp. ATTN: Dr. Keith A. Jamison Mr. Bill Fendley 1247-B N. Eglin Parkway Shalimar, FL 32579
1	SPARTA, Incorporated ATTN: Dr. Stuart N. Rosenwasser 1104 Camino Del Mar Del Mar, CA 92014
1	SPARTA, Incorporated ATTN: Mr. Moreno White 23041 De La Carlota Laguna Hills, CA 92653
1	Southwest Research Institute ATTN: Dr. C. E. Anderson 6220 Culebra Road San Antonio, TX 78284

No. of Copies	Organization
1	Dr. E. W. Sucov 1065 Lyndhurst Drive Pittsburgh, PA 15206
1	System Planning Corporation ATTN: Donald E. Shaw 1500 Wilson Blvd. Arlington, VA 22209
1	Teledyne Brown Engineering ATTN: Mr. Mike Guthrie Mailstop 50 600 Sparkman Drive Huntsville, AL 35807
1	Texas Technical University Department of EE/Computer Science ATTN: M. Kristiansen Lubbock, TX 79409-4439
1	University of Alabama Department of Physics ATTN: Prof. Tony C. H. Chan P. O. Box 1247 Huntsville, AL 35807
1	University of Dayton Research Institute ATTN: Dr. Stephan J. Bless 300 College Park, KLA-14 Dayton, OH 45469-0001
1	University of Tennessee Space Institute ATTN: Dr. Dennis Keefer Tullahoma, TN 37388-8897
1	Westinghouse Electric Corporation ATTN: Dr. Ian McNab, MS 91-2 401 East Hendy Avenue Sunnyvale, CA 94088
1	Westinghouse Science & Technology Center ATTN: Mr. Gordon Gibson 1310 Beulah Road Pittsburgh, PA 15235

USER EVALUATION SHEET/CHANGE OF ADDRESS

This Laboratory undertakes a continuing effort to improve the quality of the reports it publishes. Your comments/answers to the items/questions below will aid us in our efforts.

1. BRL Report Number BRL-CR-646 Date of Report NOVEMBER 1990

2. Date Report Received ____________________

3. Does this report satisfy a need? (Comment on purpose, related project, or other area of interest for which the report will be used.) ____________________

4. Specifically, how is the report being used? (Information source, design data, procedure, source of ideas, etc.) ____________________

5. Has the information in this report led to any quantitative savings as far as man-hours or dollars saved, operating costs avoided, or efficiencies achieved, etc? If so, please elaborate. ____________________

6. General Comments. What do you think should be changed to improve future reports? (Indicate changes to organization, technical content, format, etc.) ____________________

CURRENT ADDRESS

Name

Organization

Address

City, State, Zip Code

7. If indicating a Change of Address or Address Correction, please provide the New or Correct Address in Block 6 above and the Old or Incorrect address below.

OLD ADDRESS

Name

Organization

Address

City, State, Zip Code

(Remove this sheet, fold as indicated, staple or tape closed, and mail.)

---FOLD HERE---

DEPARTMENT OF THE ARMY

Director
U.S. Army Ballistic Research Laboratory
ATTN: SLCBR-DD-T
Aberdeen Proving Ground, MD 21(· -5066
OFFICIAL BUSINESS

NO POSTAGE
NECESSARY
IF MAILED
IN THE
UNITED STATES

BUSINESS REPLY MAIL
FIRST CLASS PERMIT No 0001, APG, MD

POSTAGE WILL BE PAID BY ADDRESSEE

Director
U.S. Army Ballistic Research Laboratory
ATTN: SLCBR-DD-T
Aberdeen Proving Ground, MD 21005-9989

---FOLD HERE---